Flow Research Report No. 440

DIRECT NUMERICAL SIMULATIONS OF AN UNPREMIXED TURBULENT JET FLAME

P. Givi, W.-H. Jou,
P. A. McMurtry, and R. W. Metcalfe
FLOW RESEARCH, INC.
21414-68th Avenue South
Kent, Washington 98032

March 1988

Final Report for 16 February 1985 through 16 February 1988
Contract No. F49620-85-C-0067

Prepared for
DEPARTMENT OF THE AIR FORCE
Air Force Office of Scientific Research (AFSC)
Bolling Air Force Base, DC 20332-6448

REPORT DOCUMENTATION PAGE

Form Approved OMB No. 0704-0188

1a. REPORT SECURITY CLASSIFICATION: Unclassified	1b. RESTRICTIVE MARKINGS
2a. SECURITY CLASSIFICATION AUTHORITY	3. DISTRIBUTION/AVAILABILITY OF REPORT: Distribution Unlimited; Approved for Public Release
2b. DECLASSIFICATION/DOWNGRADING SCHEDULE	
4. PERFORMING ORGANIZATION REPORT NUMBER(S): Flow Research Report No. 440	5. MONITORING ORGANIZATION REPORT NUMBER(S): AFOSR-TR- 88-0646
6a. NAME OF PERFORMING ORGANIZATION: Flow Research, Inc. / 6b. OFFICE SYMBOL (If applicable)	7a. NAME OF MONITORING ORGANIZATION: AFOSR/NA
6c. ADDRESS (City, State, and ZIP Code): 21414 - 68th Avenue South, Kent, WA 98032	7b. ADDRESS (City, State, and ZIP Code): Building 410, Bolling AFB DC 20332-6448
8a. NAME OF FUNDING/SPONSORING ORGANIZATION: AFOSR/NA / 8b. OFFICE SYMBOL (If applicable): NA	9. PROCUREMENT INSTRUMENT IDENTIFICATION NUMBER: F49620-85-C-0067
8c. ADDRESS (City, State, and ZIP Code): Building 410, Bolling AFB DC 20332-6448	10. SOURCE OF FUNDING NUMBERS: PROGRAM ELEMENT NO. 61102F; PROJECT NO. 2308; TASK NO A 2; WORK UNIT ACCESSION NO.

11. TITLE (Include Security Classification)

DIRECT NUMERICAL SIMULATIONS OF AN UNPREMIXED TURBULENT JET FLAME

12. PERSONAL AUTHOR(S)

P. Givi, W.-H. Jou, P.A. McMurtry and R. W. Metcalfe

13a. TYPE OF REPORT	13b. TIME COVERED	14. DATE OF REPORT (Year, Month, Day)	15. PAGE COUNT
Final	FROM 2-85 TO 2-88	March 1988	196

16. SUPPLEMENTARY NOTATION

17. COSATI CODES			18. SUBJECT TERMS (Continue on reverse if necessary and identify by block number)
FIELD	GROUP	SUB-GROUP	Reacting Flows, Turbulence, Numerical Simulations, Spectral Element Methods, Mixing Layer, Flame Extinction

19. ABSTRACT (Continue on reverse if necessary and identify by block number)

Direct numerical simulations (DNS) have been performed to study the phenomenon of mixing and its effects on chemical reactions in an unpremixed turbulent reactive flow. The type of flows considered were (1) two-dimensional temporally developing mixing layers, (2) two- and three-dimensional spatially evolving mixing layers, and (3) three-dimensional homogeneous turbulent flows. The emphasis of the simulations for the first two types of flows was the local flame extinction caused by the high rate of strain in a chemically nonequilibrium turbulent flow. It was shown that flame extinction occurs in the high strain region of the braids of the coherent structures. Preliminary investigation of the three-dimensional flow shows a highly contorted flame sheet caused by the combination of the two-dimensional coherent structures and the longitudinal (streamwise) vortices. The homogeneous turbulence simulations were performed to test Toor's hypothesis. The results of the simulations suggested a revision to the hypothesis. During the course of the research, a three-dimensional spectral-element code was developed for the three-dimensional flows. The code combined the accuracy of a pseudospectral code with the flexibility of a finite element code. Scalar transport equations are included for simulations of mixing and chemical reaction in a complex three-dimensional turbulent flow.

20. DISTRIBUTION/AVAILABILITY OF ABSTRACT	21. ABSTRACT SECURITY CLASSIFICATION
☒ UNCLASSIFIED/UNLIMITED ☐ SAME AS RPT. ☑ OTIC USERS	Unclassified

22a. NAME OF RESPONSIBLE INDIVIDUAL	22b. TELEPHONE (Include Area Code)	22c. OFFICE SYMBOL
Julian Tishkoff	(202) 767-0465	AFOSR/NA

DD Form 1473, JUN 86 — Previous editions are obsolete. — SECURITY CLASSIFICATION OF THIS PAGE

ACKNOWLEDGEMENTS

The authors are indebted to Drs. Forman Williams, James Riley, John Buckmaster, Suresh Menon and Magdi Rizk for valuable discussions and very useful suggestions during all the stages of this work. Cambridge Hydrodynamics delivered the preliminary version of the spectral-element code for modifications, which was developed by Dr. Moshe Israeli. The assistance received from Messrs. Donald Lovell, Patrick McCafferty, Daniel Grunbaum and Russell Claus in code development and other computer-related issues is gratefully acknowledged. The authors also appreciate the efforts of Ms. Kristie Hammond and Ms. Karen Janott for their skillful editing and typing of the manuscripts resulting from this work.

The majority of the calculations reported here were performed on the CRAY-XMP (48) at NASA Lewis Research Center in Cleveland, Ohio. The support of NASA Lewis and Mr. Russell Claus has been essential for the completion of this research.

TABLE OF CONTENTS

LIST OF FIGURES

OBJECTIVES

The objectives of this work are to develop and implement numerical simulation techniques that would enable us to understand the mechanisms of mixing and chemical reaction in unpremixed turbulent reactive flows. In particular, we are interested in (1) simulating spatially evolving flames and studying the phenomenon of flame extinction for an Arrhenius reaction rate, (2) understanding the mixing process in parallel shear layers, and (3) investigating the dynamics of molecular mixing in homogeneous turbulent flows.

The interest in simulating spatially evolving flames was mainly motivated by the fact that most of the flows of practical interest are spatially developing, and there is a need to develop and implement numerical schemes that are capable of simulating such flows accurately. In particular, the spatial evolution of a nonequilibrium diffusion flame and the phenomenon of lift-off in turbulent unpremixed flames have been the subjects of our investigation.

The interest in understanding mixing in parallel shear layers mainly stems from the results of recent experimental observations at Cal-Tech and Stanford. These experiments show strong evidence of mixing asymmetry in mixing layers and point to the shortcomings of the previously developed advanced turbulence models in attempting to describe the mixing process in such flows and, hence, the need for developing new models to describe the process of convective mixing in shear layer configurations.

Finally, the simulations of homogeneous turbulent flows were undertaken to investigate the isolated effects of molecular mixing in turbulent flows. This study was performed to assess the validity of stochastic models in turbulence and to address the advantages or the shortcomings of many popular mixing and reaction models that have been extensively employed for predicting the conversion rates of the reactants in unpremixed turbulent reactive flows.

The approach followed in this work is based on the direct numerical simulation (DNS) method. This method involves the accurate solving of the appropriate convection-diffusion-reaction transport equations of turbulent flows by means of very accurate numerical simulations so that no turbulence modeling is required. This approach has proven successful in investigating various aspects of turbulent reactive flows in general (for a review, see Jou and Riley, 1987), and, as will be seen in the next section, it provided a very valuable tool in our numerical experiments.

STATUS OF THE RESEARCH

During the three-year period of this research, we concentrated on both code development and on extracting useful information from the results of numerical simulations. A systematic approach was followed, and the results of every step were submitted for publication in appropriate combustion and thermal sciences journals. All these papers are provided in Appendices I through VII. In this section, the important findings of our investigation are briefly presented.

First-Year Effort

In the first year of this research, we focused on an initial understanding of the physical aspects of the problem through simulations of two-dimensional flows. Specifically, we examined the effects of large coherent structures in two-dimensional, unpremixed shear flows under either temporally evolving or spatially developing assumptions. The results are summarized below.

1. In a two-dimensional temporally evolving mixing layer, a temperature-dependent chemical reaction was incorporated into a computer code that uses pseudospectral numerical methods. The nonequilibrium effects leading to the local quenching of a diffusion flame were investigated. The results indicated that the most important parameter to be considered for flame extinction is the local instantaneous scalar dissipation rate conditioned at the scalar stoichiometric value. At locations where this value is increased beyond a critical value, the local temperature decreases and the instantaneous reaction rate drops to zero, leading to the local quenching of the flame. This finding is consistent with the model of Peters and Williams (1983), who proposed that in a turbulent mixing layer, the turbulent eddies produce highly stretched and contorted sheets across which molecular diffusion of species occurs. Combustion appears as laminar flamelets on these sheets, and the flame would be extinguished if the strain rate is sufficiently high that the local reduced Damkohler number is lower than the critical value (Linan, 1974). This work was published by Givi et al. (1987a) and is included in this report as Appendix I.

2. For the purpose of simulating spatially developing flows, as an initial effort, a two-dimensional hybrid pseudospectral-finite difference code was developed. The spectral method using Fourier transforms was employed for the periodic direction of the flow, whereas the finite difference method using a second-order upwind scheme was used for the discretization of the equations in the direction of the spatial development. The resulting code was used for simulating the pretransitional region of a laboratory mixing layer. The asymmetric nature of the mixing process was numerically simulated and the "preferred" mixed concentration value (Masutani and Bowman, 1987) was numerically calculated by constructing the profiles of the probability density functions (PDFs) of a passive scalar quantity across the shear layer. The results of this simulation were also used to explain the shortcomings associated with turbulence models using simple eddy-diffusivity concepts to model the convective flux of the PDF, such as the one used previously by Givi et al. (1985). This work was published by Givi and Jou (1988a) and is included as Appendix II.

Second-Year Effort

During the second year of this research, we were primarily concerned with developing very accurate computational tools for simulations of three-dimensional spatially developing turbulent flows. At the same time, we also continued our study to better understand the physics of mixing in parallel flows. Our accomplishments during this year are summarized below.

1. Our experience from the results obtained during the first-year effort indicated a need for developing a more accurate code than the previously used hybrid spectral-finite difference code for the simulation of spatially evolving flows. The main problem associated with second-order finite difference methods is that this form of discretization requires a maximum cell Reynolds (Peclet) number of 2 (Roache, 1972) for accurate calculations. This means that one has to use a large number of grid points to capture the physics of the problem. To circumvent this problem, different types of upwind differencing have usually been used (for a recent review of different upwind schemes, see Leonard, 1988). Although such schemes result in an improvement of the capability in resolving sharp gradients for moderate-Reynolds-number flow simulations, they contain an artificial (unphysical) numerical viscosity (diffusivity), which is not desirable. Givi and Jou (1988a) and Lowrey and Reynolds (1987) were not very concerned with that problem because their simulations were restricted to nonreacting flows in which the effects of molecular viscosity were not significant.

   In reacting flow simulations, however, the upwind differencing can lead to large errors, because the physics of the problem is directly influenced by the diffusion coefficient, and the presence of the artificial viscosity results in the unphysical higher reaction conversion rates (Jou and Riley, 1987). To improve the scheme, one can use higher-order (than the second-order) differencing schemes to better resolve the sharp gradients. The convergence of the finite difference scheme is algebraic in nature. This is in contrast to the spectral convergence of a pseudospectral scheme.

   Presumably, the finite difference discretization can be replaced by spectral methods using Chebyshev expansions in the direction of spatial development (with nonperiodic boundary conditions) of the flow. The Chebyshev polynomials do not require periodicity (as Fourier polynomials do) and can be employed for any type of boundary conditions. In practice, however, the distance between the Chebyshev collocation points near the boundaries becomes extremely small if higher-order polynomials are used to discretize a large computational domain. Consequently, time integration becomes very stiff due to numerical stability restrictions (Roache, 1972). Also, the relative grid density cannot be adjusted to reflect the flow physics. A compromise between numerical accuracy and efficiency may be achieved by combining the accuracy obtained by spectral methods with the versatility offered by other numerical schemes, such as finite element methods. Such a scheme has recently been introduced by Patera (1984) with the capability of dealing with complex flows such as spatially developing turbulent flows. This

approach of combining the accuracy of spectral methods with the versatility of finite element techniques is more flexible than either technique alone could be and, thus, provides a logical way of dealing with complex boundary conditions.

For the reasons given above, it was decided to implement this "new technology" based on a spectral-element method into our direct numerical simulations of a turbulent diffusion flame. This p-type finite element method divides the streamwise direction into a number of elements, and, within each element, the thermo-fluid variables are represented by Chebyshev polynomials. The governing equations are approximately satisfied by the discretized system at the collocation points within each element. The compromise between the accuracy and the efficient time integration can be achieved by adjusting the number of finite elements and the order of Chebyshev polynomials in each element. By increasing the number of elements and using moderately low-order polynomials within each element, the stiffness in time integration can be avoided while high accuracy is maintained.

A complete description of the algorithm was provided in our last annual report (Givi et al., 1987b). Most of our efforts during the second year were focused on developing, debugging and implementing the spectral-element code to simulate a three-dimensional spatially developing mixing layer under the influence of nonequilibrium chemical reactions. In this code, spectral methods using Fourier expansions are implemented in two of the directions with periodic (or even-odd) boundary conditions, and spectral-element methods using Chebyshev polynomials are employed in the direction of spatial evolution.

2. During the second year, we also continued our study on the mixing phenomenon in parallel shear layers. This study was motivated by the findings of Kosaly and Givi (1987), who showed that the behavior of the PDFs of a conserved scalar property is sensitive to the choice of the molecular mixing model employed in the PDF transport equation. Therefore, the calculated PDFs of a conserved scalar quantity was carried out in a temporally evolving flow, and it was emphasized that indeed it is the shortcomings associated with the gradient diffusion modeling and not the coalescence/dispersion (C/D) modeling that cannot predict the location and magnitude of the PDF of the mixed fluid concentration in parallel two-stream layers. This study points to the need for advancing turbulence models that predict the turbulent convective fluxes of the PDF in the physical space more accurately. This work was published by Givi and McMurtry (1988a) and is included as Appendix III.

3. One of the final achievements during the second-year included the publication of an updated review article on direct numerical simulations of turbulent reactive flows (Jou and Riley, 1987). This review, which resulted from an invitation extended to Dr. Jou (the lead author of the review and the principal investigator of this contract), includes a very recent bibliography of directly related work in DNS and state-of-the-art computational methods in numerical combustion. A copy of this invited review paper is included as Appendix IV.

Third-Year Effort

The final year of this research was particularly fruitful in that the results of our numerical experiments from the codes developed in the previous year started to emerge. In this year, we continued our research in two parallel directions. In one study, we investigated the spatial convolution of a reacting mixing layer under the influence of nonequilibrium chemical reactions and employed the above-mentioned spectral-element code for the simulations. In another study, we employed DNS to study a reaction of the type A + B = Products in a homogeneous turbulent flow in which the influence of molecular mixing was insulated and was studied in detail. The first study is in the direction of simulating spatially developing diffusion flames and studying the phenomenon of lift-off in such flames, while the second study was motivated by the conclusions drawn from the work of Kosaly and Givi (1987). A brief discussion of our findings is given below.

1. As an initial effort, the two-dimensional option of our spectral-element code was employed to examine the compositional structure of a diffusion flame near extinction. In this work, the structure of a nonequilibrium flame stabilized on a harmonically forced mixing layer was simulated by the spectral-element code. The instantaneous data obtained by these simulations were statistically analyzed, and the statistical results show favorable agreement with recent experimental data. It was shown that by increasing the intensity of mixing (decreasing the local Damkohler number), the flame extinction phenomenon is more pronounced. The results, in particular, indicated that as the flame approaches extinction, the mean and the rms values of the reactants' concentration fluctuations increase, whereas those of the product species and temperature decrease. These results also confirmed our previous findings that as the magnitude of the local dissipation rate is increased, the diffusion flame cannot keep pace with the large diffusive flux of the reactants into the reaction zone. As a result, the magnitude of the temperature drops and the reaction rate locally reduces to zero. However, it was concluded that the calculations should be extended for three-dimensional flows for a more meaningful comparison with the data obtained for a turbulent flame. This work was submitted for publication by Givi and Jou (1988b), and is included as Appendix V.

2. The boundaries of our research were further extended in this year by examining the phenomenon of mixing in turbulence from another perspective. It was decided to study mixing in a context that has been extensively investigated by the chemical engineering community, and there is an extensive body of literature available on their analyses. The type of flows considered are homogeneous, incompressible flows, and the type of reaction is a single-step irreversible reaction of the type A + B = Products. Such homogeneous flows have the advantage that the effects of molecular mixing are isolated from other factors influencing the rate of reactant conversion. Therefore, they make an excellent system in which the dynamics of molecular mixing can be investigated.

As an initial effort, we concentrated on the applicability of Toor's hypothesis (Toor, 1962, 1969, 1975) for the prediction of the reaction conversion rate in homogeneous turbulent flows. According to this hypothesis, if the reactants are introduced at stoichiometric conditions in a homogeneous flow, the rate of decay of the "unmixedness" term is independent of the rate of the chemical reaction and is the same under both nonreacting and reacting unpremixed conditions. This hypothesis, which has been employed extensively by the chemical engineering community, reduces the problem of turbulent reaction to the simpler (but yet unsolved) problem of turbulent mixing. Although there is an extensive body of experimental data available for validating Toor's hypothesis (see Brodkey, 1981, for a recent review), there have not been any formal "analytical" attempts to validate it.

Givi and McMurtry (1988b) used direct numerical simulations to validate Toor's hypothesis in a systematic manner. For that purpose, they simulated a three-dimensional homogeneous "box" flow under the influence of a stoichiometric reaction of the type A + B = Product. Calculations were performed with zero rate and infinitely fast rate kinetics. The results of simulations indicated that the PDF of a conserved Shvab-Zeldovich scalar quantity (which characterizes mixing) evolves from an initial "double-delta function" distribution to an asymptotic shape that can be approximated by a Gaussian distribution. Givi and McMurtry (1988b) theoretically showed that Toor's hypothesis would be valid if (and only if) the transport of the PDF can be characterized by the variation of its first two moments. However, the results of the numerical experiments indicated that this is not the case in an initially unpremixed system, in that the evolution of the PDF from an initially "double delta function" to an asymptotic Gaussian distribution cannot be described by the first two moments of the PDF. Based on these results, Givi and McMurtry (1988b) suggested a revision of Toor's hypothesis and showed that, while the hypothesis is valid for the initial stages of mixing, it should be modified to describe the asymptotic stages correctly. The form of the suggested revision depends on the asymptotic shape of the PDF distribution. Givi and McMurtry (1988b) developed an analytical expression for the case of an asymptotic Gaussian PDF distribution, and the results based on this expression and those obtained by DNS data compared very well. In conclusion, it was suggested that the laboratory experimental data available on this type of flows should be examined more carefully if they are to be used to validate Toor's hypothesis. The work by Givi and McMurtry (1988b) is included as Appendix VI.

3. The work of Givi and McMurtry (1988b) indicated a need to study molecular mixing from a more fundamental point of view. The results of this work, and those of the previous work of Kosaly and Givi (1987), encouraged us to compare the results obtained by DNS to those predicted by a class of C/D models that have been widely used to simulate mixing in homogeneous turbulence. Among the family of C/D models, the closures of Curl (1963) and Janicka et al. (1979), and the LMSE approximation of Dopazo and O'Brien (1976), have been very popular in the literature and were chosen for the purpose of comparison to DNS data.

Again, a three-dimensional homogeneous "box" flow was the subject of our numerical investigation. The evolution of the PDFs of a random scalar variable was compared with that obtained by the Monte-Carlo (Pope, 1981) calculations of a stochastic C/D transport equation for a system with the same initial statistical distribution as that of the DNS. The comparison with DNS data resulted in a number of very useful findings, which are documented in detail in Appendix VII, and is only briefly discussed here.

Our data showed that the initial stages of the mixing process are well predicted by applying the LMSE closure of Dopazo and O'Brien (1976). However, as mixing proceeds at intermediate times, the experimental results fall between those obtained by the two closure models of Dopazo and O'Brien and Janicka et al. (1979). Curl's model (1963) resulted in the least-accurate predictions. Therefore, a C/D model between these two closures is expected to result in a favorable comparison with our experimental data. The final stages of mixing were not well predicted by any of the C/D models in that all of the closures predicted an increase without bounds of the fourth- and higher-order concentration moments of the random scalar, whereas our data indicated the asymptotic distribution of the moments of the scalar can be approximated by a Gaussian distribution (with finite central moments). The exception was the Dopazo-O'Brien model, which predicted unphysical constant moments during all stages of mixing. This shortcoming associated with C/D modeling has been previously recognized by Pope (1982), who suggested an improved mixing model by an age-biasing technique to the C/D modeling. This improved model is plausible in that it results in a Gaussian asymptotic PDF; however, it is not capable of predicting the initial stages of mixing accurately. The results of our numerical experiments can be useful for constructing a mixing model (or models) that can accurately predict all the stages of molecular mixing. Such a task, however, was not performed in this work and was postponed to our future investigations.

A number of other useful realizations were also made in regard to the statistical variations of the scalar quantities under no reaction, finite-rate reactions, and infinitely fast reaction rates. The results were further analyzed in conjunction with applying Toor's hypothesis (Toor, 1962). These observations, including our other major conclusions based on the numerical experiments, were documented and submitted for publication by McMurtry and Givi (1988). This manuscript is included in this report as Appendix VII.

CURRENT ACTIVITIES

In our final effort during the closing months of this program, we concentrated on simulations of turbulent, three-dimensional, spatially developing flows, which were the main focus of the proposal. From the physical point of view, this type of flow is the most interesting, and from the computational point of view, they are the most challenging. In this section, the results of our preliminary calculations of a turbulent shear layer are presented. However, as will be seen below, we are presently only at the initial stages of these simulations, and some additional work is required for an in-depth understanding of the complex physical phenomena. Nevertheless, the results obtained to date are extremely encouraging, and form a starting place for future simulations.

In this effort, the three-dimensional "option" of our spectral-element computer code, which was developed during the second year of this research (Givi et al., 1987b), was employed to simulate a turbulent, three-dimensional, spatially developing flow under the influence of a second-order Arrhenius chemical reaction. It would have been desirable to simulate the spatial development of the flow under the influence of random perturbation (with a specified turbulence spectrum) at the inlet of the mixing layer. In this way, the response of the shear layer to the random forcing would resemble that of a laboratory experiment under the influence of random upstream turbulence. However, in the coarse simulations performed here, only the response of the layer to a harmonic forcing is presented. In the only three-dimensional simulations performed, in addition to the primary perturbation and random phase shifting between the modes [see Appendix V, Equation (6)], a secondary perturbation of the following form was also added to the random velocity perturbation:

$$A_2 \vec{U}_2(y)\, e^{i(\omega t+\phi)+i\beta z} \tag{1}$$

Low-resolution calculations with 211 Chebyshev spectral points in the streamwise X-direction and with only 64-32 Fourier modes in the cross-stream-spanwise directions were performed, and the results are presented here. If infinitely fast kinetics are assumed to describe the chemical reactions (local chemical equilibrium), the convolution of the flame structure would be described by the transport of a conserved Shvab-Zeldovich scalar variable, as presented in Fig. 1. In this figure, the convolution of the flame sheet and the influences of both the primary and secondary structures of the layer on the distortion of the flame sheet in the three-dimensional flow are displayed. It is shown that, after the initial stages of primary growth, the secondary streamwise structures play significant roles on enhancement of the reaction and convolution of the flame surface. The effects of such spanwise structures can be better observed in the three-dimensional contours of the streamwise vorticity in Fig. 2 and the absolute value of the vorticity in Fig. 3. These figures clearly display the presence of the vortex ribs and the nonlinear growth of the secondary perturbations at the region further downstream of the splitter plate.

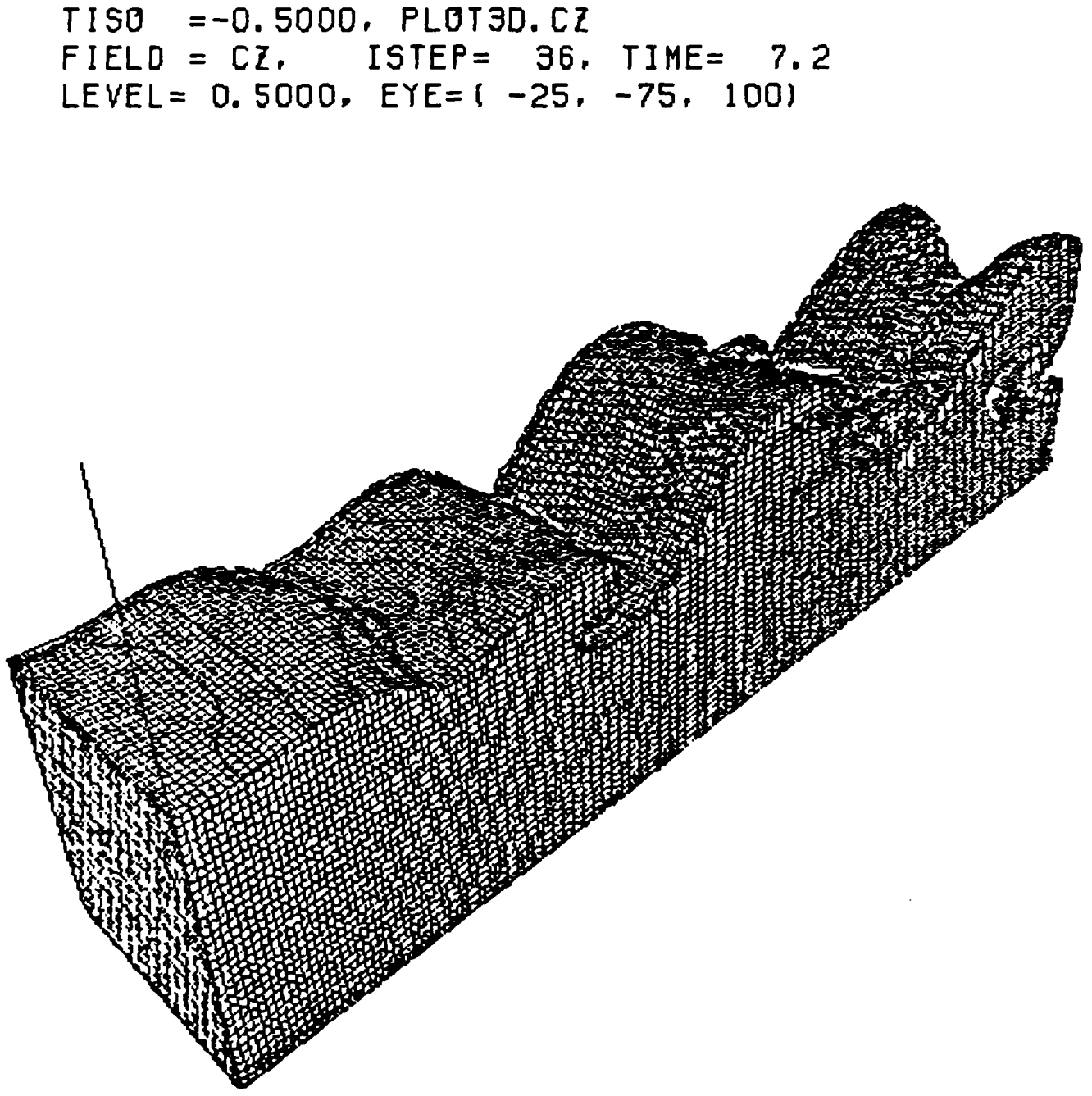

Figure 1. Convolution of the flame sheet in three-dimensional simulations

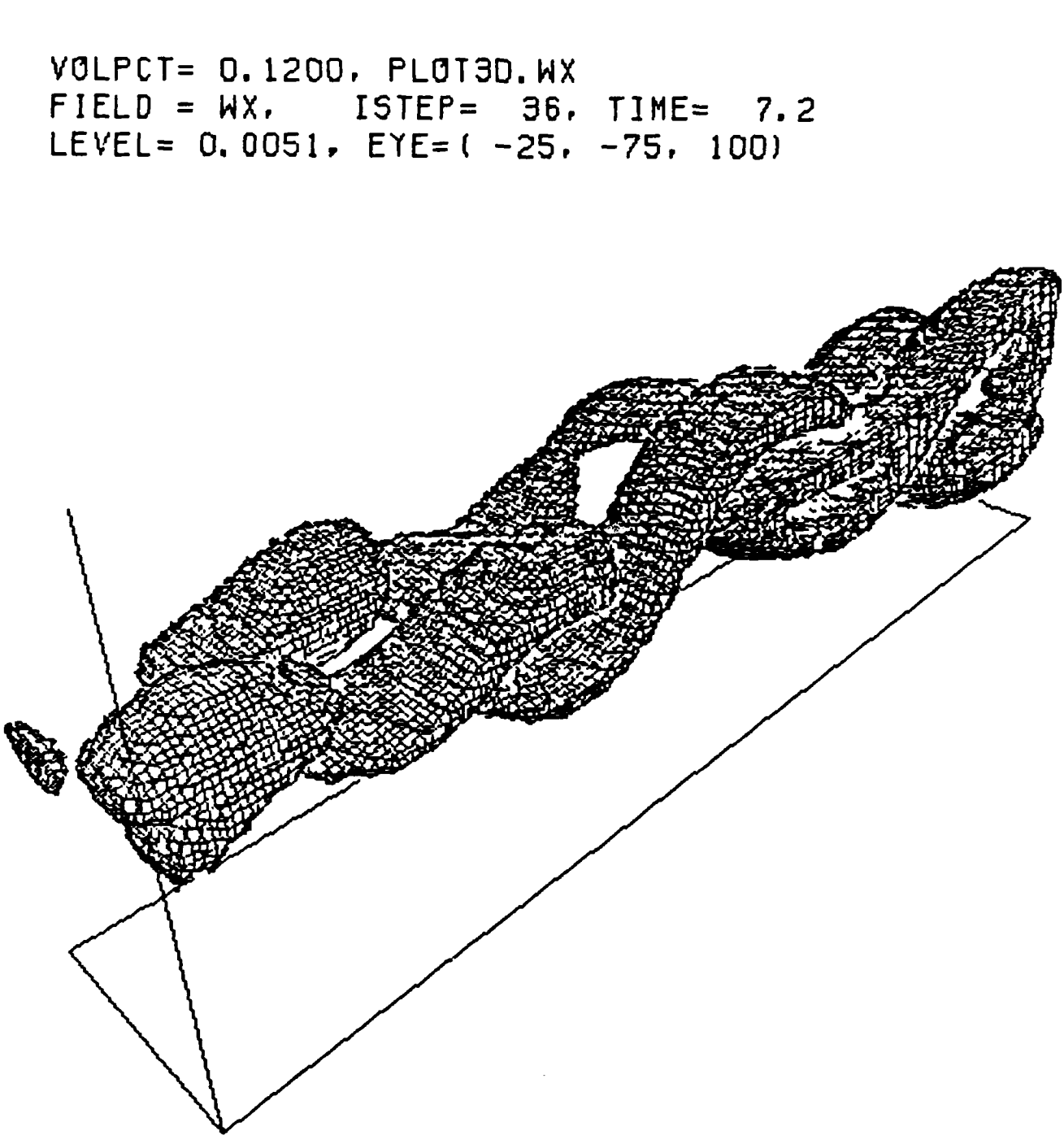

Figure 2. Three-dimensional contours of the streamwise component of the vorticity

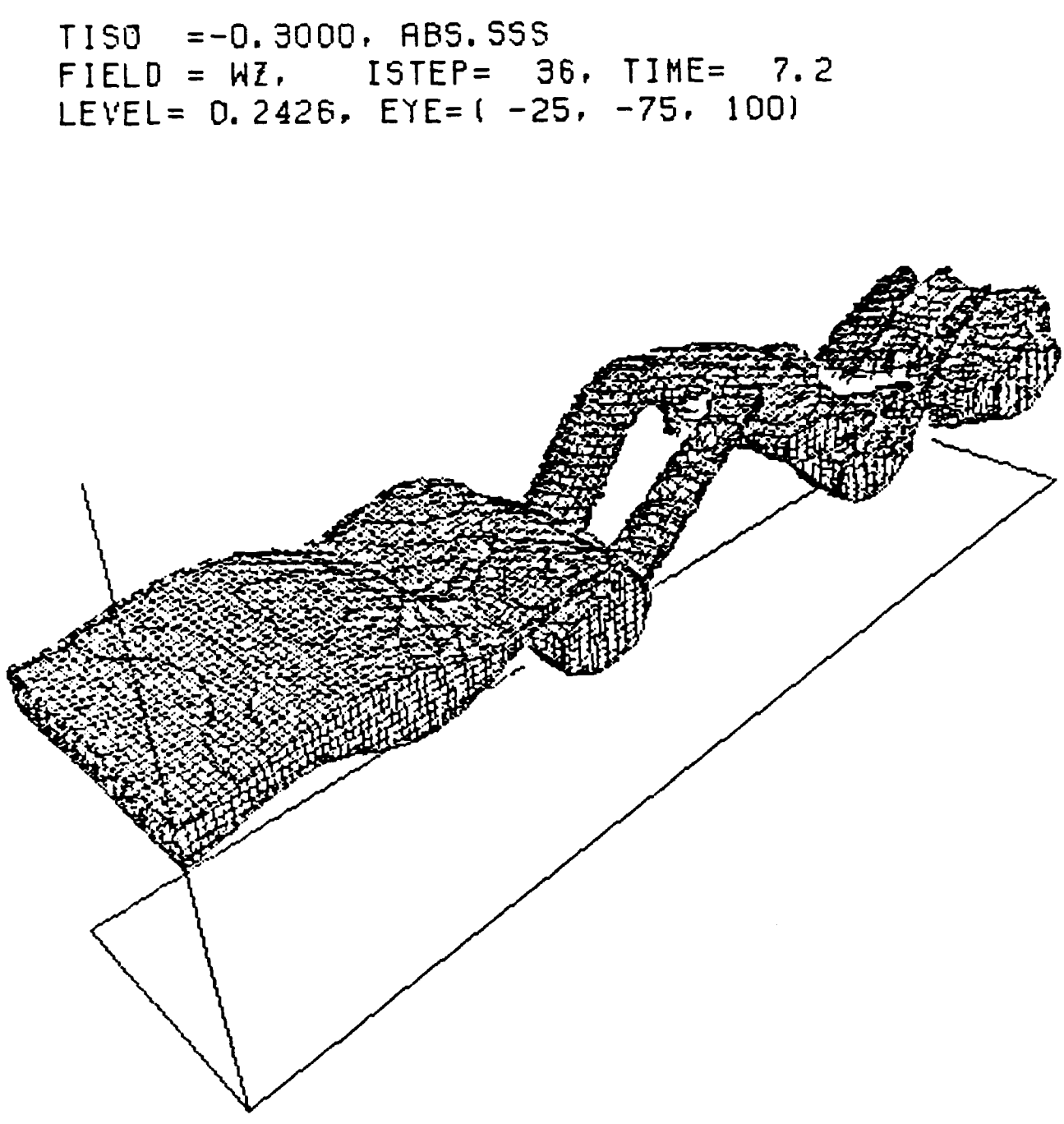

Figure 3. Three-dimensional contours of the absolute value of the total vorticity

A better display of the secondary structures is presented in the two-dimensional contour plots in Figs. 4 and 5. These figures show the streamwise contours of the X-component of the vorticity and the streamwise contours of the Shvab-Zeldovich scalar variables, respectively. Parts (a) and (b) of each figure represent conditions at X = 132 and X = 185 Chebyshev collocation planes, respectively. It is interesting to note that, even in this low-resolution simulation, the physics of the mixing layer represented by the counter-rotating vortices and the "mushroom-like" structure of the scalar variable are well-captured and resemble those recently observed in the experiments of Bernal and Roshko (1986). However, finer-grid simulations are required to capture such structures more distinctively.

The influence of complex vortex structures and the effects of increasing the local strain rate due to the three-dimensional vorticity convolution on the structure of the diffusion flame are shown in Figs. 6 and 7. These figures represent the instantaneous values of the recorded temperature across the shear layer (at Z = 0) as a function of the mixture fraction. These instantaneous data were constructed from an ensemble of 115,200 (3600 realizations multiplied by 32 cross-stream points) instantaneous data points. Fig. 6 represents conditions at the region close to the inflow where the dissipation rate is low, whereas Fig. 7 shows the overall behavior further downstream, with increasing magnitude of the local strain. It is shown in these figures that when the dissipation rate is low (Fig. 6), the magnitude of the temperature increases monotonically with the mixture fraction and attains maximum values at the region close to the stoichiometric value (equal to 0.5 in this case), and then it monotonically decreases to the ambient temperature as the value of the mixture fraction increases. In this case, the instantaneous values of the temperature are always close to the equilibrium temperature (not shown here). However, when the magnitude of the dissipation is increased, as shown in Fig. 7, the values of the temperature drop, and there are possibilities of having mixture temperatures close to the ambient value even at the stoichiometric value of the mixture fraction. This behavior, which has been clearly observed in laboratory nonequilibrium flames (see Williams, 1987, for a recent review), indicates extinction and the local quenching of the diffusion flame at the regions of large dissipation rates.

It would be very interesting to examine the behavior of the flame in the presence of random three-dimensional perturbations imposed at the inlet of a spatially developing mixing layer. In that case, the structures of the "holes" that are randomly punched into the flame sheet can be described more realistically. Our future calculations with more realistic initializations and with finer-resolution simulations are essential in addressing the interesting behavior of the lift-off phenomenon (as a result of "many holes within the flame network") in unpremixed flames.

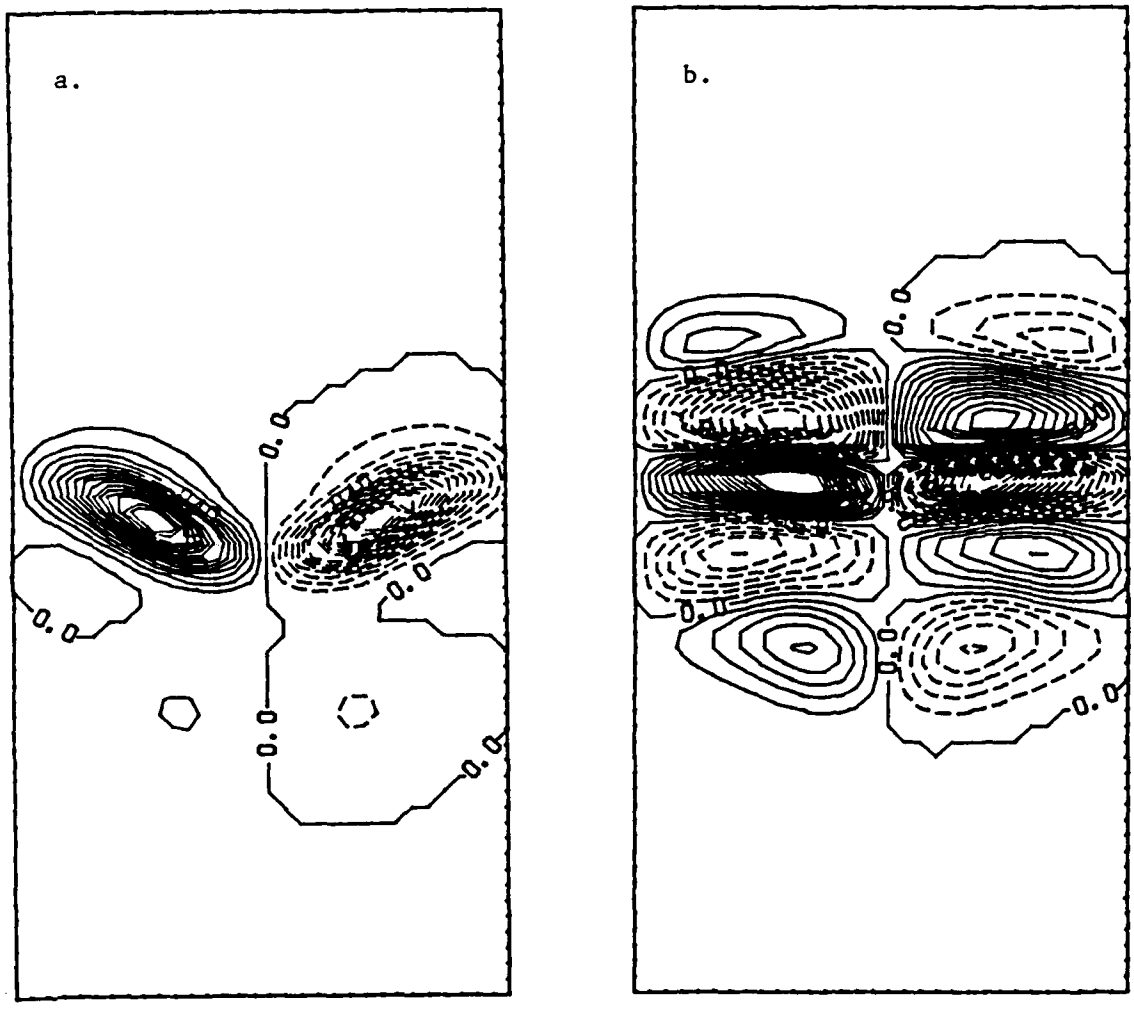

Figure 4. Two-dimensional contours of the streamwise vorticity in Y-Z planes. (a) X = 132, (b) X = 185.

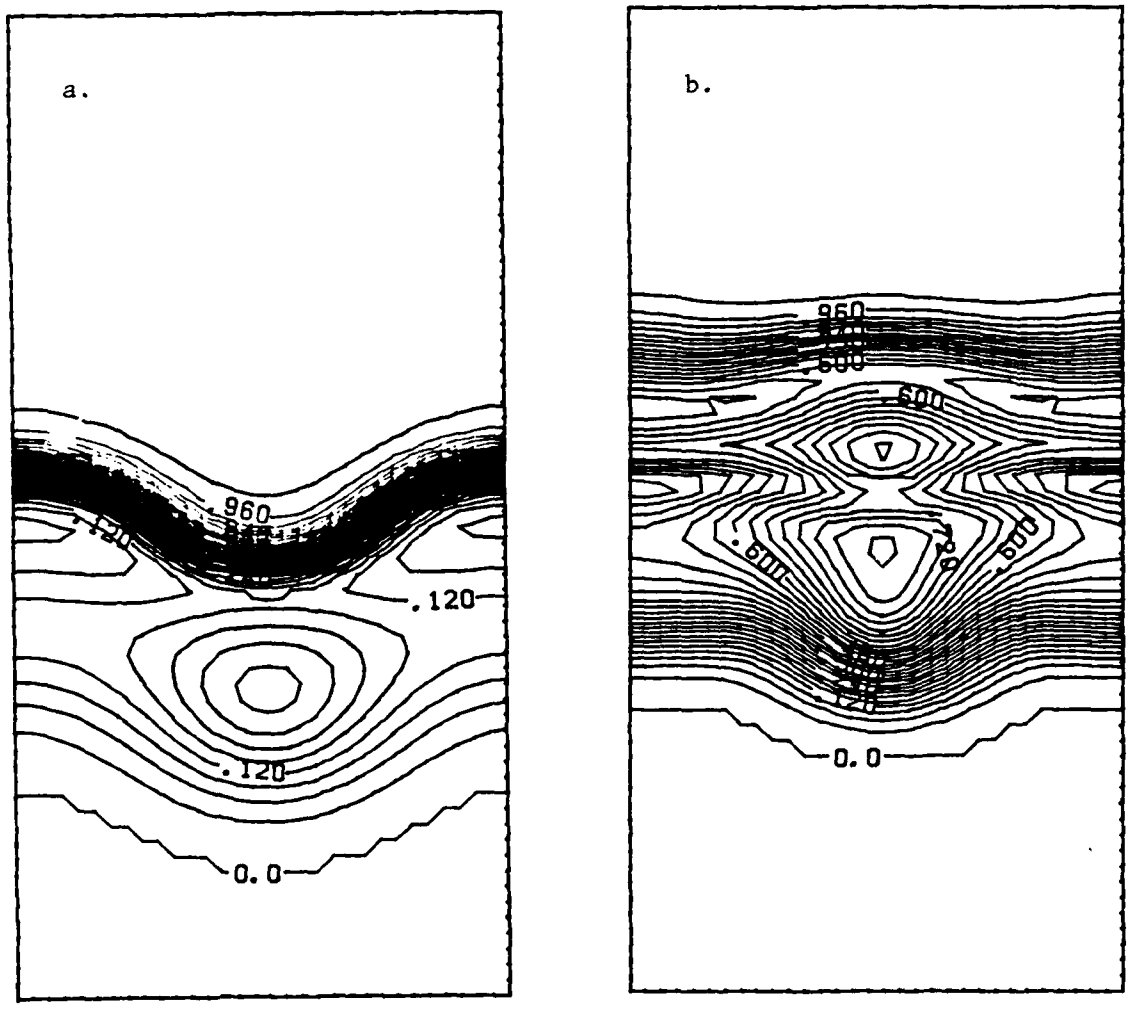

Figure 5. Two-dimensional contours of the Shvab-Zeldovich scalar variable in Y-Z planes. (a) X = 132, (b) X = 185.

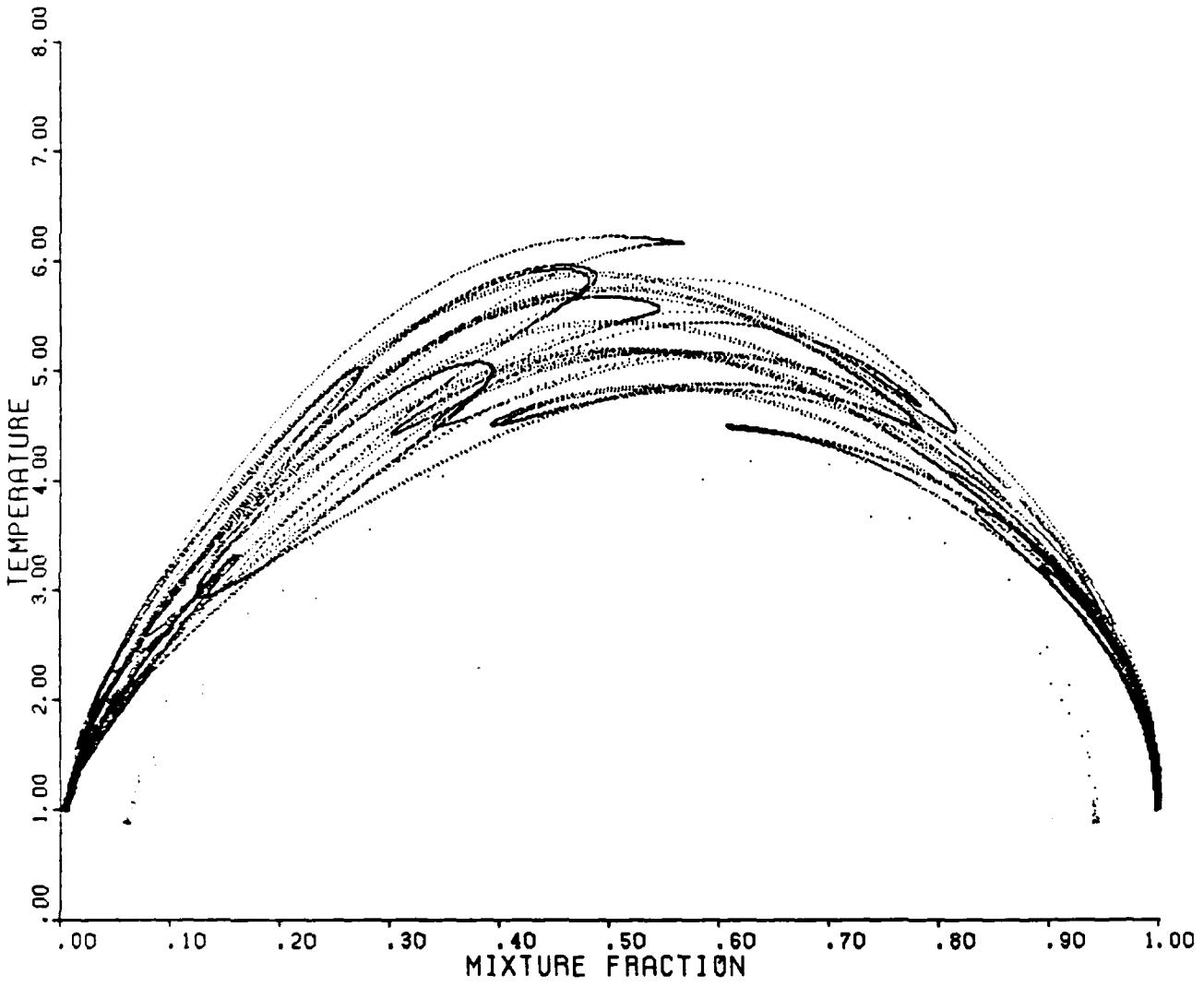

Figure 6. Instantaneous temperature as a function of mixture fraction

REFERENCES

Bernal, L. P., and Roshko, A. (1986) *Journal of Fluid Mechanics*, Vol. 170, p. 499.

Brodkey, R. S. (1981) *Chem. Eng. Comm.*, Vol. 8, p. 1.

Curl, R. L. (1963) *AIChE Journal*, Vol. 9, p. 175.

Dopazo, C., and O'Brien, E. E. (1976) *Combustion Science and Technology*, Vol. 13, p. 99.

Givi, P., and Jou, W.-H. (1988a) accepted for publication in *Journal of Non-Equilibrium Thermodynamics.*

Givi, P., and Jou, W.-H. (1988b) Submitted for presentation at the Twenty-Second Symposium (International) on Combustion.

Givi, P., and McMurtry, P. A. (1988a) *Combustion Science and Technology*, Vol. 57, 4-6, pp. 141-147.

Givi, P., and McMurtry, P. A. (1988b) accepted for publication in *AIChE Journal.*

Givi, P., Jou, W.-H., and Metcalfe, R. W. (1986) Flow Research Report No. 369, Annual Report to AFOSR.

Givi, P., Jou, W.-H., and Metcalfe, R. W. (1987a) in *Proceedings of 21st Symposium (International) on Combustion*, The Combustion Institute, Pittsburgh, PA, to appear.

Givi, P., Jou, W.-H., and Metcalfe, R. W. (1987b) Flow Research Report No. 401, Annual Report to AFOSR.

Givi, P., Ramos, J. I., and Sirignano, W. A. (1985) *Journal of Non-Equilibrium Thermodynamics*, Vol. 10, No. 2, p. 75.

Janicka, J., Kolbe, W., and Kollmann, W. (1979) *Journal of Non-Equilibrium Thermodynamics*, Vol. 4, p. 47.

Jou, W.-H., and Riley, J. J. (1987) AIAA Paper 87-1324, AIAA 19th Fluid Dynamics, Plasma Dynamics, and Lasers Conferences, Honolulu, Hawaii, June 8-10.

Kosaly, G., and Givi, P. (1987) *Combustion and Flame*, Vol. 70, p. 101.

Leonard, B. P. (1988) ICOMP Report, NASA Lewis Research Center, Cleveland, Ohio.

Linan, A. (1974) *Acta Astronautica*, Vol. 1, p. 1007.

Lowrey, P. A., and Reynolds, W. C. (1987) Stanford University Report No. TF-26.

Masutani, S. M., and Bowman, C. T. (1987) *Journal of Fluid Mechanics*, Vol. 172, p. 93.

McMurtry, P. A., and Givi, P. (1988) "Direct Numerical Simulations of a Non-Premixed Homogeneous Turbulent Flow," Submitted for Publication in *Combustion and Flame.*

Patera, A. T. (1984) *Journal of Computational Physics*, Vol. 54, p. 468.

Peters, N., and Williams, F. A. (1983) *AIAA Journal*, Vol. 21, p. 423.

Pope, S. B. (1981) *Combustion Science and Technology*, Vol. 25, p. 159.

Pope, W. B. (1982) *Combustion Science and Technology*, Vol. 28, p. 131.

Roache, P. J. (1972) *Computational Fluid Mechanics*, Hermosa Publishing Company, Albuquerque, New Mexico.

Toor, H. L. (1962) *AIChE Journal*, Vol. 8, p. 70.

Toor, H. L. (1969) *Eng. Chem. Fund.*, Vol. 8, p. 655.

Toor, H. L. (1975) in *Turbulence in Mixing Operation*, Academic Press, New York, NY.

Williams, F. A. (1987) presented at the U.S.-France workshop on Turbulent Reacting Flows, Rouen, France.

PUBLICATIONS

The following publications have resulted from our efforts during the three-year period of this research:

1. P. Givi, W.-H. Jou and R. W. Metcalfe, "Flame Extinction in a Temporally Developing Mixing Layer," Proceedings of 21st Symposium (International) on Combustion, The Combustion Institute, Pittsburgh, PA, to appear, 1987.
2. P. Givi and W.-H. Jou, "Mixing and Chemical Reactions in a Spatially Developing Mixing Layer," accepted for publication in *Journal of Non-Equilibrium Thermodynamics*, 1988.
3. P. Givi and P. A. McMurtry, "Direct Numerical Simulations of the PDF's of a Passive Scalar in a Forced Mixing Layer," *Combustion Science and Technology*, Vol. 57, 4-6, pp. 141-147, 1988.
4. P. Givi and P. A. McMurtry, "Non-Premixed Reaction in Homogeneous Turbulence: Direct Numerical Simulations," accepted for publication in *AIChE Journal*, 1988.
5. P. Givi and W.-H. Jou, "Direct Numerical Simulations of a Reacting, Spatially Developing Mixing Layer by a Spectral-Element Method," Submitted for presentation at the Twenty-Second Symposium (International) on Combustion.
6. P.A. McMurtry and P. Givi, "Direct Numerical Simulations of a Non-Premixed Homogeneous Turbulent Flow," Submitted for publication in *Combustion and Flame*, 1988.
7. W.-H. Jou and J. J. Riley, "Direct Numerical Simulations of Turbulent Reacting Flows," Submitted for publication in *AIAA Journal*, 1988.

CONFERENCE PAPERS

The following conference papers were also results of this work:

1. P. Givi and W.-H. Jou, "Mixing and Chemical Reactions in a Spatially Developing Mixing Layer," Spring Technical Meeting of the Combustion Institute, Central States Section, NASA Lewis Research Center, Cleveland, Ohio, May 5-6, 1986.
2. P. A. McMurtry and P. Givi, "Direct Numerical Simulation of Scalar Dissipation in a Turbulent Mixing Layer," *SIAM Conference on Numerical Combustion*, p. A23, Paper No. 77, San Francisco, California, March 9-11, 1987.
3. P. A. McMurtry and P. Givi, "Non-Premixed Reaction A + B = Products in Homogeneous Turbulent Flows: Direct Numerical Simulations," *Chemical and Physical Processes in Combustion*, pp. 84.1-84.4, 20th Fall Technical Meeting of the Combustion Institute, Eastern States Section, Gaithersburg, Maryland, November 2-6, 1987.
4. P. Givi and P. A. McMurtry, "Numerical Experiments on Mixing and Chemical Reactions in a Homogeneous Turbulent Flow," *Bulletin of the American Physical Society*, Vol.

32, Number 10, p. 2033, 40th Anniversary Meeting of the Division of Fluid Dynamics, Eugene, Oregon, November 22-24, 1987.

5. P. Givi, "Red + White = Pink in Homogeneous Turbulence," 5th Annual Iroquois Fluids Conference, Casowasco Conference Center, Lake Owasco, New York, March 25-27, 1988.

INTERACTIONS

In addition to the above-mentioned papers, parts of this work were presented at the following seminars:

1. P. Givi, "Direct Numerical Simulation of an Unpremixed Turbulent Jet Flame," AFOSR-ONR Contractors meeting on Turbulent Combustion, California Institute of Technology, Pasadena, California, July 23, 1985.
2. P. Givi, "Direct Numerical Simulations of a Reacting Mixing Layer: Bringing Fluid Mechanics Back to Turbulence Research," Invited Seminar, Spring Seminar Series, Department of Mechanical and Aerospace Engineering, State University of New York, Buffalo, New York, March 20, 1986.
3. W.-H. Jou, "Numerical Simulations of Chemically Reacting Flows," Invited Presentation, JANNAF Workshop on Coherent Structures in Turbulent Flows, October, 1985.
4. P. Givi, "Fundamental Studies on Turbulent Combustion and Spray Combustion," Invited Seminar, Institute for Computational Mechanics in Propulsion, NASA Lewis Research Center, Cleveland, Ohio, September 10, 1986.
5. P. Givi, "Bringing Fluid Mechanics into Turbulence Research," Invited Seminar, Fall Colloquium, Department of Aerospace and Mechanical Engineering, University of Notre Dame, Notre Dame, Indiana, September 24, 1986.
6. P. Givi, "Direct Numerical Simulations of Turbulent Diffusion Jet Flames," Invited Seminar, Fall Seminar Series, Department of Mechanical and Aerospace Engineering, Case-Western Reserve University, Cleveland, Ohio, September 26, 1986.
7. P. Givi, "Model Free Simulations of Turbulent Diffusion Flames," Invited Seminar, Graduate Seminar Series, Winter Quarter, Department of Mechanical Engineering, University of Washington, Seattle, Washington, February 3, 1987.
8. P. Givi, "Pseudospectral and Random Vortex Calculations of Diffusion Flames," Department of Mechanical Engineering, The Ohio State University, Columbus, Ohio, March 2, 1987.
9. P. Givi, "Pseudospectral and Random Vortex Calculations of Heat, Mass and Momentum Transport in Diffusion Flames," Department of Mechanical and Aerospace Engineering, State University of New York, Buffalo, New York, April 13, 1987.

10. P. Givi, "Pseudospectral and Random Vortex Calculations of Diffusion Flames," Department of Aerospace Engineering and Engineering Mechanics, University of Cincinnati, Cincinnati, Ohio, May 4, 1987.

11. P. Givi, "Direct Numerical Simulations of an Unpremixed Turbulent Jet Flame," AFOSR-ONR Contractors Meeting on Combustion and Rocket Propulsion, Pennsylvania State University, University Park, Pennsylvania, June 24, 1987.

12. P. Givi, "The Role of Supercomputers on Fluid Mechanics and Combustion Research: Spectral and Lagrangian Simulations of a Reacting Shear Layer," Invited Seminar, Spring Semester, Center for Nonlinear Science & Mathematical Computation, Department of Mathematics, New Jersey Institute of Technology, Newark, New Jersey, February 26, 1988.

13. P. Givi, "State-of-the-Art Computational Methods in Turbulent Combustion: Spectral-Element, Lagrangian, and Pseudospectral Simulations of a Reacting Shear Layer," Invited Seminar, Department of Mechanical Engineering and Laboratory for Planetary Atmosphere Research, State University of New York at Stony Brook, Stony Brook, New York, April 1, 1988.

14. W. Jou, "Direct Numerical Simulations of Chemically Reacting Flows," Lean Blow-out Workshop, Wright-Patterson Aeronautical Laboratory, March 15, 1988.

LIST OF PERSONNEL

The following professional personnel were involved in the three-year effort documented in this report:

1. Dr. Peyman Givi: Dr. Givi, a research scientist, obtained his Ph.D. degree in 1984 from Carnegie-Mellon University. He was recruited by Flow Research in 1985 to perform the present research and was the major contributor in terms of both numerical methods and the interpretation of the simulation results. Dr. Givi is now an assistant professor in the Department of Aerospace Engineering at the State University of New York at Buffalo.

2. Dr. Wen-Huei Jou: Dr. Jou is a senior research scientist. He obtained his Ph.D. degree in Aeronautical Sciences from Princeton University in 1970. He joined Flow Research in 1977 and is currently the Vice President and General Manager of the Applied Mechanics Division.

3. Dr. Patrick McMurtry: Dr. McMurtry obtained his Ph.D. degree from the University of Washington in 1987. His doctoral dissertation on direct numerical simulations of chemically reacting flows was completed at Flow Research. He is currently a research associate at Sandia National Laboratory in Livermore, California.

4. Dr. Ralph W. Metcalfe: Dr. Metcalfe received his Ph.D. in mathematics from Massachusetts Institute of Technology in 1973 and joined Flow Research in the same year. He participated in many numerical simulation studies at Flow. Dr. Metcalfe is currently a professor at the Department of Mechanical Engineering at the University of Houston.

APPENDIX I

Flame Extinction in a Temporally Developing Mixing Layer

FLAME EXTINCTION IN A TEMPORALLY DEVELOPING MIXING LAYER

by

P. GIVI, W.-H. JOU and R. W. METCALFE

Flow Research Company

21414-68th Avenue South

Kent, Washington 98032

May 1986

Manuscript Submitted for Publication in the Proceedings of the

TWENTY-FIRST SYMPOSIUM (INTERNATIONAL) ON COMBUSTION

Subject Matter

10, 11

FLAME EXTINCTION IN A TEMPORALLY DEVELOPING MIXING LAYER

P. GIVI, W.-H. JOU and R. W. METCALFE

Abstract

Nonequilibrium effects leading to the local quenching of a diffusion flame have been investigated by examining the evolution of large-scale structures in a two-dimensional temporally developing mixing layer. Pseudospectral calculations of a temperature-dependent, nonpremixed, constant-density, reacting shear layer indicate that the primary important parameter to be considered for flame extinction is the local instantaneous scalar dissipation rate, conditioned at the scalar stoichiometric value (X_{st}). At locations where this value is increased beyond a critical value (X_q), the local temperature decreases and the instantaneous reaction rate drops to zero. This is consistent with the results of perturbation methods employing large activation energy asymptotics for the study of flame extinction in nonpremixed flames.

1. Introduction

A diffusion flame is characterized by a chemical reaction time that is usually much smaller than a characteristic diffusion time. The chemical reactions occur in a narrow zone between the fuel and the oxidizer, where the concentrations of both reactants are very small. The rate at which the reactants flow into the reaction zone, and therefore the characteristic time of the flame, is dependent on the hydrodynamics of the particular flow. As the characteristic time of the chemical reactions decreases, this reaction region becomes infinitesimally thin. In this limit the chemical reaction zone approaches a "flame sheet" (local chemical equilibrium[1]), where the concentrations of both reactants are very low and the rate of combustion is governed by the rate at which fuel and oxidizer flow into the reaction zone. The flame sheet assumption is justified by the very fast chemical reaction rate of the diffusion flame. This assumption significantly reduces the complexity of the problem since it eliminates the analysis associated with the chemical kinetics. For many flows whose characteristic time scale of chemical reaction is much smaller than the hydrodynamic (convective-diffusive) time scale, the assumption of local chemical

equilibrium adequately predicts the location and the shape of the flame.[2] One important feature of the calculations based on the fast chemistry model is the introduction of a passive Shvab-Zeldovich[2] conserved scalar variable (Z), which is independent of the chemical kinetics. From this quantity, the evolution of the concentration fields of both the reactants and the products can be computed.

In turbulent flows, however, the local characteristic flow time scales vary considerably. As a result, many important and interesting problems that cannot be analyzed by local chemical equilibrium assumptions are introduced. Experimental studies of Tsuji[3] show that as the local characteristic diffusion time becomes shorter and approaches the order of magnitude of the chemical time scale, the details of the chemical reactions cannot be neglected. If the flow of reactants into the reaction zone increases further, causing the diffusion time scale to be reduced more, the chemical reaction will not be able to keep pace with the further supply of reactants. The reaction rate will be reduced, and local quenching occurs. As shown by Peters,[4] further reduction of the diffusion time scale leads to lift-off and the blow-off of the entire flame. As noted by both Tsuji and Peters, the consideration of flame extinction cannot be explained by the flame sheet model, which assumes an infinitely fast chemical reaction rate. Therefore, in order to address the quenching phenomenon, the structure of a finite reaction rate zone must be studied.

Linan[5] has employed a method of matched asymptotic expansions in the limit of large activation energy in an attempt to describe the interaction between the hydrodynamics and chemical reactions in the reaction zone of a counterflowing laminar diffusion flame. It has been shown that activation energy asymptotics are very useful in predicting flame ignition and extinction characteristics in such flows. This technique was extended to turbulent flows

by Peters[4,6] by considering turbulent diffusion flames as an ensemble of laminar diffusion flamelets.[7] By introducing a local coordinate system that moves with the stoichiometric flame sheet, Peters[4] was able to recognize that the primary "nonequilibrium" parameter for the analysis of the flame extinction is the dissipation rate of the scalar quantity evaluated at stoichiometric conditions (X_{st}). This quantity is viewed as the inverse of the diffusion time scale. If this parameter is increased beyond a critical limit (X_q), the heat conducted to both sides of the diffusion flamelets cannot be balanced by the heat production due to chemical reaction. At the critical value of the dissipation, the finite rate kinetics balance the diffusion.[3] Some numerical calculations, performed by Liew et al.[8] and compared with experimental data,[9] show also that as the maximum value of the dissipation (X_{max}) increases, the value of the maximum temperature decreases, the reaction eventually ceases, and the flame is locally quenched.

These results indicate that the dissipation rate of the conserved scalar is a useful characteristic to study in the analysis of nonequilibrium effects leading to flame extinction. In turbulent flows, however, the quantity X_{st} is a strongly fluctuating quantity that has not yet been numerically computed. Instead, statistical approaches have been chosen by Peters and Williams[10] and Janicka and Peters[11] employing different turbulence closures in predicting the lift-off height of a round diffusion jet flame. Results obtained using these methods were compared with experimental data[12] for both methane and natural gas flames and show some correct order-of-magnitude predictions. These results are encouraging; however, with the availability of larger computers, it is now possible to employ a more accurate treatment of the flame extinction and local flame quenching that occur in nonpremixed flames. It would be very useful to correlate the flame extinction with the nonequilibrium parameter X_{st}.

Also, it would be very interesting to look at the structure of the diffusion flames at the point of extinction. These are the objectives of this paper.

The present paper employs a direct numerical simulation approach to investigate the problem of local flame extinction in a time-dependent, two-dimensional mixing layer. In this flow, the governing equations are solved by an accurate numerical method without a closure model. The time-dependent flow field can be analyzed statistically to understand the underlying physics much as an experimentalist does with laboratory data. The direct numerical simulation technique has recently been successfully applied to chemically reacting flows. Riley et al.[13] considered the three-dimensional temporally growing mixing layer under the simplest possible assumption of a constant rate, non-heat-releasing chemical reaction. The main contribution of the work is the understanding of the effects of three-dimensional mixing and the diffusion of the species on the chemical reactions. McMurtry et al.[14] considered the effects of the chemical heat release and the resulting density variation on the fluid motion for a two-dimensional mixing layer. The fluid dynamics and the chemical reaction are truly coupled in this work, and the interplay between the two are discussed. However, the assumption of a constant chemical reaction rate is still employed. In the present work, we intend to understand the flame extinction problem through a two-dimensional simulation of a mixing layer. In particular, the role of large-scale features of the turbulent flow in flame extinction is studied. Due to limitations of numerical accuracy, only moderate Reynolds and Damkohler numbers are computed. For flame extinction in a three-dimensional turbulent flow, three-dimensional simulations will be performed in the future.

2. Problem Formulation

For simplicity of numerical calculations, we consider a two-dimensional shear layer as shown in Fig. 1. The flow is considered periodic in the horizontal direction (x). Although the splitter plate flow evolves spatially downstream and the numerical simulations evolve temporally, important similarities in the dynamics of these two flows make it useful to study accurate numerical simulations of the temporally growing mixing layers. By simple Galilean transformation, a flow quantity averaged in the x-direction can be related to the time average of the same quantity at a fixed location in a splitter plate configuration.[13,14] These average quantities are dependent on the transverse coordinate (y) and the time (t). Again, the inverse Galilean transformation relates the time t to the streamwise location in a splitter configuration. The presence of periodic boundary conditions allows us to use accurate pseudospectral numerical methods; these methods are discussed in Ref. 13 and will not be repeated here.

The chemical reaction between the two species is assumed to be single-step and irreversible and to obey the temperature-dependent Arrhenius law. It is assumed that the heat release rate is low so that the effects of the chemical heat release on the flow field can be neglected. This, together with the further assumptions of a low Mach number flow, result in a constant-density flow formulation.

To identify the nondimensional groupings, the variables are normalized by a velocity scale (mean velocity difference across the layer ΔU), a temperature scale (free-stream T_∞), concentration scales (free-stream $C_{A\infty}$ and $C_{B\infty}$), and a length scale ($\lambda = 2.249\,\sigma$, where σ is the distance from the plane of symmetry to the transverse plane, where the mean velocity rises to half of its freestream value). The value of 2.249 was chosen so that the size of the computational

domain would be equal to the wavelength of the most unstable mode and its normalized value would be an integer multiple of 2π.

$$\underline{x}^* = \frac{\underline{x}}{\lambda} \qquad \nabla^* = \lambda \nabla$$

$$\underline{U}^* = \frac{\underline{U}}{\Delta U} \qquad t^* = t\,\frac{\Delta U}{\lambda}$$

$$P^* = \frac{P}{(\Delta U)^2} \qquad T^* = \frac{T}{T_\infty} \tag{1}$$

$$C_A^* = \frac{C_A}{(C_A)_\infty} \qquad C_B^* = \frac{C_B}{(C_B)_\infty}$$

Assuming equal free-stream concentrations, i.e., $C_{A\infty} = C_{B\infty}$, the nondimensionalized equations are

$$\nabla \cdot \underline{U}^* = 0$$

$$L^*(\underline{U}^*, \mathrm{Re}) = \frac{\partial \underline{U}^*}{\partial t} + \underline{U}^* \cdot \nabla \underline{U}^* - \frac{1}{\mathrm{Re}} \nabla^{*2}\, \underline{U}^* = -\nabla P^*$$

$$L^*(C_A^*, \mathrm{Re\ Sc}) = L^*(C_B^*, \mathrm{Re\ Sc}) = -W^* \tag{2}$$

$$L^*(C_P^*, \mathrm{Re\ Sc}) = W^*$$

$$L^*(T^*, \mathrm{Re\ Pr}) = \mathrm{Ce}\, W^*$$

where

$$W^* = \mathrm{Da}\, e^{-\mathrm{Ze}/T^*} C_A^* C_B^*$$

$$\mathrm{Da} = \frac{A_f C_{A\infty}}{\frac{\Delta U}{\lambda}} = \text{Damkohler number}$$

$$\mathrm{Ze} = \frac{E}{RT_\infty} = \text{Zeldovich number}$$

$$\mathrm{Re} = \frac{\Delta U \lambda}{\nu} = \text{Reynolds number} \tag{3}$$

$$\mathrm{Ce} = \frac{Q}{C_v T_\infty} = \text{Heat release parameter}$$

$$\mathrm{Sc} = \frac{\nu}{D} = \text{Schmidt number}$$

$$\mathrm{Pr} = \frac{K}{D} = \text{Prandtl number}$$

The values of Sc and Pr can be set equal to unity, since this is approximately correct for gaseous diffusion flames. This results in a Lewis number of unity. The value of other nondimensional parameters is limited by the available resolution of the numerics employed in the computations.

Shvab-Zeldovich Variable

For the two-feed diffusion flame considered here, it is possible to consider only three scalar quantities rather than solving for all four scalar variables. The Shvab-Zeldovich variable (Z) and the product concentrations (G), following Givi et al.,[15] are defined as

$$\begin{aligned} Z &= C_A^* + C_P^* \\ G &= C_P^* \end{aligned} \tag{4}$$

The transport equations governing Z, G, and T^* follow:

$$\begin{aligned} L^*(Z) &= 0 \\ L^*(G) &= Da\, e^{-Ze/T^*} (1 - Z - G)\,(Z - G) \\ L^*(T^*) &= Ce\, Da\, e^{-Ze/T^*} (1 - Z - G)\,(Z - G) \end{aligned} \tag{5}$$

Initial and Boundary Conditions

The initial and boundary conditions for the velocity field are given elsewhere[16] and are only summarized here. In terms of the stream function, the initial condition is given by

$$\psi = \psi_{mean} + \psi_f + \psi_{sh} \tag{6}$$

where ψ_{mean} is the stream function associated with a mean hyperbolic tangent velocity profile, ψ_f is the stream function for the most unstable mode of this

mean velocity profile, and ψ_{sh} is the stream function for the first subharmonic of the most unstable mode. The properties of these modes have been evaluated from linear stability theory.[17] The fundamental mode in this mixing layer produces a single vortex rollup, and when the subharmonic is added in, a second rollup, or pairing, can occur.[16] In the computations reported in this paper, we have employed two initial conditions for the hydrodynamics: (1) the mean flow and the fundamental mode alone (Case I), and (2) the mean flow, the fundamental mode, and the first subharmonic mode added together in phase (Case II). In this manner, the effects that the vortex rollup have on the chemical reaction can be examined.

The initial conditions for the reactant concentration are given by

$$C_A^*(x^*, y^*, 0) = \frac{1}{y_o^* \sqrt{\pi}} \int_{-\infty}^{y_o^*} \exp\left(-\frac{\xi^2}{y_o^2}\right) d\xi$$

$$C_B^*(x^*, y^*, 0) = 1 - C_A^* \qquad (7)$$

$$C_P^*(x^*, y^*, 0) = 0$$

Note that there are no initial fluctuations in the scalar profiles.

The temperature in the free stream is equal to T_∞. Near $y = 0$, this value is increased to an ignition temperature to allow the chemical reactions to occur. The initial profile for T^* is given by an exponential function.

$$T^*(x^*, y^*, 0) = 1 + 4 \exp\left(-4 y^{*2}\right) \qquad (8)$$

A periodic boundary condition is employed in the streamwise direction, and a free-slip boundary condition in the cross-stream direction. These boundary conditions are natural when Fourier series expansions are used.

3. Presentation of Results

A pseudospectral numerical code was developed for the calculations of the incompressible reacting flow considered here. Computations were performed in a square domain with the size $0 < x < 2\pi\lambda$, $-\pi\lambda < y < \pi\lambda$ for the single vortex rollup and the domain $0 < x < 4\pi\lambda$, $-2\pi\lambda < y < 2\pi\lambda$ for the double rollup computations. The spatial resolution was 64x64 Fourier modes. The values of the Reynolds and Damkohler numbers were set equal to 200 and 10, respectively, so that the simulation would be accurately resolved on the 64x64-point grid employed here. The value of the Zeldovich number was set equal to 20. The value of the heat release parameter was selected to be small enough so that, when multiplied by the Damkohler number, it would be resolvable by the numerics and so that it would also be reasonable to neglect the effects of heat release on the flow field. However, this value should be large enough to allow the effects of temperature dependence on the chemical reaction term. A value of $Ce = 8$ is satisfactory, giving a maximum (adiabatic) temperature of $T^*_{adiabatic} = 7$.

The profiles of the conserved Shvab-Zeldovich scalar variable are chosen for the purpose of flow visualization. In Figs. 2 and 3, we present the time sequence development of this profile for Cases I and II, respectively. Initially, the perturbation associated with the fundamental mode grows until a time of $t^* = 9$, where the first vortex rollup occurs. Proceeding further in time results in diffusion of the core of the vortex with no additional rollup. Adding the subharmonic associated with this unstable mode results in a second rollup (Fig. 3) that initiates at a time of about $t^* = 12$ and is completed by $t^* = 24$. As shown in these figures, the effect of the vortex dynamics is to increase the strain rate at the braids between the vortex cores.

If a fast chemistry model was assumed to describe the chemical reactions, the surface of $Z = Z_{st} = 0.5$ would correspond to the flame location. The vortex dynamics plays an important role in increasing the area of the flame surface (Z_{st} surface) and in increasing the total amount of reaction product compared to the case where there is no rollup and the chemical reaction is only limited to the interdiffusion of the scalars at the reaction surface. In the present calculations, the increase of the equilibrium flame sheet surface due to rollup (Case I, Fig. 2b) is 153 percent in comparison with the unforced case. Merging of the vortices (Case II, Fig. 3b) increases this surface by 340 percent when compared with the unforced case.

The time sequence of the temperature is shown on Figs. 4 and 5 for Cases I and II, respectively. The mechanism of vortex rollup is to draw the reactants from the two streams to the reaction surface. The maximum temperature along the $Z = Z_{st}$ surface occurs at the core of the vortex (the hottest location), where vorticity and the product concentration are also highest, and decreases in the braids, where the gradients of the scalar are at their higher values. At the time when the computation is stopped, the maximum product concentration has not yet reached its equilibrium value. There still remain reactants, even at the core of the mixing layer, and the flame shortening phenomenon, which is usually caused by the depletion of the reactants, has not been yet observed.

The reason for this behavior of the chemical product and temperature can be explained by the contour plots of the instantaneous reaction rate W, presented in Fig. 6 for Case I. As shown in this figure, the reaction rate initially is very uniform along the species interdiffusion zone and is maximized at the reaction surface, where the reactants are in contact. At later times, the reaction rate decreases, and at points where the strain rate is sufficiently

large, the reaction rate goes to zero and the flame locally quenches. This mechanism of extinction of the diffusion flame is consistent with the experimental observations of Tsuji.[3] In the braids, as the inverse of the diffusion time scale ($1/X_{st}$) decreases (as the result of the vortex rollup), the supply of the reactants is greater than the chemical reaction can utilize. Notice from Figs. 2 through 5 that the reactants are well mixed on the braids, but the reaction rates at these places are zero. This nonequilibrium phenomenon can be explained by examining the reaction rate equation [Eq. (3)].

Unlike the temperature-independent reacting mixing layer calculation reported by Givi et al.,[18] the maximum value of the reaction rate does not necessarily correspond to the maximum value of the product of the reactants concentration, since the effects of the temperature variations influence the local conversion rate of the chemistry. If the flame temperature goes below a critical characteristic temperature, the flame becomes very rich with both reactants. However, since the value of the dissipation rate is greater than the critical value, this premixed region of the reactants cannot be reignited from the high temperature zone of the core. A higher dissipation rate results in a further decrease in temperature until it becomes equal to the background temperature. At this point, the vortex has reached the boundary of the computational domain and, therefore, further computation is not realistic.

A direct quantitative comparison of X_q, obtained in our numerical simulations (X_q is approximated here as the value of the critical instantaneous dissipation rate evaluated at the stoichiometric surface Z_{st}) with that obtained under the large activation energy asymptotics is not expected to agree exactly for several reasons. First, in asymptotic analysis, the flame thickness is very small and is only broadened near the reaction zone by a small parameter.

In the direct numerical simulations reported here, the reactants have a fairly "thick" overlap region in the reaction zone due to the numerical accuracy limitations. Furthermore, the initial conditions for the temperature profile employed here near the reaction zone are not the same as the uniform initial temperature distributions of Peters.[4] However, making the assumption that the initial concentration of the reactant and the temperature of the reactants are at some average values in the range between the free stream and the reaction zone, correct order-of-magnitude asymptotic results are verified by the results of the simulations. The temperature profiles presented in Fig. 4 show that by a time of $t^* = 15$, the value of the temperature at the braids falls to about one-fifth the flame temperature (approximately equal to the free-stream temperature). This corresponds to local quenching. The corresponding computed normalized dissipation rate X^*_{st} ($X^*_{st} = X_{st}\lambda/\Delta U$) at the point of quenching, for the given kinetics data, is about 7 for both Cases I and II. The estimated corresponding value for the dissipation rate, computed with the asymptotic methods described above, is about 8, which is in good agreement with the results of the numerical simulation.

4. Conclusions

A pseudospectral algorithm has been used for the numerical calculations of a constant-density, chemically reacting, temperature-dependent mixing layer. The nonequilibrium effects leading to the local flame quenching have been simulated in a case with fairly large Zeldovich number and moderate Reynolds and Damkohler numbers. It has been found that the rollup of an unstable shear layer creates regions with high dissipation rates at the braids, where local flame extinction occurs according to the theory of Peters[4,10]. The temperature

contour shows that the temperature drops to a value close to ambient at the braids and the reaction rate reduces to zero, even though the reactants are well mixed there. Within the limitations of numerical resolution, comparison of the critical scalar dissipation rate with that obtained by large activation energy asymptotics shows reasonable agreement. We are presently expanding this work to investigate a spatially developing mixing layer and three-dimensional turbulent flows. This should further illuminate the basic mechanisms of such phenomena as the diffusion jet flame lift-off.

Nomenclature

A_f	Preexponential factor
C	Concentration
C_v	Specific heat
Ce	Heat release parameter
D	Molecular diffusivity
Da	Damkohler number
E	Activation energy
G	Normalized product concentration
K	Thermal conductivity
L	Convective-diffusive operator
P	Pressure
Pr	Prandtl number
Q	Heat of reaction
R	Universal gas constant
Re	Reynolds number
Sc	Schmidt number
T	Temperature
t	Time
U	Streamwise velocity component
V	Cross-stream velocity component
W	Reaction rate
X	Dissipation
x	Streamwise coordinate
y	Cross-stream coordinate
Z	Shvab-Zeldovich variable
Ze	Zeldovich number

Greek

λ	Length scale
ν	Molecular viscosity
ψ	Stream function

Superscript

*	Non-dimensionalized

Subscript

A,B	Reactants
f	Fundamental
P	Product
q	Quenching
sh	Subharmonic
st	Stoichiometric
∞	Free stream

Acknowledgments

The calculations reported here were performed under research sponsored by the Air Force Office of Scientific Research under Contract F49620-85-C-00067. The United States Government is authorized to reproduce and distribute reprints for governmental purposes notwithstanding any copyright notation hereon. The authors have also appreciated the support of NASA Lewis Research Center in providing computer time.

References:

1. Bilger, R. W.: Turbulent Reacting Flows (P. A. Libby and F. A. Williams, Eds.), p. 65, Springer-Verlag, 1980.
2. Williams, F. A.: Combustion Theory, Second edition, The Benjamin/Cummings Publishing Company, Inc., 1985.
3. Tsuji, H.: Prog. Energy Comb. Sci. 8, 93 (1982).
4. Peters, N.: Comb. Sci. Tech. 30, 1 (1983).
5. Linan, A.: Acta Astronautica 1, 1007 (1974).
6. Peters, N.: Prog. Energy Comb. Sci. 10, 319 (1984).
7. Williams, F. A.: Turbulent Mixing in Non-Reactive and Reactive Flows (S. N. B. Murthy, Ed.), p. 189, Plenum Press, 1975.
8. Liew, S. K., Moss, J. B. and Bray, K. N. C.: Dynamics of Flames and Reactive Systems (J. R. Bowen, N. Manson, A. K. Oppenheime and R. I. Sdoukhin, Eds.), Progress in Astronautics and Aeronautics, Vol. 95, p. 305 (1984).
9. Mitchell, R., Sarofin, A. and Clomburg, L.: Comb. and Flame 37, 337 (1980).
10. Peters, N. and Williams, F. A.: AIAA J. 21, 423 (1983).
11. Janicka, J. and Peters, N.: Nineteenth Symposium (International) on Combustion, p. 367, The Combustion Institute, 1982.
12. Donnerhack, S. and Peters, N.: Comb. Sci. Tech. 41, 101 (1984).
13. Riley, J. J., Metcalfe, R. W. and Orszag, S. A.: Phys. Fluids 29, 406 (1986).
14. McMurtry, P. A., Jou, W.-H., Riley, J. J. and Metcalfe, R. W., AIAA Paper 85-0143, 1985.
15. Givi, P., Sirignano, W. A. and Pope, S. B.: Comb. Sci. Tech. 37, 59 (1984).

16. Kiley, J. J. and Metcalfe, R. W., AIAA Paper 80-0274, 1980.

17. Michalke, A.: J. Fluid Mech. 19, 543 (1964).

18. Givi, P., Ramos, J. I. and Sirignano, W. A.: J. Non-Equilibrium Thermodynamics 10, 75 (1985).

Figure Captions

FIG 1. Problem geometry.

FIG 2. Plots of Shvab-Zeldovich variable contours (Case I). (a) $t^* = 9$, contour minimum is 0, contour maximum is 1, contour interval is 0.1. (b) $t^* = 15$, contour minimum is 0, contour maximum is 1, contour interval is 0.1.

FIG 3. Plots of Shvab-Zeldovich variable contours (Case II). (a) $t^* = 12$, contour minimum is 0, contour maximum is 1, contour interval is 0.1. (b) $t^* = 24$, contour minimum is 0, contour maximum is 1, contour interval is 0.1.

FIG 4. Plots of normalized temperature contours (Case I). (a) $t^* = 9$, contour minimum is 0, contour maximum is 6, contour interval is 0.6. (b) $t^* = 15$, contour minimum is 0, contour maximum is 6, contour interval is 0.6.

FIG 5. Plots of normalized temperature contours (Case II). (a) $t^* = 12$, contour minimum is 0, contour maximum is 6, contour interval is 0.6. (b) $t^* = 24$, contour minimum is 0, contour maximum is 6.6, contour interval is 0.6.

FIG 6. Plots of normalized reaction rate contours (Case I). (a) $t^* = 6$, contour minimum is 0, contour maximum is 0.03, contour interval is 0.003. (b) $t^* = 9$, contour minimum is 0, contour maximum is 0.024, contour interval is 0.002. (c) $t^* = 12$, contour minimum is 0, contour maximum is 0.02, contour interval is 0.002. (d) $t^* = 24$, contour minimum is 0, contour maximum is 0.017, contour interval is 0.001.

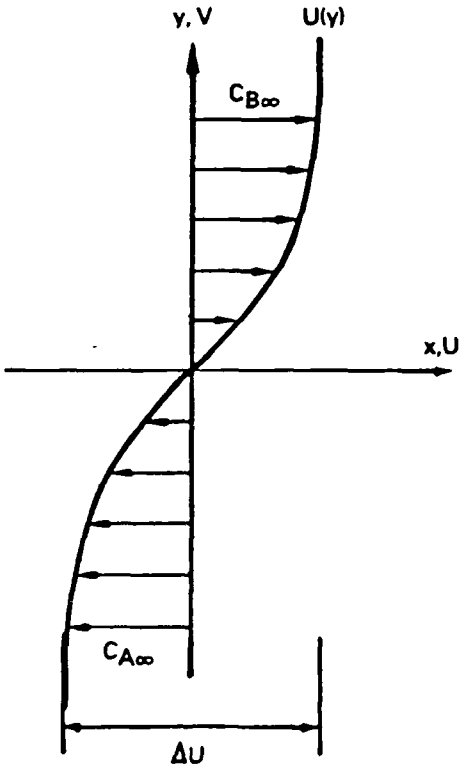

Figure 1

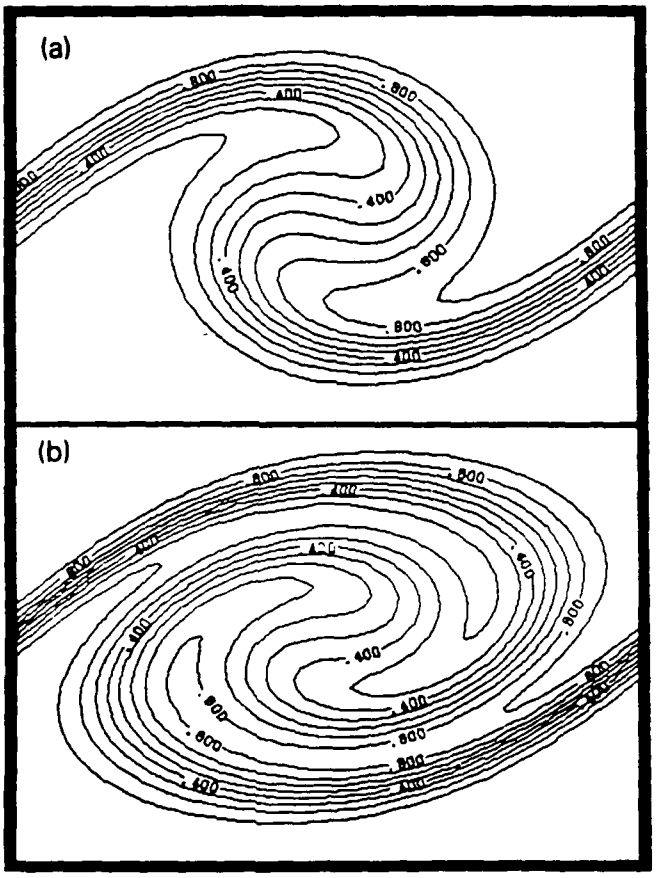
(a)
800
400
800
400
800
400
400
800
400
800
400
(b)
800
400
800
400
400
800
400
800
800
800
400
800
400

Figure 2

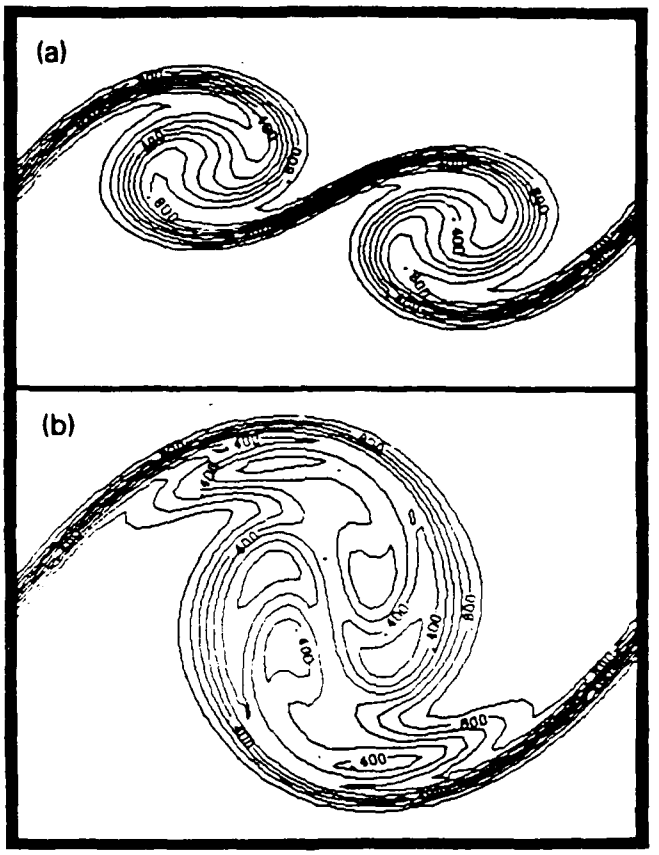

Figure 3

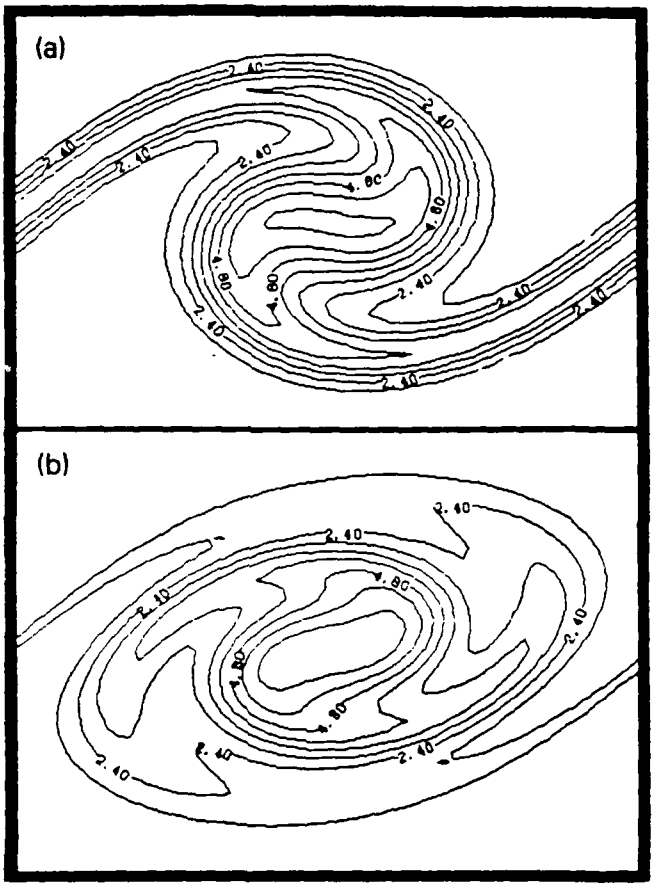
(a)
2.40
2.40
2.40
2.40
2.40
4.80
4.80
4.80
4.80
2.40
2.40
2.40
2.40
(b)
2.40
2.40
2.40
4.80
2.40
4.80
4.80
2.40
2.40
2.40

Figure 4

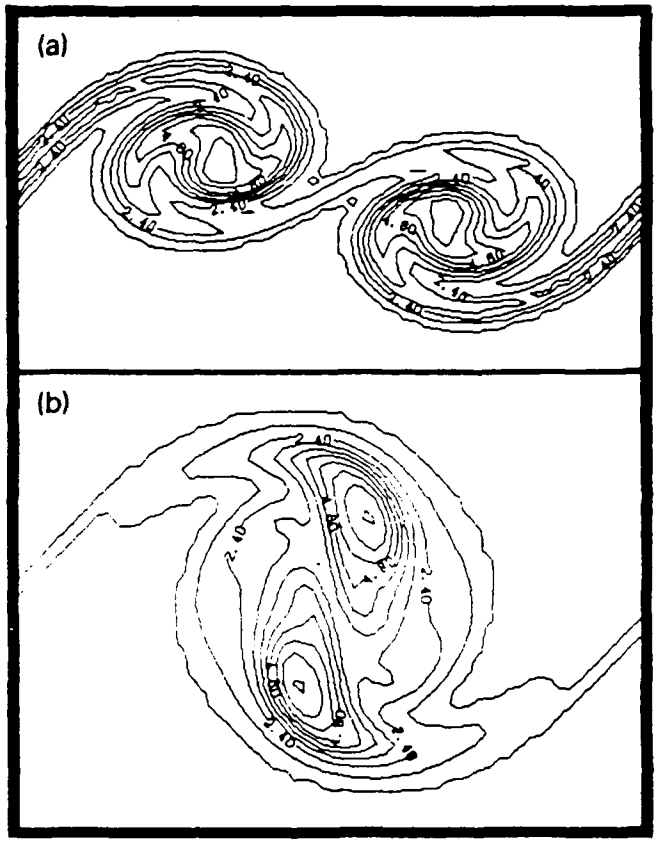

Figure 5

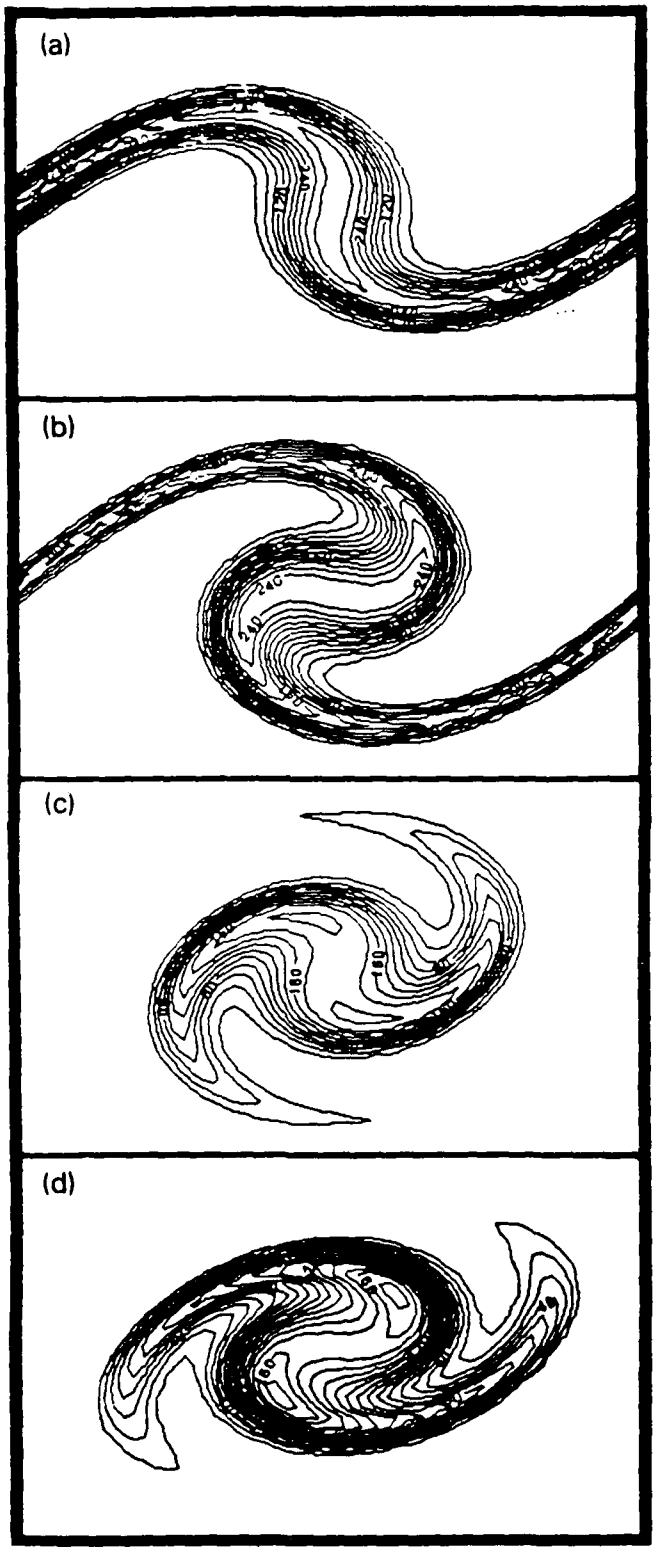

Figure 6

APPENDIX II

Mixing and Chemical Reactions in a Spatially Developing Mixing Layer

MIXING AND CHEMICAL REACTIONS IN A SPATIALLY DEVELOPING MIXING LAYER

by

Dr. P. Givi

Research Scientist
Flow Research Company
21414-68th Avenue South
Kent, Washington 98032
U.S.A.

Dr. W.-H. Jou

Vice President
Applied Mechanics Division
Flow Research Company
21414-68th Avenue South
Kent, Washington 98032
U.S.A.

February 1987

MIXING AND CHEMICAL REACTIONS IN A SPATIALLY DEVELOPING MIXING LAYER

P. Givi and W.-H. Jou

KEY NUMBERS: 32 02 93 3

KEY WORDS: Direct numerical simulations, spatially evolving mixing layers, pseudospectral methods, vortex dynamics

ABSTRACT

Direct numerical simulations have been employed to study the effects of large coherent structures in a perturbed, time-dependent, spatially developing, reacting mixing layer. It is shown that the vortex dynamics has a significant influence on the enhancement of the chemical reactions, convolution of the reaction surface, and increase of product formation in the reaction zone of the layer. Furthermore, examination of some of the statistical quantities obtained from the results of direct numerical simulations indicates the asymmetric nature of the mechanism of mixing processes in the mixing zone of the layer.

INTRODUCTION

The advancement of supercomputer technology in recent years has had a major influence on increasing our understanding of the mechanisms of many complex physical phenomena such as turbulence. The availability of high-speed, large-memory computers has made it possible, in many cases, to simulate turbulent flow problems directly by solving the appropriate basic governing transport equations without any need for additional "turbulence modeling." Such modeling is required when these equations are statistically averaged. In a complex system such as a chemically reacting flow, modeling is extremely difficult because of our lack of knowledge on the detailed dynamics of the flow. Without

using turbulence modeling, direct numerical simulations can provide the detailed information needed to increase our understanding of the physical processes involved in turbulent flows. An increase in understanding various aspects of the physics of turbulent reacting flows is evident in recent works (e.g., Riley et al. [1]).

Direct numerical simulations of turbulent reacting flows are presently applied to flows with limited dynamical and chemical parameter ranges. Continuing efforts in evaluating the advantages and also the limitations of this technique are required before the knowledge acquired can be applied to flows with practical parameter ranges. The application of direct numerical simulations to a flow with simplified geometrical configurations and well-controlled conditions is certainly the first step in understanding the physics and in evaluating the capabilities of the method.

A mixing layer, in which two parallel streams with different velocities begin to mix and react downstream of the trailing edge of a splitter plate partition, presents an ideal configuration for studying the physical processes in the mixing and reaction zones that exist in real diffusion-controlled combustors. Direct numerical simulations have been applied in studying a model problem of such flows with encouraging success [1, 2]. However, most of the previous work has employed a temporally developing mixing layer as a model. Temporally growing mixing layers refer to flows that, in a Galilean-transformed frame of reference, are assumed to evolve in time rather than in space. This is a good approximation for flows in which the difference between the freestream velocities of two streams is much less than the averaged velocity. This approximation allows simplifications in the formulation of periodic boundary conditions. A pseudospectral numerical method using Fourier series can then be employed to solve the appropriate transport equations.

Comparison of the simulation results obtained for a temporally developing mixing layer with experimental results is encouraging. The comparison shows that there is qualitative agreement between numerical simulations and laboratory data for the average reactant concentrations and the concentration correlations. However, there are some basic phenomena that cannot be explained by temporal simulations, such as (1) asymmetric mixing observed in mixing layer experiments [3], and (2) stabilization, quenching, lift-off, and blowout of turbulent jet flames [4]. A fundamental understanding of these phenomena

requires detailed calculations of spatially growing flows. Here, we have developed a numerical technique that is capable of simulating a spatially developing mixing layer as a first step to further develop the technique of direct numerical simulations.

This paper presents some preliminary results of our two-dimensional flow simulations using the resulting code in an attempt to address the first of the above-mentioned phenomena associated with spatially growing flows. The flow fields under consideration are dominated by large-scale fluctuations associated with coherent structures. The chemical reaction that occurs between the reactants on two sides of the layer is assumed to be infinitely fast, so that complications due to complex kinetics need not be considered. Therefore, the transport of a conserved Shvab-Zeldovich scalar variable is computed. There is also a nonparallel growth mechanism of the layer mainly due to diffusion, vortex rollup, and subsequent pairing of the neighboring vortices. The effects of this nonparallel growth as well as the asymmetric mixing in the shear layer are studied. Analysis of flame extinction and lift-off phenomena requires consideration of nonequilibrium chemistry. This, as well as the effects of a three-dimensional random turbulence field, are presently under study and will be reported in the future.

In the next section, the governing equations, boundary conditions, and numerical algorithms for the present problem are discussed. This is followed by the presentation of results and some conclusions.

PROBLEM FORMULATION

The mixing layer under consideration is shown in Figure 1. The reactants are introduced as dilute traces in a carrier passive gas. The chemical heat release is assumed negligible. Therefore, the density of the mixture can be assumed constant and equal to that of the carrier gas. Under these assumptions, the hydrodynamics and the transport of chemical species are decoupled. The latter is governed by passive transport equations with a given hydrodynamic velocity field.

The velocity field satisfies the incompressible Navier-Stokes equations:

$$\rho L(\underline{U}, \nu) = - \nabla P \tag{1}$$

$$\nabla \cdot \underline{U} = 0 \tag{2}$$

where P is the pressure, ρ is the density, which is assumed to be constant, ν is the kinematic viscosity, $\underline{U}$ is the velocity vector and L is the convective-diffusive operator defined by

$$L(\underline{U}, \nu) = \frac{\partial \underline{U}}{\partial t} + \underline{U} \cdot \nabla \underline{U} - \nu \nabla^2 \underline{U} \quad . \tag{3}$$

Species A is injected from the high-speed stream on the upper side of the plate, and species B is introduced from the low-speed stream. The chemical reaction between the species field is assumed to be fast and irreversible, such as

$$A + B \rightarrow C + D \quad . \tag{4}$$

The molar concentrations of the reactants (species A and B) and the product (say, species C) satisfy the following reaction-convection-diffusion equations:

$$L(C_A, D) = L(C_B, D) = - W \tag{5}$$

$$L(C_C, D) = W \tag{6}$$

where W is the reaction rate, and the stoichiometric coefficient is assumed to be equal to 1. The molecular diffusivities, D, of the species are assumed to be equal, i.e., $D_{ij} = D_{ji} = D$. If we define a Shvab-Zeldovich variable by

$$f = C_A + C_C \quad , \tag{7}$$

then the transport equation for f satisfies

$$L(f, D) = 0 \quad . \tag{8}$$

As shown by Williams [5] and Bilger [6], assuming an infinitely fast chemical reaction between species A and B, one would be able to determine the instantaneous fields of all the species involved.

In order to solve the set of Equations (1) through (8), boundary and initial conditions are needed. For the cross-stream direction, we assume the flow to be periodic with free-slip boundary conditions. At the inflow, the initial conditions for the Shvab-Zeldovich variable, f, are given by the following functional form:

$$f(0, Y) = \frac{1}{Y_o \sqrt{\pi}} \int_{-\infty}^{Y_o} \exp - \frac{\varepsilon^2}{Y_o^2} \, d\varepsilon \quad . \tag{9}$$

The initial conditions for the mean streamwise velocity are given by a hyperbolic tangent velocity profile, and the mean cross-stream velocity component is set equal to zero:

$$\underline{U} = [U(Y), 0] \tag{10}$$

$$U(Y) = U_1 [\tanh (2Y/\lambda) + 2] \tag{11}$$

where U_1 is the slow stream velocity, and λ is the vorticity thickness defined by

$$\lambda = \Delta U/(dU/dY)_{max} \quad . \tag{12}$$

The term ΔU is the difference between the velocities in the two layers.

It is well-known that a shear layer subject to white noise will develop coherent structures with predominantly the most unstable mode of its instability waves, and the subsequent pairing is caused by the subharmonic disturbance of the predominant mode. Therefore, in order to initiate the vorticity rollup and pairing, a small perturbation, in the form of the most unstable mode and its subharmonics, calculated from linear stability theory [7, 8] is added to this mean profile. In terms of stream function, we have

$$\psi = \psi_{mean} + \varepsilon_1 \psi_1 + \varepsilon_2 \psi_2 \tag{13}$$

where ψ_{mean} is the stream function associated with the mean flow, ψ_1 is the stream function for the most unstable mode, ψ_2 is that of the first subharmonic of the most unstable mode, and ε_1 and ε_2 are the amplitudes of the imposed perturbations. The presence of the fundamental mode in the mixing layer produces a single vortex rollup, and when the subharmonic perturbation is superimposed, a second rollup in the form of the merging of two vortices occurs [9]. The vortex rollup and pairing have dominant effects on the chemical reactions and the rate of formation of the products.

The downstream boundary is an artificial computational boundary and not a natural flow boundary. The boundary conditions there are difficult to formulate in a rigorous sense. We have assumed a zero-gradient condition on the velocity and species fields. This is not an exact representation of the outflow behavior. However, if the flow velocity is outgoing at the downstream boundary, which is the case here, the vorticity and species transport equations

are hyperbolic when the molecular diffusion is small. Therefore, the upstream influence may be weak. The effects of this outflow boundary condition on the solution are later assessed by comparing results of the simulations for the same flow with various lengths of the computational domain.

The periodicity of the flow in the Y direction enables us to employ a pseudospectral numerical method [10] in that direction. In the streamwise direction, however, an overall second-order finite difference scheme (Leonard, [11]) is employed with applications of a quadratic upwind differencing for the convection term where the leading dispersive truncation error of the second-order central scheme is removed. This scheme is expected to be accurate for the fine grids employed in these calculations. We use the Adams-Bashforth [12] technique for time discretization, which is a second-order-accurate scheme.

The computational domain was selected to be a region bounded by $(0 < X < 32\lambda)$ and $(-8\lambda \leq Y \leq 8\lambda)$. There are 128 equally spaced finite difference grid points in the X direction and 64 Fourier modes in the Y direction. Since the details of the chemistry are neglected and a fast chemistry model has been employed, this computational domain seems to be accurate enough for our solution procedure. The incremental time step was selected to be small enough to ensure both accuracy and stability. The value of Δt^* ($\Delta t^* = \Delta t\ \Delta U/\lambda$) was selected to be 0.0125.

The flow is conveniently characterized by two non-dimensional parameters: first, the Reynolds number, $Re = \Delta U\ \nu/\lambda$, based on the initial shear layer thickness, the mean velocity difference across the layer, and the kinematic viscosity; and second, the velocity ratio, $R = \Delta U/(U_1 + U_2)$. The Shvab-Zeldovich variable is characterized by the value of the Peclet number, $Pe = \Delta U\ D/\lambda$. The differential equations governing the transport of the hydrodynamic variables ($\underline{U}$ and P) and the scalar variable (f) can, in general, be solved for different values of the non-dimensionalized parameters Re and Pe in order to examine the effects of these parameters on the structure of the shear layer. The limited resolution due to required computational time and computer memory, however, imposes a restriction on the maximum value of these parameters in an accurate simulation. The accuracy tests of the pseudospectral method and the finite difference scheme employed in the present calculations have been reported by Riley et al. [1] and Leonard [11]. In accordance with these studies, we have selected moderate values of Reynolds and Peclet numbers and the computations

have been performed in a domain with enough number of grid points to ensure the accuracy. The validity of the results obtained from the simulations is warranted by the lack of spurious "under- or over-shoots" in the calculated values of the hydrochemical variables, as will be shown in the next section.

As discussed by Ho and Huerre [9], the two-dimensional vortex dynamics of the flow is not very sensitive to the Reynolds number, and only the shape of the vortices depends on the value of the Reynolds number employed. Therefore, simulations even at moderate Reynolds numbers provide useful information about the effects of the dynamics of vorticity on chemical reactions.

PRESENTATION OF RESULTS

Effects of Coherent Structures

As discussed in the previous section, a small perturbation at the inflow is required to trigger the initial vortex rollup. The perturbation levels, ϵ_1 and ϵ_2, are both set equal to 0.05. The velocity shear parameter R is equal to 0.5, and the values of the Reynolds and Peclet numbers are set equal to 50.

We present normalized vorticity contour plots at $t^* = 31$ for the case in which the most unstable mode is the only perturbation applied at X = 0. Figure 2 indicates the formation of rolled-up vortices at equal wavelengths. These vortices diffuse along the mixing layer as indicated by the decay of the peak value of the vorticity downstream. The formation of the rolled-up vortices is also evident in the contour plot of the Shvab-Zeldovich variable presented in Figure 3. From these two figures, it is clear that the perturbation at the inlet causes the rollup of the vorticity near the inlet. As the fluid is convected downstream, additional vortices are created at equal wavelengths from each other. The same behavior was also observed in numerical and experimental studies of McInville et al. [13] in their studies of the large coherent structures in a forced shear layer. As the vortices reach the outflow boundary, the zero-gradient condition seems to allow them to travel out of the computational domain. Employment of this weak condition at the outflow may cause some errors near the outflow boundary. Previous numerical experiments by Givi [14], however, show that the regions of the error associated with this condition are concentrated at a small area near the outflow and do not substantially affect the inner region of the computational domain. To assess the validity of this assumption, some computations were performed in two computational domains. The transverse dimensions of these two are identical, while one of the cases has a streamwise domain half the size of the other.

The grid spacing in the streamwise direction is maintained. Comparison of the results clearly showed that the boundary conditions imposed at the outflow boundary do not affect the solution in the interior of the computational domain. Therefore, it seems justified that a zero-gradient boundary condition at the outflow is adequate for our purposes.

The effects of adding the perturbation corresponding to the first subharmonic mode at X = 0 are shown in Figure 4. In this figure, we present the rollup and merging of the vortices at times of $t^* = 31$ and $t^* = 39$. The merging of the vortices caused by the subharmonic perturbation, as computed here, has been observed in experiments of Ho and Huerre [9]. These merged vortices, again, diffuse and smear as they move downstream, and no further merging is observed. The same behavior was also observed in the calculations of Davis and Moore [15]. The vortex merging associated with this subharmonic mode is also clear from the Shvab-Zeldovich variable contour plots shown in Figure 5. Again, the errors associated with the outflow boundary are concentrated only near the outflow and do not seem to affect the interior of the computational domain.

Contour plots of the computed product concentrations of the chemical reaction are presented in Figures 6 and 7. In Figure 6, only the perturbation associated with the most unstable mode is added to the mean flow, and in Figure 7, the perturbations associated with the fundamental frequency and its first subharmonic are added together to the mean flow. The regions of high product concentrations are, as expected, near the flame sheet, where the value of the Shvab-Zeldovich variable is equal to its stoichiometric value ($f = 0.5$). The vortex rollup brings unreacted species together from both streams to the chemical reaction zone. This region is marked by a very steep gradient of the chemical product near the braids of the vortices but is more diffusive in the core of the vortex. The vortex rollup increases the interface between the two streams by stretching the reaction zone and, therefore, increasing the amount of products generated. A comparison of these two figures indicates that the vortex merging results in increased formation of product in the mixing layer.

In these computations, the increase of flame sheet surface due to rollup of vortices is about 97 percent in comparison with unforced and nondiffusive computations, resulting in a 48-percent increase in total integrated products formed in the mixing layer. Merging of the vortices increases the flame sheet surface area by 163 percent and the total amount of products by 69 percent in

comparison with the unforced and nondiffusive case. Bearing in mind the low level of initial disturbance, this high level of response may one day be exploited in a practical device.

Comparison of Figures 6 and 2 and also Figures 7 and 4 shows the similarity between the profiles of the vorticity and the chemical product. Both are high near the reaction zone, gradually diffusing outward with very similar profiles. This is to be expected, since the chemical reaction is to occur where the two reactants meet near the interface, which is also a region of high velocity gradient. The same conclusions were also drawn from earlier work on spe· :al calcalculations of temporally growing mixing layers [1]. However, the asymmetric nature of the mixing mechanism in the shear layer is well represented in the spatially developing calculations, which are discussed next.

Statistical Variables

The results of direct numerical simulations have been studied to examine the validity of some of the previously used turbulence models in which the large coherent structures have not been taken into account. In previous work [16, 17], many different possibilities for the closure of the hydrochemical equations in parallel shear flows were discussed. Among the models considered, the one with the best overall performance was the combination of a modeled joint probability density function (pdf) for the scalar variables and the K-ε model of turbulence (Launder and Spalding, [18]) for the hydrodynamic closure. A formulation based on a transport equation for the pdf of scalar variables has the advantage that the effects of chemical reactions appear in a closed form. However, models are needed for the closure of the molecular mixing term and also the turbulent convection. Givi et al. [17] employed a qualesence/dispersion model for the closure of the molecular mixing term and a gradient diffusion approximation for the closure of the turbulent flux of the pdf. The results were compared with experimental data of Masutani and Bowman [19] in similar hydrochemical conditions.

As far as the first few moments are concerned, the results obtained from the pdf transport equation are in reasonable agreement with experimental data. However, a major difference between the calculated and measured shapes of the probability density function is observed. This is indicated in Figure 8. In this figure, the pdf's of a nonreacting scalar variable (similar to the variable f defined above), are presented at a streamwise location. The profile obtained from experimental measurements of Masutani and Bowman [19] is also

presented on the same figure. The experimental results indicate an intermediate peak at a fixed value of the normalized concentration between the two delta functions at 0 and 1. In the predicted pdf's two spikes also exist at the normalized concentrations of 0 and 1, indicating the concentrations at freestreams. The height of the pdf in the middle region is in reasonably correct order-of-magnitude agreement with the experimental data. However, the location of the predicted pdf peak, with respect to the normalized concentration, gradually shifts as the layer is traversed. This is a major difference between the predicted and measured pdf's, as the modeled pdf transport equation is unable to predict the bimodal pdf's observed experimentally. As suggested by Givi et al. [17], Koochesfahani [3], and Masutani [20], this discrepancy is mainly due to the shortcomings associated with the gradient diffusion modeling of the turbulent flux of the pdf. In highly intermittent flows such as mixing layers, the continuity of turbulent flow is interrupted by the presence of the nonturbulent surrounding flows. Therefore, a simple gradient diffusion model is not expected to account accurately for this discontinuity.

Direct comparison of the shape of the pdf calculated from direct numerical simulations with that of experimental measurements is not possible due to the different Reynolds numbers used. However, a great deal of understanding of the influence of the large-scale structures in the mixing mechanism of the shear layer can be gained by examining the computed concentration pdf. The profile of the pdf's calculated from the results of the direct numerical simulation at the streamwise location of $X = 24\lambda$ is presented in Figure 9. This location corresponds to the point where the first merging between the two neighboring vortices occurs. It is indicated in this figure that at any cross-stream location away from the freestreams, the pdf has approximately three peak values. The first peak is closer to the low-speed fluid concentration, the second peak is closer to the high-speed fluid concentration, and the third peak is in a mixed concentration between the other two but closer to the high-speed side. The value of the pdf of the mixed concentration is larger than the pdf corresponding to other concentrations; also, the pdf of the concentration closer to the high-speed fluid side has a larger peak than the pdf of the low-speed concentration. This trimodal nature of the pdf, and also the fact that the mixed fluid pdf has a concentration near the high-speed side concentration, indicates the asymmetry of entrainment due to large-scale structures in the mixing region of the shear layer and also indicates that

more fluid from the high-speed stream than the low-speed side is drawn into the mixing core of the layer. Comparison of this figure with Figure 8 indicates that the pdf's obtained here have a structure closer to the experimental observations of Masutani and Bowman [19] than the previous calculations employing a modeled joint pdf transport equation (Givi et al., [17]). However, the calculated predominant peak of the pdf at the mixed fluid concentration is less pronounced than that observed experimentally by Masutani and Bowman [19]. This is possibly due to the fact that, in the present two-dimensional calculations, only the isolated effects of the large coherent structures are examined, and the effects of three-dimensional random turbulent fluctuations are not presented. Nevertheless, the results obtained from direct numerical simulations indicate that the mixing mechanism in the core of the shear layer is asymmetric, and the mixed fluid has a concentration closer to the high-speed fluid concentration. This agrees with the experimental observations of Masutani and Bowman [19] and Koochesfahani [3]. Three-dimensional flow simulations with random turbulent fluctuations are currently under study and are expected to result in better agreement with experimental data.

The mean and rms values of the conserved scalar obtained from the integration of the pdf profiles, presented above, are shown in Figure 10. This figure shows that the mean value of the concentration has an apparent "plateau" in the middle region of the shear layer. This "plateau" is at a concentration where a predominant peak occurs in the pdf (Figure 9). Similar behavior has also been observed in experimental measurements [3] and indicates the influence of the large-scale structure on the mean value of the concentration. The resulting rms values of the normalized non-reacting concentrations across the layer, obtained from the direct numerical simulations, indicate that there are two apparent maximums in the rms profile. These two points correspond to the location where the gradient of the mean value is highest. The same behavior was also observed in the experimental results of Masutani [20]. Calculations using a gradient diffusion model for the pdf turbulent transport are unable to predict this detailed behavior, as the calculations of Givi et al. [17] indicate. The predicted results of the rms concentration by Givi et al. [17] form a fairly smooth bell-shaped profile with a much less clear double "hump" in the middle region. However, the pdf calculation does show that the location of the rms maximums coincides with the location of the highest gradient of the mean value.

From the discussion given above, it is clear that the intermittency caused by the large coherent structures contributes greatly to various vital statistics of turbulent flows. The results of direct numerical simulations can illuminate the qualitative behavior of large-scale structures in intermittent flow, such as the spatially developing mixing layer considered here. Quantitative comparison with the experimental data, however, is not yet possible. A three-dimensional flow simulation may be required for meaningful quantitative comparison with experimental results.

CONCLUSIONS AND FUTURE WORK

Numerical simulations have been performed for the large-scale vortex dynamics in a forced spatially developing, reacting mixing layer. A combination of a pseudospectral and a second-order finite difference technique has been employed to study the effects of the rollup of the vortices and of their merging on the rate of formation of the reaction product. As an earlier simulation [1, 2] using a temporally developing approximation indicates, the vortex rollup and merging cause the stretching of the interface between the reactants, and thereby increase the stream surface area on which the chemical reaction occurs. In addition, the present simulations of a realistic spatially developing, chemically reacting mixing layer exhibit the asymmetric properties of the entrainment, which have been observed in experimental results [19].

The results of direct numerical simulations reported here and recent experimental measurements indicate the importance of large coherent structures in the mixing region of the shear layer. This suggests the need for better turbulence models in order to predict accurately the mechanism of mixing and chemical reaction in intermittent flows such as mixing layers.

Much remains to be done in our continuing effort in numerical combustion simulations. Consideration of a temperature-dependent reaction rate with intermediate Damkohler numbers has just been successfully finished for a temporally growing mixing layer (Givi et al. [21]) and should be included with the spatially growing mixing layer studied in this paper. This simulation can address the questions regarding the quenching and extinction of diffusion flames. Next, three-dimensional calculations involving a shear layer with a random turbulence field will be studied. This is a step toward simulations of turbulent flow and will provide a better understanding of the physics of

turbulent diffusion flames. The effects of chemical heat release, at a temperature-dependent reaction rate, on the flow field and product formation in a spatially developing mixing layer would also be very interesting and will be addressed in future papers. Finally, it would be interesting to examine the effects of the vortex merging further by looking at the influence of even higher subharmonics and also the effects of phase relations between the different modes on the chemical reactions and the flame convolution in a spatially evolving mixing layer.

ACKNOWLEDGMENTS

The calculations reported here were performed under research sponsored by the Air Force Office of Scientific Research, Contract No. F49620-85-C-00067. The United States Government is authorized to reproduce and distribute reprints for government purposes nonwithstanding any copyright notation hereon. The authors have also appreciated the support of NASA Lewis Research Center in providing computer time.

REFERENCES

1. Riley, J. J., Metcalfe, R. W. and Orszag, S. A., "Direct Numerical Simulations of Chemically Reacting Turbulent Mixing Layers," Phys. Fluids, 29 (1986), 406.

2. McMurtry, P. A., Jou, W.-H., Riley, J. J., and Metcalfe, R. W., "Direct Numerical Simulations of a Reacting Mixing Layer with Chemical Heat Release," AIAA J., 24 (1986), 962.

3. Koochesfahani, M. M., "Experiments on Turbulent Mixing and Chemical Reactions in a Liquid Mixing Layer," Ph.D. Thesis, Graduate Aeronautical Laboratories, California Institute of Technology, Pasadena, California, 1984.

4. Peters, N. and Williams, F. A., "Liftoff Characteristics of Turbulent Jet Diffusion Flames," AIAA J., 21 (1983), 423.

5. Williams, F. A., Combustion Theory, The Benjamin Cummings Publishing Company, Inc., Menlo Park, California, 1985.

6. Bilger, R. W., "Turbulent Flows with Nonpremixed Reactants," in Turbulent Reacting Flows, Springer-Verlag, New York, 1980.

7. Michalke, A., "On Spatially Growing Disturbances in an Inviscid Shear Layer," J. Fluid Mech., 23 (1965), 521.

8. Monkewitz, P. A. and Huerre, P., "Influence of the Velocity Ratio on the Spatial Instability of Mixing Layers," Phys. Fluids, 25 (1982), 1137.

9. Ho, C.-M. and Huerre, P., "Perturbed Free Shear Layers," Ann. Rev. Fluid Mech., 16 (1984), 365.

10. Gottlieb, D. and Orszag, S. A., Numerical Analysis of Spectral Methods: Theory and Applications, SIAM, Philadelphia, 1977.

11. Leonard, B. P., "A Stable and Accurate Convective Modeling Procedure Based on Quadratic Upstream Interpolation," Computer Meth. in Appl. Mech. and Eng., 19 (1979), 59.

12. Roach, P. J., Computational Fluid Mechanics, Hermosa Publishers, Albuquerque, New Mexico, 1972.

13. McInville, R. M., Gatski, T. B., and Hassan, H. A., "Analysis of Large Vortical Structures in Shear Layers," AIAA J., 23 (1985), 1165.

14. Givi, P., "Upstream and Downstream Boundary Conditions in Computational Fluid Dynamics," Department of Mechanical Engineering, Carnegie-Mellon University, Report CFD/81/11, Pittsburgh, Pennsylvania, 1981.

15. Davis, R. W. and Moore, E. F., "A Numerical Study of Vortex Merging in Mixing Layers," Phys. Fluids, 28 (1985), 1626.

16. Givi, P., Ramos, J. I., and Sirignano, W. A., "Turbulent Reacting Conce. ic Jets: Comparison Between Pdf and Moment Calculations," Prog. in Astro. and Aero., 95 (1984), 384.

17. Givi, P., Ramos, J. I., and Sirignano, W. A., "Probability Density Function Calculations in Turbulent Chemically Reacting Round Jets, Mixing Layers and One-Dimensional Reactors," J. Non-Equilib. Thermodyn., 10 (1985), 75.

18. Launder, B. E., and Spalding, D. B., Lectures in Mathematical Models of Turbulence, Academic Press, New York, 1972.

19. Masutani, S. M., and Bowman, C. T., "The Structure of a Chemically Reacting Plane Mixing Layer," Paper 84-44, Western States Section/The Combustion Institute, Boulder, CO, 1984.

20. Masutani, S. M., "An Experimental Investigation of Mixing and Chemical Reaction in a Plane Mixing Layer," Ph.D. Thesis, Stanford University, Stanford, California, 1985.

21. Givi, P., Jou, W.-H., and Metcalfe, R. W., "Flame Extinction in a Temporally Developing Mixing Layer," Twenty-First Symp. (Int.) Comb., The Combustion Institute, Pittsburgh, to appear.

FIGURE CAPTIONS

Figure 1. Schematic diagram of the two stream plane mixing layer and the hyperbolic tangent streamwise velocity boundary condition at X = 0. Species A and B are introduced into the high- and low-speed streams of the layer, respectively.

Figure 2. Plot of non-dimensionalized vorticity contours at $t^* = 31$ for the single rollup case. $0 \leq X/\lambda \leq 32$ and $-8 \leq Y/\lambda \leq 8$. Contour minimum is -2.10, contour maximum is 0, contour interval is 0.1.

Figure 3. Plot of Shvab-Zeldovich variable (f) contours at $t^* = 31$ for the single rollup case. $0 \leq X/\lambda \leq 32$ and $-8 \leq Y/\lambda \leq 8$. Contour minimum is 0 (indicating no species from the high-speed stream), contour maximum is 1 (indicating the species from the high-speed stream), contour interval is 0.1.

Figure 4. Plots of non-dimensionalized vorticity contours for the double rollup case. $0 \leq X/\lambda \leq 32$ and $-8 \leq Y/\lambda \leq 8$. (a) $t^* = 31$, contour minimum is -2.50, contour maximum is 0, contour interval is 0.1. (b) $t^* = 39$, contour minimum is -1.76, contour maximum is 0, contour interval is 0.08.

Figure 5. Plots of Shvab-Zeldovich variable (f) contours for the double rollup case. $0 \leq X/\lambda \leq 32$ and $-8 \leq Y/\lambda \leq 8$. Contour minimum is 0, contour maximum is 1, contour interval is 0.1 (a) $t^* = 31$, (b) $t^* = 39$. (Also see the caption on Figure 3.)

Figure 6. Contour plot of concentration of the product of chemical reaction in the limit of infinitely fast chemistry at $t^* = 31$. Single rollup case, $0 \leq X/\lambda \leq 32$ and $-8 \leq Y/\lambda \leq 8$. Contour minimum is 0 (indicating no reaction), contour maximum is 0.5 (indicating maximum reaction), contour interval is 0.05.

Figure 7. Contour plots of concentration of the product of chemical reaction in the limit of infinitely fast chemistry at (a) $t^* = 31$, (b) $t^* = 39$. Double rollup case, $0 \leq X/\lambda \leq 32$ and $-8 \leq Y/\lambda \leq 8$. Contour minimum is 0.5, contour interval is 0.05. (Also see the caption on Figure 6.)

Figure 8. Comparison of predicted and measured PDF's of the conserved scalar variable (f) at points across the width of the mixing layer. (a) predictions based on a modeled transport equation for PDF (Givi et al. [17]), (b) experimental data obtained by Masutani and Bowman [19]. The cross stream coordinate (y) is normalized by use of $y'_o = [y(< f > = 0.5)]$, the virtual origin of the mixing layer (x'_o) and the streamwise distance (x). These PDF's represent conditions at a distance of x = 7 cm from the tip of the splitter plate used in the experiments of Masutani and Bowman [19].

Figure 9. PDF's of the conserved Shvab-Zeldovich scalar variable (f) at points across the mixing layer calculated directly from the results of present direct numerical simulations. These PDF's represent conditions at a distance of $X = 24\ \lambda$ from the tip of the splitter plate.

Figure 10. Calculated mean and RMS values of the Shvab-Zeldovich scalar variable (f) from the results of direct numerical simulations, versus the non-dimensionalized cross stream coordinate (Y/λ) at $X/\lambda = 24$.

4963R

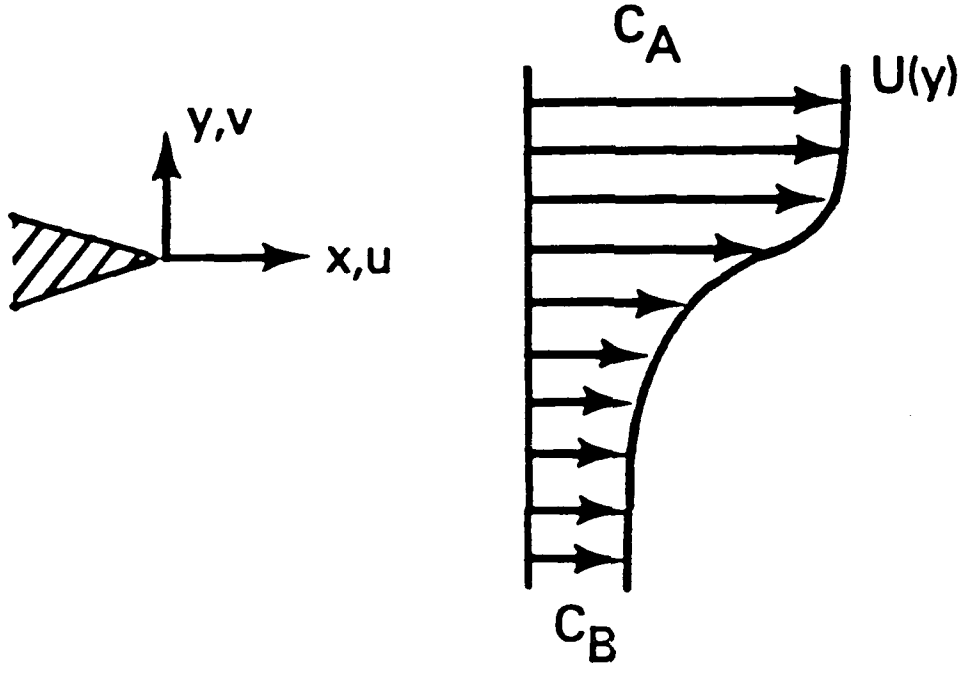

Figure 1

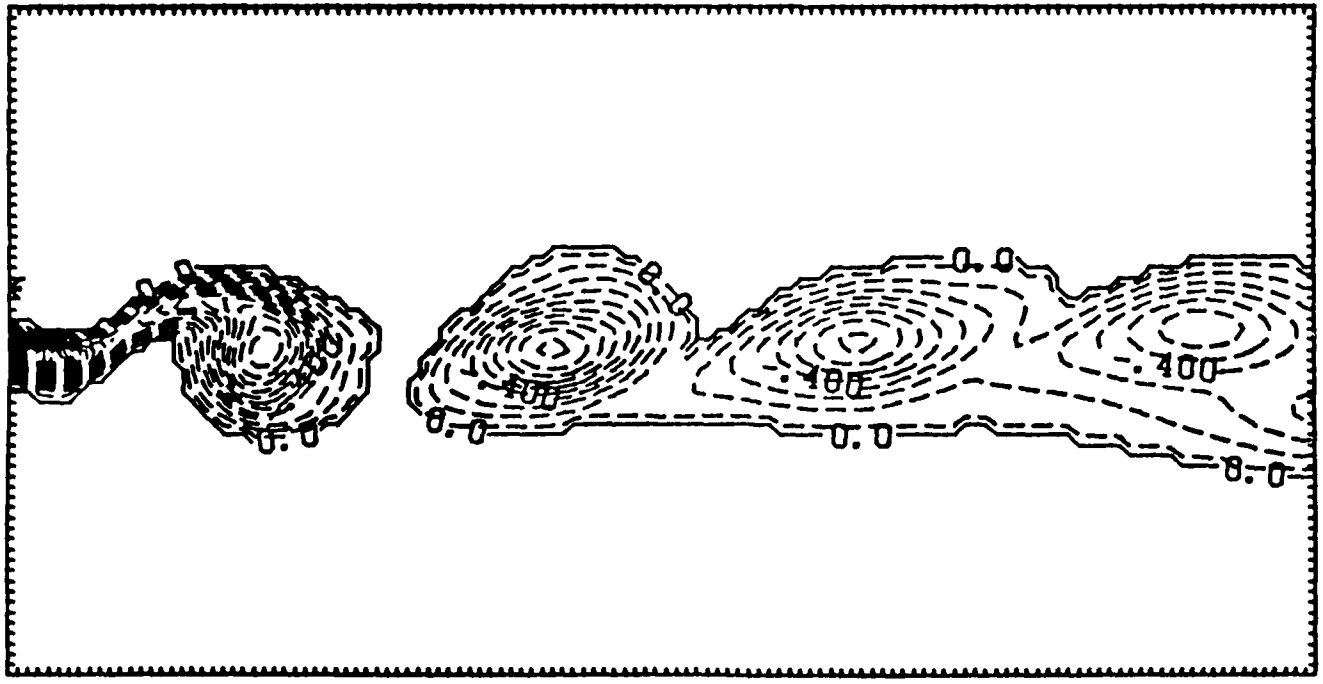

CONTOUR FROM -2.10 TO 0.
CONTOUR INTERVAL IS 0.100

Figure 2

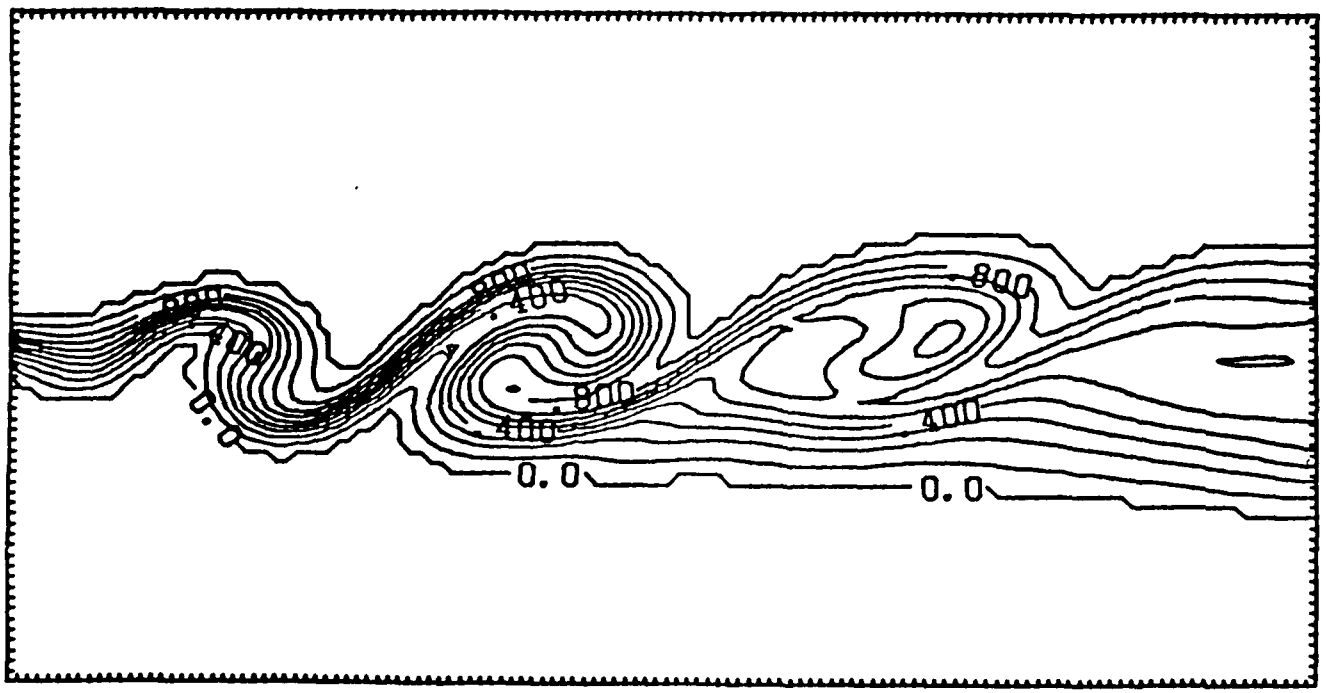

CONTOUR FROM 0. TO 1.00
CONTOUR INTERVAL IS 0.100

Figure 3

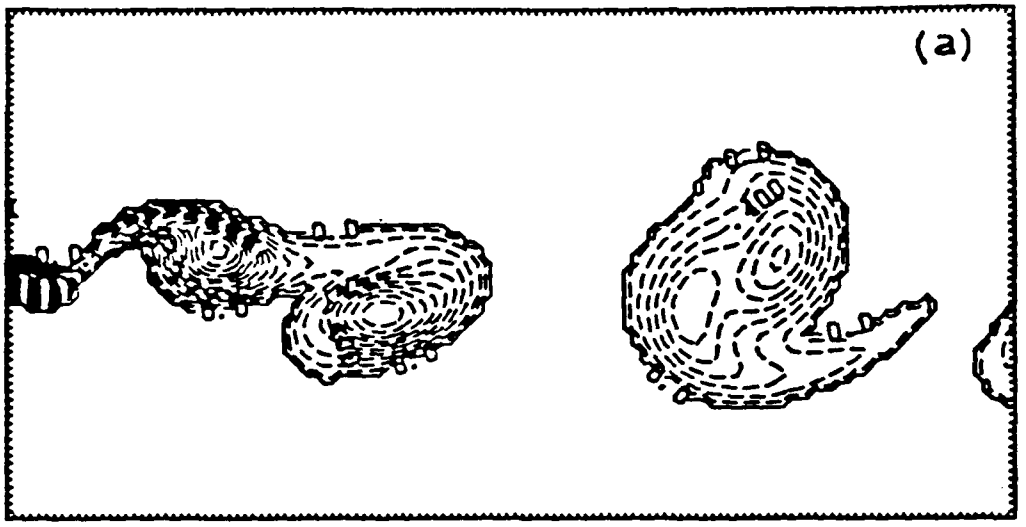

CONTOUR FROM -2.50 TO 0.
CONTOUR INTERVAL IS 0.100

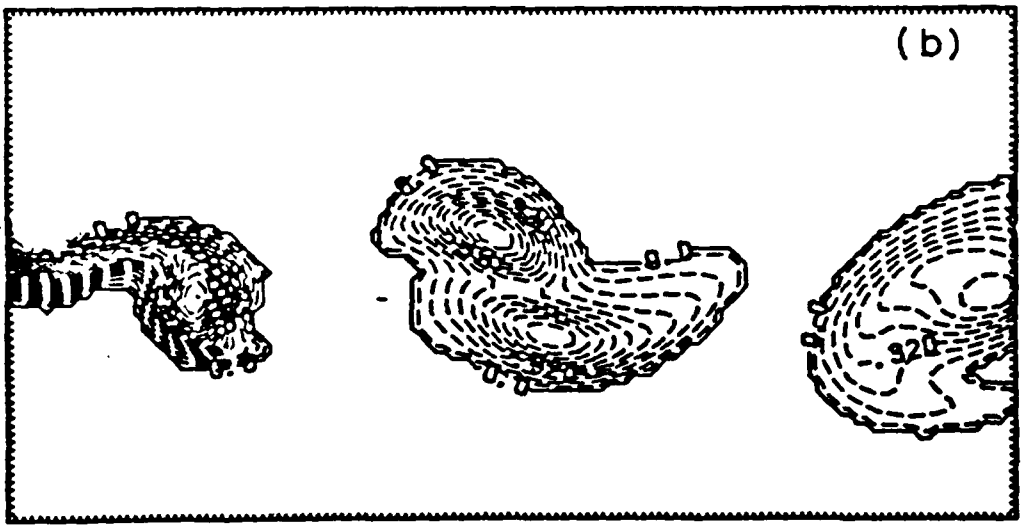

CONTOUR FROM -1.76 TO 0.
CONTOUR INTERVAL IS 0.800E-01

Figure 4

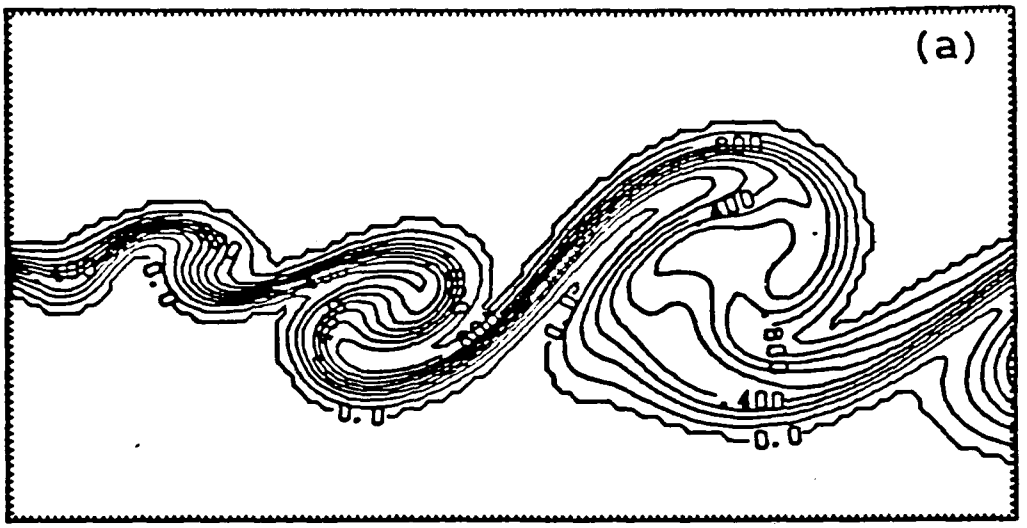

CONTOUR FROM 0. TO 1.00
CONTOUR INTERVAL IS 0.100

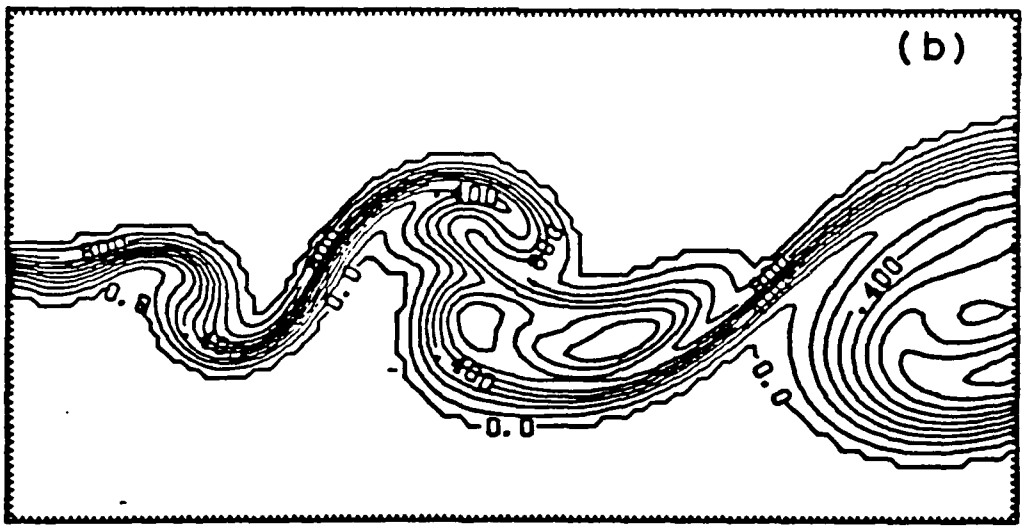

CONTOUR FROM 0. TO 1.00
CONTOUR INTERVAL IS 0.100

Figure 5

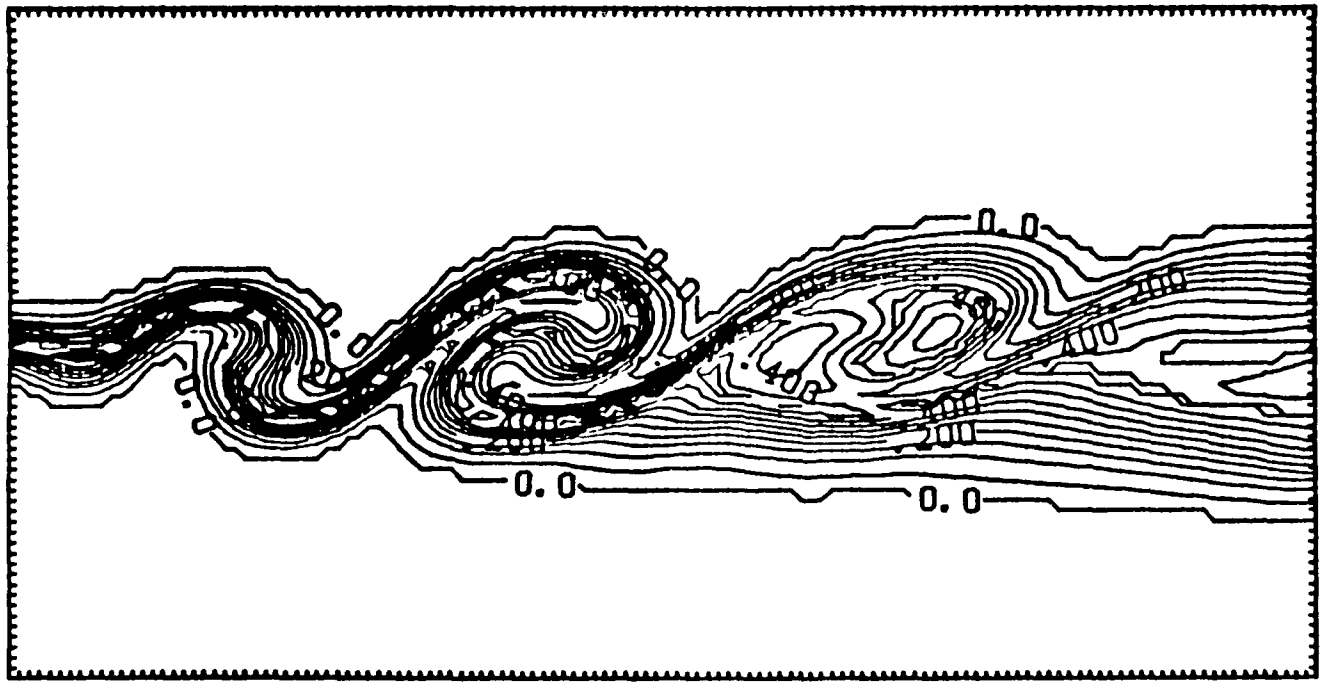

CONTOUR FROM 0. TO 0.500
CONTOUR INTERVAL IS 0.500E-01

Figure 6

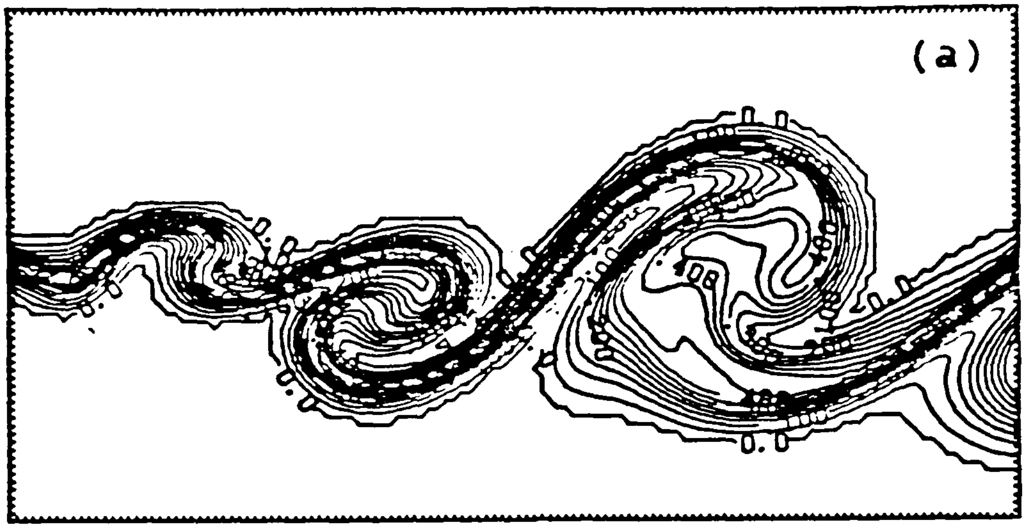

CONTOUR FROM 0. TO 0.450
CONTOUR INTERVAL IS 0.500E-01

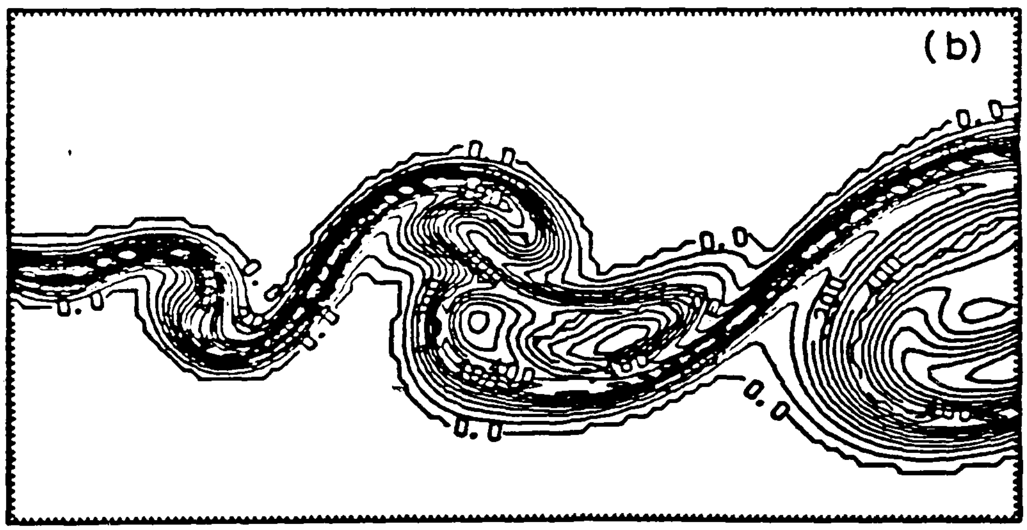

CONTOUR FROM 0. TO 0.500
CONTOUR INTERVAL IS 0.500E-01

Figure 7

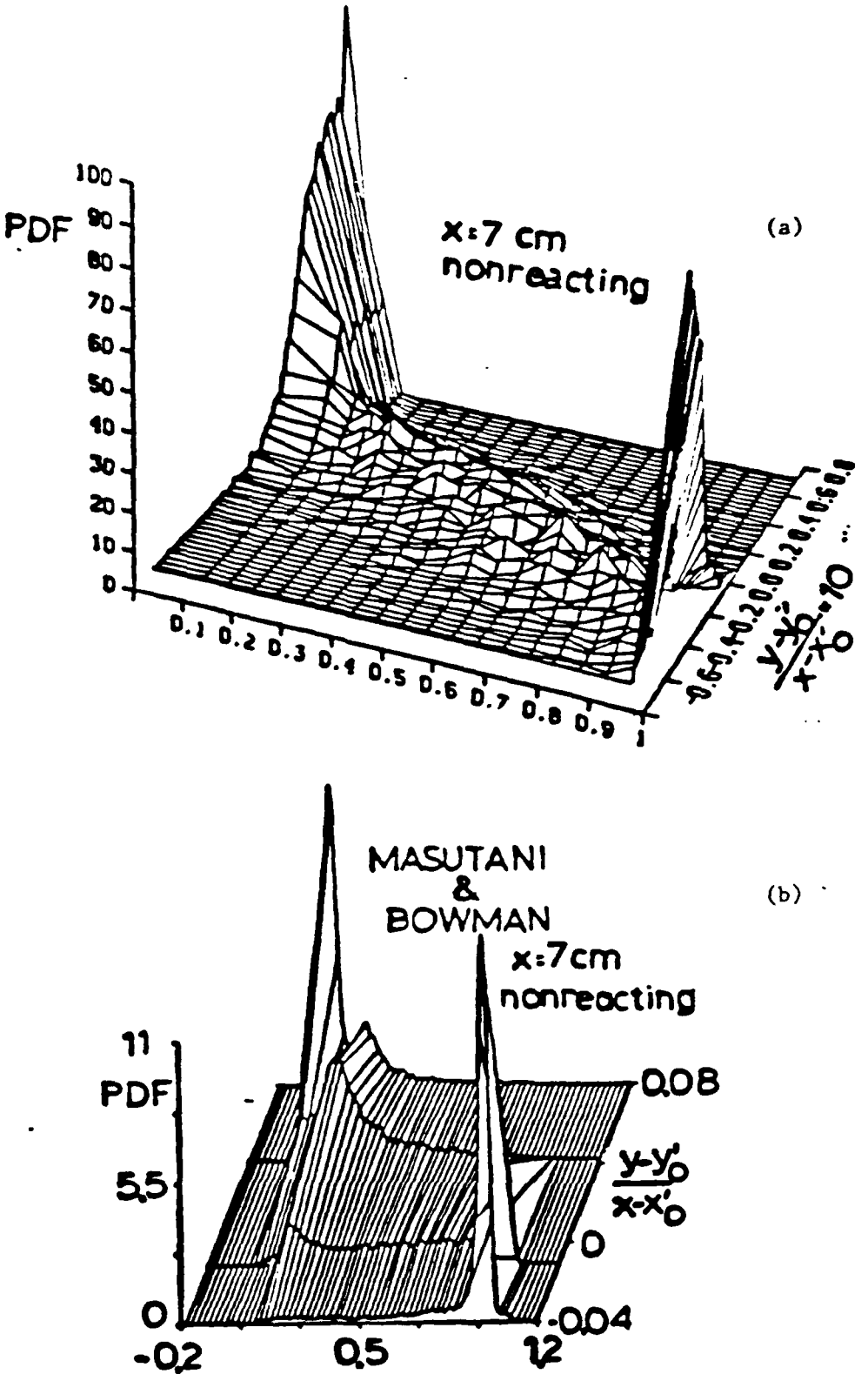
PDF
100
90
80
70
60
50
40
30
20
10
0
x=7 cm
nonreacting
(a)
0.1 0.2 0.3 0.4 0.5 0.6 0.7 0.8 0.9 1
y-y'o / x-x'o
MASUTANI
&
BOWMAN
x=7cm
nonreacting
(b)
11
PDF
5.5
0
-0.2
0.5
1.2
0.08
0
-0.04
y-y'o / x-x'o

Figure 8

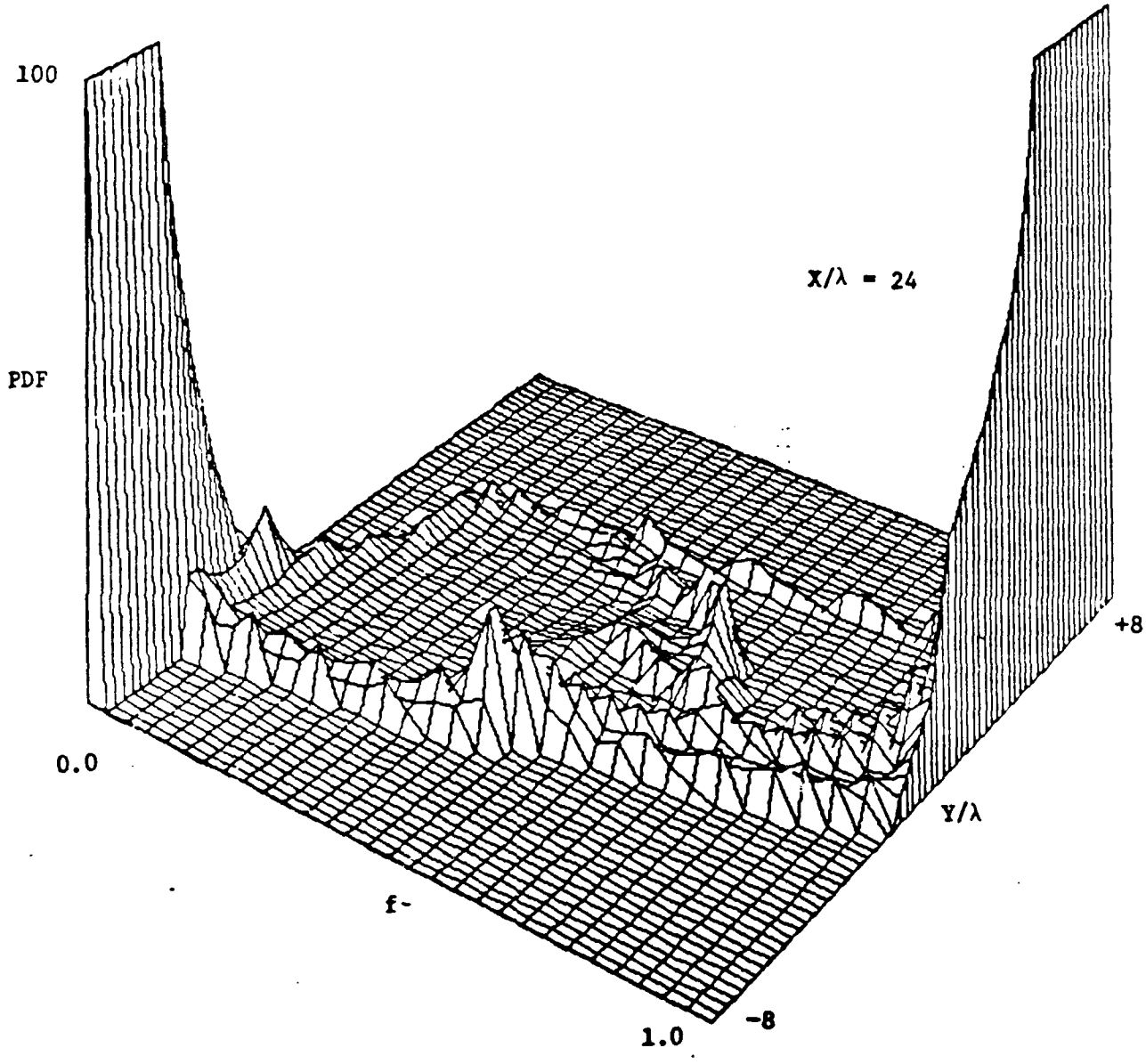

Figure 9

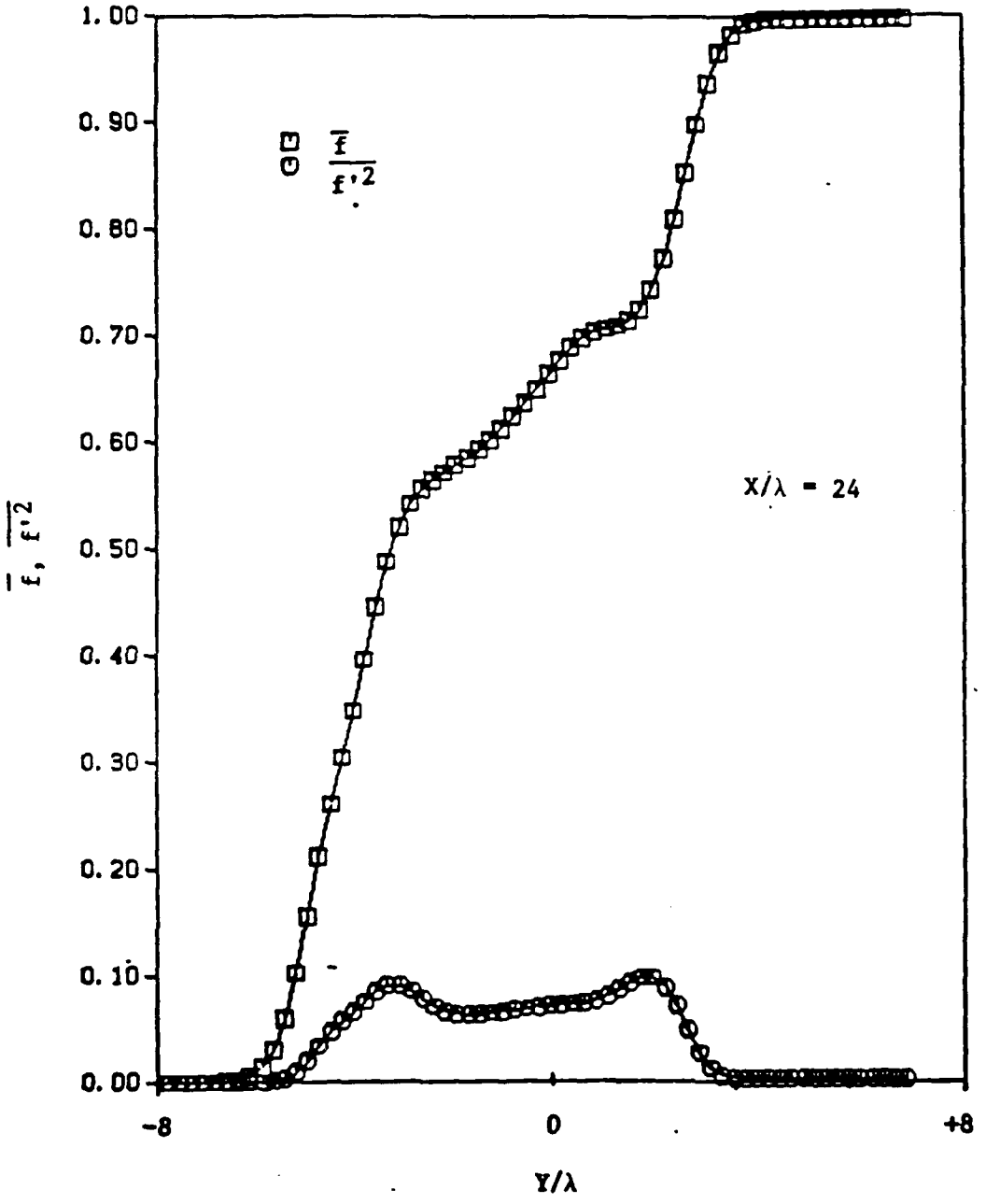
1.00
0.90
0.80
0.70
0.60
0.50
0.40
0.30
0.20
0.10
0.00
$\overline{f}$, $\overline{f'^2}$
$\frac{\overline{f}}{f'^2}$
X/λ = 24
-8
0
+8
Y/λ

Figure 10

APPENDIX III

Direct Numerical Simulations of the PDF's of a Passive Scalar in a Forced Mixing Layer

DIRECT NUMERICAL SIMULATIONS OF THE PDF'S OF A PASSIVE SCALAR IN A FORCED MIXING LAYER

by

P. Givi and P.A. McMurtry
Flow Research Company
21414 68th Avenue South
Kent, WA 98032

September 1987

Revised Manuscript Accepted for Publication as a
Short Communication in Combustion Science and Technology

DIRECT NUMERICAL SIMULATIONS OF THE PDF'S OF A PASSIVE SCALAR IN A FORCED MIXING LAYER

P. Givi Flow Research Company, 21414-68th Ave. South, Kent, Washington 98032

P. A. McMurtry Department of Mechanical Engineering, University of Washington, Seattle, Washington 98195

Abstract - The probability density functions of a passive scalar quantity are calculated in a perturbed mixing layer by means of direct numerical simulations. The results indicate that the two-dimensional rollup of the unsteady shear layer, and the pairing process in particular, contributes greatly to the generation of the predominant peak of the PDF's within the mixing region.

Key Words - Direct Numerical Simulation, Mixing Layers, Probability Density Functions, Coherent Structures, Entrainment.

INTRODUCTION

Probability Density Functions (PDF's) have proven very useful in the theoretical treatment of turbulent reacting flows since the early work of Hawthorne et al. (1949). An approach based on the solution of a transport equation governing the probability density function of the scalar quantities has the advantage that it provides a complete statistical description of all the scalars (Pope, 1979). Therefore, the effects of chemical reactions appear in a closed form eliminating the need for any turbulence modeling associated with the scalar fluctuations. However, models are needed for the closure of the molecular mixing term and also the turbulent convection (O'Brien, 1981).

In most of the previous work employing the PDF approach, the effects of molecular mixing have usually been modeled by using different stochastic models originating from the same "family" of the coalesence-dispersion models (Pope, 1982), whereas simple gradient-diffusion approximations have been employed for the closure of the turbulent flux of the PDF (Givi et al., 1984).

Among these previous works, Givi et al. (1985) used a Monte Carlo numerical routine for the calculations of a modeled transport equation governing the evolution of a passive scalar PDF in a nonreacting two-stream turbulent mixing layer. The results of the prediction were compared with the experimental data of Masutani and Bowman (1986), which were obtained under similar hydrodynamical conditions. Good agreement between predicted results and the measured data was obtained for the first two moments of the scalar quantity. There was a major difference, however, between the calculated and measured profiles of the PDF's. The experimental results indicated that the apparent functional form of the PDF changes very little across the mixing layer and has an intermediate peak at a fixed "preferred" value of the concentration (although the magnitude of this peak changes as the mixing layer is traversed). This behavior was originally documented in the measurments of Konrad (1976) and Koochesfahani (1984) in the mixing transition and post-mixing transition (Breidenthal, 1981) regions of the layer and indicates that a given mixed fluid concentration has the same probability relative to other mixed fluid concentrations, regardless of the position in the layer. The predicted results, however, indicate that the location of the PDF peak, with respect to the concentration coordinate, changes as the layer is traversed, meaning that the PDF of the mixed fluid concentration varies with the cross stream direction of the layer.

The major reason for this discrepancy, as suggested by Givi et al. (1985) and Masutani and Bowman (1986), is due to the shortcomings associated with the gradient diffusion modeling of the turbulent flux of the PDF and is fairly independent of the modeling of the molecular mixing term (Kosaly and Givi, 1987). In a highly intermittent flow such as a mixing layer, regions of turbulent fluid are interrupted by the presence of nonturbulent surrounding fluid. A simple gradient diffusion model is not expected to accurately account for this discontinuity.

By the use of direct numerical simulations, it is now possible to simulate the mixing layer directly without resorting to turbulence models (Riley and Metcalfe, 1980). Direct numerical simulation refers to the numerical solution of the exact transport equations of turbulent flows by means of very accurate and efficient numerical methods. Transport coefficients are chosen to assure that all relevant flow characteristics are accurately resolved so that no turbulence modeling is required. The results of such simulations can be used

to obtain useful information on the statistics of the variables characterizing the structure of the flow, which in turn can be used as a basis for turbulence modeling.

In this communication, the results of direct numerical simulations are used to construct the PDF of a passive scalar quantitiy in a perturbed two-dimensional mixing layer. The profiles of the PDF constructed in this manner are used to address the shortcomings associated with the modeling of the turbulent flux of the PDF in the transport equation governing its evolution.

RESULTS

A pseudospectral numerical code developed by McMurtry et al. (1986) was modified to simulate a two-dimensional temporally evolving mixing layer under the influence of harmonic forcing. The numerical resolution was upgraded from the previously used 64 x 64 grid to 256 x 256 equally spaced Fourier modes. This upgrade was required for better statistical analysis of the data used for constructing the PDF's. The flow is assumed periodic in the streamwise direction and free slip, impermeable boundary conditions are employed at the transverse boundaries. Although, the laboratory splitter plate mixing layers evolve spatially downstream and the numerical simulations evolve temporally, important similarities in the dynamics of these two flows make it useful to study accurate numerical simulations of the temporally growing layers. By simple Galilean transformation, a flow quantity averaged in the streamwise direction can be related to the time average of the same quantity at a fixed location in a splitter plate configuration. These averaged quantitities are dependent on the tranverse coordinate and the time. Again, the inverse Galilean transformation relates time to the streamwise location in a splitter plate configuration. There is one structure within the periodic domain at each time step. Statistical analysis are perfromed by sampling 256 data points in the streamwise direction at each transverse location and at each time step. The presence of periodic boundary conditions allows us to use accurate pseudospectral numerical methods; these methods are discussed by McMurtry (1987) and will not be repeated here.

The flow field is initialized with a hyperbolic tangent mean streamwise velocity profile and perturbations corresponding to the most unstable mode of

this profile and the first subharmonic of the most unstable mode. The properties of these modes have been evaluated from linear stability theory (Michalke, 1964). The fundamental mode in the mixing layer produces a single vortex rollup. When the subharmonic is added in, a second rollup, or pairing, can occur.

The normalized initial value of the conserved scalar concentration, f, varies from 0 in the bottom stream to 1 in the top stream, and its shape is approximated by the following functional form:

$$f(x,y,0) = \frac{1}{y_0\sqrt{\pi}} \int_{-\infty}^{y} \exp(-\xi/y_0)^2 d\xi$$

The flow is conveniently characterized by two nondimensional parameters: the Reynolds number, $Re = \Delta U\delta/\nu$, based on the mean velocity difference across the layer, the velocity half width, and the kinematic viscosity; and the Peclet number, $Pe = Re\ Sc$, where Sc is the molecular Schmidt number. The values of these two parameters were set equal to 200, so that the scales would be accurately resolved on the 256-256 grid points employed in the numerical simulations. The value of y_o was chosen so that the initial concentration thickness and the initial velocity thickness were identical. The time dependent transport equations governing the hydrodynamical variables (velocities and pressure) and the scalar variable (f) are solved with use of the pseudo-spectral code, the results of which are discussed next.

The contour plots of the conserved scalar variable are shown for the purpose of flow visualization. In Fig. 1, we present the time development of the contours of the variable f at four different computational times. Initially, the perturbation associated with the fundamental mode grows until a time of t* ($t^*=t_{\Delta u}/\delta$) equal to 12, when the first rollup occurs. Proceeding in time results in the diffusion of the core of the vortex and the growth of the subharmonic mode, which expresses itself in the form of a second rollup and the pairing of two neighboring vortices. This second rollup is completed by a time of t*=36. Proceeding further in time results in the diffusion of the vortex core with no additional rollup.

The profiles of the PDF's of the variable f obtained by statistical analysis of the instantaneous values of f are shown in Fig. 2. In this figure, the PDF has been plotted as a function of the instantaneous concentration f,

and the cross-stream direction of the shear layer. These PDF's represent conditions at the initial stages of the growth ($t^*=3$) and the final stage after the pairing process is completed ($t^*=36$).

A comparison between the two parts of Fig. 2 reveals the effects of vortex dynamics on the structure of the PDF's. Fig. 2a shows that, at the early stages of the development, before any rollup or pairing has occurred, the PDF's can be simply characterized by two delta functions that are located at $f=0$ and $f=1$, with only a negligible amount of mixed fluid at the mixing core of the layer. This indicates that, at any location in the cross-stream direction, the fluid originates from either the top stream or the bottom stream without any significant amount of mixing in the core. Fig. 2b shows that after the occurance of the rollup and the completion of pairing, a third spike appears in the profiles of the PDF at a region in the neighborhood of a concentration value of 0.5. The presence of this third peak suggests the existence of a preferred mixed fluid concentration equal to 0.5. The combined effects of vortex rollup and diffusion are to engulf fluids from the two streams and mix them in the cores of the vortices. As the layer is traversed, the preferred value of this concentration does not seem to change considerably and remains in close proximity to $f=0.5$.

The trimodal shape of the PDF is consistent with that observed experimentally (Koochesfahani, 1984). However, the experimental measurements were performed in the transition and post-transition regions of the mixing layer, whereas the numerical data presented here resulted strictly from a two-dimensional simulation. This indicates that the two-dimensional rollup of the unsteady shear layer can be considered as one possible mechanism by which the third peak is generated in the PDF profiles.

It should be mentioned that the presently calculated third peak of the PDF at the preferred mixed fluid concentration of $f=0.5$ is less pronounced than that observed experimentally by Masutani and Bowman (1986). This may be due to the fact that in the present calculations, the effects of random turbulent motion, which can further enhance mixing, are not taken into account. In order to consider the contributions of turbulent motion into the generation of the third peak in the PDF profile, three-dimensional simulations are required. Furthermore, the asymmetry of the mixing mechanisms, which has been both experimentally (Koochesfahani et al., 1985; Koochesfahani and Dimotakis, 1986; Mungal and Dimotakis, 1984) and numerically (Givi and Jou, 1987) observed for

spatially evolving flows cannot be represented in the temporal simulations presented here. The asymmetric mixing mechanism results in a preferred concentration value that is closer to that of the high speed stream and may depend on the ratio of the free stream velocities (Dimotakis, 1986). In the present temporal simulations, the ratio of the magnitude of the free stream velocities is equal to unity and the structure of the flow is symmetric with respect to the streamwise coordinates (as shown by the symmetry of the PDF's with respect to the location (f,y)=(0.5,0) in Fig. 2). Therefore, the numerical simulations cannot predict any other than the arithmatic average of the concentration values of the two streams (i.e., 0.5). Nevertheless, the results indicate that the rollup of the unsteady shear layer contributes greatly to the generation of the predominant peak of the PDF's. The exact role of the small scale turbulence motion on the enhancement of such generation requires full three-dimensional simulation and is the subject of our future research.

Finally, the reason that the methods based on simple gradient diffusion modeling of the turbulent flux of the PDF, such as that employed by Givi et al. (1985), cannot predict the trimodal shape of the PDF obtained in the present simulation is due to the fact that such methods do not consider the influence of intermittency caused by the large coherent structures in the formulation. The results of the direct numerical simulations reported here indicate the importance of such structures in the mixing region of the shear layer and suggest the need for better turbulence models in order to accurately predict the mechanisms of mixing and entrainment in such flows.

ACKNOWLEDGEMENTS

The authors are indebted to Dr. Manoochehr Koochesfahani for valuable discussions on the topic during all the stages of this research. Dr. Wen-Huei Jou is also acknowledged for many useful suggestions. This research was part of an effort sponsored by the Air Force Office of Scientific Research under Contract No. F49620-85-C-00067. The United States government is authorized to reproduce and distribute reprints for governmental purposes notwithstanding any copyright notation hereon. The authors also appreciate the support of NASA Lewis Research Center in providing computer time on CRAY-XMP.

REFERENCES

Breidenthal, R. E. (1981) "Structure in Turbulent Mixing Layers and Wakes Using a Chemical Reaction", Journal of Fluid Mechanics, Vol. 125, pp. 397-410.

Dimotakis, P. E. (1986) "Two-Dimensional Shear-Layer Entrainment," AIAA Journal, Vol. 24, Number 11, pp. 1791-1796.

Givi, P. and Jou, W.-H. (1987) "Mixing and Chemical Reactions in a Spatially Developing Mixing Layer," Journal of Non-Equilibrium Thermodynamics, in press.

Givi, P., Ramos, J. I., and Sirignano, W. A. (1985) "Probability Density Function Calculations in Turbulent, Chemically Reacting Round Jets, Mixing Layers and One-Dimensional Reactors," Journal of Non-Equilibrium Thermodynamics, Vol. 10, pp. 75-104.

Givi, P., Sirignano, W. A. and Pope, S. B. (1984) "Probability Calculations for Turbulent Jet Flows with Mixing and Reaction of NO and O_3," Combustion Science and Technology, Vol. 37, pp. 59-74.

Hawthorne, W. R., Wedell, D. S., and Hottel, H. C. (1949) "Mixing and Combustion in Turbulent Gas Jets," Third Symposium on Combustion, Flames and Explosion Phenomena, The Combustion Institute, Pittsburgh, PA, pp. 266-288.

Konrad, J. H. (1976) "An Experimental Investigation of Mixing in Two-Dimensional Turbulent Shear Flows with Application to Diffusion Limited Chemical Reactions", Ph.D. Thesis, California Institute of Technology, Pasadena, CA.

Koochesfahani, M. M. (1984) "Experiments on Turbulent Mixing and Chemical Reactions in a Liquid Mixing Layer," Ph.D. Thesis, California Institute of Technology, Pasadena, CA.

Koochesfahani, M. M. and Dimotakis, P. E. (1986) "Mixing and Chemical Reactions in a Turbulent Liquid Mixing Layer," Journal of Fluid Mechanics, Vol.170, pp. 83-112.

Koochesfahani, M. M., Dimotakis, P. E. and Broadwell, J. E. (1985) "A Flip Experiment in a Chemically Reacting Turbulent Mixing Layer," AIAA Journal, Vol. 23, Number 8, pp. 1191-1194.

Kosaly, G. and Givi, P. (1987) "Modeling of Turbulent Molecular Mixing," Combustion and Flame, in press.

Masutani, S. M. and Bowman, C. T. (1986) "The Structure of a Chemically Reacting Plane Mixing Layer," Journal of Fluid Mechanics, Vol. 172, pp. 93-126.

McMurtry, P. A. (1987) "Direct Numerical Simulations of a Reacting Mixing Layer with Chemical Heat Release," Ph.D. Thesis, University of Washington, Seattle, WA.

McMurtry, P. A., Jou, W.-H., Riley, J. J. and Metcalfe, R. W. (1986) "Direct Numerical Simulations of a Reacting Mixing Layer with Chemical Heat Release," AIAA Journal, Vol. 24, Number 6, pp. 962-970.

Michalke, A. (1964) "On the Inviscid Instability of a Hyperbolic-Tangent Velocity Profile," Journal of Fluid Mechanics, Vol. 19, pp. 543-556.

Mungal, M. G. and Dimotakis, P. E. (1984) "Mixing and Combustion with Low Heat Release in a Turbulent Shear Layer," Journal of Fluid Mechanics, Vol. 148, pp. 349-382.

O'Brien, E. E. (1981) "The Probability Density Function (pdf) Approach to Reacting Turbulent Flows," Topics in Applied Physics, Turbulent Reacting Flows, Libby, P. A. and Williams, F. A. (eds.), Springer-Verlag, New York, Chapter 5, pp. 185-218.

Pope, S. B. (1979) "The Statistical Theory of Turbulent Flames," Philosophical Transactions of the Royal Society of London, Vol. 291, pp. 529-568.

Pope, S. B. (1982) "An Improved Turbulent Mixing Model," Combustion Science and Technology, Vol. 28, pp. 131-145.

Riley, J. J. and Metcalfe, R. W. (1980) "Direct Numerical Simulations of a Perturbed Turbulent Mixing Layer," AIAA Paper 80-0274.

FIGURE CAPTIONS

Figure 1: Plot of the Conserved Scalar Variable (f) Contours at Four Different Computational Times. Contour Minimum is 0, Contour Maximum is 1, Contour Interval is 0.1. (a) $t^*=3$, (b) $t^*=12$, (c) $t^*=24$, (d) $t^*=36$.

Figure 2: PDF's of the Conserved Scalar Variable (f) at Points Across the Mixing Layer Width. (a) $t^*=3$, (b) $t^*=36$.

5642R

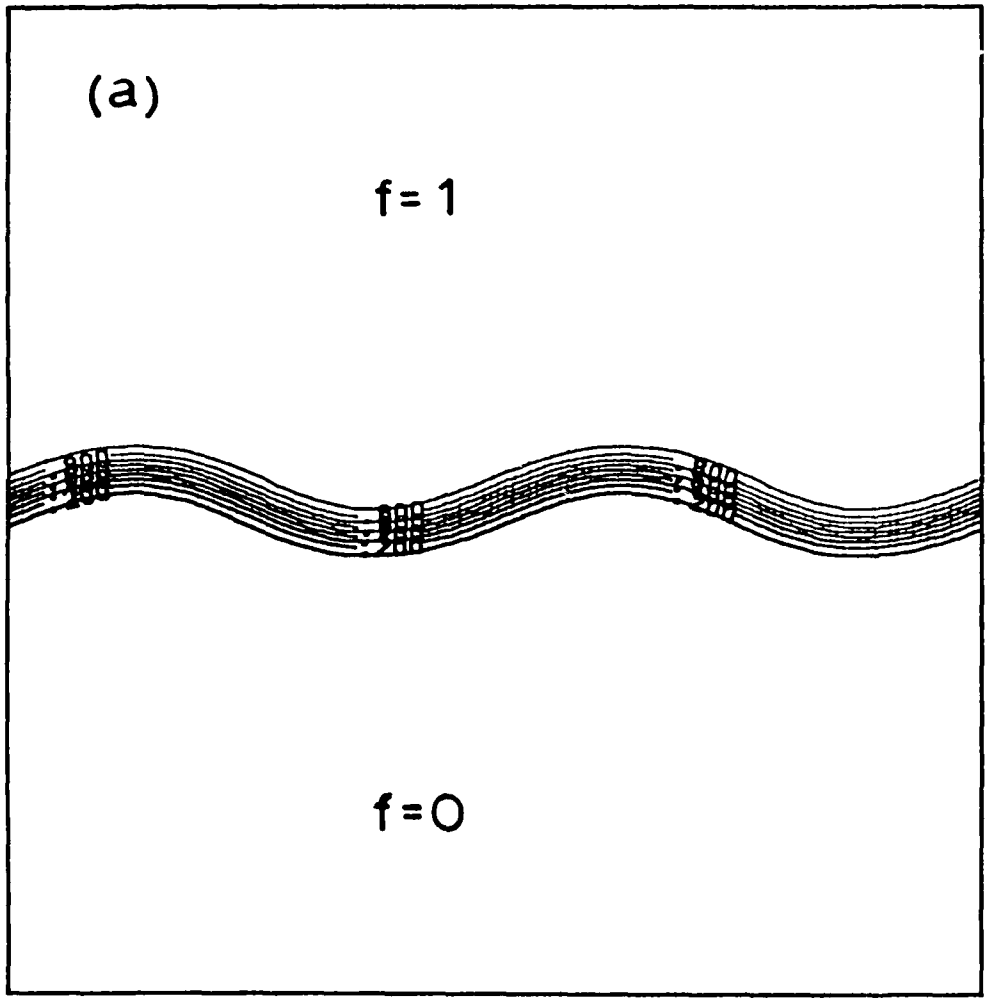

Figure 1a

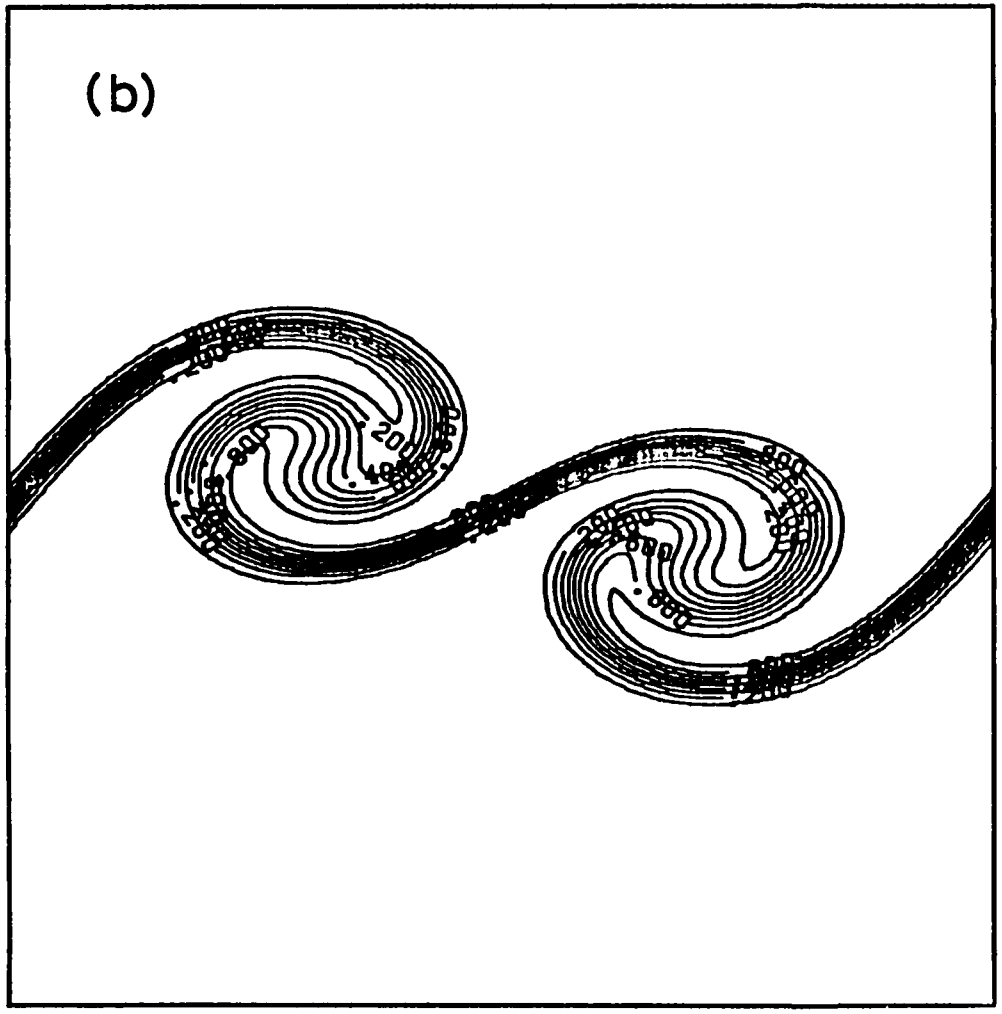

Figure 1b

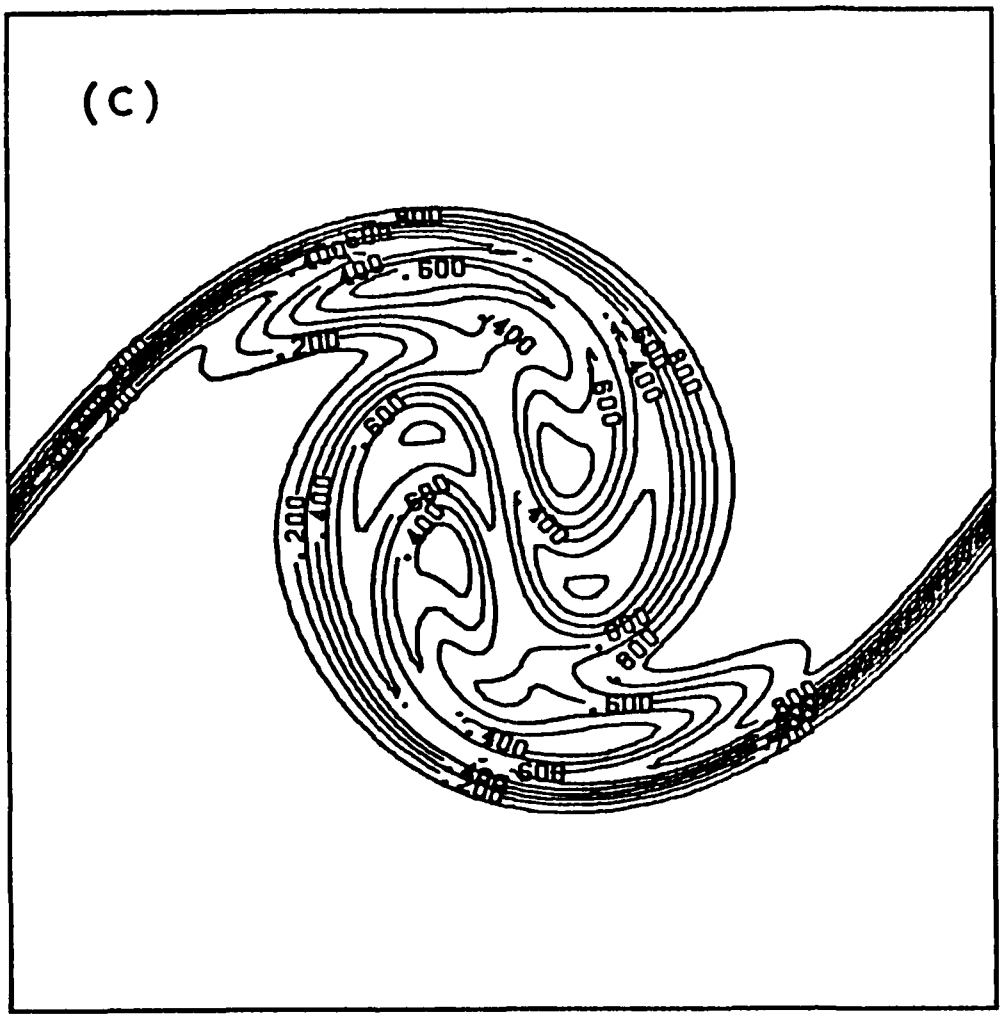

Figure 1C

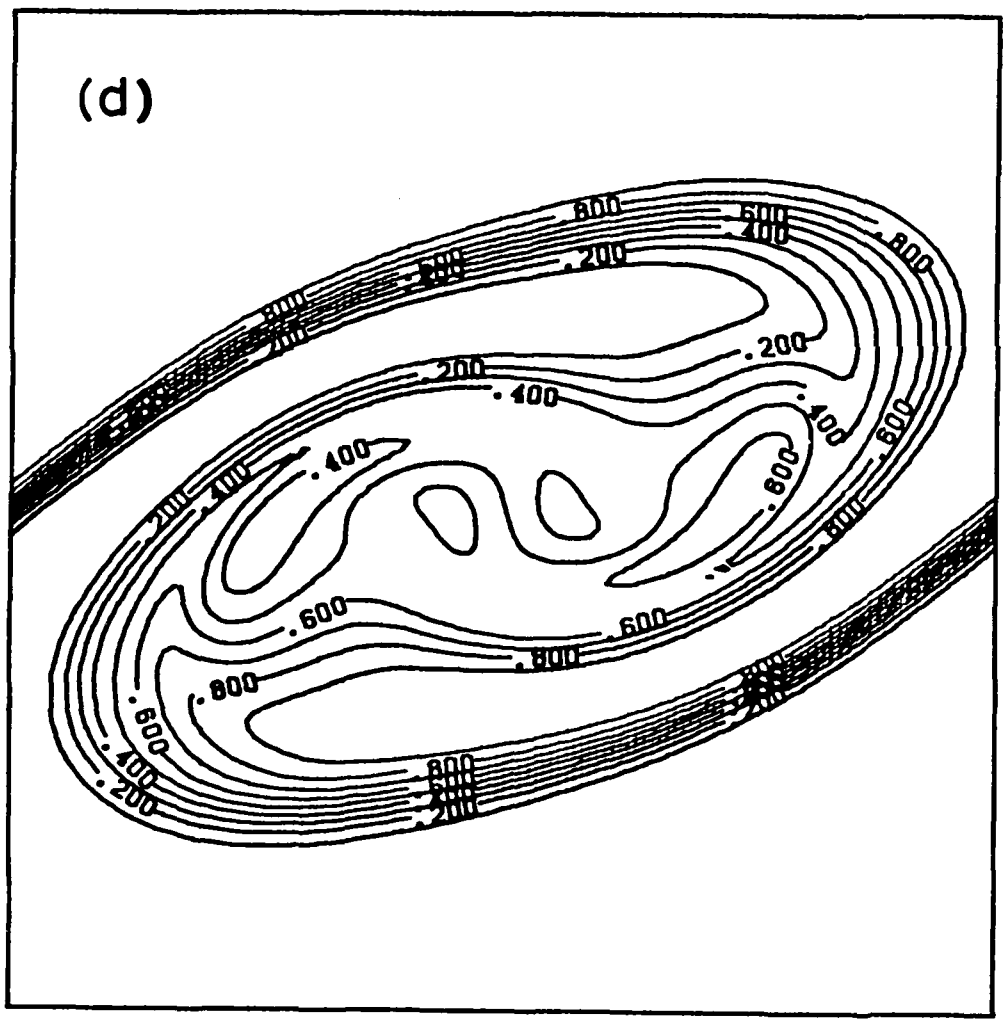

Figure 1d

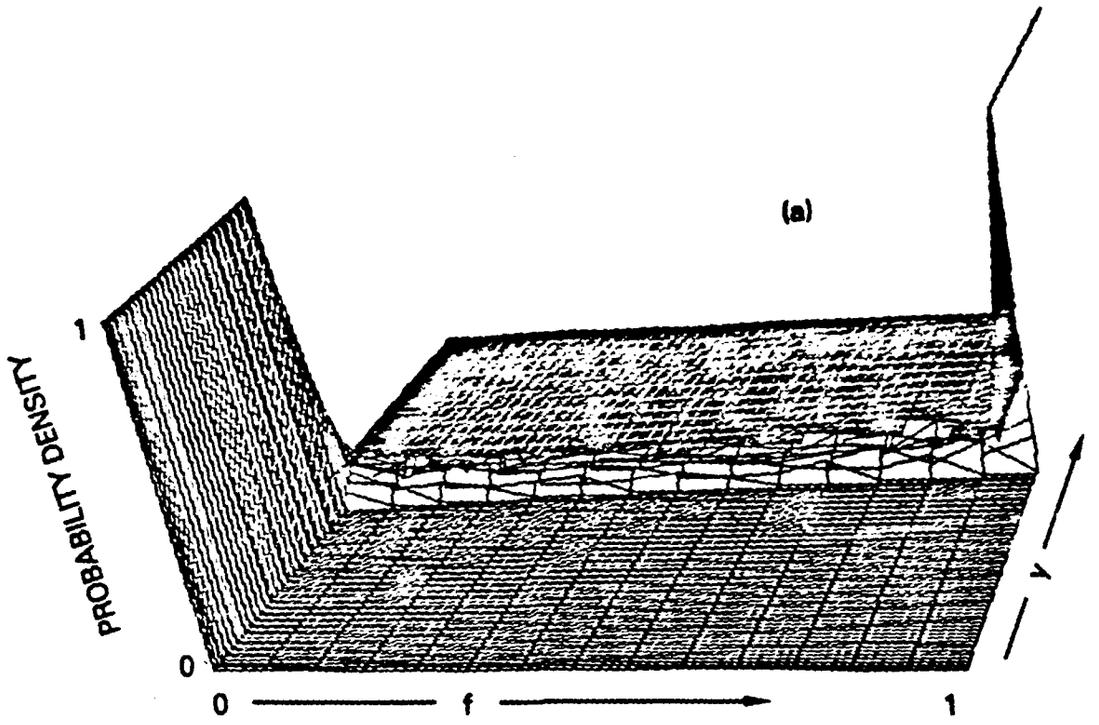
(a)
PROBABILITY DENSITY
1
0
0
f
1
v

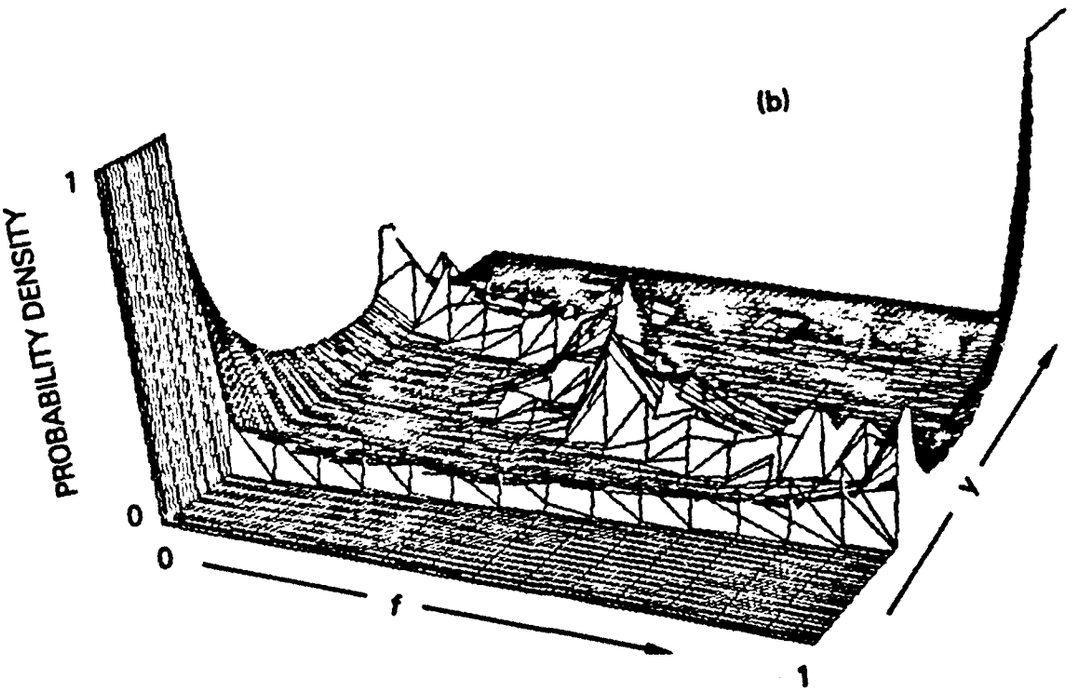
(b)
PROBABILITY DENSITY
1
0
0
f
1
v

Figure 2

APPENDIX IV

Direct Numerical Simulations of Turbulent Reacting Flows

AIAA'87

AIAA-87-1324

On Direct Numerical Simulations of Turbulent Reacting Flows

W.-H. Jou, Flow Research Company, Kent, WA, and J. J. Riley, University of Washington, Seattle, WA

AIAA 19th Fluid Dynamics, Plasma Dynamics, and Lasers Conference
June 8-10, 1987/Honolulu, Hawaii

ON DIRECT NUMERICAL SIMULATIONS OF TURBULENT REACTING FLOWS

W.-H. Jou*
Flow Research Company, Kent, Washington 98032

James J. Riley†
University of Washington, Seattle, Washington 98195

Abstract

We present a description of the emerging field of direct numerical simulations of turbulent, chemically-reacting flows. The types of direct numerical simulations, physical issues related to implementing the simulations, as well as the various numerical methods used are described. Examples are presented of recent applications of direct numerical simulations to a variety of problems, displaying both the potential of the method and also some of its limitations. Finally, our view of the potential role of direct numerical simulations in future research on turbulent, chemically-reacting flows is presented.

1 Introduction

Turbulent flow dynamics are often a critical element in combustion processes. For example, in non-premixed reactions the overall rate of product formation is usually controlled by the ability of the turbulence to mix the reacting species down to the microscale. The present ability to model turbulence in combustion processes is very limited, however, due to the lack of understanding of the physical processes involved. This has led Waltrup[1] (see also Northam[2]), e. g., in a discussion of the development of liquid fueled, supersonic combustion ramjets, to list research into turbulent shear layers and turbulent boundary layers as the highest priority items deserving further research.

Most modeling of turbulent reacting flows to date is based upon either the Reynolds- (or Favre-) averaged equations, or the probability density function equations (or some combination of the two). Both approaches suffer from the closure problem, and hence rely heavily on empirical models which are of questionable validity and generality, especially for combustion processes. An alternative predictive approach to this problem, which avoids some of the problems of these other methods, is direct numerical simulations. This approach, as applied to chemically-reacting flows, is in its infancy. A significant amount of work using this methodology has been initiated over the past few years, and the method has tremendous potential in the future, as computers become larger and faster, and as numerical methods become more efficient and more accurate. The objective of this article is to explain the basic methodology of direct numerical simulations when applied to turbulent, chemically-reacting flows. The discussion will include the various methods of approach, the different numerical methods which are presently used, and the problems which can and cannot be addressed with this methodology. Since we are emphasizing the methodology, this article is not meant to be a complete review of past and current work. We will draw on examples from this work only to the extent that it helps to explain the methodology.

Direct numerical simulations involve the numerical solution of the time-development of the detailed, unsteady structures in a turbulent flow field. Using very efficient numerical methods and, usually, supercomputers, the fully nonlinear governing equations are solved directly so that, at most, only the smaller-scale motions need to be modeled. Statistical data are then obtained by performing averages over the computed flow fields. The procedure is analogous to laboratory experiments, but has the advantages that (i) most of the physical quantities of interest are known and their relevant statistical properties can be computed (since the entire flow field is known at every time step), (ii) the parameters can easily be varied, and (iii) experimental conditions are more controllable. The advantage over other numerical approaches is that the clo-

*Senior Research Scientist, Member AIAA
†Professor, Mechanical Engineering, Member AIAA

sure problem can be circumvented, and the behavior of large-scale structures directly addressed. The main disadvantage is the limited spatial and temporal resolution available, which limits the range of space and time scales (and hence maximum Reynolds and Damköhler numbers) that can be included in the simulations. At the present time direct numerical simulations are limited to use as a research tool. It is possible, however, that within the next decade certain types of direct numerical simulations will be used in applications.

The approach has been used successfully in the study of turbulent, nonreacting flows. For example, it has been applied to testing turbulence theories, from analytic theories (Orszag and Patterson[3]; Herring et al[4]) to second order closure modeling assumptions (Herring[5]; Schumann and Patterson[6]; Bardina et al[7]). Important advances have been made in the study of the atmospheric boundary layer (Deardorff[8]) as well as of neutral boundary layers (Moin and Kim[9]), of homogeneous shear and homogeneous straining flows (Rogallo[10]), and of density-stratified flows (Riley et al[11]). The method has been validated by comparing simulation results with laboratory data for the cases of homogeneous, turbulence decay (Mansour et al[12]), turbulent wakes (Riley and Metcalfe[13]), turbulent mixing layers (Riley and Metcalfe[14]), and turbulent boundary layers (Moin and Kim[9]).

In this paper we will first discuss in detail the methodology involved in direct numerical simulations of chemically-reacting turbulent flows. This involves discussions of the various types of direct simulations, of some physical issues related to the implementation of direct simulations, and of the numerical methods employed in simulations to date. We next discuss examples of direct simulations, pointing out in particular some of the ways that direct simulations can be used to address important issues. Finally we will discuss how we believe the methodology should be used in the future, including the critical areas of research in further developing the methodology, and problems that are best addressed by this methodology. For an excellent review of the methodology and applications of direct numerical simulations to nonreacting flows see Rogallo and Moin[15].

2 Methodology

As the field of direct numerical simulations has developed over the past 17 years, a variety of implementations has emerged, and several different numerical methods employed. In this section we will discuss these different implementations and the numerical methods used, as well as several physics issues which must be addressed if one is to properly apply the methodology.

2.1 Direct Numerical Simulations

By the term direct numerical simulation we mean a numerical calculation which solves for the time development of detailed, unsteady structures in a turbulent flow field. In particular, we exclude any calculation using the Reynolds- (or Favre-) averaged equations, even if applied to a (statistically) unsteady turbulent flow. There are several implementations of direct numerical simulations, which can be classified as follows.

Full turbulence simulations (FTS) are calculations in which all of the dynamically significant length and time scales of motion are included. This implies resolving length scales ranging from the size of the domain of interest down to scales smaller than those at which viscous dissipation and chemical reaction occur. We can obtain an estimate of this range of scales for nonreacting flows by examining the ratio of a length scale characterizing the energy-containing range (L_ϵ) to the Kolmogorov length scale (L_k), which characterizes the dissipation range. The Kolmogorov length scale is defined by $L_k = (\nu^3/\epsilon)^{1/4}$, where ϵ is the energy dissipation rate. Estimating ϵ by u'^3/L_ϵ (Batchelor[16]), where u' is an rms turbulent velocity scale, the ratio of the energy-containing scale to the Kolmogorov scale is approximately

$$\frac{L_\epsilon}{L_k} \sim \frac{L_\epsilon}{(\nu^3/\epsilon)^{1/4}} \sim \left(\frac{u' L_\epsilon}{\nu}\right)^{3/4}. \qquad (1)$$

We see that this ratio of length scales is roughly proportional to $R_L^{3/4}$, where $R_L = u' L_\epsilon/\nu$ is a Reynolds number based upon the energy-containing range of scales. Therefore the number of grid points N in a particular direction is expected to be proportional to $R_L^{3/4}$, so that, in a three-dimensional simulation, the total number of grid points will be proportional to $(u' L_\epsilon/\nu)^{9/4}$. Most technological flows have Reynolds numbers in the tens of thousands or more, which would require more grid points than computers of the present or near future could handle. With present-day supercomputers, the maximum Reynolds numbers achieved in such simulations are in the range of several hundred. This limits this approach to basic research studies.

Full turbulence simulations originated with the work of Orszag and Patterson[3], who studied homogeneous decaying turbulence and the validity of certain analytical theories of turbulence. The approach has been employed further in many basic research issues, including turbulent diffusion (Riley and Patterson[17]), magnetic turbulence (Schumann[18]), the behavior of pressure/strain-rate correlations (Schumann and Patterson[6]; Feiereisen et al[19]), turbulent wakes (Orszag and Pao[20]; Riley and Metcalfe[13]), turbulent mixing layers (Riley and Metcalfe[14]), and turbulent boundary layers (Moin and Kim[6]). Examples of full turbulence simulations of chemically-reacting flows are the work of Riley et al[21] and McMurtry et al[22].

In order to avoid the Reynolds number limitations inherent in full turbulence simulations, Lilly[23] and Deardorff[24] introduced the methodology which is now know as large eddy simulations (LES). In large eddy simulations the equations of motion are prefiltered to eliminate the scales of motion smaller than those resolvable on the computational mesh. This produces equations analogous to the Reynolds averaged equations, only the averaged (filtered) terms now represent the unresolved motions. Models are proposed for the filtered terms, and then the equations are solved for the resolvable scales of motion (large eddies).

The advantage of this approach over FTS is that it has the potential to treat very high Reynolds number (and very fast reaction) flows. The disadvantage is that *ad hoc* models are necessary to close the equations, which introduce some uncertainty into the validity of the results. The advantage of the method over solving the usual Reynolds-averaged equations is that the large-scale turbulent motions are treated almost exactly, and only the smaller scales are modeled. In the Reynolds-averaged approach, however, all scales of the turbulence are modeled. Therefore it would be expected that the LES would provide a more accurate simulation of the turbulence, that the LES results would be less sensitive to modeling assumptions (since scales comprising only a small percentage of the energy are usually modeled), and that this sensitivity would decrease as the resolution increases. Another advantage is that information about the detailed structures of the larger-scale motions is provided by LES. The disadvantage is that lengthy computations of unsteady three-dimensional (or possibly two-dimensional) flows are required, whereas, in the Reynolds-averaged approach, usually steady-state and lower dimensional equations are considered. Furthermore a much larger range of length and time scales is necessary in the LES approach, so that a significantly greater computational effort is required.

Large eddy simulations can be classified into two categories, two-dimensional (or axisymmetric), and three-dimensional. In two-dimensional LES, in addition to filtering out the subgrid-scale motions, the equations are also averaged in one spatial direction. This results in a much simpler numerical problem. More of the scales of motion need to be modeled, however, decreasing the reliability of the model. Furthermore, key three-dimensional aspects of turbulence, e. g., vortex-tube stretching, are eliminated, which considerably limits the dynamics that can be simulated. Two-dimensional LES have been mainly applied to the study of plane turbulent mixing layers, where it is argued that a significant portion of the turbulence dynamics are two-dimensional. Studies have been carried out of both nonreacting (e. g., Patnaik et al[25]; Riley and Metcalfe[14]; Lesieur et al[26]; Jou and Menon[27]; Menon and Jou[28]) and reacting flows (e. g., Ashurst and Barr[29]; Ghoniem et al[30]; McMurtry et al[22]).

Three-dimensional LES have been used in a variety of problems, beginning with the boundary layer studies of Deardorff[5,24], and continuing with calculations of homogeneous decay (Mansour et al[12]), channel flows (Moin and Kim[6]; Grötzbach and Schumann[31]), and more recent work on the atmospheric boundary layer (Moeng[32]). At the present no three-dimensional LES of chemically-reacting turbulent flows have been performed.

2.2 Some Physics Issues

In direct numerical simulations it is important to estimate the length scales of the physical phenomena of interest so that an appropriate choice of the approaches discussed above can be made, and so that the phenomena can be adequately resolved numerically. This is particularly true when full turbulence simulations are employed. Usually it is also important to estimate the parameter range for which the simulations can accurately predict the phenomena of interest. Given the performance of supercomputers available now and in the near future, approximately two decades of length scales can be resolved in a three-dimensional simulation. As mentioned in the previous section, using Equation (1) to estimate the maximum Reynolds number in terms of the ratio of the largest to the smallest length scales which can be resolved,

the maximum Reynolds number is found to be several hundred.

When chemical reaction is included, additional physical parameters are involved. We shall use a nonpremixed reaction to demonstrate how the physical parameters related to chemical reaction may affect the scaling and thus the technique for direct numerical simulations. For convenience in our discussion we assume that the Prandtl and Lewis numbers are both unity, so that only one dissipative coefficient, namely the viscosity, is an independent parameter. The chemical reaction rate is characterized by the Damköhler number Da_I defined as

$$Da_I = \frac{r C_\infty L_C}{u'}. \qquad (2)$$

where r is the the rate coefficient, C_∞ a characteristic value of the chemical concentration field C, and L_C a length scale characterizing C. This Damköhler number gives an estimate of the ratio of the reaction terms to the advection terms in the conservation equation for the chemical concentration, and when it is of the order unity, the diffusion length scale, i. e., the Batchelor length scale $(D\nu/\epsilon)^{1/2}$, and the thickness of the reaction zone are of the same order. (Here D is the molecular diffusivity of C). A simulation which resolves the diffusion scale will then also resolve the reaction zone. At high Damköhler numbers, for binary reactions the ratio of thickness of the reaction zone to the diffusion length scale decreases as $O(Da_I^{-1/3})$ (Gibson and Libby[33]). Inside the reaction zone, the species concentration is small and of the same order in Da_I as the thickness of the reaction zone. Thus, well designed direct numerical simulations can probably handle up to about $Da_I = 30$ without losing numerical accuracy.

For very high Damköhler numbers, the reaction zone cannot be resolved using currently available computers. It is well known, however, that the rate of chemical reaction is controlled by the rate of diffusion of the reactants into the reaction zone, which is extremely thin. If the reaction zone is treated as a sheet with zero thickness, the gradient of the concentration of the reactants is discontinuous there. The numerical solutions of the species concentration equation may encounter loss of accuracy. Fortunately, a conserved scalar, which is smooth across the reaction sheet, can be defined for cases in which the species diffusion coefficients are equal and the Lewis number is unity (Williams[34]). The species concentrations, including the reaction product, can be inferred from the conserved scalar. For a flow with constant density, accurate results can be obtained by numerical simulations using this approach (Riley et al[21]).

For a flow in which the chemical heat release affects the dynamics of the fluid through variable density, the situation is somewhat different. Although the species concentrations as well as the temperature field, and thus the density field, can still be inferred from the conserved scalar, the fiist spatial derivatives of these quantities are discontinuous at the reaction sheet. In the solution of the conservation equations for a variable density flow, spatial derivatives of the density field are required. Numerical inaccuracy due to the Gibb's phenomena may thus result near the reaction sheet in any numerical method intended to capture the reaction sheet. This discontinuity in derivatives is due to the discontinuous nature of the relationship between the conserved scalar and temperature (see Figure 1), and may be circumvented by smoothing this relationship. In physical space, this smoothing process artificially broadens the reaction zone into a region of finite thickness. The structure of this reaction zone is then entirely artificial. If the smoothing process, however, can be contained within a scale small with respect to the diffusion length, the effects of the artificial broadening of the reaction zone on the fluid dynamics as well as on the species diffusion may not be affected. Since the reaction is diffusion controlled, it is expected to be independent of the structure of temperature and density field within the artificial reaction zone. The potential of this method has not yet been explored.

For a reaction with an Arrhenius temperature dependent rate, an additional parameter E, the activation energy nondimensionalized by the adiabatic flame temperature, is present. This additional parameter is usually large so that the large activation energy asymptotic analysis (Williams[34]; Buckmaster and Ludford[35]) can provide valuable information. Since the Damköhler number, the nondimensional activation energy, and the Reynolds number are all large numbers, there is a relative ordering among these parameters which determines the structure of the flame. It is known that in a flow field where the local dissipation rate is high enough, flame extinction occurs (Liñán[36]; Givi et al[37]). Heat is diffused away from the flame rapidly enough so that the chemical heat release fails to sustain the flame temperature at a value above which the chemical reaction occurs. Because of the exponential nature of the temperature dependent reaction rate, the heat release is reduced rapidly

once the temperature falls below the flame temperature. To establish the relative ordering of the parameters involved, we start with the known scaling of the flame thickness of $O(E^{-1})$ when the flame extinction occurs (Liñán[36]). The species concentration in the flame sheet is also of the same order in E. Therefore, the balance between the diffusion term and the reaction term gives

$$\frac{\nu}{L_t^2 E^{-2}} \sim r_f C_\infty E^{-1} \exp(-E). \qquad (3)$$

where the activation energy E is normalized by the adiabatic flame temperature, and r_f is the frequency factor of the chemical reaction. This relation can be rewritten in terms of a redefined Damköhler number D_a as

$$D_a = \frac{Da_I R_L^{-1/2}}{E^3 e^E} = O(1), \qquad (4)$$

where Equation (1) has been used, and Da_I only includes the frequency factor r_f. This is the relative ordering among the three parameters R_L, Da_I, and E for local flame extinction to occur. In this parameter range, the assumption of chemical equilibrium in the region outside of the flame sheet is no longer valid, as part of the flow field is chemically frozen. If the Damköhler number is so large that the above relation is not satisfied, the chemical reaction is again in equilibrium and the flame thickness is scaled by an additional factor of $Da^{-1/3}$.

In many practical flows, both the Reynolds number and the Damköhler number are very large and are beyond the range for accurate full turbulence simulations. Interesting information on flame extinction occurring in a high Reynolds number, high Damköhler number flow may, however, be obtained by a simulation with moderate Reynolds number, Damköhler number and activation energy if the above relation can be satisfied. This conclusion, of course, is based on the assumption that a high enough Reynolds number can be attained in the simulations so that the estimate given by Equation (1) can be employed. With continued improvement in the computational power of supercomputers, the simulation of dissipative behavior of a turbulent flow becomes increasingly possible.

Since both chemical equilibrium flows and chemically frozen flows can be computed using a conserved scalar, one may be tempted to think that such an approach, with the reaction sheet treated asymptotically as a discontinuity, can be used when the activation energy is very high. The problem, however, turns out to be nontrivial. Along the sheet where the value of conserved scalar is at the stoichiometric ratio, the instantaneous local Damköhler number can be computed and the flame extinction criterion of Liñán[36] can be applied. The difficulty lies in the fact that the flow field outside of the reaction zone is divided into a part that is in chemical equilibrium and a part that is chemically frozen. The transition at the edge of the flame sheet to chemically frozen flow must be treated. If the reaction zone is treated as a sheet, this transition region is a point flame tip. The relationships between the conserved scalar and other relevant scalar quantities are different for an equilibrium flow and for a frozen flow. It is not clear how the scalar variables in a mixed equilibrium-frozen flow can be inferred from a conserved scalar, even if the edge of the flame sheet can be located. Ingenious methods must be invented for treatment of the flame sheet with local extinction in a full turbulence simulation.

Despite the technical obstacles one may encounter, the treatment of the reaction zone as a discontinuous sheet in the simulation of turbulent reacting flows seems to be an important direction in the future.

2.3 Numerical Methods

With the understanding of the length scales of the physical phenomena involved and of the accuracy requirements of various approaches of direct numerical simulations, an appropriate numerical scheme must be chosen for resolving the physics. Various numerical schemes can be used in direct numerical simulations of turbulent reacting flows. These methods can be classified into three main categories: spectral and pseudo-spectral methods, finite difference and finite volume methods, and vortex methods. These methods vary in accuracy, computing efficiency, and flexibility in treating boundary conditions. Each method has certain advantages and disadvantages, with no one method the obvious choice for all problems. In selecting a numerical method for a specific problem, it is important to understand the properties of methods, so that one may make the optimum choice of numerical method for the particular problem of interest.

Much of the work on direct numerical simulations of nonreacting turbulent flows has employed spectral or pseudo-spectral numerical methods.[1] The application of these methods to turbulent reacting flows was initiated by Riley et al[21], and continued by McMurtry et

[1] This has led, in fact, to some confusion, as some people have tended to equate direct numerical simulations with spectral numerical methods.

al[22], Givi et al[37], Leonard and Hill[38], and McMurtry et al[39].

In the spectral or pseudospectral method (see Gottlieb and Orszag[40] for a rather complete discussion of these methods), the dependent variables are expanded in truncated series of orthogonal functions satisfying the required boundary conditions. Spatial derivatives are then evaluated locally in the transformed domain, while nonlinear products are evaluated locally in the physical domain. Mainly Fourier series and Chebyschev polynomials have been used. With these functions, the mapping between the physical space and the configuration space can be efficiently performed using a Fast Fourier Transform algorithm. The spectral method, which is equivalent to a Galerkin method, involves eliminating entirely the aliasing errors that arise in evaluating the nonlinear terms. The pseudospectral method, which is equivalent to collocation, retains some of these aliasing terms. The pseudospectral methods, which are much easier to implement and run several times faster, have been most often used, although not exclusively (e. g., Orszag and Patterson[3]; Kerr[41]; Rogallo[10]). Various time-stepping schemes have been employed with these methods, including leap-frog, Adams-Bashforth, and higher-order Runga-Kutta schemes.

Spectral and pseudospectral methods have the advantages that phase errors are very small and rates of convergence are very high. If the dependent variable is sufficiently smooth and the orthogonal functions have been properly chosen, then as the number of orthogonal functions N becomes large, the truncation error decreases faster than algebraically (Gottlieb and Orszag[40]). Various authors (e. g., Peyret and Taylor[42]; Haidvogel et al[43]) have found that the pseudospectral methods are at least twice as accurate in each spatial dimensions compared to finite difference schemes using the same resolution.

In order to explore the capabilities of pseudospectral numerical methods when applied to chemically reacting flows, Riley et al[21] applied the method to the color problem with diffusion and reaction. It was found that both diffusive and dispersive errors decay rapidly with N (the number of Fourier modes) when a sufficiently small time step is used. Because of this high convergence rate and the lack of phase errors, high gradient regions could be accurately and efficiently computed with a moderate number of Fourier modes. This property of the method is important for simulations of a reacting flow where the molecular diffusion is of primary concern. When the number of modes was not sufficient to resolve the dependent variables, a build-up of amplitude near the cut-off wave number occurred, leading to significant errors in the solutions.

There are several drawbacks with this method. The class of complete basis functions which allow matching the boundary conditions and which also possess the properties of rapid convergence are limited. The application of Fourier series is restricted to problems with periodic or with free-slip boundary conditions. While Chebyschev polynomials can be applied to problems with arbitrary boundary conditions, the distribution of collocation points for the method may not be ideal for many problems. These collocation points are densely packed near the boundary with spacing of $O(N^2)$. Additional mapping is required, particularly in the far field, to adjust the spacing to a more reasonable distribution. The method in its original form is limited in its capabilities for computing flows around a complex geometrical shapes and for treating inflow and outflow boundary conditions. Recent work on the spectral element method (Korczak and Patera[44]; Ghaddar et al[45]), however, has made considerable progress in removing these limitations. Spectral methods, because of their inherent nonlocal properties, also have difficulty in capturing discontinuities such as shocks while maintaining spectral accuracy. Gibb's phenomenon develops at the discontinuities, degrading the accuracy of the solution.

Finite difference methods can be constructed to arbitrarily high order of accuracy, but with increasing computational effort. In general, second or fourth order schemes are used in computing complex flow fields. Unfortunately, the large dispersive and dissipative errors in second order central difference schemes produce results which are not acceptable for moderately high Reynolds number flows or for flows with shock waves. To circumvent this problem, either explicit artificial dissipation is added to the scheme, or the scheme is constructed in such a way that artificial dissipation is implicitly included. Examples of the former can be found in Beam and Warming[46] and Jameson et al[47], and those of latter in MacCormack's[48] scheme and the QUICK (Quadratic Upstream Interpolation for Convective Kinematics) scheme (Leonard[49]). The methods can thus be applied to smooth flows at moderate Reynolds number. In fact, many schemes can compute flow with extremely high Reynolds number while retaining numerical stability. The Reynolds number in these computations probably loses its meaning, however, as the numerical dissipation dominates the molecular viscosity. Therefore, only large-scale

phenomena may be captured accurately using such a method at high Reynolds number. Hence, in applying these schemes to reacting flows, one should be careful in the interpretation of the results. Examples of using MacCormack's scheme for large eddy simulations can be found in the simulations of flow in a propulsion device (Menon and Jou[28]; Jou and Menon[27]).

To prevent artificial viscosity from smearing discontinuities (e. g., shocks) over a large number of grid points while eliminating spurious oscillations around a discontinuity, a class of numerical schemes has been developed. Boris and Book[50] were the first to construct a finite difference scheme, the Flux Corrected Transport scheme, which preserves the monotonicity of flow variables in a high gradient region. Recent development of the so-called Total Variation Diminishing (TVD) schemes (e. g., Harten[51]; Davis[52]; Roe[53]; Yee[54]) also belong to this category. The essential feature of these schemes is a "smart" artificial viscosity, in the form of a flux limiter, which is small in the region of smooth flow, but which reduces the numerical scheme to a low order one near sharp gradients. The solution can thus "negotiate" the sharp gradient without producing spurious oscillations. Study of the dissipative properties of TVD schemes using a color problem is discussed by Smolarkiewicz[55]. It was found that the solution maintains the monotonicity property. Dissipative errors, however, are substantial. Again, molecular diffusion can not be treated accurately for a high Reynolds number flow, even when the computations are stable. This type of scheme is quite successful in computing very complex patterns of detonation waves (e. g., Guirguis et al[56]). Its applications to other reacting flows can be found in the work by Kailasanath et al[57], where the flow is assumed inviscid and the chemical reaction is modeled.

For a full turbulence simulation of a reacting flow in which no phenomenological model is desirable, the detailed molecular dissipative processes are essential elements of the physics. Thus, the careful construction of a finite difference scheme without numerical dissipation in high gradient regions is important. The Reynolds number, the Damköhler number, and the activation energy for these simulations will then be restricted to moderate values. These restrictions are likely to be more stringent for finite difference methods than those for pseudospectral methods. For large eddy simulations, however, the numerical dissipation can be considered as a crude subgrid-scale model.

Finite difference methods have advantages over spectral methods in several aspects. It is easier to construct a finite difference code than a pseudospectral code for flow with complex geometry. If properly implemented, shock waves can be captured more accurately with finite difference schemes. Finally, for the same number of grid points, the computational efficiency of a finite difference scheme is generally higher than for a pseudospectral scheme.

An interesting numerical method for solving thermo-fluid problems is the vortex, or perhaps more appropriately, the distributed singularity, method. Examples of the application of this method to reacting flows can be found in the research of Ghoniem et al[30], Ghoniem and Givi[58] and Ashurst and Barr[29] for two-dimensional flows. Applications to three-dimensional nonreacting flows are just emerging (Leonard[59]; Ashurst and Meiburg[60]; Ghoniem et al[61]). Only two-dimensional flows will be discussed here. In solving the governing equations subject to the small Mach number approximation, the velocity field is decomposed into a solenoidal part and a potential part:

$$\mathbf{u} = \nabla \wedge \Psi + \nabla \Phi.$$

If the vorticity distribution is discretized and its spatial distribution is known, then the solenoidal velocity field can be obtained using a Green's function which satisfies the required boundary conditions. Note that the Green's function can be singular at a convex corner. The heat of combustion produces a local dilatation which is idealized as a mass source term in the Poisson equation governing the potential field Φ. Again, a Green's function approach can be employed to find the potential flow field. The combined flow velocity induced at the locations of each discrete vortex and dilatation source convects these sources to new locations. If a convex corner is present, then new vortices must be shed at the corner in order that the Kutta condition be satisfied there. Viscous diffusion is simulated by a random walk of the discrete vortices.

In its application to the combustion of a premixed gas, the flame sheet is treated as a discontinuous surface and its location is tracked using the local laminar flame velocity (Sethian[62]). It is equivalent, in spirit, to the shock-fitting method in the computation of compressible flows with shock waves. The smoothing of flame location, however, may be required to prevent a saw-tooth instability (Pindera[63]). This is equivalent of adding some form of artificial dissipation, the effects on the accuracy of the computation of which are not understood.

Since the flow field away from the sources is expressed analytically in terms of the Green's function,

only highly complex source regions require discretized numerical computations. Presumably, the computations can be made much more efficient than the numerical solution of the primitive equations. No direct comparison, however, between the computational efficiencies of the distributed singularity method and the discretized field methods is available.

The methodology described above applies to constant density flows, but with concentrated mass sources to represent local volume expansion due to heat release. Certain dynamics are lost, however. For a flow with density discontinuity, such as a flame front in a premixed reaction, the velocity induced by the vortices and computed on each side of the discontinuity by the Biot-Savart law will be equal. The dynamic boundary condition at the density discontinuity therefore cannot be satisfied unless new vortices are introduced there. This is the manifestation of the effect of baroclinic torque. Recently, the generation of vorticity at the flame front was taken into consideration by Pindera[63] using the vorticity jump condition across a discontinuity derived by Hayes. The effects of this baroclinic torque on the evolution of the flow field were shown to be very strong.

The vortex method presents a useful tool to compute in two spatial dimensions the large-scale features of complex phenomena associated with reacting flows. The computation is stable for very high Reynolds number. Whether the resulting flow field, however, contains all features of a high Reynolds number turbulent flow is still a subject for debate. The results of simulations using this method in two dimensions must be interpreted in the context of a large eddy simulation. Applications of this method to three-dimensional nonreacting flows have just begun, and the three-dimensional vortex stretching mechanism can thus now be simulated. As discussed in the previous section, the spectral bandwidth of a flow increases as the Reynolds number increases. Therefore, although the vortex method may produce stable computations, in order to describe all scales of turbulence accurately the number of singular vortex elements may increase with Reynolds number at a similar rate as the computational elements in a pseudospectral or a finite difference calculation.

3 Examples

In this section we introduce examples of direct numerical simulations in order to demonstrate how such simulations can be used in the study of turbulent, chemically-reacting flows. We begin with a sequence of related numerical experiments.

3.1 A Step-by-Step Sequence

Perhaps, the best way to illustrate the use of direct numerical simulations of reacting turbulent flows is to describe some examples from the recent literature. These examples are not meant to be exhaustive, but are chosen to illustrate the general approach. We shall begin with a series of studies in which we have been directly involved. This series starts with the very simple case of a constant density flow, and gradually the complexity of the physical model is increased. In doing so, each of the physical mechanisms can be turned on and off in order to isolate their individual effects on the overall behavior of the flow and chemical reaction. In this manner a systematic understanding of the physics of turbulent reacting flows can be obtained.

The series started with the work of Riley et al[21]. The flow under consideration is a two stream mixing layer with one reactant on each side. The fluid is assumed to be constant density, so that the fluid dynamics are independent of chemical reaction. The species concentrations are influenced by advection, molecular diffusion, and chemical reaction. The chemical reaction is taken as a binary, single step, irreversible reaction with a constant rate coefficient. (Hence, in particular, the reaction rate is temperature independent.) This simple model addresses effects of the fluid dynamics on the chemical reaction, but not vice versa. In order to avoid the significant numerical difficulties associated with inflow and outflow boundary conditions, and to take advantage of Fourier pseudospectral numerical methods, the flow is assumed to be periodic in the streamwise direction. Therefore the temporally growing mixing layer was studied, whereas in laboratory flows the spatially growing layer is investigated. The temporal problem is, however, closely related to the spatial problem when viewed in a reference frame moving at the average velocity, and many of the dynamic characteristics of the spatial problem are contained in the temporal case. Full turbulence simulations in three spatial dimensions were performed using 64x64x64 point Fourier decomposition of the flow variables. Typical values of important parameters for the simulations are: $Re = \Gamma L_{1/2}/\nu = 92$, $Da_I = rC_\infty L_r/U = 0.25$, and $Sc = \nu/D = 0.6$. (Here Γ is the velocity difference across the mixing layer, and $L_{1/2}$ is the mean velocity half-width). Also, cases

with infinite Damköhler number were computed using a conserved scalar approach.

Figure 2 shows a series of concentration contour plots in a streamwise section, displaying the time-development of the layer and, in particular, the general behavior of the reaction zone. Even with this limited range of parameters, several important observations and conclusions are obtained concerning the fluid dynamical effects on chemical reactions. Qualitatively, the coherent structures in a turbulent flow increase the interface between the two species, thus increasing the overall reaction rate. Quantitative information is obtained by taking (spatial) averages of various flow variables from the results of simulations. Mean product thicknesses are computed at various times, and show that the profiles of chemical species concentrations are self-similar. A most interesting result is obtained from the averages of the reaction term at various times. With constant reaction rate, the reaction term can be averaged to give

$$r\overline{C''_A C''_B} = r\overline{C''_A}\,\overline{C''_B} + r\overline{C''_A C''_B}$$

The individual components of the above relation as a function of the cross stream coordinate are given in Figure 3. The two terms on the right hand side are of the same order of magnitude and are of opposite sign. It is very clear that the modeling of the correlation of the fluctuations of species concentration must be performed carefully to ensure that the overall chemical reaction rate is accurately computed. A surprising result from the study is the weak dependence of the product thickness on the Damköhler number. The product thickness for the infinite reaction rate case, which is completely diffusion controlled, is only about 10% greater than for cases with moderate Damköhler numbers. Finally the similarity profiles for the average product, computed from the infinite reaction rate case, compared favorably with the experimental results of Mungal[64], giving some confidence in the results of simulations.

The parameter range investigated in these experiments was very limited. The effects of Damköhler number can probably be examined in further detail by performing simulations with values of up to about 20 to 30. The behavior of solutions can be studied as the reaction rate is systematically increased. The grid resolution has restricted the scales of turbulence being simulated. With a supercomputer such as National Aerodynamic Simulator, a 256x256x256 grid point simulation is possible and would greatly enhance the understanding of the physical process at higher Reynolds and Damköhler numbers.

After addressing the fluid dynamical effects on chemical reaction, a logical extension of the work is to investigate how the chemical reaction modifies the flow field. The chemical reaction can affect the fluid dynamics through the variable density, which is caused by the thermal expansion of the fluid associated with chemical heat release. This aspect of the problem was addressed by McMurtry et al[22,39]. These authors assumed that the characteristic Mach number of the flow is much smaller that unity. (In practice this was accomplished by keeping the Mach number of the flow sufficiently small (< 0.3) and the chemical reaction sufficiently weak.) For the fully-compressible flow equations including chemical heat release, a formal expansion of the independent variables, in terms of a power series in the Mach number, is made. This results in a set of equations as the lowest order approximation in which acoustic waves, a result of the elastic properties of the gas medium, are filtered out from the system, while the density variations due to heat release effects are retained (Rehm and Baum[65], Sivashinsky[66], Buckmaster[67], Majda and Sethian[68], McMurtry et al[22]). The advantage of using this set of *approximate equations is that* the numerical method does not need to track high frequency acoustic waves. Thus larger time steps can be used, so that the computation is much more efficient. With the variable density of the fluid taken into consideration, the chemical reaction and the fluid dynamics are truly coupled.

McMurtry et al[22] first developed a pseudospectral numerical scheme which solves the equations for variable density flows in two spatial dimensions. The flow under consideration is the temporally developing mixing layer as formulated by Riley et al[21]. Qualitative effects of the heat release are obtained, e. g., by comparing vorticity contour plots from these simulations to those obtained with no heat release (see Figure 4). The roll-up of vorticies is substantially suppressed by the heat release, as is evident from this figure.

In a two-dimensional flow, the vorticity transport equation can be written in the following form:

$$\frac{D}{Dt}\left(\frac{\omega}{\rho}\right) = \frac{1}{\rho^2}\nabla\rho\wedge\nabla p + \frac{\mu}{\rho}\nabla^2\omega.$$

Here ω is the vorticity vector, ρ is the density, and p the pressure. There are two principal mechanisms by which the density of the fluid can affect the vorticity dynamics. The first is through baroclinic torques, represented by the first term on the right hand side. These torques are most effective in the neighborhood

of the reaction surface, where the density is lowest and the density gradient highest. This surface separates a region of production of vorticity from one of destruction. The ultimate effect appears to be to reduce the vorticity in the center part of the mixing layer, while increasing it at the outer edges, thus causing a more diffuse vorticity field. Without the baroclinic torques, the vorticity per unit mass, ω/ρ, would be conserved following the flow when viscous diffusion is neglected. Thus decreasing the local density and hence increasing the local volume (e. g., through heat release) will result in a decrease in the strength of the vorticity. Again the vorticity in the layer is made more diffuse. The combined effect is to weaken vortex rollup, causing less reactants to be entrained into the layer, and hence resulting in lower product formation.

Based on this preliminary work in two dimensions, McMurtry et al[30] developed a three-dimensional simulation code using the same methodology. In three-dimensional simulations, the additional effect of vortex line stretching is included, so that the simulations can more properly represent turbulence. Typical parameter values of $Re = 500$ and $Da_I = 2$ were chosen. Here $Re = \Delta U \delta/\nu$, where ΔU is the mean velocity difference across the layer, and δ is the initial vorticity thickness of the layer.

Secondary instabilities in the form of streamwise vortices have been observed in the simulations of a constant density flow (Riley et al[21]). Figure 5 shows a comparison from McMurtry et al[30] of instantaneous concentration contour plots in a cross-stream section for cases with and without heat release, revealing the three-dimensional nature of the flow. The heat release suppresses the secondary instabilites as well as the spanwise vortex rollup. The simulations generally confirmed what was observed in the two-dimensional case. In addition, the turbulent Favre-averaged kinetic energy equation was examined, and the magnitude of each term in the case with heat release was compared to that from a constant density case in order to better understand the effects of heat release. The turbulence production resulting from the work done by turbulent stress is shown to decrease in the case with heat release. It is interesting also to examine the left hand side of the turbulent kinetic energy equation:

$$\frac{\partial}{\partial t}(\bar{\rho}\tilde{q}) + \nabla \cdot (\mathbf{U}\bar{\rho}\tilde{q}) = \frac{D}{Dt}(\bar{\rho}\tilde{q}) + \bar{\rho}\tilde{q}\nabla \cdot \mathbf{U}.$$

Here $\bar{\rho}\tilde{q}$ is the Favre-averaged turbulent kinetic energy. The left hand side can thus be written as the substantial derivative of the turbulent kinetic energy and a term which gives the contribution from the dilatation $\nabla \cdot \mathbf{U}$. The dilatation field is, of course, the result of thermal expansion due to heat release. If the term with dilatation field is moved to the right hand side of the Favre-averaged turbulent kinetic energy equation, it will represent destruction of turbulent kinetic energy due to thermal expansion, a conclusion consistent with that obtained by using the vorticity transport equation.

The type of methodology used in this study has significant potential in future research. In particular, the use of a conserved scalar for infinite Damköhler number cases, with possible artificial smoothing of the flame structure, is a potentially fruitful research direction. High Damköhler number simulations, with $Da_I = O(30)$, may be performed to validate the infinite Damköhler number results using flame smoothing.

With a preliminary understanding of the heat release effects on turbulent mixing, the next step has been to examine how a temperature dependent chemical reaction rate would affect the flow field, and vice versa. According to the asymptotic analysis of ignition-extinction phenomena by Liñán[36], a diffusion flame in a medium with given activation energy may be extinguished when the local scalar dissipation rate exceeds a certain limit. For convenience of discussion, we assume that the temperature, concentration, and all the gas properties are the same for both the fuel and oxidizer, and that the frequency factor for chemical reaction and the density of the gas are both constants. The extinction limit is given by a lower bound on the local, instantaneous reduced Damköhler number as

$$0.125 Da_{II} |\nabla Z|^{-2} (E^{-3} e^{-E}) \leq 0.315 e,$$

where Z is an appropriately defined conserved scalar, $|\nabla Z|$ is evaluated locally at the stochiometric surface, and Da_{II} is the second Damköhler number, defined in terms of the free stream values and a characteristic length. For more details of this extinction limit, see Williams[34]. Peters and Williams[69] argued that, in the turbulent diffusion flame of a jet, the scalar dissipation rate near the jet exit is so large that regions of local extinction (holes) in the flame sheet may become connected so that the flame sheet is ruptured. A flame can thus not be sustained there. Hence, the flame lifts off and stabilizes at a location further downstream, where the local dissipation rate is smaller than the extinction limit. This explanation of flame liftoff is certainly plausible, although it is difficult to confirm

experimentally. Numerical simulations of this phenomena can be used to learn more about the structure of the flame sheet in a turbulent flow, and also to obtain a better understanding of the details of the mechanism of the rupturing of the flame sheet.

Givi et al[37] initiated an investigation of this problem using a temporally growing mixing layer simulation. The simulations were two-dimensional, and typical parameter values were $Re = 200$, $Da_I = 10$, and an activation energy of $E = 3$ when normalized by the adiabatic flame temperature. Figure 6 shows the contours of instantaneous rate of reaction. Along the braids of the rolled up vortex, where the strain rate is high, the temperature is reduced to a very low value and the flame becomes extinct. Givi et al also solve the equation for a conserved scalar field. For the infinite reaction rate case, the surface where the scalar achieves the stochiometric value is the flame sheet. An examination of the extinction condition given above, obtained from asymptotic theory, shows that, at the edge of the flame sheet in the simulation, the dissipation rate does satisfy the extinction criterion.

Further interesting questions regarding flame extinction can be addressed using numerical simulations. For example, after the flame becomes extinct, the reactants diffuse towards each other to form a premixed fuel mixture. Subsequent events are not clear. For example, when the dissipation rate has decreased to a low enough level as a result of diffusion, would the flame then propagate into the mixture in the form of a premixed flame? The preliminary simulation results indicate that reignition does not occur, and the reacting sheet continues to shrink. Of course, only cases within a restricted range of parameters were simulated. Whether the conclusion can be generalized or not remains to be determined. The mechanism by which the flame is reignited is important in understanding the nature of flame liftoff. To further investigate the structure of a flame sheet, a numerical code for simulating the three-dimensional turbulent motion in a plane jet with chemical reaction is currently being developed (Givi and Isreali[70]). Simulations of the flame extinction phenomena using this code will provide a more complete picture than the previous two-dimensional simulations. As we have discussed, the activation energy in a practical system is large. The flame, when it exists, has a thickness of the order of E^{-1} compared to the diffusion scale. Therefore numerical resolution is a serious problem. Yet a conserved scalar approach is not suitable since only part of the flow field is in chemical equilibrium; the remainder is chemically frozen. An ingenious approach is needed which would treat the flame sheet as a discontinuity.

3.2 Other Examples

An example of the use of full turbulence simulations to test theoretical hypotheses for chemically-reacting turbulent flows is given by Leonard and Hill[38]. They studied the behavior of two chemical species undergoing an irreversible, isothermal, second order chemical reaction in a homogeneous, incompressible, decaying turbulent flow. The initial concentrations for the two species were in stochiometric proportion and were defined as square waves which were out-of-phase so that the reactants were approximately segregated. In order to determine the effect of the reaction rate on various statistical properties, three calculations were performed, for Damköhler numbers of 0, 5, and 10. Pseudospectral numerical methods were used, the calculations being performed on 32x32x32 point computational grids. The initial turbulent Reynolds number (based upon the Taylor microscale) was 25, and the Schmidt number for both species was 0.7.

Two hypotheses were tested. The first was Toor's[71] hypothesis, which was made for reactants which are initially in stochiometric proportion and have equal diffusivities. Based upon results from certain limiting cases, Toor hypothesized that the reactant concentration covariance $\overline{C'_A C'_B}$ was independent of the reaction rate and therefore could be determined from a mixing experiment (without chemical reaction). Patterson[72] proposed a model for the joint probability density function (pdf) for (C'_A, C'_B) which does not explicitly depend on the initial stoichiometry and which enables the prediction of various terms in the moment equations for C'_A and C'_B, e. g., the reaction covariance term.

From the numerical simulations Leonard and Hill computed, in particular, the reaction covariance term for the three cases for different Damköhler numbers. They found that, as hypothesized by Toor, this term was approximately independent of the reaction rate. This allowed, e. g., the closure of the equations for $\overline{C'_A}$ and $\overline{C'_B}$, and their accurate estimation. The predictions of Patterson's model did not compare well with simulation results. In order to explain this discrepancy the joint pdf of C'_A and C'_B were computed from the simulation results, and were found to not retain the form assumed by Patterson.

The results of Leonard and Hill are only preliminary.

The resolution was fairly course and the Reynolds number, especially towards the end of the simulations, was very low. The work gives a good example, however, of how direct numerical simulations can be used to test theoretical hypotheses regarding chemically-reacting turbulent flows. We expect that this will be one of the principal uses of direct numerical simulations in the near future.

Another use of direct numerical simulations is in the prediction and study of reactant (and other parameter) probability density functions. There are a number of advantages in theoretical approaches to chemically-reacting turbulent flows which employ the pdf conservation equation (see, e. g., O'Brien[73]). For example, the reaction term in the pdf equation is closed, and the conserved scalar approach can be readily utilized. Closure problems for other terms, e. g., the mixing terms, remain a primary difficulty, however. Another difficulty with this approach is in the solution of the resulting equations. The dimensionality of the equations is the sum of the usual dimensions (e. g., $\mathbf{x}$, t) *plus* the usual dependent variables. Therefore for reacting flows the dimensionality of the system can become very large, obviating a solution by standard numerical methods. To circumvent this problem, Monte-Carlo methods have ben used to indirectly solve the the pdf equation (and to obtain other statistical quantities: Pratt[74]; Pope[75]).

In the Monte-Carlo approach, in order to solve the pdf equation an auxiliary problem, sometimes called a Langevin problem, is often introduced. The Langevin problem is a (theoretically) realizable process which has, as its pdf equation, the original pdf equation of interest. To solve for the pdf (or other statistics) of interest then, the auxiliary problem is solved (often many times), and either ensemble, time, or spatial averages are performed. The advantage of this approach is that the Langevin problem is usually much easier to solve numerically, and the computational time increases approximately linearly as additional dependent variables are included.

When applied to chemically-reacting turbulent flows, the Langevin problem for a modeled pdf equation is usually some simplified reacting flow system. As more sophistication is added to the modeled terms in the pdf equations, the Langevin problem becomes more like the original turbulent reacting flow. The realism of the pdf equation is then indicated by the sophistication of the corresponding Langevin system. As pointed out by Riley and Metcalfe[76], direct numerical simulations can be considered as Langevin systems for particular pdf model equations. And in fact considerable physics can be incorporate into this system, making the pdf model highly realistic.

Past Langevin systems used in Monte-Carlo approaches to solving the pdf equations have not directly included, e. g., the physics of the large-scale structures occurring in the flow, nor of the Schmidt and Reynolds number effects on micromixing. Those features were recently included in a study by Lin and Pratt[77] of a chemically-reacting, spatially-growing free shear layer. They considered a diffusion flame with an isothermal, irreversible, infinite-rate, binary chemical reaction. A two-dimensional large eddy simulation was employed, using a modified vortex method to compute the unsteady (incompressible) velocity field. The chemical reaction was treated using the conserved scalar approach, and, in particular, molecular mixing was treated using Curl's[78] model. The mixing rate β was determined from the estimation by Broadwell and Breidenthal[79] of the time scale required to diffuse across the Kolmogorov length scale. They used

$$\beta = C' |\boldsymbol{\omega}(\mathbf{x}, t)| \frac{Re^{1/2}}{Sc},$$

where C' is an empirical constant and $\boldsymbol{\omega}$ is the local grid-scale vorticity. Their work can be considered one of the first where subgrid-scale models were employed in a large eddy simulation involving chemical reaction.

Lin and Pratt carried out simulations for three different velocity ratios ($r = U_1/U_2 = 0$, 0.3, and 0.6), and two different Schmidt numbers (0.7 and 600). The latter corresponded to values for experiments carried out by Konrad[80] and Breidenthal[81], respectively. Their results for various velocity statistics gave reasonable agreement with laboratory data, except for the lateral rms velocity. Predictions of various concentration statistics, in particular, the dependence of the nondimensional product thickness on the Schmidt number, showed reasonable agreement with the laboratory data.

We think that the utilization of direct numerical simulations for Langevin systems for pdf model equations has considerable potential. It allows the input of rather sophisticated models into the pdf equations. On the other hand, pdf models might suggest particular subgrid-scale closures to be implemented in large eddy simulations.

The numerical simulation of compressible, turbulent, chemically reacting flows is in an embryonic state. There are specific physical phenomena in which acoustic waves are an integral component. For ex-

ample, turbulent reacting flows in a ramjet combustor may interact with acoustic waves to produce large amplitude pressure oscillations (e. g., Smith and Zukoski[52]). Furthermore Kelvin-Helmholtz instabilities are much weaker in supersonic mixing layers, which may result in drastic reductions in the rate of chemical reaction. Several preliminary attempts have been made to simulate these flows. For the ramjet problem, Menon and Jou[28] and Jou and Menon[27] used direct numerical simulations to address the interaction between vorticity fluctuations and acoustic waves in a combustor with no chemical reactions. Guirguis et al[56] included chemical reaction in a similar configuration. We shall briefly review the work of Jou and Menon[27] as an example of how one can deduce acoustic information from the results of the simulations.

Menon and Jou[28] considered the flow in a simplified model of a ramjet combustion chamber by solving the compressible Navier-Stokes equations in axisymmetric form using MacCormack's[48] explicit algorithm. Because the computer requirements for a three-dimensional simulation of this flow are beyond the capability of the existing computers, they addressed the effects of large scale vortical structures, which may be predominantly axisymmetric in this case. It is expected that only the longitudinal acoustic mode will interact with the vortical disturbances to produce the low frequency pressure oscillations prevalent in the combustor. Thus, axisymmetric vortical disturbances may be predominant. The flow field was started from rest by lowering the downstream pressure to a prescribed value. After an initial transient period, the flow field settles into a stationary oscillatory state.

As shown in the vorticity contour plot in Figure 7, the shear layer behind the backward facing step rolls up into vorticies, and the merged large structures subsequently impinge on the nozzle wall downstream. To understand the physical phenomena, the acoustic field is visualized in a unique way. If one defines the acoustic component of the disturbances to be that of an unsteady potential flow (Yates[83]), the instantaneous dilatation field $\mathcal{D}$ and the acoustic potential Φ are related as follows:

$$\nabla^2\Phi = \mathcal{D}.$$

Comparing this with the equation relating the vorticity to the stream function ($\nabla^2\psi = -\omega$), which represents the solenoidal field, it is seen that the dilatation field plays a role in acoustics analogous to that of vorticity for a solenoidal field. Since vorticity has been successfully used to visualize rotational disturbances, the dilatation field may be taken as a representative quantity for visualizing acoustic disturbances.

Figure 8 shows an instantaneous dilatation field together with the corresponding vorticity field. It was found that the near-field dilatation is dominated by the pseudo-sound and the propagational aspects of acoustic waves are lost. The dilatation field thus gives the detailed characteristics of the acoustic sources. Around each vortex a quadrupole dilatation field is clearly identifiable. Near the region where large vortex structures impinge on the nozzle, the structure of dilatation field appears very complex. The wavelengths of the longitudinal acoustic waves in the combustion chamber are of the order of the length of the combustor, and hence are much larger than the length scale of the impinging vortex. Thus, the acoustic sources near the vortex impingement point can be considered compact. The behavior of such a compact source can be represented by its multipole expansion in terms of a distributed dilatation field. Therefore, we take the first two spatial moments of the complex dilatation field over a region to give the monopole and dipole as:

$$Q_1 = \int\int_V \mathcal{D}\, dV$$

$$\mathbf{Q_2} = -\int\int_V \mathcal{D}\,\mathbf{x}\, dV + \frac{Q_1}{V}\int\int_V \mathbf{x}\, dV.$$

The time variation of the vorticity fluctuations in the same region are also determined by integration over the same volume. Figure 9 shows the time variation of the monopole, the dipole and the vorticity. It is evident that, as the large vortical structures impinge on the nozzle wall, a strong dipole which is approximately 180° out-of-phase with the vorticity fluctuation is present.

Jou and Menon[27] used this information to construct a model for acoustic wave/vortex interactions. This method of simulation and data analysis demonstrates the potential use of numerical simulations of compressible flow in analyzing the behavior of flow variables such as the dilatation field which are difficult or impossible to measure experimentally. The extension of this simulation method to cases with chemical reaction, which may create strong acoustic monopoles, is currently under investigation. Extension of this code to three-dimensions requires the capabilities of the next generation of supercomputers. Preliminary simulations of the combustion and flow field in a ramjet have been reported by Kailasanath et al.[57]

Supersonic combustion is an active area of research, partly because of the currently interest in the National

Aerospace Plane. Drummond[84] attempted to simulate a mixing layer with a realistic hydrogen-oxygen reaction. Some further results were presented by Zang et al[85]. The Mach number of 1.5 and Reynolds number of 3700 were chosen. The finite-thickness trailing edge of a splitter plate was suspected of playing a primary role in triggering the instabilities in a supersonic flow. The results are preliminary, and require further research.

4 Conclusions

Direct numerical simulations of turbulent reacting flows have begun to attract interest among combustion scientists, fluid mechanicists and numericists. The present article reviews some research on turbulent reacting flows using direct simulations, emphasizing the methodology, the kinds of results obtainable, and the strengths and limitations of the approach.

There are two implementations of direct numerical simulations: full turbulence simulations (FTS), in which all of the dynamically significant space and time scales are resolved; and large eddy simulations (LES), in which the governing equations are filtered at the numerical grid scale, and the subgrid-scale motions modeled. Because of limited numerical resolution FTS is restricted to moderate Reynolds and Damköhler numbers (although the conserved scalar approach can for certain cases eliminate the latter restriction), whereas LES can be applied, at least in concept, to high Reynolds number, high Damköhler flows. Three general classes of numerical methods have been used in the implementation of direct simulations: spectral methods, finite-difference methods, and vortex methods (and some combinations of the three). Each numerical method has its own advantages and disadvantages, with no one method the obvious choice for all problems.

The potential advantages of direct numerical simulations, when the method can be applied, are the following: the flow can be examined in detail, since all quantities are known at each point in space and time; parameters can be easily varied and experimental conditions are easily controlled; large-scale structures are directly addressed; and results are less sensitive to the models used, since only, at most, the smaller scales are modeled. The main disadvantage is the limitation in the spatial and temporal resolution available, which can be severe. Typical applications at the present are similar to those of laboratory experiments, i.e., understanding particular physical processes, and developing and testing of models.

In the foreseeable future only two to three decades of length scale can be resolved using the most powerful computational facilities available. Full turbulence simulations require the resolution of all relevant length scales, down to the Kolmogorov scale for a nonreacting flow. Thus, only flows with moderate Reynolds number can be simulated. Furthermore, in chemically reacting flows, the Damköhler number and the activation energy are usually very large. An additional length scale, the thickness of the reaction zone, which can be much smaller than the Kolmogorov scale, must be resolved. Fortunately, in the limit of chemical equilibrium and for a restricted class of transport coefficients, a conserved scalar can be defined for which the governing equation is simple. Under this simplification, the reaction zone degenerates to a discontinuous sheet. Therefore, if the discontinuity can be captured, full turbulence simulations using the conserved scalar approach will then require the same resolution as the nonreacting case. This direction is one of the most promising for future research. With moderate Reynolds number, the simulations can be used as a research tool to provide important information on the intricate interactions between fluid dynamics and chemical reactions. The nature of these interactions may, in many cases, be approximately independent of the Reynolds number. This information can then be utilized to construct turbulence models for the computation of chemically reacting flows with higher Reynolds number, and subgrid-scale models for large eddy simulations.

There are, however, phenomena for which it is not clear how an approach using a discontinuous reaction zone can be formulated. An example is the simulation of local flame extinction and ignition. Local asymptotic analysis using large activation energy provides a criterion for extinction. Construction of a global solution using this local information in a numerical simulation may, however, be difficult. The question of the behavior of the flame tip, which interfaces a region in chemical equilibrium with a frozen region, and its role in extinction and ignition will require further research.

For computations of turbulent reacting flows with parameter ranges encountered in most practical systems, large eddy simulations are required. Thus, the development of accurate subgrid-scale models is a most urgent task. (See Oran and Boris[86] for a discussion of some of the difficulties in develop-

ing subgrid-scale models for chemically-reacting flows, and some criteria that a subgrid-scale model should meet.) Present subgrid-scale models for nonreacting flows rely on several physical hypotheses. In particular a continuous flux of energy (or scalar variance) from low to high wave numbers is assumed, which implies at most a weak dependence of the larger scales of motion on the smaller scales. Furthermore, some sort of universality (e. g., a Kolmogorov spectrum) at high wave numbers is hypothesized. The validity of both of these hypotheses is probably also required for the successful application of LES to turbulent, reacting flows. For example, if the direct effects of the subgrid-scale motions on the computation scales of motion are very strong, then it is unlikely that accurate subgrid-scale models can be developed and reliable large eddy simulations performed. If the effects of the subgrid-scale motions are weak, however, then there is reason to conclude that the LES may be successfully employed.

For large Damköhler number reactions the smaller scales can be very energetic due to the chemistry at the narrow flame sheet. Hence the small scale behavior would be expected to be very different from that of nonreacting flows, so that the development of subgrid-scale models may be very difficult. One approach which appears to be providing useful information for nonreacting flows is renormalization group theory (Yakhot and Orszag[87]), which can be formulated to directly address subgrid-scale issues. This approach also relies on the assumptions of energy flux and universality mentioned above, however, and so may have to be somewhat modified to treat chemically-reacting turbulent flows.

For direct numerical simulations of compressible, chemically reacting flows, several important issues require attention. The first is the treatment of sound waves. Unlike vortical disturbances which decay rapidly away from the source, acoustic waves may propagate great distances and, upon interacting with a boundary, be reflected and refocused into the turbulent region. A simulation of a subsonic flow using a finite domain may excite certain acoustic eigenmodes if the boundary of the computational domain is a surface which reflects sound waves. Therefore, careful formulation of the boundary conditions is required to simulate the true physical properties of the computational boundary. A second issue involves the computation of shock waves in a supersonic flow. In order to capture shock waves without spurious oscillations, most of the numerical schemes must contain some form of artificial dissipation. To resolve the dissipation scale in a full turbulence simulation, instantaneous high gradient regions must be properly treated. Although most of the finite difference schemes with high gradient regions will be stable, the relative magnitudes of the artificial dissipation terms and those of the real dissipation terms must be monitored continuously to ensure the accuracy.

Acknowledgements: Research on direct numerical simulations of turbulent reacting flows at Flow Research Company and at the University of Washington forms the basis of this article. Work at Flow Research has been suppo ed by NASA Lewis Research Center through Contract No. NAS3-23531 and Contract No. NAS3-24229, by Air Force Office of Scientific Research through Contract No. F49620-85-C0067, and by the Office of Naval Research through Contract No. N00014-84-C0359. Research at the University of Washington has been supported through ONR Contract No. N00014-87-K-0174 and the Johns Hopkins University Applied Physics Laboratory Contract No. 602673-0. The computer resources were obtained from the NASA Lewis Research Center and more recently from the National Aerodynamic Simulator at the NASA Ames Research Center. The authors would like to acknowledge the contributions from the members of the excellent research team at Flow Research and the University of Washington. In particular, contributions from Drs. P. Givi, P. McMurtry, S. Menon and R. Metcalfe are gratefully acknowledged. Discussions of the conserved scalar approach and flame extinction phenomena with Professor F. A. Williams have been very beneficial.

References

[1]Waltrup, P. J., "Liquid Fueled Supersonic Combustion Ramjets: A Research Perspective of the Past, Present and Future", AIAA-86-0158, 1986.

[2]Northam, G. B., "Combustion in Supersonic Flow", 21st JANNAF Combustion Meeting, Oct., 1984.

[3]Orszag, S. A., and Patterson, G. S., Jr., "Numerical Simulation of Turbulelnce", in *Statistical Models and Turbulence*, Springer-Verlag, 1972, p. 127.

[4]Herring, J. A., Riley, J. J., Patterson, G. S., Jr., and Kraichnan, R. H., "Growth of Uncertainty in Decaying Isotropic Turbulence", *J. Atmos. Sci.*, Vol. 30, 1973, p. 303.

[5]Herring, J. A., "Approach of Axisymmetric Turbulence to Isotropy", *Phys. Fl.*, Vol. 30, 1974, p. 859.

[6]Schumann, U., and Patterson, G. S., Jr., "Numerical Study of the Return of Axisymmetric Turbulence to Isotropy", *J. Fluid Mech.*, Vol. 33, 1978, p. 711.

[7]Bardina, J., Ferziger, J. H., Reynolds, W. C., "Improved subgrid-scale models for large-eddy simulations", *AIAA Paper No. 80-1357*, 1980.

[8]Deardorff, J. W., "Three-Dimensional Numerical Study of the Height and Mean Structure of a Heated Planetary Boundary Layer", *Bound. Layer Met.*, Vol. 7, 1974, p. 81.

[9]Moin, P., and Kim, J., "Numerical Investigation of Turbulent Channel Flow", *J. Fluid Mech.*, Vol. 118, 1982, p. 341.

[10]Rogallo, R. S., "Numerical Experiments in Homogeneous Turbulence", *NASA TM-81315*, 1981.

[11]Riley, J. J., Metcalfe, R. W., and Weissman, M. A., "Direct Numerical Simulations of Homogeneous Turbulence in Density-Stratified Fluids", in *Nonlinear Properties of Internal Waves*, B. J. West, ed., AIP Conference Proceedings No. 76, 1981, p. 79.

[12]Mansour, N. N., Moin P., Reynolds, W. C., and J. H. Ferziger, "Improved Methods for Large Eddy Simulations of Turbulence", in *Turbulent Shear Flows I*, Springer-Verlag, 1979.

[13]Riley, J. J., and Metcalfe, R. W., "Direct Numerical Simulations of the Turbulent Wake of an Axisymmetric Body", in *Turbulent Shear Flows II*, Springer-Verlag, 1980, p. 78.

[14]Riley, J. J., and Metcalfe, R. W., "Direct Numerical Simulations of a Perturbed, Turbulent Mixing Layer", AIAA-80-0274, 1980.

[15]Rogallo, R. S., and Moin, P., "Numerical Simulation of Turbulent Flows", *Ann. Rev. Fluid Mech.*, Vol. 16, 1984.

[16]Batchelor, G. K., *Theory of Homogeneous Turbulence*, Cambridge University Press, 1953.

[17]Riley, J. J., and Patterson, G. S., Jr., "Diffusion Experiments with Numerically Integrated Isotropic Turbulence", *Phys. Fl.*, Vol. 17, p. 292, 1974.

[18]Schumann, U., "Numerical Simulation of the Transition from Three- to Two-Dimensional Turbulence under a Uniform Magnetic Field", *J. Fluid Mech.*, Vol. 74, 1976, p. 31.

[19]Feiereisen, W. J., Reynolds, W. C., and Ferziger, J. H., "Numerical Simulation of Compressible, Homogeneous, Turbulent Shear Flow", Stanford Report No. TF-13, 1981.

[20]Orszag, S. A., and Pao, Y.-H., "Numerical Computation of Turbulent Shear Flows", *Adv. Geophysics*, Vol. 18A, 1974, p. 225.

[21]Riley, J. J., Metcalfe, R. W., and Orszag, S. A., "Direct Numerical Simulations of Chemically-Reacting Turbulent Mixing Layers", *Phys. Fl.*, Vol. 25, 1986, p. 406.

[22]McMurtry, P. A., Jou, W.-H., Riley, J. J., and Metcalfe, R. W., "Direct Numerical Simulations of a Reacting Mixing Layer with Chemical Heat Release", *AIAA J.*, Vol. 24, 1986, p. 962.

[23]Lilly, D. K., "On the Application of the Eddy Viscosity Concept in the Inertial Subrange of Turbulence", *NCAR Manuscript No. 123*, 1966.

[24]Deardorff, J. W., "A Numerical Study of Three-Dimensional Turbulent Channel Flow at Large Reynolds Numbers", J. Fluid Mech., Vol. 41, 1970, p. 453.

[25]Patnaik, P. C., Sherman, F. S., and Corcos, G. M., "A Numerical Simulation of Kelvin-Helmholtz Waves of Finite Amplitude", *J. Fluid Mech.*, Vol. 73, 1976, p. 215.

[26]Lesieur, M., Staquet, C., Leroy, P., and Lecomte, P., "A Study of the Mixing Layer from the Point of View of Two-Dimensional Turbulence", submitted to the *J. Fluid Mech.*, 1987.

[27]Jou, W.-H., and Menon, S., "Numerical Simulations of the Flow Field in a Ramjet Combustor: Part II - The Origin of Pressure Oscillations", AIAA-87-1422, 1987.

[28]Menon, S., and Jou, W.-H., "Numerical Simulations of the Flow Field in a Ramjet Combustor: Part I - Numerical Model, Large-Scale Motion, and Mean Field", AIAA-87-1421, 1987.

[29]Ashurst, W. T., and Barr, P. K., "Lagrangian-Eulerian Calculation of Turbulent Diffusion Flame Propagation", in *Third Symp. Turb. Shear Flows*, 1981, p. 3.44.

[30]Ghoniem, A. F., Chorin, A. J., and Oppenheim, A. K., "Numerical Modeling of Turbulent Flow in a Combustion Tunnel", *Phil. Trans. R. Soc. London*, Ser. A, Vol. 304, 1982, p. 303.

[31]Grötzbach, G., and Schumann, U., "Direct Numerical Simulations of Turbulent Velocity-, Pressure-, and Temperature-Fields in Channel Flows", *Symp. Turb. Shear Flows*, 1977, p. 14.11.

[32]Moeng, C.-H., "A Large-Eddy Simulation Model for the Study of Planetary Boundary Layer Turbulence", *J. Atmos. Sci.*, Vol. 41, 1984, p. 2052.

[33]Gibson, C. H., and Libby, P. A., "On Turbulent Flows with Fast Chemical Reactions. Part II. The Distribution of Reactants and Products Near a Reacting Surface", *Comb. Sci. Tech.*, Vol. 6, 1972, p. 29.

[34]Williams, F. A., *Combustion Theory*, Second Edition, Benjamin/Cummings, 1985.

[35]Buckmaster, J. D., and Ludford, G. S. S., *Lectures on Mathematical Combustion*, SIAM, 1983.

[36]Liñán, A., "The Asymptotic Structure of Counterflow Diffusion Flames for Large Activation Energy", *Acta Astron.*, Vol. 1, pp. 1007-1039.

[37]Givi, P., Jou, W.-H., and Metcalfe, R. W., "Flame Extinction in a Temporally Developing Mixing Layer", *Proc. 21st Symposium (International) on Combustion*, Combustion Institute, 1986.

[38]Leonard, A. D., Hill, J. C., "A Simple Chemical Reaction in Numerically Simulated Homogeneous Turbulence", AIAA-87-0134, 1987.

[39]McMurtry, P. A., Riley, J. J., and Metcalfe, R. W., "Mechanisms by Which Heat Release Affects the Flow Field in a Chemically Reacting, Turbulent Mixing Layer", AIAA-87-0131, 1987.

[40]Gottlieb, D., and Orszag, S. A., *Numerical Analysis of Spectral Methods: Theory and Application*, CBMS-NSF Reg. Conf. Ser. Appl. Math., Vol. 26, SIAM, 1977.

[41]Kerr, R. M., "Higher-Order Derivative Correlations and the Alignment of Small-Scale Structures in Isotropic Numerical Turbulence", *J. Fluid Mech.*, Vol. 153, 1985, p. 31.

[42]Peyret, P., and Taylor, T. D., *Computational Methods for Fluid Flows*, Springer-Verlag, 1983.

[43]Haidvogel, D. B., Robinson, A. R., and Schulman, E. D., "The Accuracy, Efficiency, and Stability of Three Numerical Models with Application to Open Ocean Problems", *J. Comp. Phys.*, Vol. 34, 1980, p. 1.

[44]Korczak, K. Z., and Patera, A. T., "An Isoparametric Spectral Element Method for Solution of the Navier-Stokes Equations in Complex Geometry", *J. Comp. Phys.*, Vol. 62, 1986, pp. 361-382.

[45]Ghaddar, N. K., Karniadakis, G. E., and Patera, A. T., "A Conservative Isoparametric Spectral Element Method for Forced Convection; Application to Fully Developed Flow in Periodic Geometries", *Num. Heat Trans.*, Vol. 9, 1986, pp. 277-300.

[46]Beam, R. M., and Warming, R. F., "An Implicit Factored Scheme for the Compressible Navier-Stokes Equations", AIAA-77-645, 1977.

[47]Jameson, A., Schmidt, W., and Turkel, E., "Numerical Solutions of the Euler Equations by Finite Volume Methods Using a Runga-Kutta Time-Stepping Scheme", AIAA-81-1259, 1981.

[48]MacCormack, R. W., "The Effect of Viscosity in Hypervelocity Impact Cratering", AIAA-69-354, 1969.

[49]Leonard, B. P., "A Stable and Accurate Convective Modeling Procedure Based on Quadratic Upstream Interpolation", *Comp. Meth. Appl. Mech. and Engin.*, Vol. 19, 1979, pp. 59-98.

[50]Boris, J. P., and Book, D. L., "Flux-Corrected Transport. I. SHASTA, A Fluid Transport Algorithm that Works", *J. Comp. Phys.*, Vol. 11, 1973, p. 38.

[51]Harten, A., "On a Class of High Resolution Total-Variation-Stable Finite Difference Schemes", *SIAM J. Num. Anal.*, Vol. 21, 1983, pp. 1-23.

[52]Davis, S. F., "TVD Finite Difference Schemes and Artificial Viscosity", ICASE Report No. 84-20.

[53]Roe, P. L., "Some Contributions to the Modeling of Discontinuous Flows", AMS Publications, *Lectures in Applied Mathematics*, Vol. 22, 1985.

[54]Yee, H. C., "Construction of Explicit and Implicit Symmetric TVD Schemes and Their Applications", *J. Comp. Phys.*, Vol. 68, 1987, pp. 151-179.

[55]Smolarkiewicz, P. K., "A Fully Multidimensional Positive Definite Advection Transport Algorithm with Small Implicit Diffusion", *J. Comp. Phys.*, Vol. 54, 1984, pp. 325-362.

[56]Guirguis, R., Oran, E. S., and Kailasanath, K., "Numerical Simulations of the Cellular Structure of *Detonations in* Liquid Nitromethane – Regularity of the Cell Structure" *Comb. Flame*, Vol. 61, 1986, pp. 199-209.

[57] Kailasanath, K., Gardner, J. H., Oran, E. S., and Boris, J. P., "Numerical Simulation of Combustion Oscillations in Compact Ramjets", *Proc. JANNAF Propulsion Mtg.* CPIA, Johns Hopkins University, Applied Physics Laboratory, 1986.

[58]Ghoniem, A. F., and Givi, P., "Vortex-Scalar Element Calculations of a Diffusion Flame", AIAA-87-0225, 1987.

[59]Leonard, A., "Computing Three-Dimensional Incompressible Flows with Vortex Elements", *Ann. Rev. Fluid Mech.*, Vol. 17, 1985, p. 523.

[60]Ashurst, W. T., and Meiburg, E., "Three-Dimensional Shear Layers via Vortex Dynamics", submitted to *J. Fluid Mech.*, 1986.

[61]Ghoniem, A. F., Aly, H. M., and Knio, O. M., "Three-Dimensional Vortex Simulation with Application to Axisymmetric Shear Layers", AIAA-87-0379, 1987.

[62]Sethian, J. A., "Turbulent Combustion in Open and Closed Vessels", *J. Comp. Phys.*, Vol. 54, 1984, p. 425.

[63]Pindera, M. Z., "On the Aerodynamics of Flames", Ph. D. Thesis, University of California, Berkeley, 1986.

[64]Mungal, M. G., "Experiments on Mixing and Combustion with Low heat Release in a Turbulent Shear Flow", Ph. D. Thesis, California Institute of Technology, 1983.

[65]Rehm, R. G., and Baum, H. R., "The Equations of Motion for Thermally Driven, Buoyant Flows", *J. of Res. Nat'l Bur. Stand.*, Vol. 83, 1978, p. 297.

[66]Sivashinsky, G. J., "Hydrodynamic Theory of Flame Propagation in an Enclosed Volume", *Acta Astr.*, Vol. 6, 1979, p. 631.

[67]Buckmaster, J. D., "An Introduction to Combustion Theory", in *The Mathematics of Combustion*, J. D. Buckmaster, ed., SIAM, 1985.

[68]Majda, A., and Sethian, J., "The Derivation and Numerical Solution of the Equations for Zero Mach Number Combustion", *Comb. Sci. Tech.*, Vol. 42, 1985, pp. 185-205.

[69]Peters, N., and Williams, F. A., "Liftoff Characteristics of Turbulent Jet Diffusion Flames", *AIAA J.*, Vol. 21, 1983, p. 423.

[70]Givi, P., and Isreali, M., 1987, to be published.

[71]Toor, H. L., "Turbulent Mixing of Two Species With and Without Chemical Reactions", *Ind. Eng. Chem. Fundam.*, Vol. 8, 1969, p. 655.

[72]Patterson, G. K., *Chem. Eng. Commun.*, Vol. 8, 1981, p. 25.

[73]O'Brien, E. E., "Statistical Methods in Turbulent Reacting Flows", *AIAA J.*, Vol. 19, 1981, p. 366.

[74]Pratt, D. T., "Mixing and Chemical Reaction in Continuous Combustion", *Progr. Energy Comb. Sci.*, Vol. 1, 1976, p. 73.

[75]Pope, S. B., *Phil. Trans. Roy. Soc. London*, Ser. A, Vol. 291, 1979, p. 529.

[76]Riley, J. J., and Metcalfe, R. W., "Direct Numerical Simulations of Chemically Reacting Turbulent Mixing Layers", NASA CR 17460, 1984.

[77]Lin, P., and Pratt, D. T., "Numerical Simulation of a Plane Turbulent Mixing Layer, with Applications to Isothermal, Rapid Reactions", AIAA-87-0224, 1987.

[78]Curl, R. L., "Dispersed Phase Mixing: I. Theory and Effects of Simple Reactors", *AIChE J.*, Vol. 9, 1963, p. 175.

[79]Broadwell, J. E., and Breidenthal, R. E., "A Simple Model of Mixing and Chemical Reaction in a Turbulent Shear Layer", *J. Fluid Mech.*, Vol. 125, 1982, p. 397.

[80]Konrad, J. J., "An Experimental Investigation of Mixing in Two-Dimensional Turbulent Shear Flows with Application to Diffusion Limited Chemical Reactions", Ph. D. Thesis, California Institute of Technology, 1977.

[81]Breidenthal, R. E., "A Chemically Reacting Turbulent Shear Layer", Ph. D. Thesis, California Institute of Technology, 1978.

[82]Smith, D. A., and Zukoski, E. E., "Combustion Instability Sustained by Unsteady Vortex Combustion", AIAA/SAE/ASME/ASEE 21st Joint Propulsion Conference, Monterey, California, 1985.

[83]Yates, J. E., "Application of the Bernoulli Enthalpy Concept to the Study of Vortex Noise and Jet Impingement Noise", NASA CR2987.

[84]Drummond, J. P., "Numerical Simulation of a Supersonic Chemically Reacting Mixing Layer", D. Sc. Thesis, The George Washington University, 1987.

[85]Zang, T. A., Drummond, J. P., Erlebacher, G., Speziale, C., and Hussaini, M. Y., "Numerical Simulation of Transition, Compressible Turbulence, and Reacting Flows", AIAA-87-0130, 1987.

[86]Oran, E. S., and Boris, J. P., "Detailed Modeling of Combustion Systems", *Progr. Energy Comb. Sci.*, Vol. 7, 1981, pp. 1-72.

[87]Yakhot, V., and Orszag, S. A., "Renormalization Group Analysis of Turbulence. I. Basic Theory", *J. Sci. Comp.*, Vol. 1, 1986, pp. 3-51.

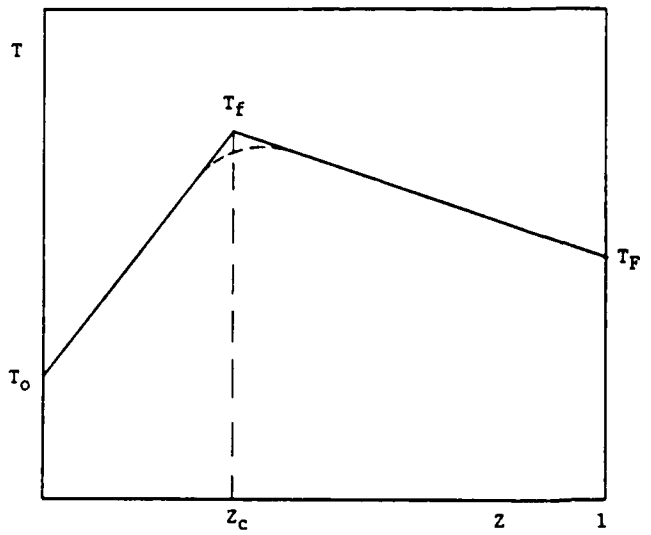

Figure 1. Relationship between the temperature T and the conserved scalar Z.

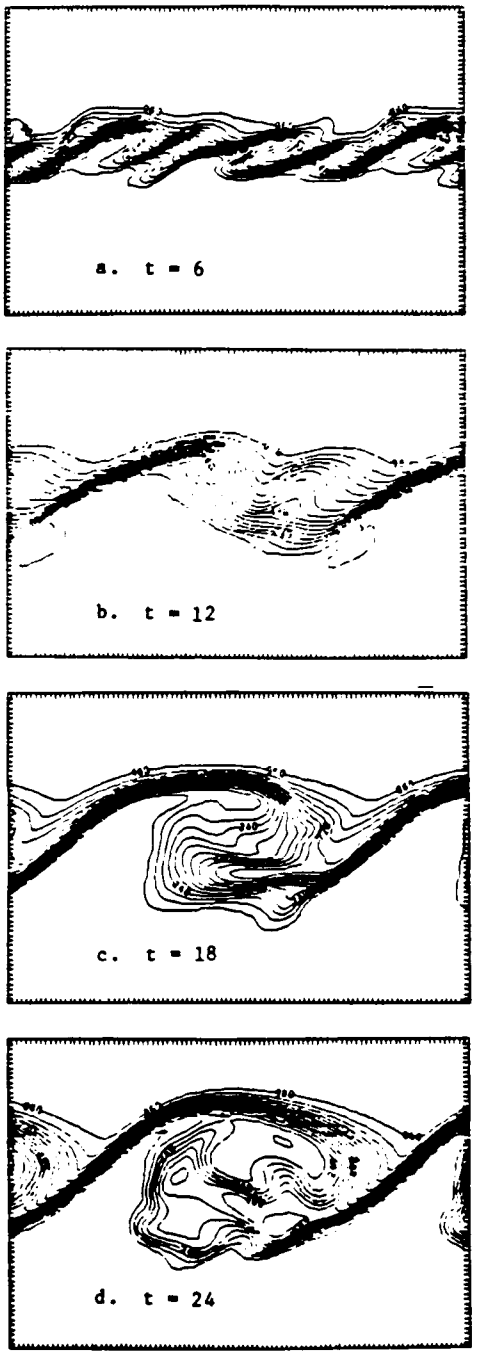

Figure 2. Time sequence of concentration contours in streamwise section for an isothermal reaction.

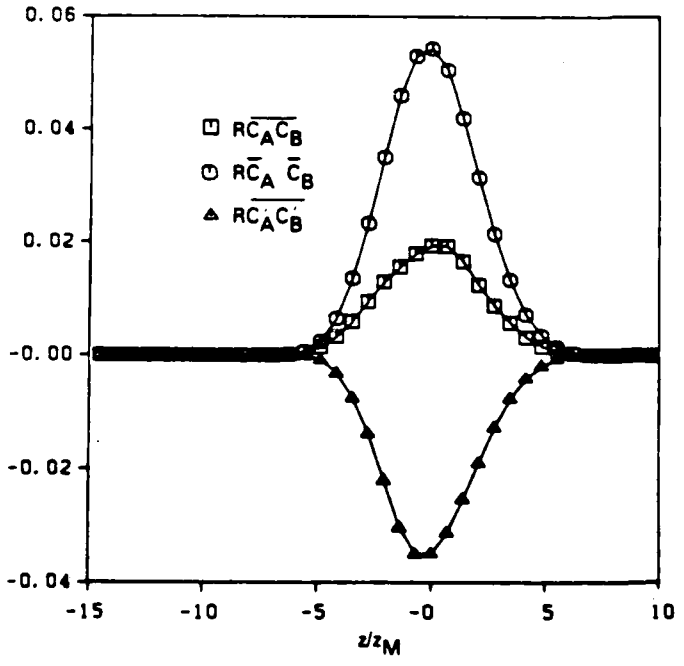

Figure 3. Average of the product of the concentrations, the product of the averages, and the concentration correlation.

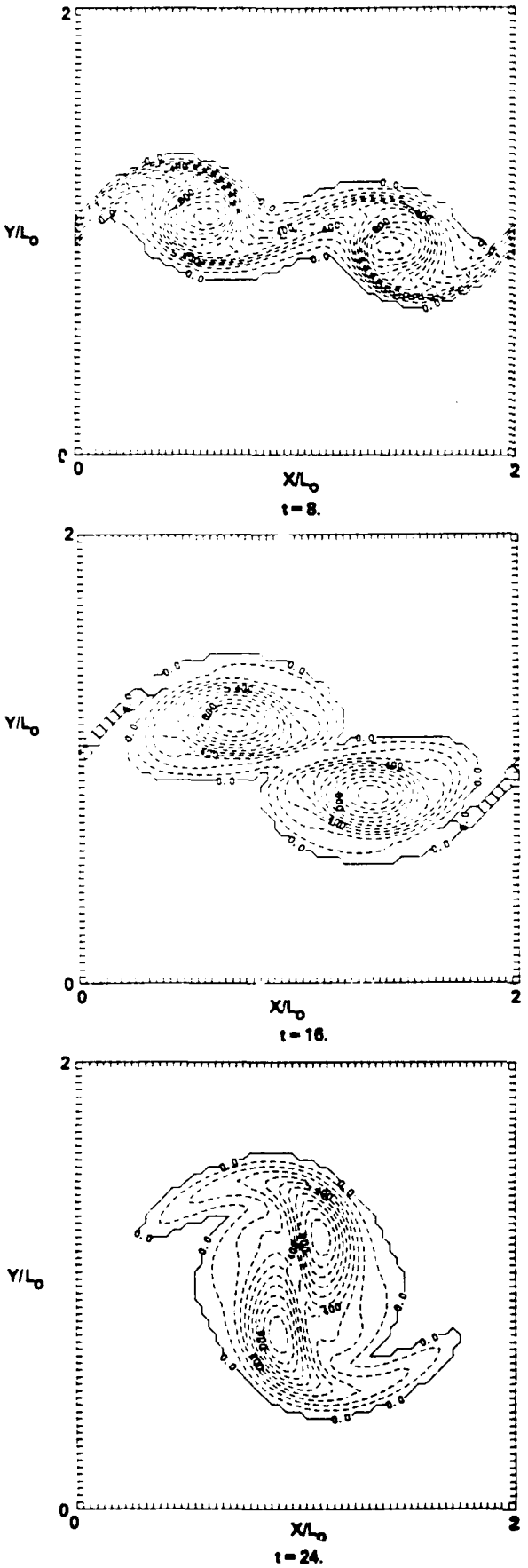

a. Vorticity contour plots, no heat release (Ce = 0)

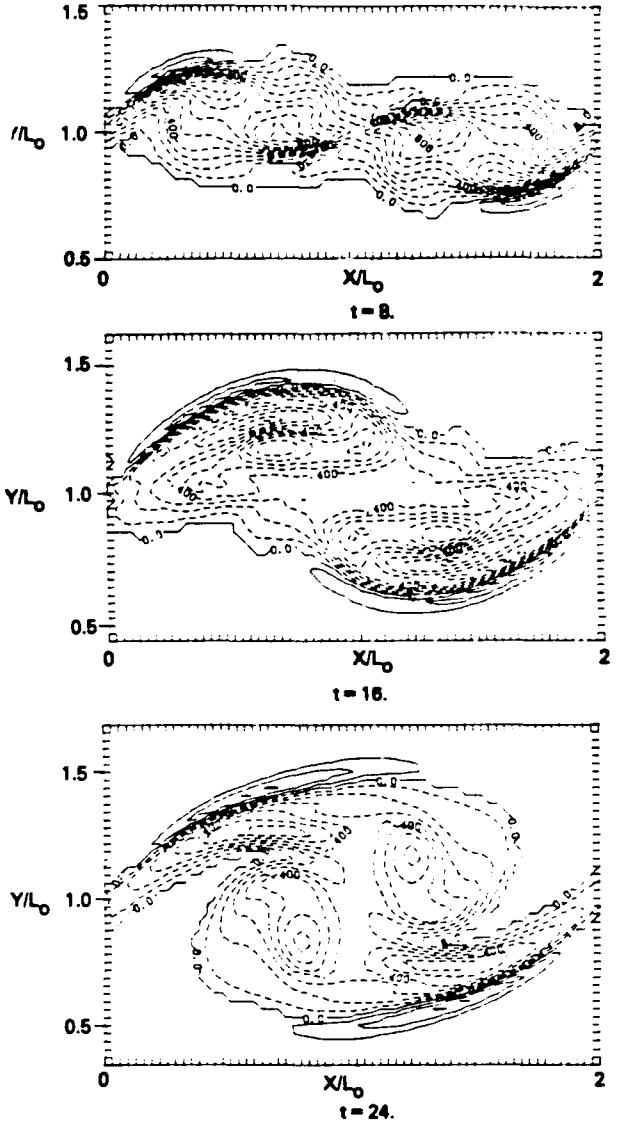

b. Vorticity contour plots, with heat release (Ce = 5)

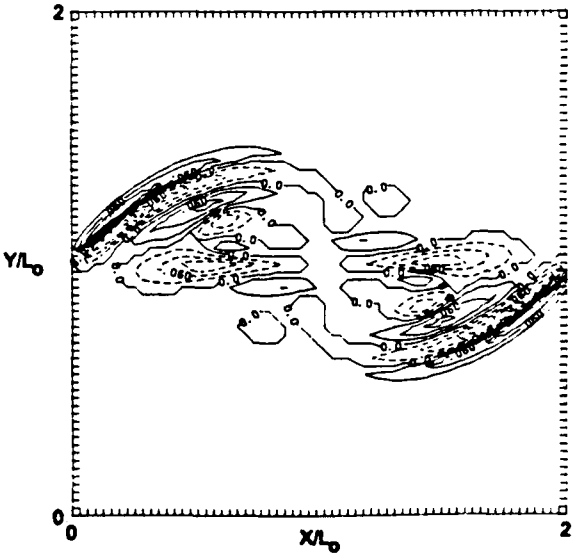

c. Baroclinic torque, Ce = 5, t = 16

Figure 4. Comparison of vorticity contour plots for cases with and without heat release.

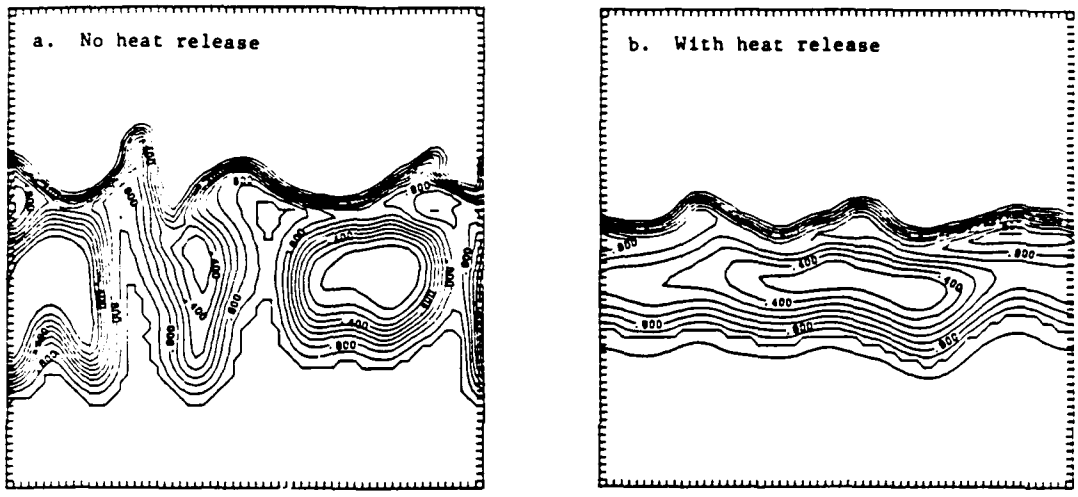

Figure 5. Instantaneous species contour plots on a cross-stream section y-z.

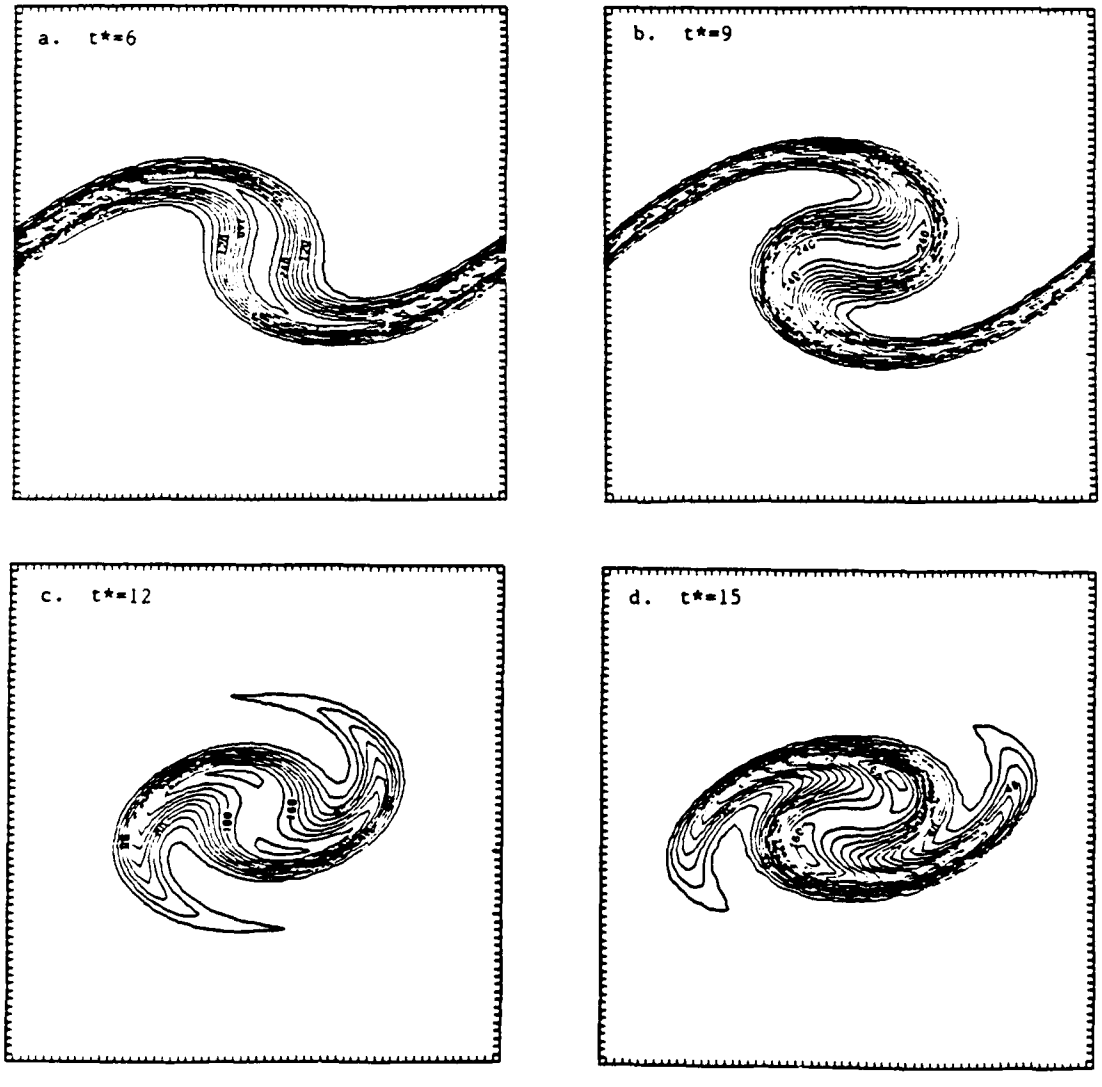

Figure 6. Instantaneous reaction rate (Arrhenius temperature-dependent reaction rate).

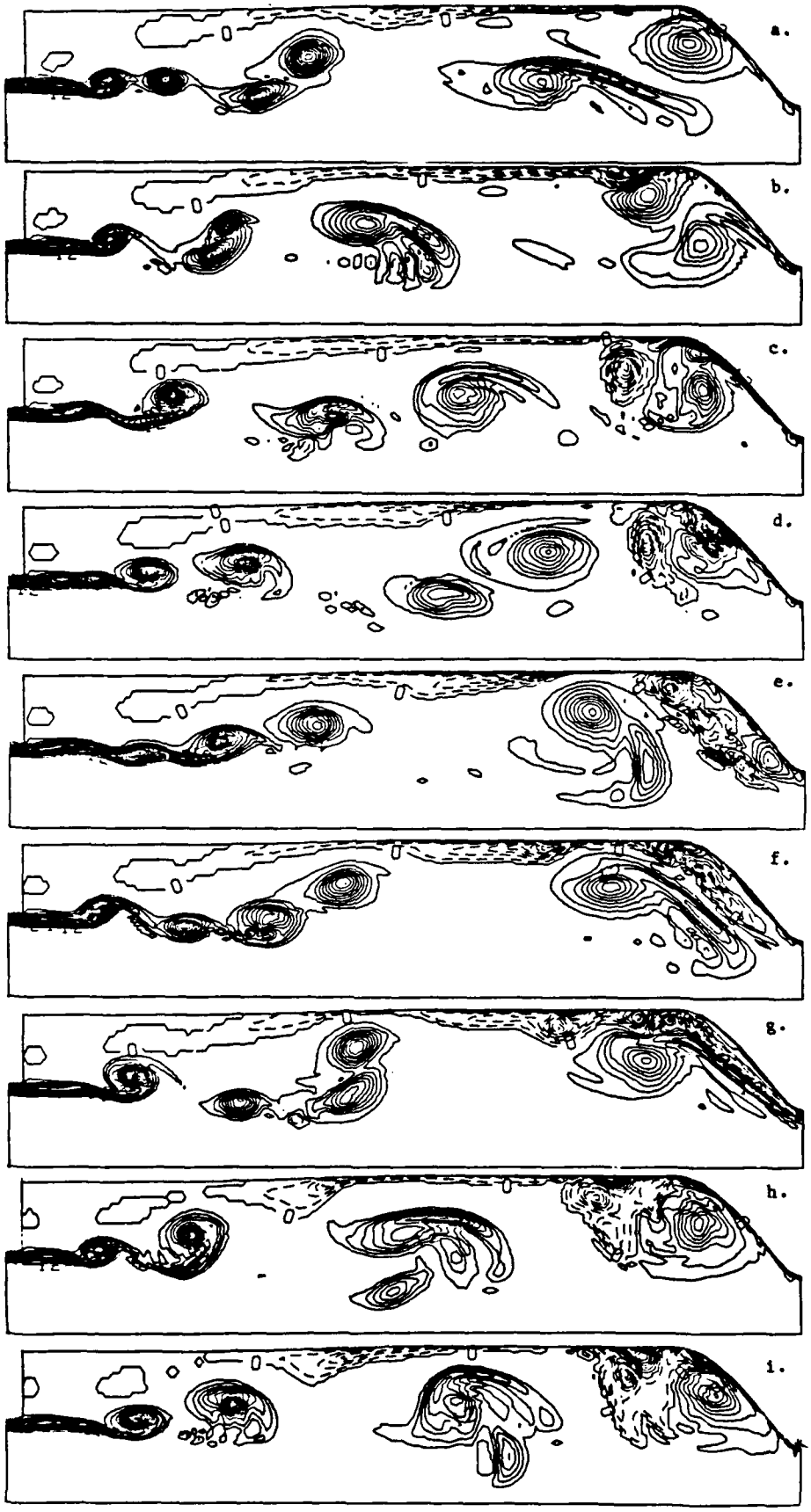

Figure 7. Time sequence of vorticity contour plots in a ramjet combustor. Mach number 0.32.

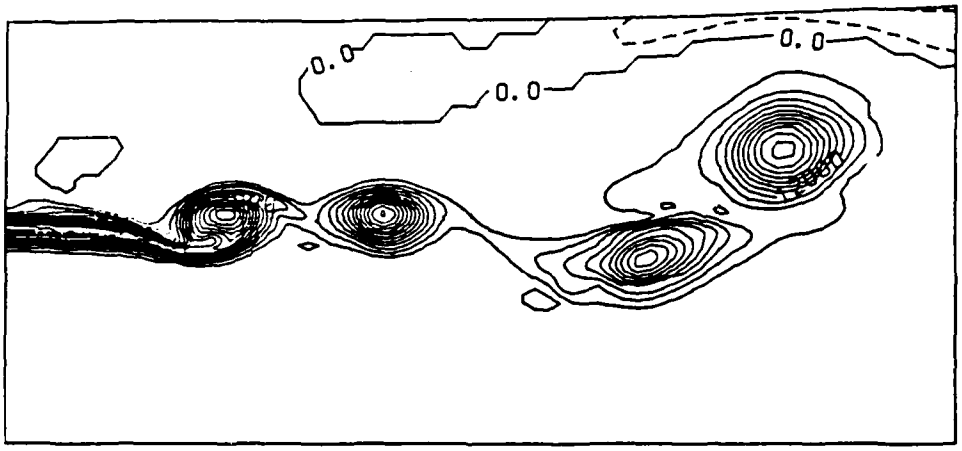

a. Vorticity contour

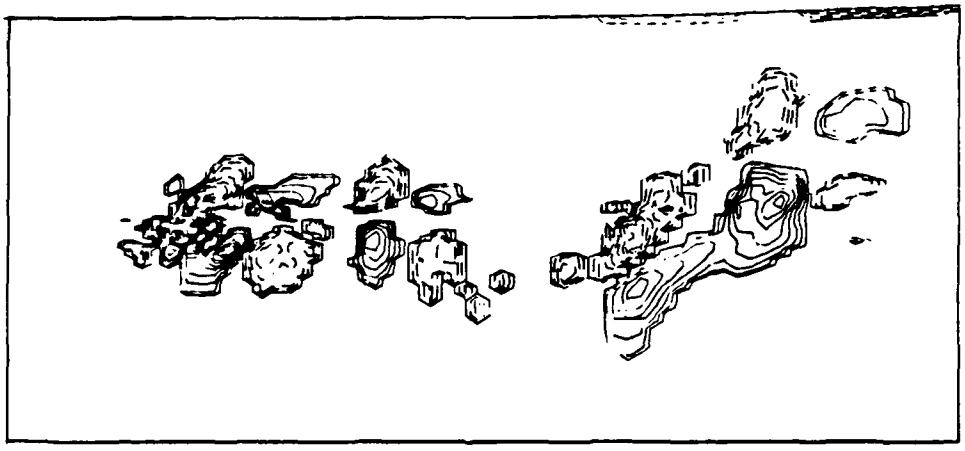

b. Dilatation contour

Figure 8. Instantaneous dilatation field and vorticity field.

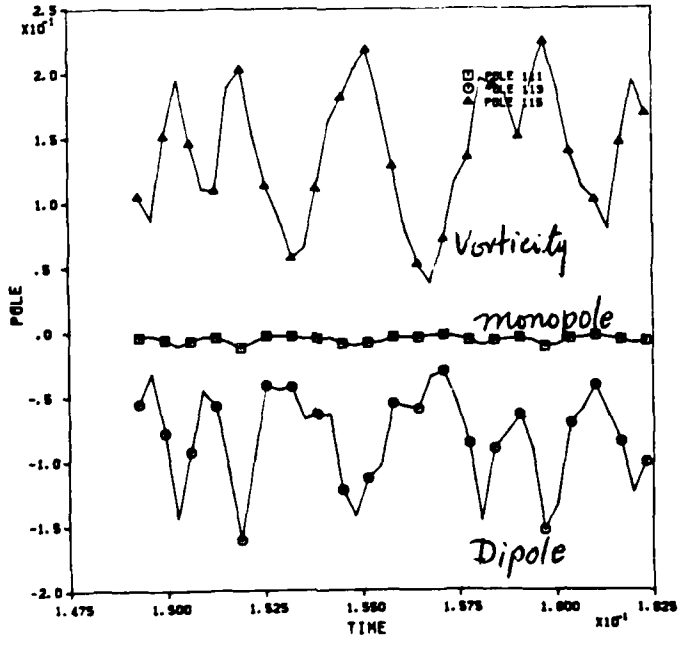

Figure 9. Time histories of vorticity, acoustic monopole and dipole in a ramjet nozzle.

APPENDIX V

Direct Numerical Simulations of a Reacting, Spatially Developing Mixing Layer by a Spectral-Element Method

Direct Numerical Simulations of a Reacting, Spatially Developing Mixing Layer by a Spectral-Element Method

by

P. Givi and W.-H. Jou
Flow Research Company
21414-68th Avenue South
Kent, WA 98032
U.S.A.

Manuscript Submitted for Presentation at the Twenty-Second Symposium (International) on Combustion

Subject Matter: 19, 30

(December, 1987)

TP-219/12-87

Direct Numerical Simulations of a Reacting, Spatially Developing Mixing Layer by a Spectral-Element Method

P. Givi and W.-H. Jou
Flow Research Company
Kent, WA 98032

Abstract

The spectral-element method, a numerical scheme that combines the accuracy of spectral methods with the versatility of finite element techniques, has been employed to study the mechanisms of mixing and chemical reactions in a diffusion flame stabilized on a two-stream planar mixing layer. The results of simulations of the harmonically forced, spatially developing flow are statistically analyzed to examine the compositional structure of the flame near quenching. The results indicate that as the flame approaches extinction, the mean and the rms values of the reactant concentrations decrease while those of the product concentration and temperature increase. This behavior is enhanced by increasing the hydrodynamics characteristic time (reducing the local Damkohler number) and is consistent with that observed experimentally.

1. Introduction

Many recent investigations [1-3] on the developments of theoretical models capable of describing the behavior of nonequilibrium turbulent diffusion flames, point to the necessity of obtaining experimental data for the purpose of validation of the closure assumptions employed in these models. The results of some recent experiments [4,5] have proven extremely valuable if not completely adequate. However, since detailed experimental measurements are difficult to obtain, it would be useful to supplement the measurements with some results obtained by the method of direct numerical simulations. This method refers to solving the exact governing hydro-chemical transport equations without resorting to turbulence modeling [6]. Time evolutions of the thermochemical variables are computed by using highly accurate numerical schemes. Therefore, detailed flow field information is available within the computational space-time domain, from which statistical properties and other relevant information can be extracted. There are, certainly, restrictions on the resolvable space and time scales, which in turn restrict the range of physical parameters that can be accurately simulated. However, depending on the particular physical phenomenon of interest, certain thermo-fluid dynamic similitude exists [6]. By simulations of flows in a restricted parameter range while satisfying the required similitude, the results are useful for extracting some important information for understanding the behavior of that particular phenomenon. This approach is followed in this paper to investigate the nonequilibrium phenomena of extinction in a non-premixed flame.

Although direct simulations of chemically reacting mixing layers have been investigated previously, the numerical model of a temporally developing, spatially periodic layer has usually been used [7-10]. Although the simulations yield a wealth of information on the behavior of a reacting mixing layer, there is always some uncertainty of what might have been missed by such an approximation. For example, it has been established that in spatially developing mixing layers, the mechanism of mixing between the fluids from the two streams is asymmetric [11-13]. This behavior cannot be predicted by assuming spatial periodicity, and a spatial evolution model should be employed to simulate such flows more realistically.

In this paper, we shall describe the development of a spectral-element code capable of accurately computing a spatially developing, chemically reacting mixing layer. This method enables us to simulate flows at higher Reynolds (Peclet) numbers than those of previous approaches using conventional second-order finite difference schemes [10,14]. The resulting code is used for simulations of a spatially developing shear layer under the influence of a nonequilibrium chemical reaction. The results are statistically analyzed to obtain valuable information on the compositional structure of the reacting flow.

A three-dimensional code has been developed. In the present paper, however, only the results of two-dimensional simulations are presented. Detailed three-dimensional simulations that include the effects of small-scale turbulence will be reported in the future.

2. Formulation

A mixing layer in which two parallel streams with different velocities begin to mix and react downstream of the trailing edge of a splitter plate partition presents an ideal configuration for studying the physical processes in the reaction zone of a real combustor. A schematic diagram of the layer considered here is shown in Fig. 1. The reactant C_B (fuel) enters the computational domain on the upper, high-speed stream, while the other reactant C_A (oxidizer) enters on the lower, low-speed side. The chemical reaction between the two species is assumed to be single step and to obey the temperature dependent Arrhenius law.

$$A + B \rightarrow P \tag{1}$$

The effect of chemical heat release is assumed negligible, which together with the further assumption of a low Mach number flow, results in a constant density formulation. Under these assumptions, the hydrodynamics and the transport of the chemical species and temperature are decoupled. The incompressible Navier-Stokes equations together with the species diffusion-reaction equations are the governing equations to be numerically integrated.

The appropriate reference quantities for normalizing the transport equations are the velocity difference between two streams ΔU, the free-stream temperature T_∞, the free stream concentrations $C_{A\infty}$ and $C_{B\infty}$, and the unperturbed shear layer thickness at the entrance σ. With these reference quantities, the relevant parameters are the Reynolds number Re, the Damkohler number Da, the Zeldovich number Ze, and the heat release parameter Ce. The values of the Prandtl and Schmidt numbers are assumed to be unity, and the magnitudes of other non-dimensional parameters used in the simulations will be given below.

Spectral Element Method

In the flow configurations shown in Fig. 1, impermeable free slip boundary conditions are employed on the upper and lower boundaries. Therefore, pseudospectral methods with Fourier transforms can be used in the cross-stream direction Y for the discretization of the governing equations. This technique was used in previous investigations of a spatially periodic, temporally evolving mixing layer [7-10].

In the stream-wise direction, the flow field is not periodic, and basis functions other than Fourier series must be used. Presumably, Chebyshev polynomials can be employed for a problem with non-periodic boundary conditions. In practice, however, the distance between the neighboring Chebyshev collocation points near the boundaries becomes extremely small if high order polynomials are used to discretize a large computational domain. Consequently, time integration becomes very stiff because of numerical stability restrictions [15]. A compromise between numerical accuracy and efficiency can be achieved by using the spectral-element method [17]. This p-type finite element method divides the stream-wise

domain into N_E number of elements. Within each element, the thermo-fluid variables are represented by Chebyshev polynomials. The governing equations are approximately satisfied by the discretized system at the collocation points within each element. The compromise between the accuracy and the efficient time integration can be achieved by adjusting the number of finite elements and the order of the Chebyshev polynomials in each element. By increasing the number of elements and using moderately low order polynomials within each element, the stiffness in time integration can be avoided while high accuracy is maintained.

For the purpose of demonstrating this technique, we shall consider the solution of the species transport equation in which the velocity field is given:

$$\frac{\partial C}{\partial t} = -\nabla\cdot(\vec{u}C) - \dot{\omega} + \frac{1}{Pe}\nabla^2 C \tag{2}$$

where Pe is the Peclet number and $\dot{\omega}$ is the reaction rate. To advance the dependent variable C in time, the fractional time stepping scheme is used. The solution is first advanced to an intermediate time by using a second order accurate Adams-Bashforth scheme for the nonlinear term in Eq. (2), i.e.,

$$\frac{C^* - C^n}{\Delta t} = \frac{3}{2}(\nabla\cdot(\vec{u}C) - \dot{\omega})^n - \frac{1}{2}(\nabla\cdot(\vec{u}C) - \dot{\omega})^{n-1} \tag{3}$$

where Δt is the time increment, and the superscripts n and * refer to the previous and the intermediate time steps, respectively. The spatial discretizations in the above equation are performed by employing spectral methods using Fourier transforms in Y and Chebyshev expansions in X.

The advancement of the scalar equations from computational time n to n+1 is accomplished by the completion of the viscous (diffusion) step. In this step, the influences of both spectral methods and finite element techniques become apparent. Taking the Fourier transform of the equation in the cross-stream direction, we have:

$$\frac{\partial^2 \tilde{C}^{n+1}}{\partial x^2} - (K^2 + \frac{Pe}{\Delta t})\tilde{C}^{n+1} = -\frac{Pe}{\Delta t}\tilde{C}^* \tag{4}$$

Where K is the Fourier wave number in the Y-direction, and ~ denotes the variables in the

Fourier domain. Now we can use the variational principle [17] to solve this equation. According to this principle, solving Eq. (4) is equivalent to minimizing the functional

$$I = \int [-\frac{1}{2}(\frac{\partial \tilde{C}^{n+1}}{\partial x})^2 - \frac{1}{2}(K^2 + \frac{Pe}{\Delta t})(\tilde{C}^{n+1})^2$$

$$+ \frac{Pe}{\Delta t}\tilde{C}^{*}\tilde{C}^{n+1}]dx \qquad (5)$$

within each element.

Using the Lagrangian interpolant (Chebyshev expansion) of $\tilde{C}^{n+1}$ as a trial function in Eq (5) and requiring that the variation of I with respect to the nodal values vanishes, we obtain a set of elemental equations for the interior nodes within each element. By using a direct stiffness method [17] we can construct the system matrix from the elemental matrix [16]. Solutions of the resulting linear algebraic systems give the unknown variables at the interior and the interface collocation points for all wave numbers (K's) in the other direction of the flow. The variable at the new time level, i.e., C^{n+1} is recovered by the inverse Fourier transform of $\tilde{C}$.

Boundary Conditions

The inflow and outflow boundary conditions are required to complete the formulation of the present problem. Ideally, a random velocity field with a spectrum similar to what was measured experimentally can be specified. In the present simulations, however, only the dominant two-dimensional features of a turbulent shear layer are examined. It is known that the mixing layer is most responsive to disturbances corresponding to the most unstable instability wave and its subharmonics. Therefore, these disturbances are imposed at the inflow boundary for capturing the dominant two-dimensional coherent structures. The inflow velocity profile is therefore given by :

$$\vec{U}(0, y, t) = \vec{U}_o(y) + Real[A_1 \vec{U}_1(y) e^{i(\omega t + \phi_1)} \tag{6}$$

$$+A_{1/2} \vec{U}_{1/2}(y) e^{i/2(\omega t + \phi_2)} + A_{1/4} \vec{U}_{1/4}(y) e^{i/4(\omega t + \phi_4)}]$$

where the unperturbed velocity profile is

$$\vec{U}_o(y) = [U_m + \frac{\Delta U}{2} \tanh(\frac{y}{\delta})]\vec{e}_x \tag{7}$$

and $U_i(y)$ are the eigenfunctions of the most unstable mode and its subharmonics computed from the Orr-Sommerfield equations for the unperturbed velocity profile. A_n are the amplitudes and ϕ_n are the phase shift between the modes. The amplitudes in the simulations are chosen so that the rms disturbance is approximately 12 percent of the mean flow velocity.

At the outflow boundary, a weak condition of zero second derivatives is applied for all variables. From Eq. (4) this condition can be written as :

$$(\tilde{C}^{n+1})_{outflow} = \frac{\frac{Pe}{\Delta t} \tilde{C}^*}{K^2 + \frac{Pe}{\Delta t}} \tag{8}$$

Numerical tests were performed to examine the extent of the influence of this approximation. It was found that the effects of the approximate boundary condition are confined within the last finite element. This is consistent with that found by Korszak [18]. Therefore, the solution in the last computational element was discarded in our simulations.

3. Results of Simulations

Computations were performed in a domain with the size $34\sigma > x > 0$, $6.75\sigma > y > -6.75\sigma$. There are 64 Fourier modes in the cross-stream direction and 52 finite elements are used for the stream-wise discretization. A fifth order Chebyshev polynomial is used to approximate the variables within each element. This discretization is equivalent to, at least, a fifth order accurate finite difference technique even if the spectral convergence is not considered. This results in a total number of 211 points in the stream-wise direction. With this 211x64 grid resolution, accurate simulations with Re = Pe = 100 and Ze = 20 are possible. The

computation time increment is selected to be $\Delta t = 0.04$, which is small enough to accurately simulate a chemical reaction with $Ce = 8$. Simulations are performed with two different values of ΔU while other parameters are kept fixed to assess the influence of the characteristic flow frequency on the compositional structure and the temperature within the reaction zone.

The magnitudes of the phase shifts between the modes ϕ_j in Eq. (6) are randomly selected from a random seed with a top hat probability density function. This technique was suggested by Reynolds [19] for nonreacting flow simulations. This selection was performed in such a way that $<\phi_j> = 0$ and the fluctuating phase shift with $<\phi'_j{}^2> = 5°$, where $<>$ indicates the mean value of the random numbers selected from the seed. The implementation of these phase shifts is the only mechanism to introduce randomness into an otherwise deterministic simulation. This is to mimic partially the random perturbations which are present in laboratory turbulent flows, in a two-dimensional simulation. In the three-dimensional simulation of a mixing layer currently being undertaken, the random phase shift will be replaced by specifying an initial random turbulent spectrum [20].

For the purpose of flow visualization, a time sequence of contour plots for a conserved Shvab-Zeldovich scalar variable is presented in Fig. 2. The variable Z is defined as $Z = (C_B - C_A - C_{B\infty})/(C_{B\infty}+C_{A\infty})$ and has normalized values equal to unity and zero in the fuel and oxidizer streams, respectively. This figure shows how the small perturbations at the inflow are amplified to form large scale structures downstream. The perturbations associated with the most unstable mode alone would cause the initial roll-up of the vortices, which are created at equal wavelengths from each other. Adding the perturbations corresponding to the first subharmonic mode results in a second roll-up in the form of the merging of neighboring vortices. Finally, the presence of the perturbations corresponding to the second subharmonic, generates a third roll-up (second merging) at a region near the outflow. It is observed in this figure that as the vortices reach the outflow, the zero second derivatives condition seems to allow them to travel out of the computational domain. As mentioned in the previous section, the errors associated with this boundary condition tend to be confined within the last computational element. Within this domain, the computed spreading rate of the mixing layer $\frac{\partial \delta}{\partial x}$ is approximately 0.105, which is slightly higher than the measured value of 0.07 [21] for a planar layer with the same free-stream velocity ratio.

The vortex roll-up of the unsteady shear layer brings unreacted species from the two streams into the chemical reaction zone. This region is marked by a very steep gradient of the Shvab-Zeldovich variable across the braids of the vortices, while in the core of the vortex the magnitude of the gradient is small. The stretching of the reaction zone by the vortex roll-up is further enhanced by each subsequent roll-up, and the diffusion across the high strain braids is further increased.

If an infinitely fast chemistry was assumed to describe the chemical reaction, the enhancement of the mixing by the vortex roll-up would directly result in the augmentation of the chemical reactions and the increase of product formation. For the finite rate, nonequilibrium chemistry employed in the present calculations, however, this may not be the case, as the increased mixing rate might have a reverse effect on the product formation rate. To examine this effect, the time sequence of the product concentration and that of the instantaneous reaction rate are presented in Figs. 3 and 4, respectively. Figure 3 indicates that the amount of products along the $Z = Z_{st}$ iso-surface attains a maximum value at the core of the vortex and reaches a minimum at the braids. Figure 4 shows that the reaction rate is fairly uniform along the mixing layer near the inlet where the reactants are first brought into contact. Further downstream from the inflow, as the magnitude of the instantaneous dissipation increases due to vortex roll-ups and pairings, the reaction rate approaches zero at the braids of the vortices, and the flame locally quenches at those locations. This mechanism of flame extinction is consistent with the previous temporal simulations of Givi et al. [9] and also with the experimental observations reviewed by Tsuji [22]. As explained by Peters [1], at the regions of high strain the supply of the reactants is greater than what can be digested by the chemical reaction. Therefore, the local temperature decreases below a critical value and the flame becomes very rich with both reactants. As a result, the flame cannot be sustained.

Statistical Analysis

To examine the compositional structure of the flame near extinction, the instantaneous values of the species concentration and temperature at a downstream location were statistically analyzed. This analysis was performed by recording the instantaneous values at every time step within the period $144 < t < 288$. At $t = 144$, the elapsed time is long enough for the flow to sweep through the computational domain once. Therefore, the effects of the initial

transients are eliminated. During the recording period, an ensemble of 3600 instantaneous values was recorded at selected grid points for analysis. As was mentioned previously, the chemistry parameters and the velocity ratio were kept constant, while the velocity difference across the layer was changed in the simulations to assess the influence of the mixing intensity on the structure of the flame. In the discussions below, Case I corresponds to $\Delta U = 0.5$, and Case II corresponds to $\Delta U = 1$. This is, effectively, equivalent to changing the magnitude of the local Damkohler number as discussed previously by Givi et al. [23] and Dibble and Marge [24].

For both Case I and Case II, the mean profiles of the fuel (species B) and of the products (species P) at the stream-wise location $x = 17\sigma$ are presented in Figs. 5 and 6, respectively. It is shown on these figures that as the mixing rate is increased, the mean value of the fuel concentrations increases. This suggests that as the flame approaches extinction, the concentration of the reactants in the reaction zone increase and, as a result of local flame quenching, the rate of product formation decreases. The same behavior was also observed in the mean temperature profiles (not shown here), which indicates that the mixture tends to be hotter at lower mixing rates.

The influence of mixing on the second order moments of the scalar quantities is presented in Figs. 7, 8, and 9, which show the profiles of $<C'_A{}^2>$, $<C'_B{}^2>$ and $<C'_P{}^2>$, respectively. Figures 7 and 8 indicate that as the flame approaches extinction, the magnitude of the fluctuations of the concentration of reactants decreases. On the other hand, Fig. 9 shows that the rms fluctuation of the product concentration is higher for Case I. Again, similar behavior was observed for the temperature fluctuations (not shown here). As the mixing rate increases and the flame is quenched, the magnitude of the temperature fluctuations decreases.

The results of our numerical simulations are in favorable agreement with the recent experiments of Masri et al. [5]. Their spontaneous Raman/Rayleigh measurements of species concentration and temperature in a non-premixed methane flame indicate that as the flame approaches extinction, the mean values of the concentrations of the reactants CH_4 and O_2 increase, while those of the products decrease. This is consistent with our calculations, as displayed in Figs. 5 and 6. The experimental measurements also indicate that the rms fluctuations of the product concentration, temperature, and O_2 decrease, whereas those of the CH_4 concentration slightly increase with the increase in the intensity of mixing. While the

results of our numerical simulations indicate the same behavior for the product species (Fig. 9) and the mixture temperature, they show an increase of the fluctuations of both of the reactants A and B (Figs. 7 and 8). This discrepancy between the results of our simulations with the experimental data may be due to the use of a one-step kinetic model for the chemistry in our simulations. It is well known that, although such approximations may be valid for simulating hydrogen flames, they are inadequate in predicting the compositional structure of hydrocarbon flames near extinction [25]. Experimental measurements [26,27] and recent numerical investigations [28,29] of the transport equations for the structures of methane diffusion flames with detailed chemical kinetics in parallel flows show that increasing the magnitude of the local strain rate results in an increase in the leakage of the O_2 through the reaction zone but no CH_4 leakage [25]. This behavior is contrary to the activation energy asymptotics with one-step chemistry, and multi-step kinetic mechanisms have to be incorporated to yield the correct behavior [25]. However, the flame structure predicted by our direct numerical simulations shows the same qualitative behavior as those observed in the laboratory for both hydrogen [30] and methane [29] flames. Future calculations with recently developed multi-step chemical kinetics chemistry models [31,32,33,2] are required for better comparison to nonequilibrium methane flame data.

4. Conclusions

A spectral-element numerical algorithm has been developed for the numerical calculation of a harmonically forced reacting mixing layer. This method combines the advantage of the versatility offered by finite element techniques with the accuracy of the spectral methods in a more flexible manner than that can be found in either technique alone. This approach allows the application of non-periodic boundary conditions and, therefore, is applicable to the simulation of spatially evolving flows.

The results of our numerical simulations indicate that as the magnitude of the instantaneous dissipation rate is increased, the diffusion flame cannot keep pace with the large diffusive flux of the reactants into the reaction zone. As a result, the magnitude of the temperature drops and the reaction rate locally reduces to zero. The compositional structure of the flame was studied by examining the statistical behavior of the species concentrations and the temperature near extinction. It is shown that by increasing the intensity of mixing (decreasing

the local Damkohler number), the effects of finite rate kinetics are more pronounced. The results of the statistical analysis indicate that as the flame approaches extinction, the mean and the rms values of the reactants concentrations increase whereas those of the product species and temperature decrease. This is consistent with the recent measurements of Masri et al. [5] for a nonequilibrium methane flame near extinction.

Acknowledgements

The assistance received from Dr. Moshe Israeli in developing the preliminary version of the computer code is gratefully acknowledged. This research was part of an effort sponsored by the Air Force Office of Scientific Research under Contract No. F49620-85-C-00067. The United States government is authorized to reproduce and distribute reprints for governmental purposes nonwithstanding any copyright notation hereon. The authors also appreciate the support of NASA Lewis Research Center in providing computer time on the CRAY-XMP computer.

References

1. Peters, N.: *Prog. Energy Comb. Sci*, 10, 319 (1984).

2. Bilger, R. W.: *Combustion and Flame*, submitted for publication (1987).

3. Liew, S. K., Bray, K.N.C. and Moss, J. B.: *Combustion and Flame*, 56, 199 (1984).

4. Masri, A. and Bilger, R. W.: Proceedings of Twenty-First Symposium (International) on Combustion, The Combustion Institute, in press (1987).

5. Masri, A., Dibble, R. W. and Bilger, R. W.: *Combustion and Flame*, in press (1987).

6. Jou, W.-H. and Riley, J. J.: AIAA paper 87-1324 (1987).

7. Riley, J. J., Metcalfe, R. W. and Orszag, S. A.: *Phys. Fluids*, 25, 406 (1986).

8. McMurtry, P. A., Jou, W.-H., Riley, J. J. and Metcalfe, R. W.: *AIAA Journal*, 24, 962 (1986).

9. Givi, P., Jou, W.-H. and Metcalfe, R. W.: Proceedings of Twenty-First Symposium (International) on Combustion, The Combustion Institute, in press (1987).

10. Givi, P. and McMurtry, P. A.: *Combust. Sci. Tech.*, 57, 141 (1988).

11. Givi, P. and Jou, W.-H.: *Journal of Nonequilibrium Thermodynamics*, in press (1987).

12. Masutani, S. M. and Bowman, C. T.: *Journal of Fluid Mechanics*, 172, 93 (1986).

13. Koocheshfahani, M. M. and Dimotakis, P. E.: *Journal of Fluid Mechanics*, 170, 83 (1986).

14. Lowery, P. S. and Reynolds, W. C.: Stanford University Report No. TF-26 (1987).

15. Roache, P. J.: *Computational Fluid Mechanics*, Hermosa Publishing Co., Albuquerque, New Mexico (1972).

16. Patera, A. T.: *Journal of Computational Physics*, 54, 468 (1984).

17. Baker, A. J.: *Finite Element Computational Fluid Mechanics*, Hemisphere Washington, D.C. (1983).

18. Korszak, K.: AIAA Paper 87-0133 (1987).

19. Reynolds, W. C.: Presented at AFOSR Contractors Meeting on Airbreathing Combustion, Pennsylvania State University, June (1987).

20. Givi, P. and Jou, W.-H.: work under progress (1987).

21. Rodi, W.: Ph.D. Thesis, University of London (1972).

22. Tsuji, H.: *Prog. Energy Comb. Sci.*, 8, 93 (1982).

23. Givi, P., Sirignano, W. A. and Pope, S. B.: *Combust. Sci. Tech.*, 37, 59 (1984).

24. Dibble, R. W. and Marge, P.: Sandia Report SAND87-8601, Sandia National Laboratories (1987).

25. Williams, F. A.: Presented at U.S.-France Workshop on Turbulent Reacting Flows, Rouen, France (1987).

26. Isizuka, S. and Tsuji, H.: Proceedings of Eighteenth Symposium (International) on Combustion, The Combustion Institute, 695, (1981).

27. Puri, I. K. and Seshardi, K.: *Combustion and Flame*, 65, 137 (1986).

28. Smooke, M. D., Puri, I. K. and Seshardi, K.: Proceedings of Twenty-First Symposium (International) on Combustion, in press (1987).

29. Dixon-Lewis, G., David, T., Gaskell, P. H., Fukutani, H., Jinno, H., Miller, J. A., Kee, R. T., Smooke, M. D., Peters, N., Effelsburgh, E., Warnatz, J., and Behrendt, F.: Proceedings of Twentieth Symposium (International) On Combustion, 1893 (1984).

30. Drake, M. C.: Proceedings of Twenty-First Symposium (International) on Combustion, in press (1987).

31. Peters, N. and Kee, R. J.: *Combustion and Flame*, in press (1987).

32. Seshardi, K. and Peters, N.: *Combustion and Flame*, in press (1987).

33. Trevino, C. and Williams, F. A.: Presented at Eleventh International Colloquium on Dynamics of Explosions and Reactive Systems, Warsaw, Poland, (1987).

Figure Captions:

Figure 1: Geometrical configuration showing the spectral elements and the collocation points.

Figure 2: Time sequence of Shvab-Zeldovich variable contours. Contour minimum is 0, contour maximum is 1.0, contour interval is 0.05. (a) t=176 (b) t=208 (c) t=240.

Figure 3: Time sequence of product concentration contours. contour minimum is 0, contour maximum is 0.8, contour interval is 0.05. (a) t=176 (b) t=208 (c) t=240.

Figure 4: Time sequence of instantaneous reaction rates contours. Contour minimum is 0, contour maximum is 0.039, contour interval is 0.001. (a) t=176 (b) t=208 (c) t=240.

Figure 5: Mean concentration values of species B at every other grid point in Y.

Figure 6: Mean product concentration values at every other grid point in Y.

Figure 7: Mean fluctuations of species A at every other grid point in Y.

Figure 8: Mean fluctuations of species B at every other grid point in Y.

Figure 9: Mean fluctuations of product species at every other grid point in Y.

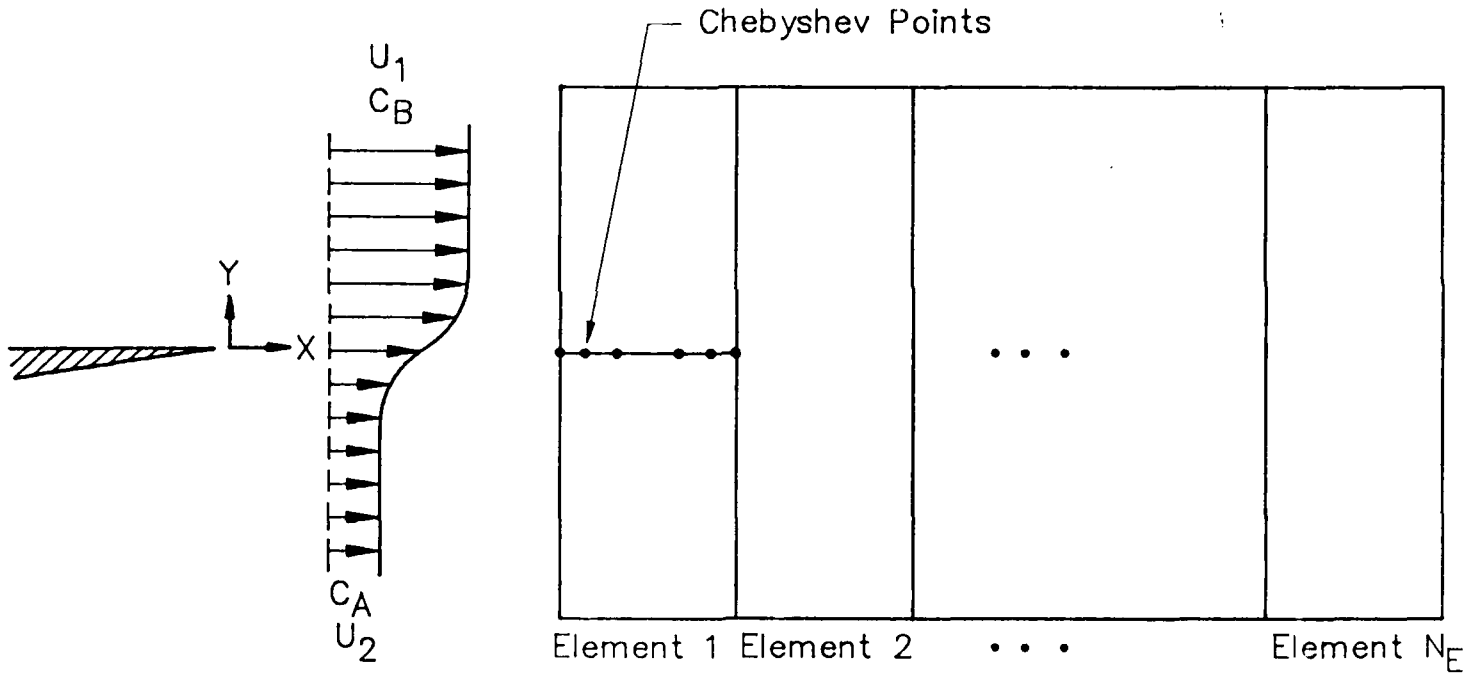
Chebyshev Points
U_1
C_B
Y
X
C_A
U_2
Element 1
Element 2
Element N_E

Figure 1

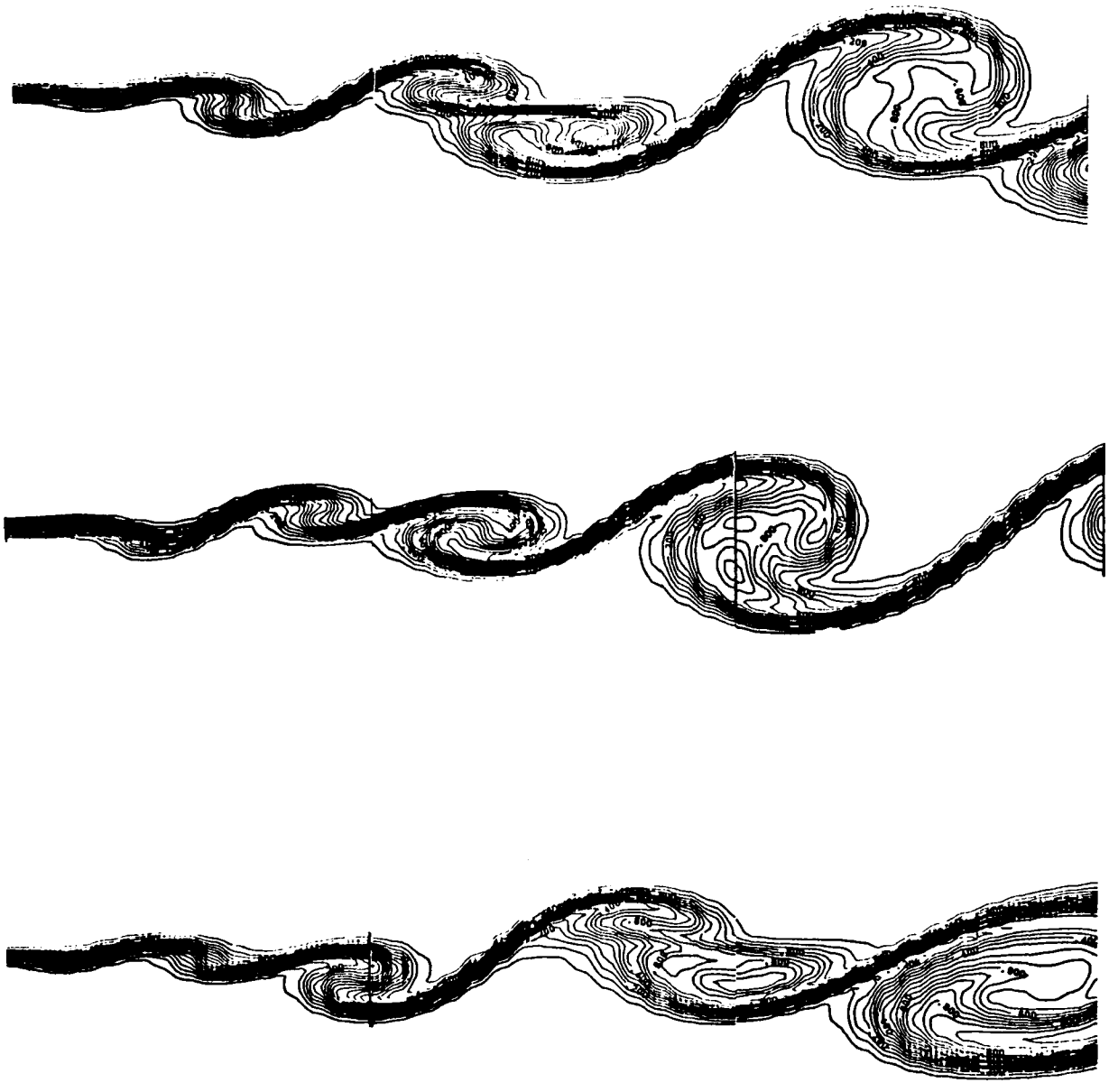

Figure 2

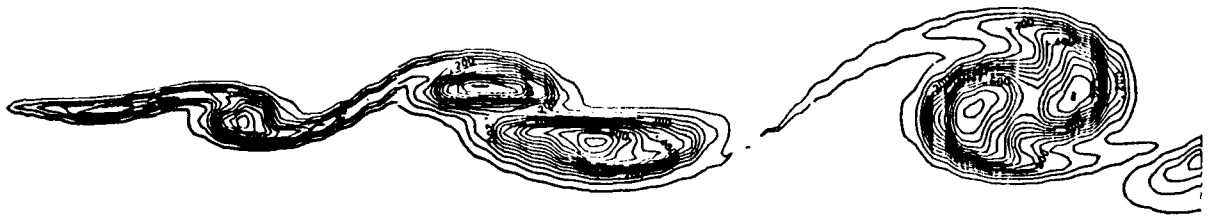

(a)

(b)

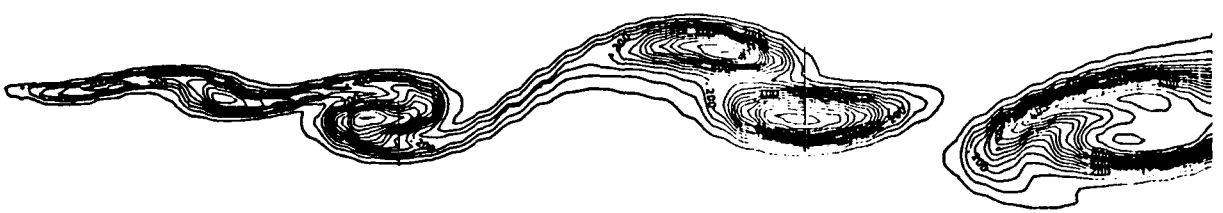

(c)

Figure 3

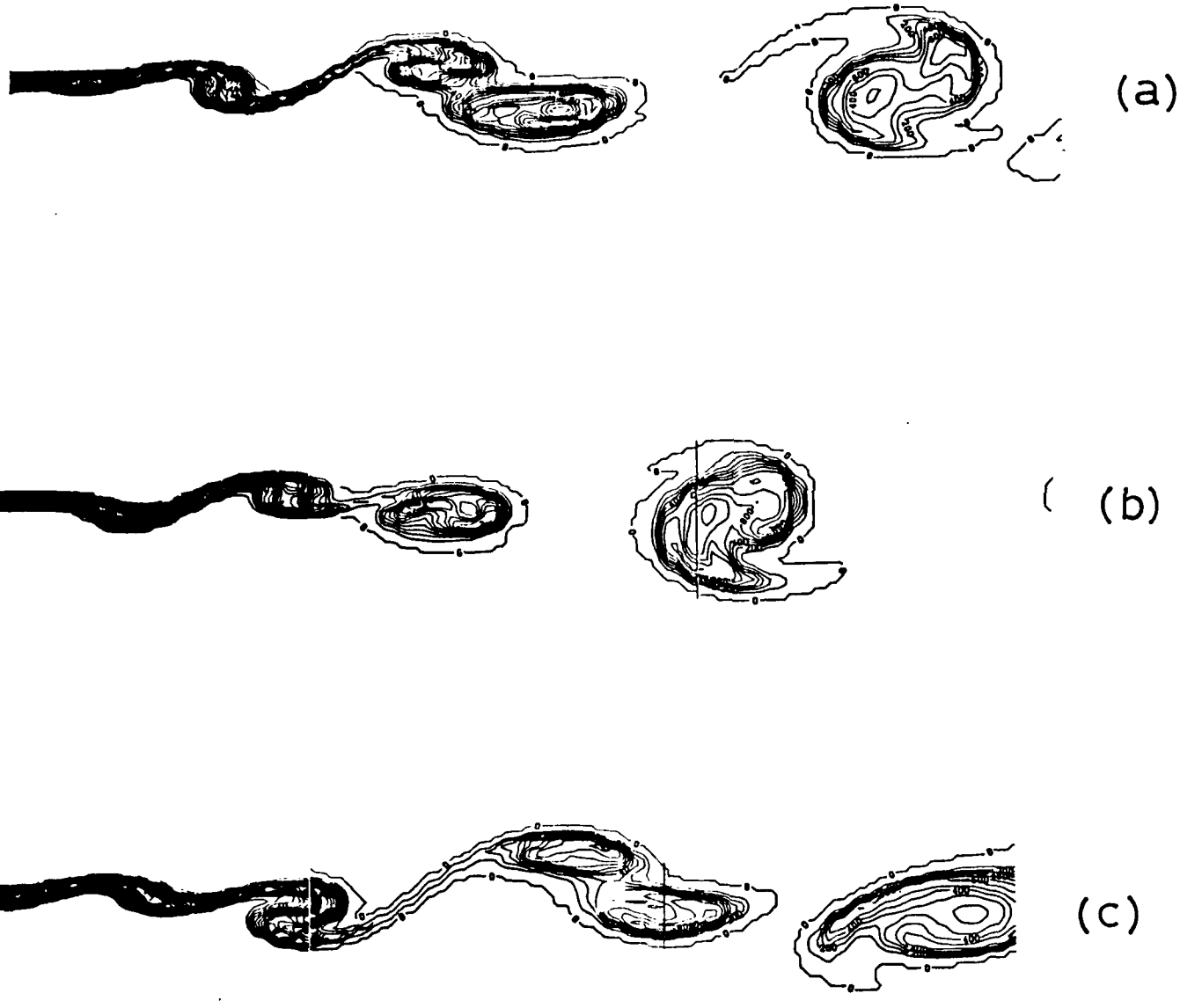

Figure 4

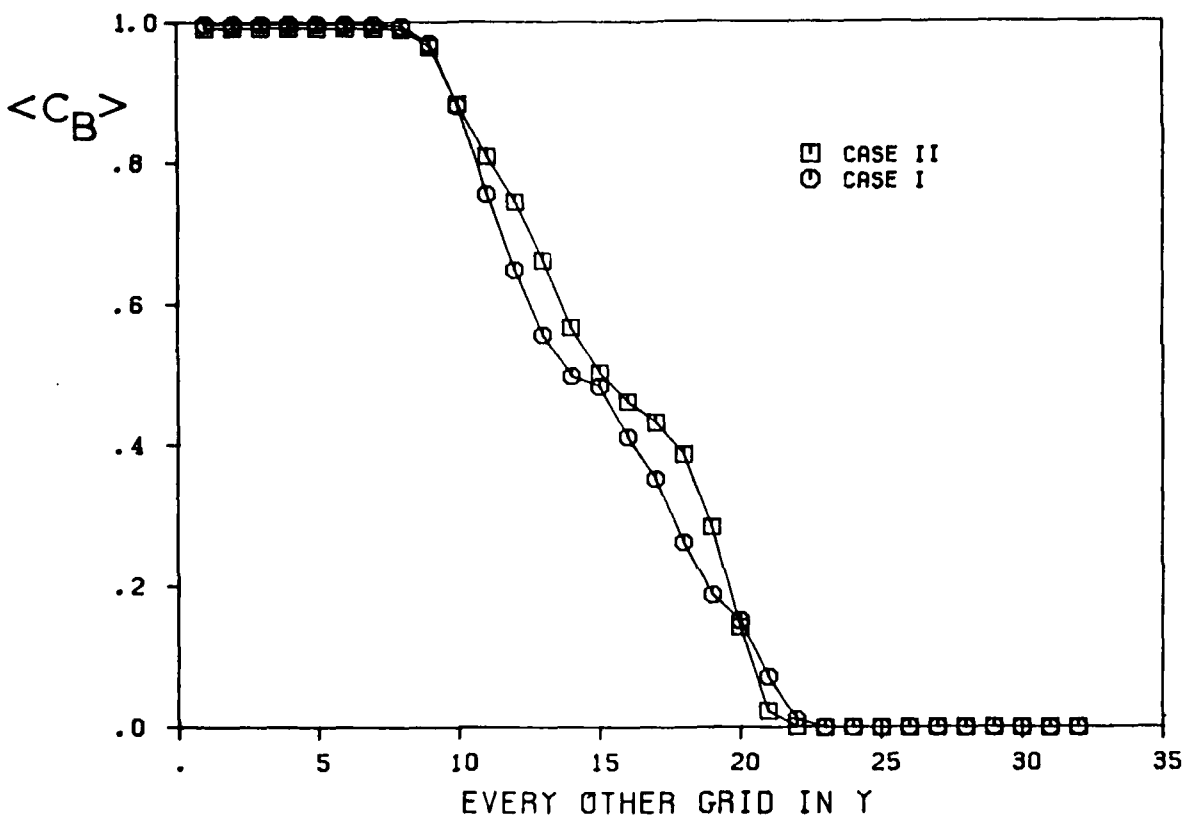
1.0
.8
.6
.4
.2
.0
<C_B>
CASE II
CASE I
5
10
15
20
25
30
35
EVERY OTHER GRID IN Y

Figure 5

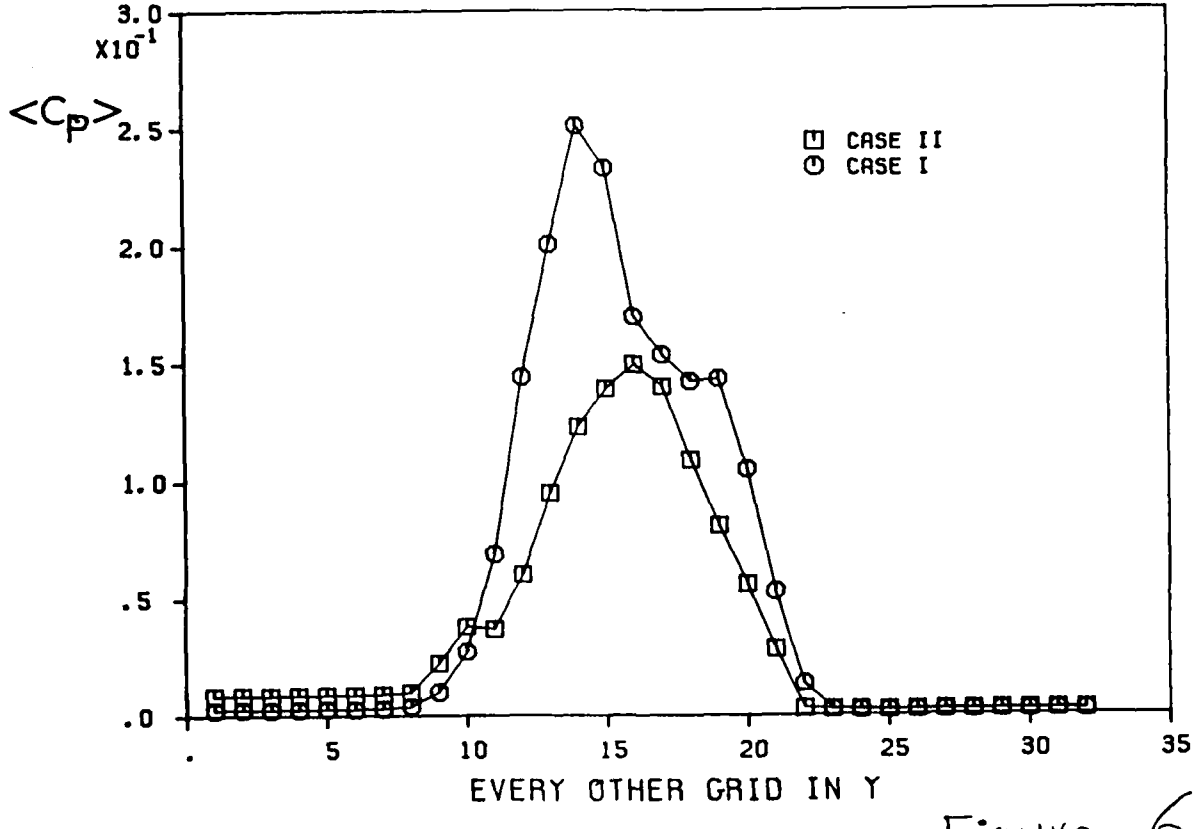
3.0
X10⁻¹
<Cp>
2.5
2.0
1.5
1.0
.5
.0
5
10
15
20
25
30
35
CASE II
CASE I
EVERY OTHER GRID IN Y

Figure 6

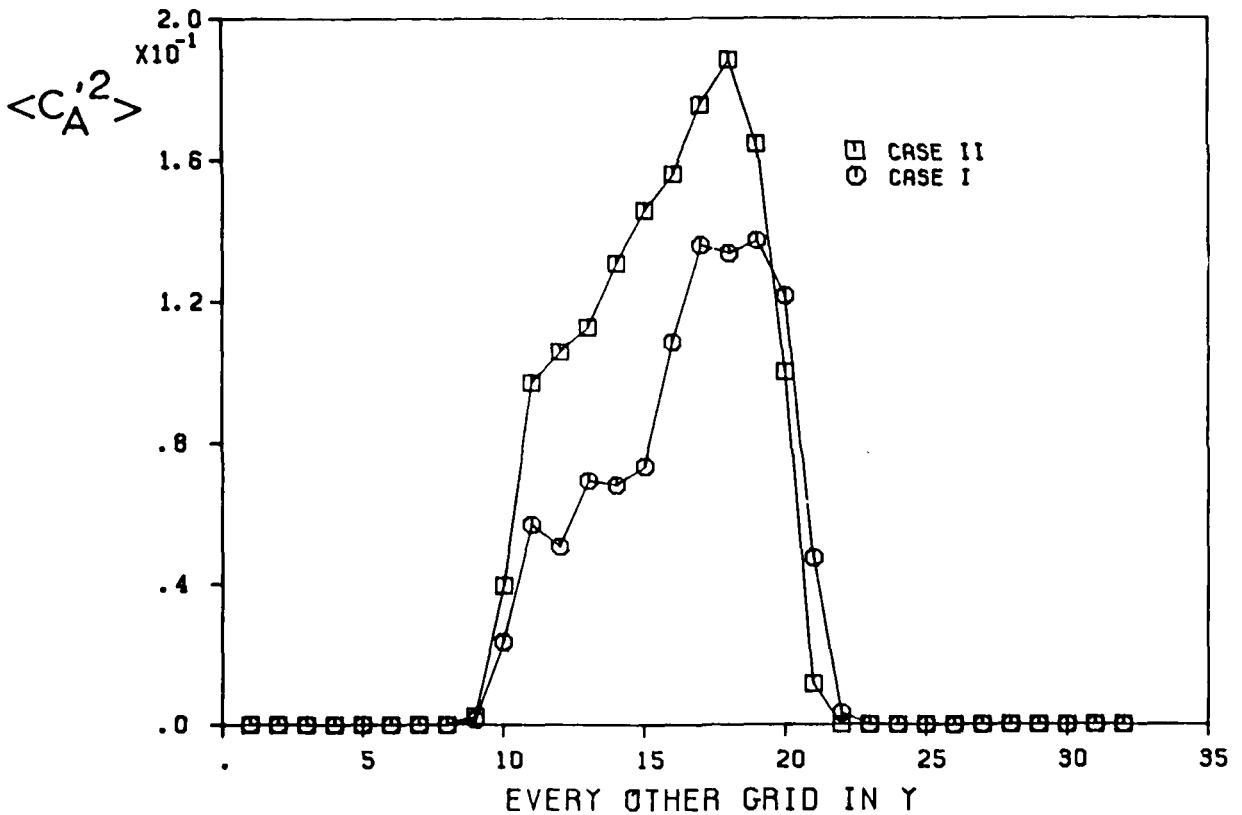
2.0
X10⁻¹
<C'A²>
1.6
1.2
.8
.4
.0
CASE II
CASE I
5
10
15
20
25
30
35
EVERY OTHER GRID IN Y

Figure 7

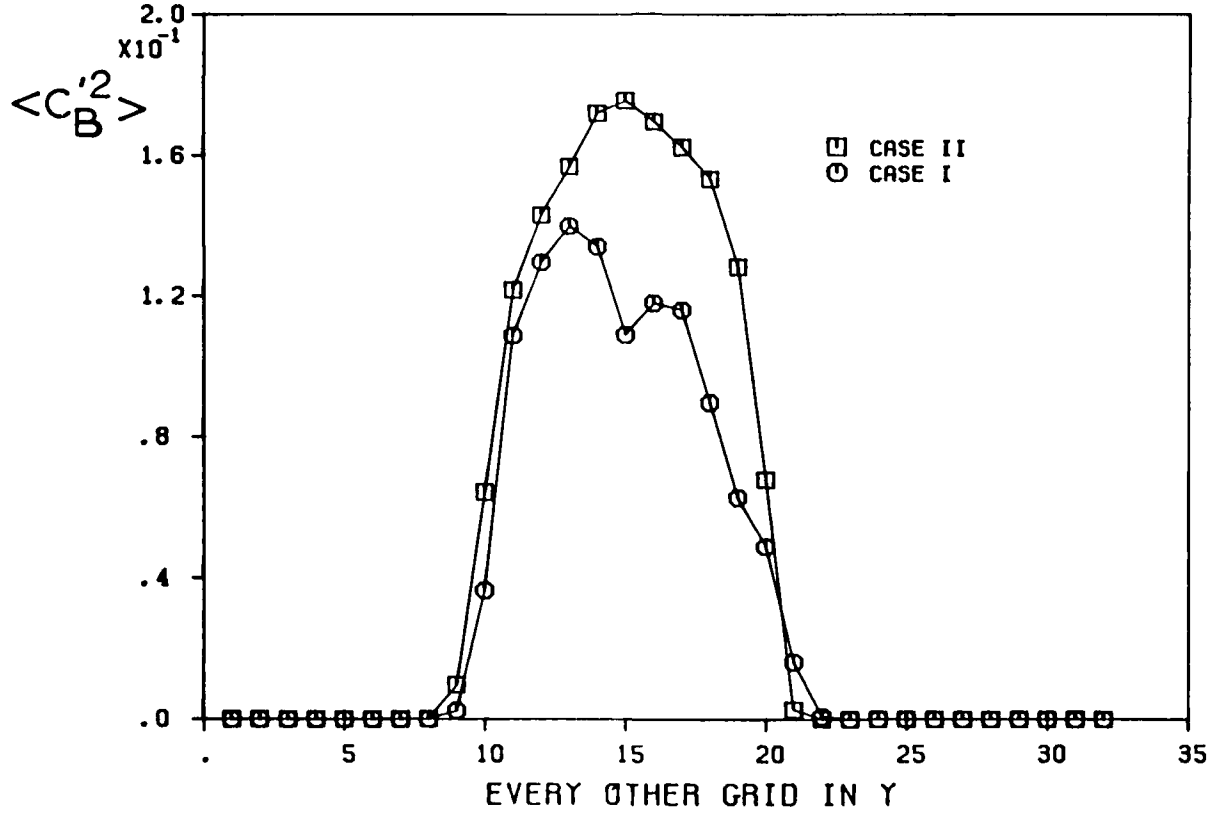
2.0
X10⁻¹
<C'²B>
1.6
1.2
.8
.4
.0
CASE II
CASE I
5
10
15
20
25
30
35
EVERY OTHER GRID IN Y

Figure 8

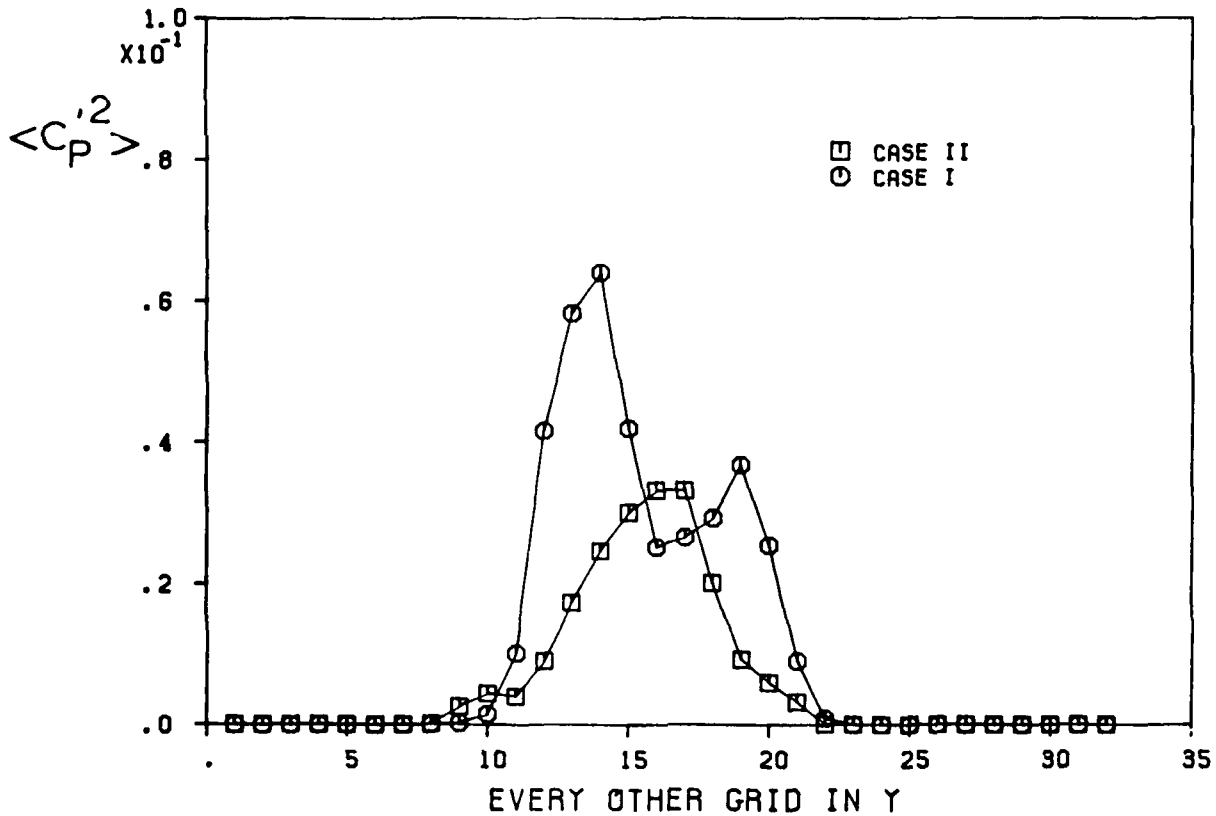
1.0
X10^-1
<C_P'^2>
.8
.6
.4
.2
.0
CASE II
CASE I
5
10
15
20
25
30
35
EVERY OTHER GRID IN Y

Figure 9

APPENDIX VI

Non-Premixed Reaction in Homogeneous Turbulence: Direct Numerical Simulations

NON-PREMIXED REACTION IN HOMOGENEOUS TURBULENCE: DIRECT NUMERICAL SIMULATIONS

by

Peyman Givi* and Patrick A. McMurtry
Flow Research Company
21414-68th Avenue South
Kent, WA 98032

December 1987

Revised Manuscript Accepted for Publication as an
R&D Note in AIChE Journal

*To whom all the correspondence should be addressed.

INTRODUCTION

In accordance with Toor's original paper (1962), consider an irreversible, one-step isothermal reaction of the type A + B → Products in a non-premixed homogeneous turbulent flow. Let $A(\underline{x},t)$ and $B(\underline{x},t)$ define the instantaneous concentration of the two species and decompose each concentration into an ensemble mean value (denoted by $< >$) and its fluctuation from the mean value (represented by small letters):

$$A = \langle A \rangle + a$$
$$B = \langle B \rangle + b \tag{1}$$

Under the assumptions given above, the transport equations governing the evolution of the mean concentrations are

$$L(\langle A \rangle) = \frac{d\langle A \rangle}{dt} = -W \tag{2}$$

$$L(\langle B \rangle) = -W \tag{3}$$

$$W = K\,[\langle A \rangle \langle B \rangle + \langle ab \rangle] \tag{4}$$

where W is the mean reaction rate, K is the kinetic speed of the reaction, and L is the convection-diffusion operator, which is the same for the two reactants if their diffusion coefficients are identical. The second term on the right-hand side of Equation (4) is unclosed and needs to be modeled. This term can be written, in normalized form (Toor, 1975; Kosaly, 1987),

$$\psi^2(t) = \frac{\langle ab \rangle_t}{\langle ab \rangle_o} \tag{5}$$

where the subscripts t and o refer to the time and the initial time (i.e., the inlet of a plug flow reactor), respectively. Turbulent mixing is characterized by the root-mean-square of one of the reactants in the absence of reaction:

$$d^2(t) = \frac{\langle a_m^2 \rangle_t}{\langle a_m^2 \rangle_o} \tag{6}$$

where m refers to "pure mixing" only. It is obvious that, in the limit of zero rate chemistry, $d^2(t)$ and $\psi^2(t)$ are identical (Toor, 1975), i.e.,

$$d^2(t) = \lim_{K \to 0} \psi^2(t) \tag{7}$$

In the limit of infinitely fast chemistry under stoichiometric conditions, and assuming a Gaussian shape* for the probability density function (PDF) of the mixture fraction $J(\underline{x},t)$ [defined by $J(\underline{x},t) = A(\underline{x},t) - B(\underline{x},t)$], Toor showed that

$$d^2(t) = \lim_{K \to \infty} \psi^2(t) \tag{8}$$

Based on Equations (7) and (8), Toor assumed that

$$\psi^2(t) = d^2(t) \text{ for any } K \tag{9}$$

Equation (9) summarizes Toor's hypothesis.

In the recent paper of Kosaly (1987), it is shown that the application of Toor's hypothesis is not valid for the predictions of plug flow reactors in which the initial shape of the PDF of the variable $J(\underline{x},t)$ is not Gaussian but rather of bimodal shape determined by initial conditions. Kosaly showed that, while $d^2(t)$ and $\psi^2(t)$ are identical for zero rate chemistry [i.e., Equation (7)] and at $t = 0$ for all K, Equation (8) should be replaced by

$$\lim_{K \to \infty} \psi^2(t) = \frac{2}{\pi} d^2(t) \tag{10}$$

at later times. The factor $2/\pi$ was a result of algebraic manipulation assuming the PDF of J becomes Gaussian (see Kosaly, 1987, for details).

In this note, we first provide a generalization of Kosaly's result and, by use of direct numerical simulation (DNS), further investigate the validity of Toor's hypothesis and the revisions proposed by Kosaly. In this application DNS refers to the numerical solution of the aerothermodynamic transport equations of turbulent reacting flows for the detailed time development of the flow field. This technique uses no closure modeling, and no assumptions are

---

*This assumption can be relaxed for symmetric PDF's (O'Brien, 1971).

made pertaining to the turbulent behavior of the fluid. DNS has proven very useful in computational studies of turbulence (see Rogallo and Moin, 1984, for a review) and is used here as a means of performing experiments on the computer. This approach offers advantages over laboratory experiments in that the instantaneous values of the hydrochemical variables are known at all locations at each time step, allowing better statistical analysis of the data. Computer limitations restrict, of course, the ranges of time and space scales that can be accurately resolved.

GENERALIZATION OF TOOR'S HYPOTHESIS

Kosaly's results can be generalized by defining the normalized variable $\hat{\phi}$ and the standard PDF $P(\hat{\phi},\hat{t})$ as (Pope, 1982)

$$\hat{\phi} = \frac{\phi}{\sigma(t)} \tag{11}$$

$$\hat{P}(\hat{\phi},t) = P(\phi,t)\ \sigma(t) \tag{12}$$

where $P(\phi,t)$ is the PDF of J, and σ is the standard deviation. Assuming that the PDF approaches an asymptotic time-independent form (whether Gaussian or not), we have

$$\hat{P}(\hat{\phi},t) \approx \hat{P}(\hat{\phi}) \tag{13}$$

or

$$P(\phi,t) \approx \frac{\hat{P}[\phi/\sigma(t)]}{\sigma(t)} \tag{14}$$

With an asymptotic shape of $\hat{P}(\hat{\phi})$, Kosaly's results generalize to

$$\Psi^2(t) = C\ d^2(t) \tag{15}$$

where

$$C = 4\left[\int_0^\infty \hat{\phi}\ \hat{P}(\hat{\phi})\ d\hat{\phi}\right]^2 \tag{16}$$

For a PDF that asymptotically assumes a Gaussian form,

$$\hat{P}(\hat{\phi}) = \frac{1}{\sqrt{2\pi}}\ \exp\ (-\hat{\phi}^2/2) \tag{17}$$

the value of C would be the same as that given by Kosaly (1987), i.e., $C = 2/\pi$. The exact asymptotic shape of the PDF, therefore, determines the constant of proportionality in Equation (15). The magnitude of this constant, which is valid only in the final stages of mixing, cannot be predicted mathematically and can only be estimated experimentally or numerically.

SIMULATION RESULTS

A pseudospectral numerical method developed by McMurtry (1987) was modified for the calculations of the homogeneous turbulent flow considered here. This method is very similar to that employed previously by Riley et al. (1986), McMurtry et al. (1986, 1987), Givi et al. (1987) and Givi and Jou (1987) and, therefore, will not be explained here. The scalar fields are defined to be square waves with the two reactants out of phase and at stoichiometric conditions. This is similar to that used previously by Leonard and Hill (1986, 1987). The flow field is initialized by specifying the turbulence spectrum (similar to that used by McMurtry, 1987), and a forcing mechanism is employed to keep the turbulence stationary by adding energy artificially to the large scale motions (low wave numbers in Fourier space). This forcing was applied in such a way to conpensate for small scale dissipation without affecting the small scale statistics of interest (McMurtry and Givi, 1987). Periodic boundary conditions are employed in all three directions, and the aerothermodynamical variables are spectrally approximated on 64X64X64 collocation points within the computational domain. The values of the Reynolds and Peclet numbers are kept within moderate levels to ensure the accuracy of the simulations on the grids used. Calculations were performed with zero rate and infinitely fast chemical reactions to assess the influence of the chemistry on the decay rate of the unmixedness parameter (ψ^2). In the zero rate chemistry simulations, the value of K was set to zero in Equation (4), whereas, in the infinitely fast rate chemistry calculations, the statistical variations of the two reactants A and B were related to that of the conserved scalar variable J (Bilger, 1980; Kosaly and Givi, 1987).

For the purpose of flow visualization, two-dimensional contour plots of species A are presented in Figure 1. Parts (a) and (b) of this figure correspond to zero rate and infinitely fast chemical reactions, respectively. Time is normalized by the large-scale turbulence frequency, and the nondimensional time of $t = 1.2$ corresponds to the case when the average

concentration of species A under reacting conditions has reduced to 30% of its initial value. This figure exhibits the effects of three-dimensional turbulent motion on the distortion of the scalar field and the mixing of the two initially segregated reactants (the contours form parallel lines at t = 0). The effects of chemical reactions are to increase the steepness of the scalar gradients and, obviously, to reduce the instantaneous values of the reactants as indicated by a comparison between parts (a) and (b) of Figure 1. The influence of the chemical reactions on the decay rate of the unmixedness is shown in Figure 2. In this figure, the ratio $\Psi^2(t)/d^2(t)$ is presented versus time for zero rate and infinitely fast chemical reactions. For zero rate chemistry, the ratio, obviously, remains at unity. For the reacting case, at the initial time (t = 0), the influence of chemistry is nil. At later times, however, the value of the unmixedness for the fast chemistry is lower than that under zero rate chemistry. The results shown in this figure indicate that, for initially non-premixed reactants, the decay rate of the unmixedness is not independent of the chemical reactions and depends on the magnitude of the local Damkohler number.

The theoretical discussion given in the previous section on the lack of agreement with Toor's hypothesis is verified by examining the temporal evolution of the PDF of J (i.e., $P(\phi,t)$, $-1 \leq \phi \leq 1$) in Figure 3. It is clearly seen that the evolution of the PDF from its initial bimodal shape (composed of two delta functions at $\phi = \pm 1$ to its asymptotic shape (composed of a single delta function at $\phi = 0$) cannot be characterized by its first two moments (i.e., 0 and σ). Therefore, Equation (9) is not valid for intermediate times, and the application of Toor's hypothesis is not appropriate for the prediction of the conversion rate in plug flow-type reactors with initially segregated reactants.

Figure 2 further indicates the interesting result that the ratio of Ψ^2/d^2 for the infinitely fast chemistry approaches the value of 0.64 ($\simeq 2/\pi$). This value corresponds to the case if $\hat{P}(\hat{\phi})$ asymptotically adopts a Gaussian Profile (Kosaly, 1987). To ascertain the asymptotic shape of the PDF, the temporal variation of the kurtosis (μ_4 = normalized fourth moment) of species A is presented in Figure 4. It is seen that, under no chemical reaction, the value of this variable approaches $\mu_4 = 2.9$. The asymptotic values of the normalized sixth (superskewness) and eight moments are $\mu_6 = 13.9$ and $\mu_8 = 98$, and all the odd moments remain close to zero (not shown here). A comparison of these values with those of a Gaussian profile (i.e., $\mu_4 = 3$, $\mu_6 = 15$, and $\mu_8 = 105$)

indicates that the approximation of a Gaussian PDF for the final stages of mixing of a nonreacting scalar is justified. Better agreements would require a larger sample size than the presently used 64^3 data points for more accurate statistical analysis. For the reacting case, however, the values of the normalized fourth and higher order moments are larger than those of an inert scalar. This is shown in Figure 4 for the Kurtosis of one of the reactants and is consistent with our previous calculations (Kosaly and Givi, 1987). Therefore, a Gaussian PDF assumption is not justified in this case.

Finally, it must be mentioned that the results of our present calculations are not in agreement with those previously obtained by Leonard and Hill (1986). In their calculations, the ratio of ψ^2/d^2 initially decreases from unity with time but asymptotically returns to unity for longer times. This lack of agreement with Leonard and Hill's calculations may be attributed to the fact that, in their finite rate chemistry simulations, the magnitude of the Damkohler number is not large enough to justify the infinitely fast chemistry assumption adopted here.

The results of this work and those of Kosaly (1987) indicate the need for detailed measurements in plug flow reactors for comparison with numerical simulations. The present simulations indicate that Toor's hypothesis ($\psi^2 = d^2$) should be modified by Equation (15) for infinite rate chemistry at the temporal asymptote. For finite rate chemistry and intermediate times, however, the application of the hypothesis is not valid and full simulations are required. The numerical experiments reported here indicate that the asymptotic shape of the PDF of a conserved scalar characterizing mixing is approximately Gaussian. This suggests a value of $C = 2/\pi$ in Equation (15).

5619R

REFERENCES

Bilger, R. W, "Turbulent Flows with Non-premixed Reactants," In Turbulent Reacting Flows (P. A. Libby and F. A. Williams, eds.), Springer-Verlag, Heidelberg, Vol. 44, Topics in Applied Physics (1980).

Givi, P., and W.-H. Jou, "Mixing and Chemical Reactions in a Spatially Developing Mixing Layer," Accepted for publication in J. Nonequil. Thermodyn., in press (1987).

Givi, P., W.-H. Jou and R. W. Metcalfe, "Flame Extinction in a Temporally Developing Mixing Layer," In Proceedings of 21st Symposium (Int.) on Combustion, in press (1987).

Kosaly, G., "Non-Premixed Simple Reaction in Homogeneous Turbulence," Accepted for publication in AIChE J., (1987).

Kosaly, G. and P. Givi, "Modeling of Turbulent Molecular Mixing," Combustion and Flame, 70, 101 (1987).

Leonard, A. D., and J. C. Hill, "Direct Simulation of Turbulent Mixing with Irreversible Chemical Reaction," Paper presented at the Third World Congress of Chem. Eng., Tokyo, Sept. (1986).

Leonard, A. D., and J. C. Hill, "A Simple Chemical Reaction in Numerically Simulated Homogeneous Turbulence," AIAA Paper 87-0134, 25th Aerospace Sciences Meeting, January 12-15, Reno, Nevada (1987).

McMurtry, P. A., "Direct Numerical Simulations of a Reacting Mixing Layer with Chemical Heat Release," Ph.D. Thesis, University of Washington, Seattle, WA, February (1987).

McMurtry, P. A., and P. Givi, paper in progress (1987).

McMurtry, P. A., W.-H. Jou, J. J. Riley, and R. W. Metcalfe, "Direct Numerical Simulation of a Reacting Mixing Layer with Chemical Heat Release," AIAA J., 24(6), 962 (1986).

McMurtry, P. A., J. J. Riley and R. W. Metcalfe, "Mechanisms by Which Heat Release Affects the Flow Field in a Chemically Reacting, Turbulent Mixing Layer," AIAA Paper 87-0121, 25th Aerospace Sciences Meeting, January 12-15, Reno, Nevada (1987).

O'Brien, E. E., "Turbulent Mixing of Two Rapidly Reacting Chemical Species," Phys. Fluids, 14, 1326 (1971).

Pope, S. B., "An Improved Turbulent Mixing Model," Combust. Sci. and Tech., 28, 131 (1982).

Riley, J. J., R. W. Metcalfe and S. A. Orszag, "Direct Numerical Simulations of Chemically Reacting Mixing Layer," Phys. Fluids, 29, 406 (1986).

Rogallo, R. S. and Moin, P., "Numerical Simulation of Turbulent Flows," Ann. Rev. Fluid Mech., 16, 99 (1984).

Toor, H. L., "Mass Transfer in Dilute Turbulent and Nonturbulent Systems with Rapid Irreversible Reactions and Equal Diffusivities," AIChE J., 8, 70 (1962).

Toor, H. L., "Turbulent Mixing of Two Species With and Without Chemical Reactions," Ind. Eng. Chem. Fundamentals, 8, 655 (1969).

Toor, H. L., "The Non-premixed Reaction; A + B → Products," In Turbulence in Mixing Operations (R. S. Brodkey, ed.), Academic Press, New York (1975).

ACKNOWLEDGEMENT

The authors are indebted to Drs. James Hill and George Kosaly for valuable discussions on the topic. The first author wishes to acknowledge Professor Herbert Toor for introducing him to Toor's hypothesis. This research was part of an effort sponsored by the Air Force Office of Scientific Research under Contract No. F49620-85-C-00067. The United States government is authorized to reproduce and distribute reprints for governmental purposes nonwithstanding any copyright notation hereon. The authors also appreciate the support of NASA Lewis Research Center for providing computer time on CRAY-XMP.

NOTATION

A,B	=	instantaneous concentration of reacting species
a,b	=	instantaneous concentration fluctuation of reacting species
$d^2(t)$	=	$< a_m^2 >_t / < a_m^2 >_o$
J	=	A - B
K	=	kinetic reaction rate
P	=	PDF
t	=	time
W	=	reaction rate
σ	=	standard deviation
ϕ	=	scalar space
$\Psi^2(t)$	=	$< ab >_t / < ab >_o$

Indices

o	=	initial
m	=	mixing in absence of chemical reaction

Other Notations

< >	=	ensemble average

FIGURE CAPTIONS

Figure 1: Plots of species A concentration contours at t = 1.2.
(a) nonreacting case, contour minimum is 0.06, contour maximum is 0.72, contour interval is 0.06. Labels are scaled by 1000.
(b) reacting case, contour minimum is 0, contour maximum is 0.66, contour interval is 0.06.

Figure 2: Temporal variation of ψ^2/d^2.

Figure 3: Temporal variation of $P(\phi)$.

Figure 4: Temporal variation of μ_4.

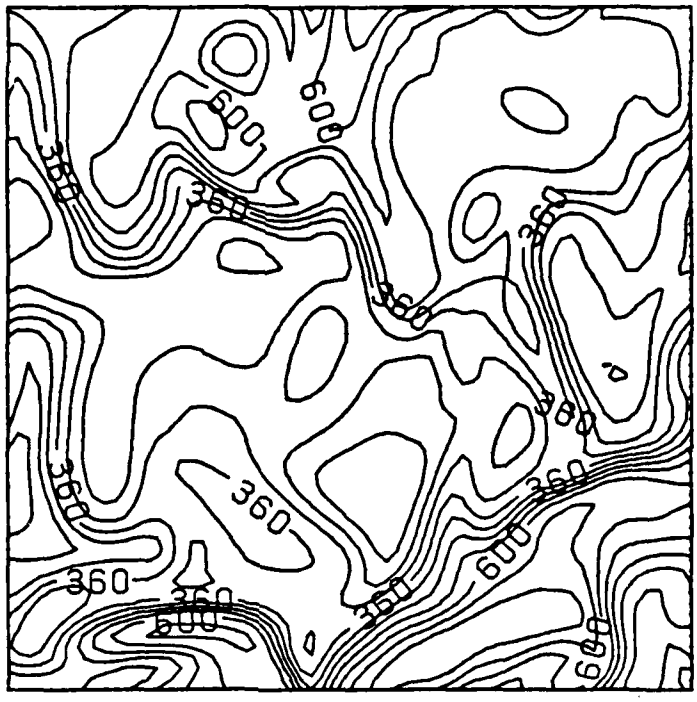

(a)

(b)

Figure 1

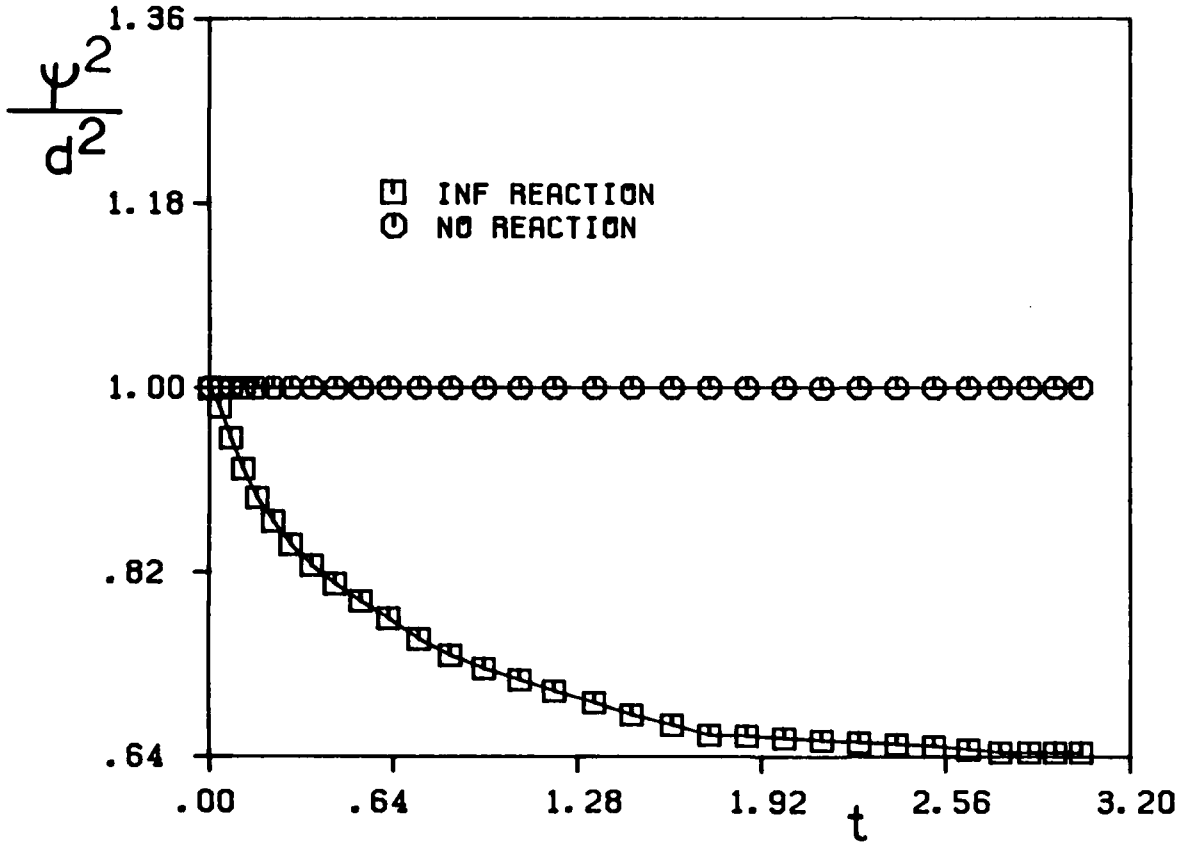
1.36
1.18
1.00
.82
.64
$\frac{\psi^2}{d^2}$
INF REACTION
NO REACTION
.00
.64
1.28
1.92
2.56
3.20
t

Figure 2

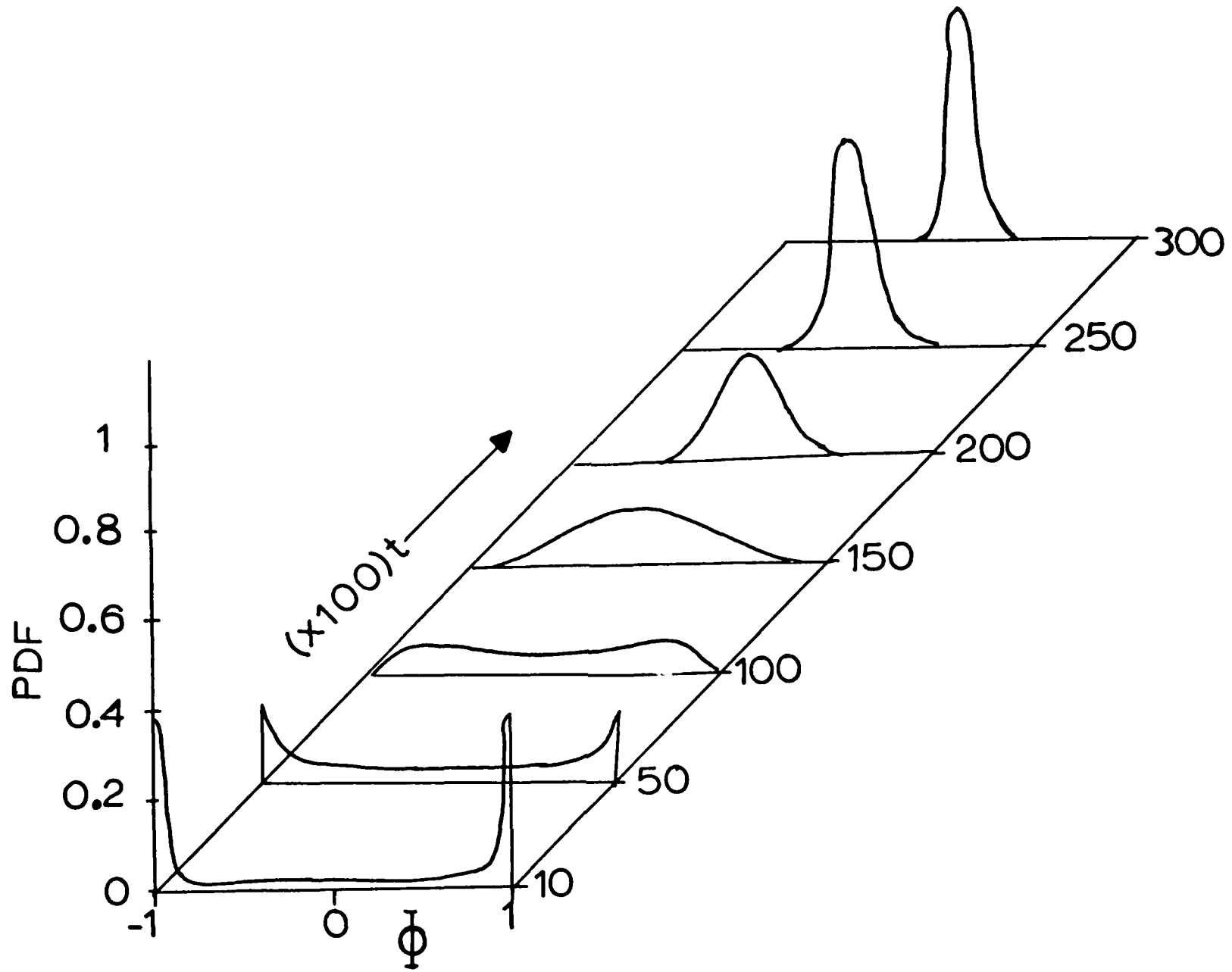

Figure 3

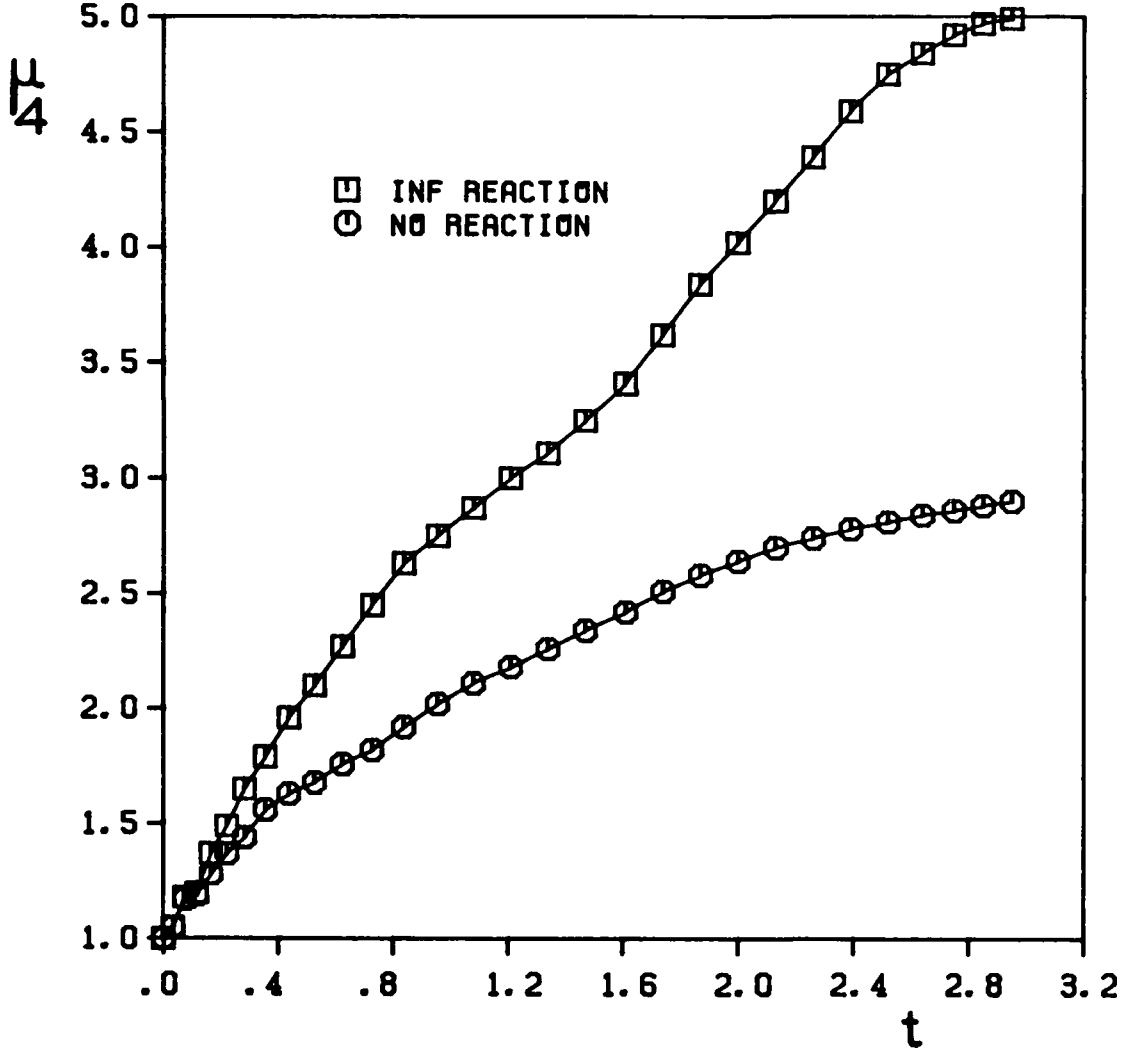
5.0
4.5
4.0
3.5
3.0
2.5
2.0
1.5
1.0
μ4
INF REACTION
NO REACTION
.0
.4
.8
1.2
1.6
2.0
2.4
2.8
3.2
t

Figure 4

APPENDIX VII

Direct Numerical Simulations of a Non-Premixed Homogeneous Turbulent Flow

DIRECT NUMERICAL SIMULATIONS OF A NON-PREMIXED HOMOGENEOUS TURBULENT FLOW

by

P. A. McMurtry and P. Givi
Flow Research Company
21414-68th Avenue South
Kent, WA 98032

Manuscript submitted for publication to Combustion and Flame

December 1987

ABSTRACT

Direct numerical simulations have been performed to study the mechanisms of mixing and chemical reaction in a three-dimensional, homogeneous turbulent flow under the influence of the reaction of the type A + B → Products. The results are used to examine the applicability of Toor's hypothesis [1] and also to determine the range of validity of various coalescence/dispersion (C/D) turbulence models that have been used previously to model the effects of turbulent mixing in such flows [2]. The results of numerical experiments indicate that the probability density function (PDF) of a conserved Shvab-Zeldovich scalar quantity, characterizing the mixing process, evolves from an initial double-delta distribution to an asymptotic shape that can be approximated by a Gaussian distribution. During this evolution, the PDF cannot be characterized by its first two moments; therefore, the application of Toor's hypothesis is not appropriate for the prediction of such flows. The results further indicate that the initial stages of mixing are well represented by the Dopazo-O'Brien C/D model, whereas, at intermediate times, the experimental results fall between those obtained by the two closures of Dopazo and O'Brien [3] and Janicka et al. [4], and deviate the most from those of Curl [5]. Therefore, a C/D model between the two closures of Dopazo-O'Brien and Janicka et al. is expected to result in favorable comparison with our data. The final stages of mixing are not well predicted by any of the C/D closures in that none of the models is capable of predicting a Gaussian asymptotic PDF for the Shvab-Zeldovich scalar variable. The results of our numerical experiments may be used to generate a C/D model (or models) that can predict all the stages of mixing accurately.

1. INTRODUCTION

In a recent paper, Kosaly and Givi [2] studied the mechanisms of mixing and reaction in a non-premixed, homogeneous turbulent flow under the influence of an isothermal chemical reaction of the type A + B → Products. In their calculations, single-point probability density function (PDF) methods were employed for the transport of scalar quantities, and various coalescence/dispersion (C/D) mixing models were used for the closure of the molecular mixing term in the PDF evolution equation. Calculations were performed with zero-rate, as well as infinitely fast chemical reactions, and the results indicated sensitivity to the choice of the C/D model employed. In that work, a set of new observations was presented that helped to clarify the relationship between the different types of C/D models. Also, new insight was gained regarding the nature of C/D modeling by comparing the results of such models to those obtained by applying Toor's hypothesis [1,6,7]. Despite encouraging results, it was concluded that, since C/D modeling is fundamentally phenomenological in nature, comparison to experimental data is the only way to determine its applicability and range of validity.

In the present work, we intend to provide such experimental data for the purpose given above. The data provided here, however, are not obtained from conventional laboratory measurements but rather using the method of direct numerical simulations (DNS). DNS refers to the numerical solution of the exact aerothermodynamical equations (nonaveraged) of the unsteady, turbulent reacting flow field. No turbulence modeling is used so that no assumptions are made concerning the turbulent behavior of the fluid. Computational requirements of DNS are very severe, however, and restrict the range of time and space scales that can be resolved. Full simulations require on the order of hours of CPU time on the fastest available computers and are limited to relatively simple systems, as studied here. Despite these limitations, this approach has proven very useful in computational studies of turbulence (see Rogallo and Moin [8] for a review) and turbulent reacting flows (Riley et al. [9]; McMurtry et al. [10]; Givi et al. [11]; Givi and Jou [12]). In conjunction with laboratory measurements, DNS offers a useful alternative of probing data when experimental techniques may fail.

Here, direct numerical simulations are employed to study the process of mixing and the influence of chemical reaction in a non-premixed, homogeneous, constant-density flow under the influence of a single-step, irreversible,

isothermal reaction of the type A + B → Products. This type of reacting system has been extensively used by Toor and associates (see Toor [1] for a review) and provides a simplified system in which the effects of mixing and chemical reactions can be isolated. The DNS results are compared with those obtained by calculation based on C/D closures to address the shortcomings associated with the presently used C/D models. A comparison between the results of simulations and Toor's results is also presented, and the validity of applying Toor's hypothesis for initially segregated binary scalar field is discussed. Pure mixing, finite-rate, and infinitely fast reaction rate calculations are performed to examine the effects of chemistry on the transport of concentration fluctuations. Higher order concentration moments are also calculated, and the results are compared with calculations based on C/D closures to further study the sensitivity of high concentration moments to chemistry.

In the next section, the methodology of direct numerical simulation applied to a non-premixed turbulent flow field is discussed. A brief description of the geometrical configuration and flow initialization are also given. In Sections 3 and 4, we briefly review Toor's hypothesis and C/D modeling in anticipation of our numerical results, which are presented in Section 5. These results are used to examine the validity of Toor's hypothesis and, in general, to study the statistical behavior of the reacting species. The evolution of the PDF of a conserved scalar is presented to further clarify the process of mixing in this system. Comparisons of the simulation results, and those of various C/D models are also made in this section. The results are summarized in Section 6, and we also summarize and present the conclusions of our findings.

2. DIRECT NUMERICAL SIMULATIONS

The subject in these numerical experiments is a three-dimensional homogeneous turbulent ("box") flow field under the influence of an isothermal binary reaction of the type A + B → Products (Fig. 1). To impose homogeneity, periodic boundary conditions are employed in all three directions of the flow identifying the "box" as a homogeneous member of a turbulent universe. This periodicity allows the mapping of all the aerothermodynamical variables from the physical domain into a Fourier space using Fourier transforms. Therefore, rather than approximating the variables on discrete

grid points (which is usually the case for typical finite difference schemes), they are represented by functions passing through the collocation points. This allows the use of pseudospectral numerical methods for simulating the flow in the wave number domain [13]. Compared to typical finite difference schemes, this approach has the advantage of resolving the various small scales of the flow more accurately (and in fewer grid points), making it more attractive for turbulence simulations. The values of the nondimensional parameters characterizing the flow (i.e., Reynolds, Peclet, and Damkohler numbers), however, must be kept at moderate levels to ensure the accuracy of the simulations (as will be discussed in the next section).

The flow field is initialized by zero mean velocity and random three-dimensional velocity fluctuations. These fluctuations have a specified energy spectrum and are imposed in such a way to satisfy continuity [14]. The initial spectrum used in these simulations is given by:

$$E_u(k) = \varepsilon_{3d} \Lambda \frac{k^2 \Lambda^2}{(1 + k^2 \Lambda^2)^3} \tag{1}$$

This spectrum is a fairly broad-banded spectrum; Λ is the integral length scale and ε_{3d} determines the amplitude of the fluctuations. All the variables are spectrally approximated on $N = 64^3$ collocation points within the couputational domain. The spatially honogeneous flow evolves in time, and, at each time step, N defines the sample data size for the purpose of statistical analysis. A forcing mechanism was employed to keep the turbulence stationary by adding energy artificially to the large-scale motions. This forcing was applied in such a way to compensate for small-scale dissipation without affecting the small-scale statistics of interest [15]. The scalar fields are defined to be square waves with the two reactants out of phase and at stoichiometric conditions. This is shown schematically in Fig. 1, where it is seen that the two reactants are initially unmixed. The normalized initial concentration values vary only in Y-direction and are constant in each X-Z planes. In accordance with Toor's hypothesis, the reactants are assumed to have identical diffusion coefficients and are introduced at stoichiometric conditions.

To identify the nondimensional groupings, the variables are normalized by a velocity scale characterizing the turbulence ($U_o = \sqrt{u'^2}$), a concentration scale (Maximum A = A_∞), and a length scale, L_o, conveniently chosen such that the nondimensional computational domain size is 2π. With such normalization, the nondimensionalized instantaneous transport equations are

$$\nabla \cdot U = 0 \tag{2}$$

$$L(U,Re) = \frac{\partial U}{\partial t} + U \cdot \nabla U - \frac{1}{Re} \nabla^2 U = -\nabla P \tag{3}$$

$$L(A,ReSc) = L(B,ReSc) = -W \tag{4}$$

where L is the convective-diffusive operator, and, for a second-order reaction,

$$W = Da\ A\ B \tag{5}$$

$$Da = \frac{kA_\infty}{U_o L_o} \qquad \text{Damkohler number} \tag{6}$$

$$Re = \frac{U_o L_o}{\nu} \qquad \text{Reynolds number} \tag{7}$$

$$Sc = \frac{\nu}{D} \qquad \text{Schmidt number} \tag{8}$$

The Damkohler number, the Reynolds number and the Schmidt number are the important nondimensional groupings that appear in the formulation. The value of Sc can be set to unity, since this is approximately correct for gaseous reactants. The values of other nondimensional parameters are limited by the available resolution of the numerics employed in the computations. For both zero-rate and infinitely fast chemical reactions, solution of a conserved scalar variable with no chemistry source [similar to Eq. (4) with W = 0] predicts the conversion rate. For finite-rate chemistry, the full solution of Eq. (4) is required.

3. TOOR'S HYPOTHESIS

For the purpose of examining Toor's hypothesis, we decompose each concentration, $A(\underline{x},t)$ and $B(\underline{x},t,)$, into an ensemble mean value (denoted by $< >$) and a fluctuation from the mean value (represented by small letters):

$$A = \langle A \rangle + a \tag{9}$$

$$B = \langle B \rangle + b \tag{10}$$

The transport equations governing the mean values are

$$L(\langle A \rangle, Pe) = L(\langle B \rangle, Pe) = -\langle W \rangle \tag{11}$$

$$\langle W \rangle = Da(\langle A \rangle \langle B \rangle + \langle ab \rangle) \tag{12}$$

The first term on the right-hand side of Eq. (12) is the homogeneous mean rate, and the second term is the unmixedness term, which needs to be modeled. This term can be written in normalized form [1]:

$$\psi^2(t) = \langle ab \rangle_t / \langle ab \rangle_o \tag{13}$$

where the subscripts t and o refer to time and the initial time (i.e., at the inlet of the plug flow reactor), respectively. A conserved, Shvab-Zeldovich scalar variable, $J(\underline{x},t)$ is defined by [16]

$$J(\underline{x},t) = A(\underline{x},t) - B(\underline{x},t) \tag{14}$$

Turbulent mixing is characterized by the rms of the Shvab-Zeldovich variable:

$$d^2(t) = \sigma^2(t)/\sigma^2(o) \tag{15}$$

It is obvious that, in the limit of zero-rate chemistry, $d^2(t)$ and $\psi^2(t)$ are identical:

$$d^2(t) = \lim_{Da \to 0} \psi^2(t) \tag{16}$$

In the limit of infinitely fast chemistry, under stoichiometric conditions, and assuming a Gaussian shape* for the PDF of the Shvab-Zeldovich variable, Toor showed that

$$d^2(t) = \lim_{Da \to \infty} \psi^2(t) \tag{17}$$

Based on Eqs. (16) and (17), Toor assumed that

$$d^2(t) = \psi^2(t) \text{ for any Da} \tag{18}$$

Equation (18) defines Toor's hypothesis. This hypothesis has been used for calculations of a variety of reacting flows (for reviews, see Givi [18] and Brodkey [19]). In this paper, its validity is studied by means of numerical data presented in Section 5.

4. COALESENCE/DISPERSION MODELING

The general C/D model is expressed by a transport equation for the PDF of the Shvab-Zeldovich variable, $J(\underline{x},t)$ [defined by $P(\phi,t)$]. In the homogeneous flow considered here, the evolution of the probability is given by Pope [20]:

$$\frac{\partial P(\phi,t)}{\partial t} = -2\beta\Omega P(\phi,t) + 2\beta\Omega \int_{-\infty}^{+\infty}\int d\phi' d\phi'' p(\phi',t)\, p(\phi''t)$$
$$\times \int_{-\infty}^{+\infty} d\alpha\, A(\alpha)\, \delta[\phi - (1-\alpha)\phi' - \frac{1}{2}\alpha(\phi'+\phi'')] \tag{19}$$

The kernal $A(\alpha)$ is the PDF of α, and the random variable α is a measure of mixing. The function $A(\alpha)$ is zero outside the interval (0,1) and is non-negative and normalized to unity within (0,1). The parameter β is defined by Pope:

$$\beta = \frac{1}{a_1 - \frac{1}{2} a_2} \tag{20}$$

*This assumption can be relaxed for symmetric PDFs [17].

where

$$a_m = \int_0^1 \alpha^m A(\alpha) d\alpha \tag{21}$$

Multiplying Eq. (19) by ϕ^2 and integrating, the time evolution of the standard deviation, which characterizes turbulent mixing, is defined:

$$\sigma(t) = \sigma(o) \exp\left[-\int_0^t \Omega(t')dt'\right] \tag{22}$$

where Ω is the appropriate turbulent mixing frequency and needs to be specified.

To complete the closure, the function $A(\alpha)$ must be specified. Different choices of $A(\alpha)$ result in different C/D models. Curl's original model [5] is defined by setting $A(\alpha) = \delta(\alpha - 1)$. The closure of Janicka et al. [4] is equivalent to using $A(\alpha) = 1$ within [0,1]. The Dopazo-O'Brien [3] approximation is recovered by setting (Kosaly and Givi [2])

$$A(\alpha) = \lim_{\varepsilon \to 0} \delta(\alpha - \varepsilon) \tag{23}$$

Note that the models of Curl [5] and Dopazo and O'Brien [3] appear as two opposite limiting cases. $A(\alpha) = \delta(\alpha - 1)$ is obviously the most extreme of all the cases that peak at $\alpha = 1$ and decrease as α tends to zero. $A(\alpha) = \delta(\alpha - \varepsilon)$, $\varepsilon \to 0$, at the other limit, is the extreme representative of the physically acceptable shapes at $\alpha = 0$ that decrease with increasing values of α. The $A(\alpha) = 1$ choice can be considered to be halfway between the two extremes.

Depending on the shape of $A(\alpha)$, obviously, there is an infinite number of choices, each leading to a different C/D model. The sensitivity to the choice of the model can be expressed by examining the central and standardized moments of $J(\underline{x},t)$, defined in order as

$$\mu_n(t) = \int_{-\infty}^{+\infty} \phi^n P(\phi,t) d\phi \tag{24}$$

$$\hat{\mu}_n(t) = \mu_n(t)/\sigma^n(t) \quad (n = 1,2, \ldots) \tag{25}$$

It has been shown by Kosaly and Givi [2] that the first three moments are independent of the choice of $A(\alpha)$. It is the fourth (and higher even moments) that depend on the $A(\alpha)$ shape. For a constant Ω,

$$\hat{\mu}_4(t) = [3 + \hat{\mu}_4(0)]\, e^{\gamma\Omega t} - 3 \tag{26}$$

where

$$\gamma = (a_2 + \frac{1}{4} a_4 - a_3)/(a_1 - \frac{1}{2} a_2) \tag{27}$$

It is seen that all models with $\gamma > 0$ yield $\mu_4 \to \infty$ as $t \to \infty$, which indicates the shortcomings associated with the presently used C/D models.

The above relations hold for any inert scalar, i.e., species A without chemical reactions. In the presence of chemistry, the situation is markedly different for the behavior of the higher-order concentration moments. In the previous work, Kosaly and Givi [2] showed that only the Dopazo-O'Brien closure results in equal central moments in the presence and in the absence of chemical reaction, and employing other C/D models predicts higher concentration moments under reacting conditions than those under nonreacting conditions. However, since all the C/D models employed are phenomenological in nature, the examination of the exact role of chemistry on higher-order concentration moments was not possible. Here, examination is possible by means of numerical experiments, as discussed in the next section.

5. RESULTS OF NUMERICAL EXPERIMENTS

Computations were performed on a cubic domain with dimensions of 2π. The values of the Reynolds and the Peclet numbers were set to 100, so that the simulations would be accurately resolved on a 64^3 grid. The Reynolds number, based on the Taylor microscale and the turbulence rms level (this is the non-dimensional parameter of interest for describing the turbulence), was approximately 50 throughout the calculations. Calculations were performed with zero-rate chemistry (Da = 0), infinite rate chemistry (Da $\to \infty$), and at intermediate finite rates (Da = 2, 8, and 30) to assess the influence of the chemical reaction on the statistics of the concentrations.

It is well known that the formulation based on a one-point PDF [Eq. (19)] does not include any information about the mixing frequency (Ω). This frequency has usually been modeled by ad hoc closures [21] but can be evaluated from the results of our direct numerical simulations. A discussion on the evaluation of mixing frequency, as well as other hydrodynamical variables characterizing the turbulent flow field, is reported elsewhere (McMurtry and Givi [15]) and is not repeated here. For the time being, the influence of the turbulence frequency is included in normalized time, which is defined by

$$t^* = \int_0^t \Omega(t')dt' = -\ln \frac{\sigma(t)}{\sigma(0)} \tag{28}$$

In the discussions below, this normalized time is used to exhibit the evolution of the chemical quantities that are of interest to mixing and reaction of the scalars.

The contours of one of the reactants (species A) are chosen for the purpose of flow visualization. In Figs. 2, 3, and 4, we present the time sequence development of these contours for (a) Da = 0, and (b) Da $\to \infty$. These figures represent conditions at one particular X-Y plane cut through Z = 10 (Fig. 1). Nondimensional times of $t^* = 0.625$, $t^* = 1.20$, and $t^* = 3$ correspond to the case when the average concentration of species A, under the infinite rate chemistry, has reduced to 52%, 28%, and 4.2% of its initial value, respectively. These figures exhibit the effects of three-dimensional turbulent motion on the distortion of the scalar field and the mixing of the two initially segregated reactants (with parallel contour lines). The effects of chemical reations are to increase the steepness of the scalar gradients and, obviously, to reduce the instantaneous values of the reactants, as indicated by a comparison between parts (a) and (b) of Figs. 2-4. The magnitude of this reduction increases with the increase in the value of the Damkohler number. This is clearly shown in Fig. 5, where the influence of chemical reaction on the consumption rate of the reactant concentration is presented. It is indicated in this figure that, for finite values of Da, the combined effects of mixing and reaction are to reduce the mean concentration of the reacting species. As the magnitude of the Damkohler number increases, more reactants are consumed and the rate of decay increases until it reaches a maximum value as Da $\to \infty$. In this limit, the chemistry does not play any role, and the consumption rate is determined solely by the mechanism of the molecular mixing.

For the purpose of evaluating the C/D closure, the results of predictions using such models as $Da \to \infty$ are presented in Fig. 6. All the calculations using C/D models were performed by means of a Monte-Carlo numerical method (Kosaly and Givi [2]) in a configuration with an identical statistical initialization and mixing frequency, as used in the DNS. Implementation of the Monte-Carlo method, developed originally by Pope [22], is discussed by Givi et al. [21] for the present problem.

Figure 6 indicates that, at initial times, the results of numerical experiments are closest to those of predictions using the Dopazo-O'Brien closure. This is mainly due to the fact that the initial stages of mixing are realistically described by those members of the family of C/D models with an $A(\alpha)$ shape concentrated at $\alpha = 0$ (for a theoretical discussion, see Kosaly and Givi [2]). The Dopazo-O'Brien closure is the extreme representative of shapes that peak at $\alpha = 0$ and decrease with increasing values of α. Other C/D models that do not possess this property for the shape of $A(\alpha)$ are not expected to result in realistic predictions at the initial stages of mixing (Kosaly and Givi [2]). This is clearly shown in Fig. 6 and indicates that, as Curl's model is approached [i.e., $A(\alpha) = \delta(\alpha - 1)$], the agreement with the results of numerical experiments gets worse.

At later times, none of the C/D models is capable of accurately predicting the conversion rate, and the experimental curve falls between the two cases given by the results of Janicka et al. [4] and of Dopazo-O'Brien. This discrepancy between the results of C/D closures and those of DNS is attributed to the fact that none of the C/D models results in acceptable asymptotic ($t \to \infty$) behavior. As indicated originally by Pope [20] and later by Kosaly and Givi [2], all the C/D models predict infinite fourth and higher even standardized moments as $t \to \infty$ for the conserved Shvab-Zeldovich scalar quantity, J [Eqs. (26) and (27)]. The exception is the Dopazo-O'Brien model, which predicts an unphysical constant value for those moments.

The asymptotic behavior of scalar mixing cannot be predicted by a mathematical theory, and its determination is the subject of our numerical experiments. The time evolution of the PDF of the random variable $J(\underline{x},t)$ is presented in Fig. 7. As shown in this figure, at initial times ($t^* \simeq 0$) the PDF is composed of two delta functions at $\phi = \pm 1$, indicating the two initially non-premixed reactants. As mixing proceeds, the gap between the two delta functions is filled, and the original two delta functions smear and move closer

to each other. At moderate times ($t^* \approx 1.5$), the PDF is composed of a peak at the mixed concentration of $\phi = 0$, and proceeding further in time results in a sharper peak at this mixed concentration. As time proceeds, it seems that the PDF is approaching a self-similar Gaussian profile. To ascertain this asymptotic shape, the temporal variations of the standardized moments characterizing the PDF must be examined. The standardized fourth ($\hat{\mu}_4$) moment of the variable $J(\underline{x},t)$ is presented in Fig. 8. While all the odd moments remain in close proximity to zero (not shown here), Fig. 8 indicates a monotontic increase in the magnitude of all the even-order moments. In this experiment, the values of the kurtosis, superskewness and superkurtosis approach the values of $\hat{\mu}_4 = 2.9$, $\hat{\mu}_6 = 13.9$, and $\hat{\mu}_8 = 98$, respectively. A comparison of these values with those of a Gaussian profile (i.e., $\hat{\mu}_4 = 3$, $\hat{\mu}_6 = 15$, $\hat{\mu}_8 = 105$) indicates that the approximation of a Gaussian PDF for the final stages of mixing of a conserved scalar is well justified and is in agreement with the findings of some recent experimental results [23,24]. Note that the accuracy of our statistics is limited by the size of the data sample, i.e., 64^3. Future Future higher-resolution simulations (i.e., 128^3 or higher) might improve the accuracy and, therefore, might result in better agreements for higher-order moments. In Fig. 8, the temporal variation of the kurtosis obtained by C/D modeling is also presented. The unacceptable behavior of the models of Curl and Janicka et al. in predicting a continuously increasing fourth-order moment, and also the nonphysical constant value of the kurtosis predicted by the Dopazo-O'Brien model, are shown in this figure.

The influence of chemical reactions on the decay rate of the unmixedness is shown in Fig. 9. In this figure, the ratio (Ψ^2/d^2) is presented versus normalized time for zero-rate, infinitely fast rate, and three intermediate rates (Da = 2, Da = 8, Da = 30) chemical ractions. For zero-rate chemistry, the ratio, as expected, remains at unity. For the reacting cases at the initial time ($t^* = 0$), the influence of chemistry is nil. At later times, however, the values of the unmixedness for the reacting cases are lower than those under zero-rate chemistry. This is in contrast with Toor's hypothesis and indicates that the decay rate of the unmixedness is not independent of the chemical reactions and depends on the magnitude of the local Damkohler number. A theoretical discussion on the lack of agreement with Toor's hypothesis is given by

Givi and McMurtry [25], who showed that, for initially non-premixed reactants, Toor's hypothesis should be modified by replacing Eq. (17), at a temporal asymptote, with

$$C\, d^2(t) = \lim_{Da \to \infty} \psi^2(t) \tag{29}$$

where the constant C is determined from the asymptotic shape of the PDF of J, i.e., $P(\phi,t)$

$$C = 4 \left[\int_0^\infty \phi p(\phi) d\phi \right]^2 \tag{30}$$

This modification of Toor's hypothesis is due to the fact that the evolution of $P(\phi,t)$ from its initial binary shape to its asymptotic profile (Fig. 7) cannot be characterized by the first two moments (i.e., 0 and σ). Therefore, Toor's hypothesis, which is based on the assumption of Gaussian PDFs at all times, is not appropriate in this case, and Eq. (18) must be replaced by Eq. (16) for zero-rate and Eq. (29) for $Da \to \infty$ at the temporal asymptote. For an asymptotic Gaussian PDF, i.e.,

$$p(\phi) = \frac{1}{\sqrt{2\pi}} \exp\left(-\frac{\phi^2}{2}\right) \tag{31}$$

the value of the constant C in Eq. (30) would be

$$C = \frac{2}{\pi} \tag{32}$$

which is the same as that given by Kosaly [26].

The validation of this modification is clearly represented in Fig. 9. Note that the ratio of $\psi^2(t)/d^2(t)$ is always between unity and $0.64 \approx 2/\pi$. Also, note that the modification of the hypothesis [Eq. (29)] is valid only for $Da \to \infty$ at the temporal asymptote. For finite-rate chemistry and intermediate times, the application of the hypothesis is not valid and full numerical simulations are required.

The results of our numerical experiments are further examined to study a recent result of Hsieh and O'Brien [27], who found that higher-concentration moments are not sensitive to chemistry. The possible reason behind this finding is investigated by comparing infinite-rate chemistry and pure mixing

results in Figs. 10 and 11. In these figures, the skewness and the kurtosis of species A are presented. For the purpose of comparison, the results obtained by employing various C/D models are also presented and, for each case, two curves are shown: one without chemistry and another with infinite-rate chemistry. It is clearly observed that, in the Dopazo-O'Brien approximation, the two curves coincide, whereas the results of Curl's model show a maximum difference between the two curves. In each case, the standardized moments are higher for the reacting scalar than for the conserved scalar. As the moments of the nonreacting scalar approach the asymptotic values corresponding approximately to those of a Gaussian distribution, the moments of the reacting scalar approach higher values, which indicates that the assumption of a Gaussian distribution for the reacting scalar is not well justified. These results confirm Kosaly and Givi's speculations that it is the use of moderate rate chemistry by Hsieh and O'Brien [27] that makes the skewness and Kurtosis values similar to those calculated with pure mixing. Increasing the rate of chemical reactions would probably change the results of Hsieh and O'Brien considerably.

Figures 10 and 11 further indicate that the results of our numerical experiments fall between those of predictions using the closures of Dopazo-O'Brien and Janicka et al. Therefore, a closure model between the two approximations may be used for the purpose of predicting the intermediate stages of mixing. At the later stages of the developments, however, none of the C/D models are satisfactory in that they all (except the Dopazo-O'Brien model) predict an increase without bound of all the fourth and higher order moments.

Pope [20] made an attempt to remedy this problem by introducing an age-biasing technique that, together with an appropriate $A(\alpha)$ shape [(Eq. 19)], would result in an asymptotic Gaussian PDF. Although such a technique is very successful in predicting the asymptotic behavior correctly, the shapes of $A(\alpha)$ suggested by Pope do not predict the initial stages of mixing accurately [28]. The results of direct numerical simulations presented here will be very useful in optimizing the $A(\alpha)$ shape, as well as in developing an age-biasing technique that can be used to predict the mechanism of mixing, both at the initial time and at asymptotic times.

6. CONCLUSIONS

A pseudospectral algorithm has been employed to study the mechanism of mixing and reaction in a non-premixed, three-dimensional, homogeneous turbulent flow. The evolution of the species field in an isothermal, one-step, stoichiometric reaction of the type A + B → Products was the subject of investigations in our numerical experiments. Calculations were performed for zero-rate, infinitely fast-rate, and intermediate moderate finite-rates chemical reactions to assess the influence of chemistry on the transport of the scalar variables.

Mixing is characterized by the evolution of a Shvab-Zeldovich conserved scalar quantity, $J(\underline{x},t)$, defined by Eq. (14). The results of our numerical simulations indicate that the PDF of J, i.e., $P(\phi,t)$, evolves from its initial double-delta function distribution to an asymptotic shape, which can be approximated by a Gaussian distribution. During this evolution, the PDF cannot be characterized by its first two moments (except when it adopts the asymptotic Gaussian shape). Therefore, the application of Toor's hypothesis is not appropriate for the prediction of the conversion rate in such flows. The results indicate that, while Toor's hypothesis ($\psi^2 = d^2$) is valid for zero-rate chemistry (Da = 0), it should be modified by ($\psi^2 = Cd^2$) for Da → ∞ and at a temporal asymptote. The parameter C is determined by the asymptotic shape of the $P(\phi)$ [Eq. (30)]. In the present experiment where $P(\phi)$ adopts a Gaussian asymptotic profile, the value of this constant is equal to $2/\pi$, which is consistent with that given by Kosaly [26].

The results of numerical experiments are further compared with those obtained by employing various C/D mixing models applied to a homogeneous flow with the same statistical initialization. The results indicate that the initial stages of the mixing process are well predicted by applying the Dopazo-O'Brien [3] closure. As mixing proceeds at intermediate times, the experimental results fall between those obtained by the two closure models of Dopazo-O'Brien and Janicka et al. [4]. Therefore, a C/D model between these two closures is expected to result in favorable comparison with our experimental data. The final stages of mixing are not well-predicted by any of the C/D models in that all of the closures predict an increase without bounds of the fourth and higher-order concentration moments. The exception is the Dopazo-O'Brien model, which predicts unphysical constant moments during all stages of mixing. This shortcoming associated with C/D modeling has been previously recognized by Pope [20], who suggested an improved mixing model by

introducing an age-biasing technique to the C/D modeling. This improved model is plausible in that it results in a Gaussian asymptotic PDF; however, it is not capable of predicting the initial stages of mixing accurately. The results of our numerical experiments can be useful for constructing a mixing model (or models) that can accurately predict all stages of the molecular mixing. Such a task is one of the goals of our ongoing investigations.

While the assumption of a Gaussian asymptotic PDF is well justified for the conserved scalar quantities (e.g., J), our experiments show that this is not the case for the reacting scalars. The results of our direct numerical simulations indicate that the higher moments (third, fourth, ...) of the species under reacting conditions increase faster than those under no chemical reaction. This is consistent with that found by C/D modeling and, again, the experimental results fall between the two closures of Dopazo-O'Brien and Janicka et al. In all the comparisons with C/D modelings, our results show the greatest deviations from those obtained by using the Curl's model and indicate that the models of Janicka et al. and Dopazo-O'Brien bracket the range of the C/D models that, in conjunction with an appropriate age-biasing technique, can predict our experimental results accurately. Thus, questions such as "Does such model predicting a correct PDF evolution exist?" and if so, "Is it universal?" are to be addressed in future studies.

At this point, it should be pointed out that all the C/D models evaluated here are mainly used for single-point PDF closures. This requires the introduction of a mixing frequency into the formulation, as defined by Eq. (22). Employing the results of direct numerical simulations to evaluate (or to generate) models for more than one-point-level closures [29, 30] remains to be a challenging task. Also, it must be mentioned that the simulations presented here are similar to most of the laboratory investigations in that they include the results of only one experimental realization. More future numerical experiments with different initializations and possibly with better numerical resolutions (i.e., 128^3 or 256^3 grids) would be logical extensions of the present work. The rapid advancements in super-computer technology and the expected better capabilities of such machines in the future will play significant roles in the continuation of the work presented here.

REFERENCES

1. Toor, H. L., Turbulence in Mixing Operations, Ed. Brodkey, R. S., Academic Press, New York, 1975.

2. Kosaly, G., and Givi, P., Combustion and Flame, 70, 101, 1987.

3. Dopazo, D., and O'Brien, E. E., Combust. Sci. Tech., 13, 99, 1976.

4. Janicka, J., Kolbe, W. and Kollmann, W., J. Nonequil. Thermodyn., 4, 47, 1979.

5. Curl, R. L., AIChEJ., 9, 175, 1963.

6. Toor, H. L., AIChEJ., 8, 70, 1962.

7. Toor, H. L., Eng. Chem. Fundamentals, 8, 655, 1969.

8. Rogallo, R. S., and Moin, P., Ann. Rev. Fluid Mech., 16, 99, 1984.

9. Riley, J. J., Metcalfe, R. W., and Orszag, S. A., Phys. Fluids, 29(2), 406, 1986.

10. McMurtry, P. A., Jou, W.-H., Riley, J. J., and Metcalfe, R. W., AIAA J., 24(6), 962, 1986.

11. Givi, P., Jou, W.-H., and Metcalfe, R. W., Proceedings of 21st Symposium (Int.) on Combustion, The Combustion Institute, Pittsburgh, PA, in press, 1987.

12. Givi, P., and Jou, W.-H., J. Nonequil. Thermodyn., in press, 1987.

13. Gottlieb, D., and Orszag, S. A., Numerical Analysis of Spectral Methods, SIAM, Philadelphia, 1977.

14. McMurtry, P. A., Ph.D. Thesis, University of Washington, Seattle, WA.

15. McMurtry, P. A., and Givi, P., paper in progress, 1987.

16. Williams, F. A., Combustion Theory, second edition, Benjamin Cummings Publishing Co., Inc., Menlo Park, CA, 1985.

17. O'Brien, E. E., Phys. Fluids 14, 1326, 1971.

18. Givi, P., Ph.D. Thesis, Carnegie-Mellon University, Pittsburgh, PA.

19. Brodkey, R. S., Chem. Eng. Comm. 8, 1, 1981.

20. Pope, S. B., Combust. Sci. Tech., 28, 131, 1982.

21. Givi, P., Ramos, J. I., and Sirignano, W. A., J. Nonequil. Thermodyn., 10, 75, 1985.

22. Pope, S. B., Combust. Sci. Tech., 25, 159, 1981.

23. Miyawaki, O., Tsujikawa, H., and Uraguchi, Y., J. Chem. Eng. Japan, 7, 52, 1974.

24. Tavoularis, S., and Corssin, S., J. Fluid Mech., 104, 311, 1981.

25. Givi, P., and McMurtry, P. A., AIChE Journal, in press, 1987.

26. Kosaly, G., AIChE Journal, in press, 1987.

27. Hsieh, T. H. J., and O'Brien, E. E., Combust. Sci. Tech., 46, 267, 1986.

28. Kosaly, G., Combust. Sci. Tech., 49, 227, 1986.

29. O'Brien, E. E., in Turbulent Reacting Flows, Libby, P.A. and Williams, F. A., (eds.), Springer-Verlag, Heidelberg, Vol. 44, Topics in Applied Physics, Chap. 5, 1980.

30. O'Brien, E. E. in Frontiers in Fluid Mechanics, Davis, S. W. and Lumely, J. L. (Eds.), Springer-Verlag, 113, 1985.

FIGURE CAPTIONS

Figure 1. Geometrical configuration showing a schematic diagram of the initial instantaneous reactant concentrations.

Figure 2. Two-dimensional plots of species A contours at $t^* = 0.625$. Contour interval is 0.05. (a) Da = 0, contour minimum is 0, contour maximum is 0.9. (b) $Da \to \infty$, contour minimum is 0, contour maximum is 0.9.

Figure 3. Two-dimensional plots of species A contours at $t^* = 1.20$. Contour interval is 0.05. (a) Da = 0, contour minimum is 0.10, contour maximum is 0.75, (b) $Da \to \infty$, contour minimum is 0, contour maximum is 0.65.

Figure 4. Two-dimensional plots of species A contours at $t^* = 3$. Contour inteval is 0.005. (a) Da = 0, contour minimum is 0.370, contour maximum is 0.495. (b) $Da \to \infty$, contour minimum is 0, contour maximum is 0.135.

Figure 5. $\langle A \rangle_t / \langle A \rangle_o$ versus time for various values of the Damkohler number.

Figure 6. $\langle A \rangle_t / \langle A \rangle_o$ versus time for $Da \to \infty$.

Figure 7. Temporal evolution of $P(\phi,t)$.

Figure 8. Kurtosis of the random variable $J(\underline{x},t)$ versus time.

Figure 9. ψ^2/d^2 versus time for various values of the Damkohler number.

Figure 10. Skewness of species A versus time with infinite rate chemistry and with pure mixing. In the pure mixing case, the skewness is zero.

Figure 11. Kurtosis of species A versus time with infinite rate chemistry with pure mixing.

5628R

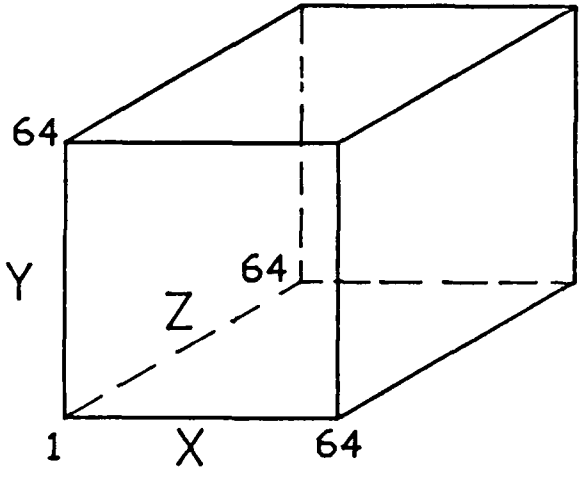

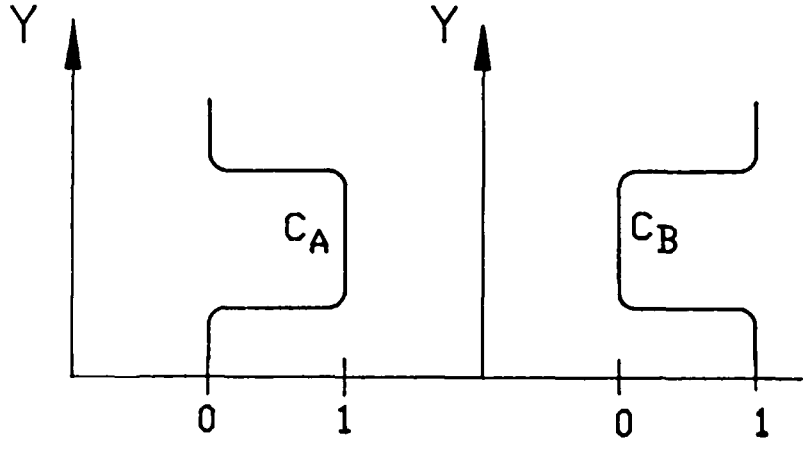

CONCENTRATION

Figure 1

(2a)

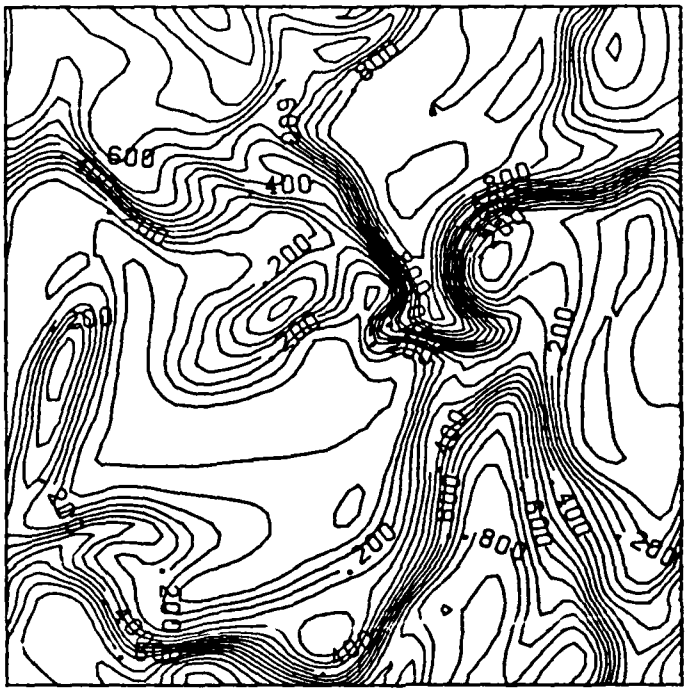

(2b)

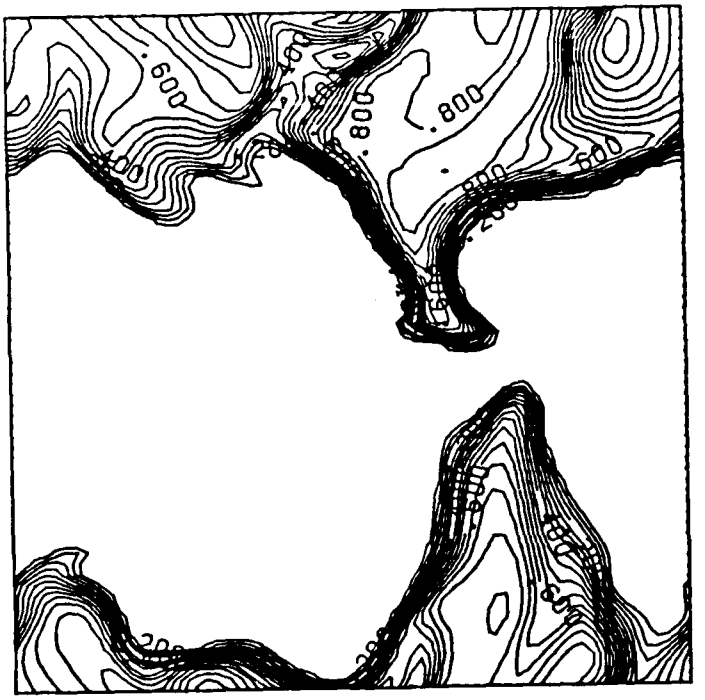

Figure 2

(3a)

(3b)

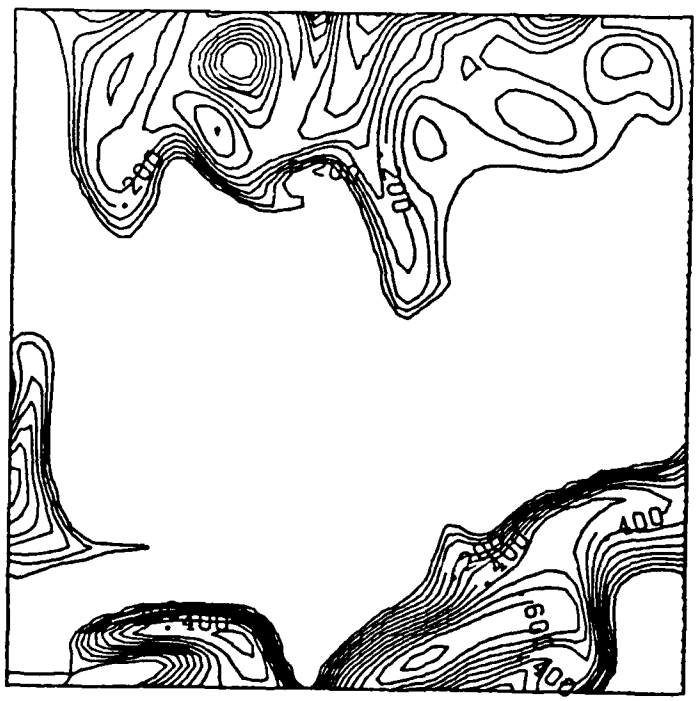

Figure 3

(4a)

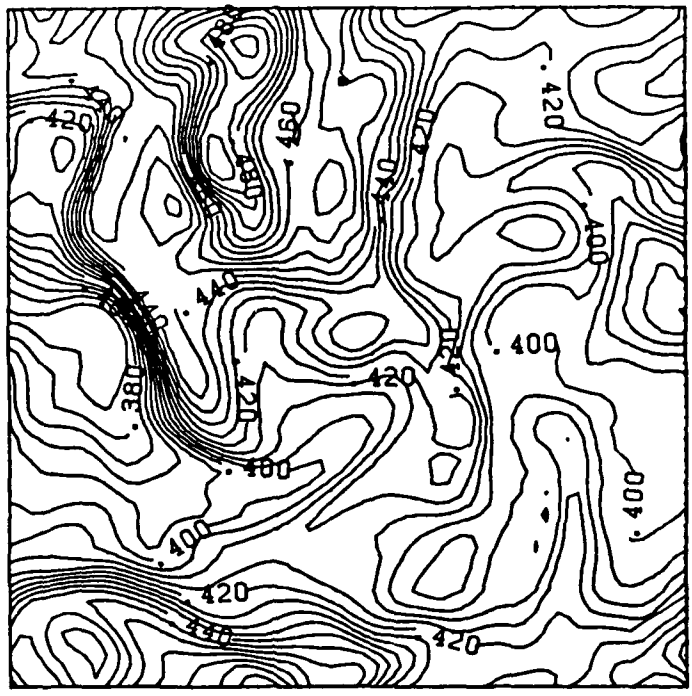

(4b)

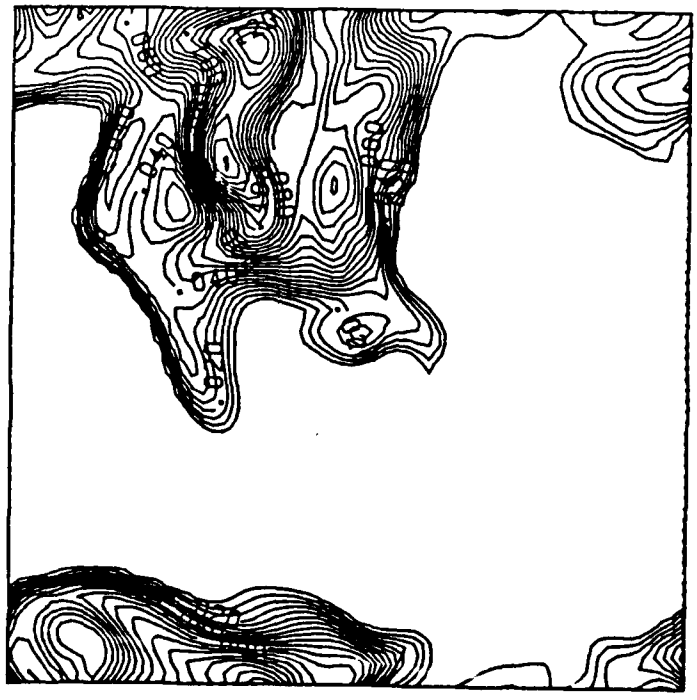

Figure

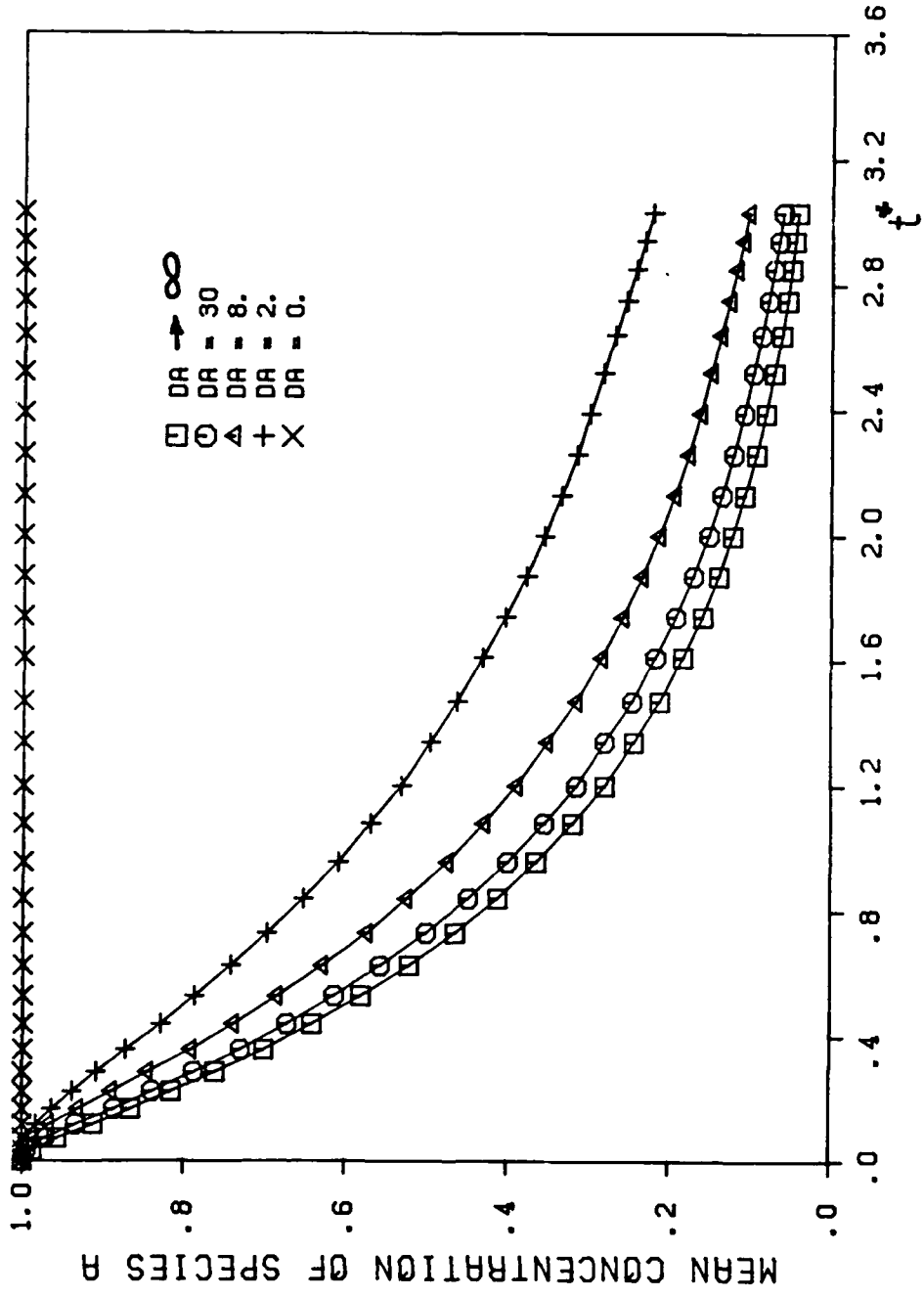
MEAN CONCENTRATION OF SPECIES A
1.0
.8
.6
.4
.2
.0
.0
.4
.8
1.2
1.6
2.0
2.4
2.8
3.2
3.6
t*
DA = ∞
DA = 30
DA = 8.
DA = 2.
DA = 0.

Figure 5

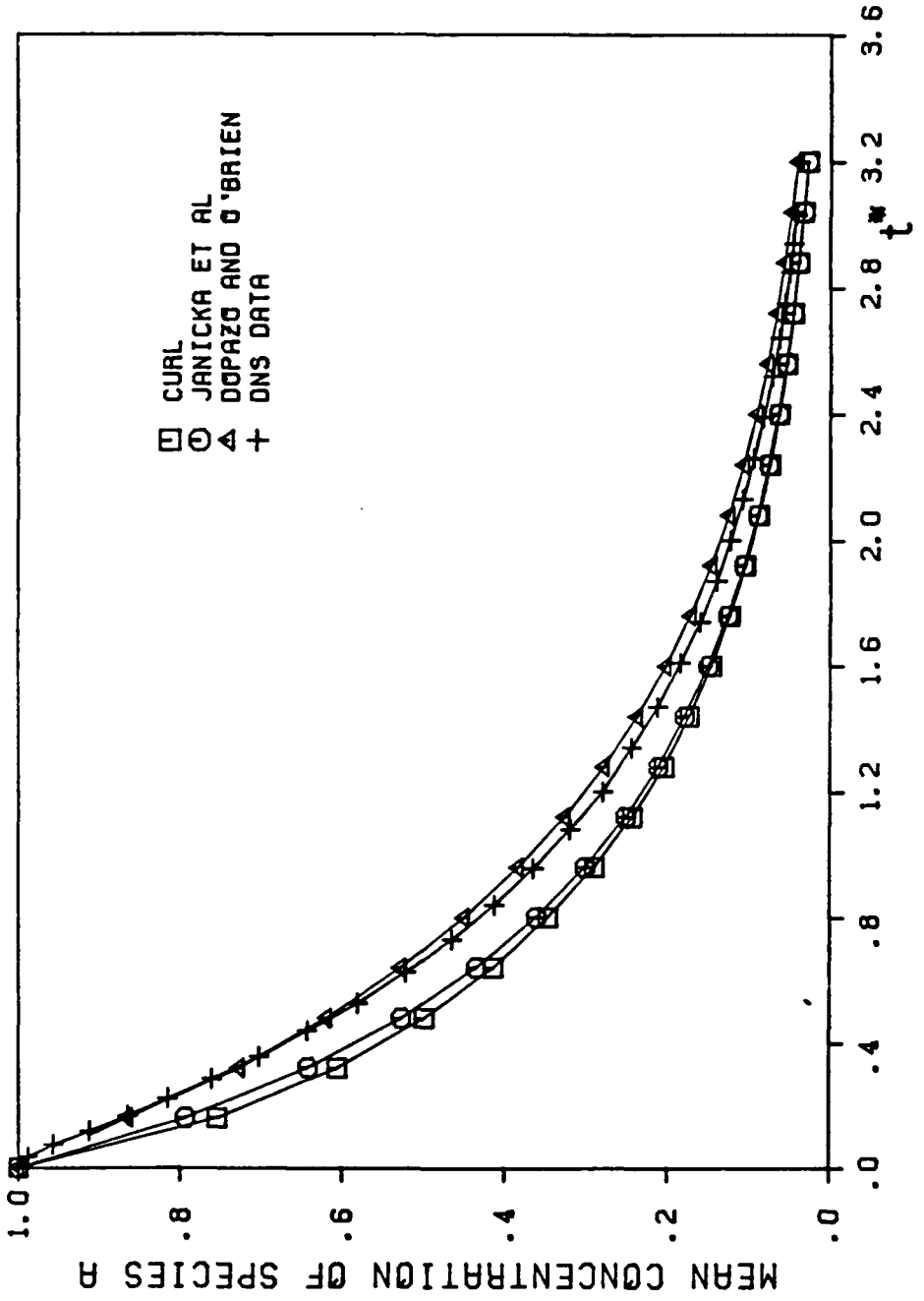
CURL
JANICKA ET AL
DOPAZO AND O'BRIEN
DNS DATA
MEAN CONCENTRATION OF SPECIES A
t*
0.0
.4
.8
1.2
1.6
2.0
2.4
2.8
3.2
3.6
.0
.2
.4
.6
.8
1.0

Figure 6

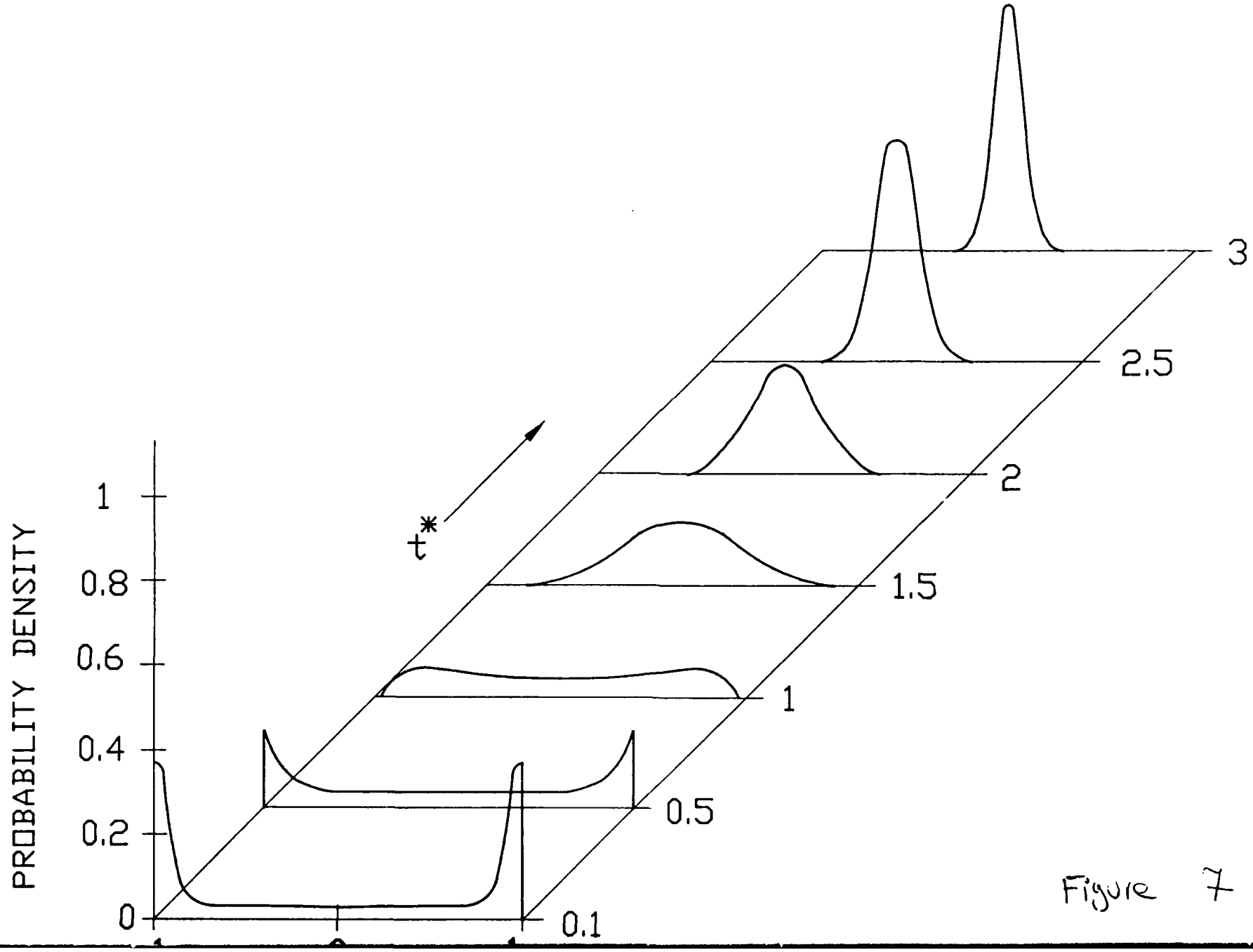

Figure 7

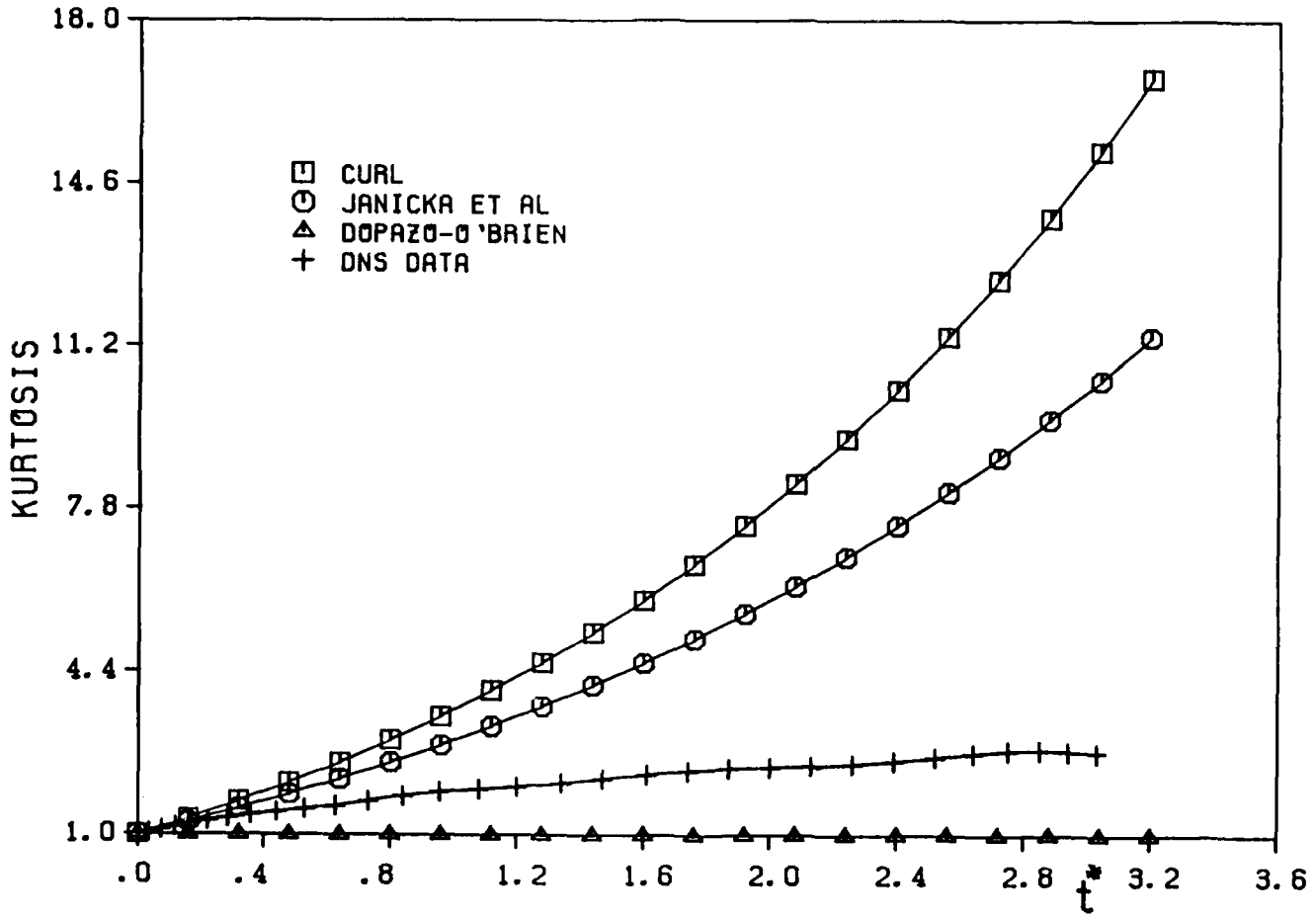
18.0
14.6
11.2
7.8
4.4
1.0
KURTOSIS
CURL
JANICKA ET AL
DOPAZO-O'BRIEN
DNS DATA
.0
.4
.8
1.2
1.6
2.0
2.4
2.8
3.2
3.6
t*

Figure 8

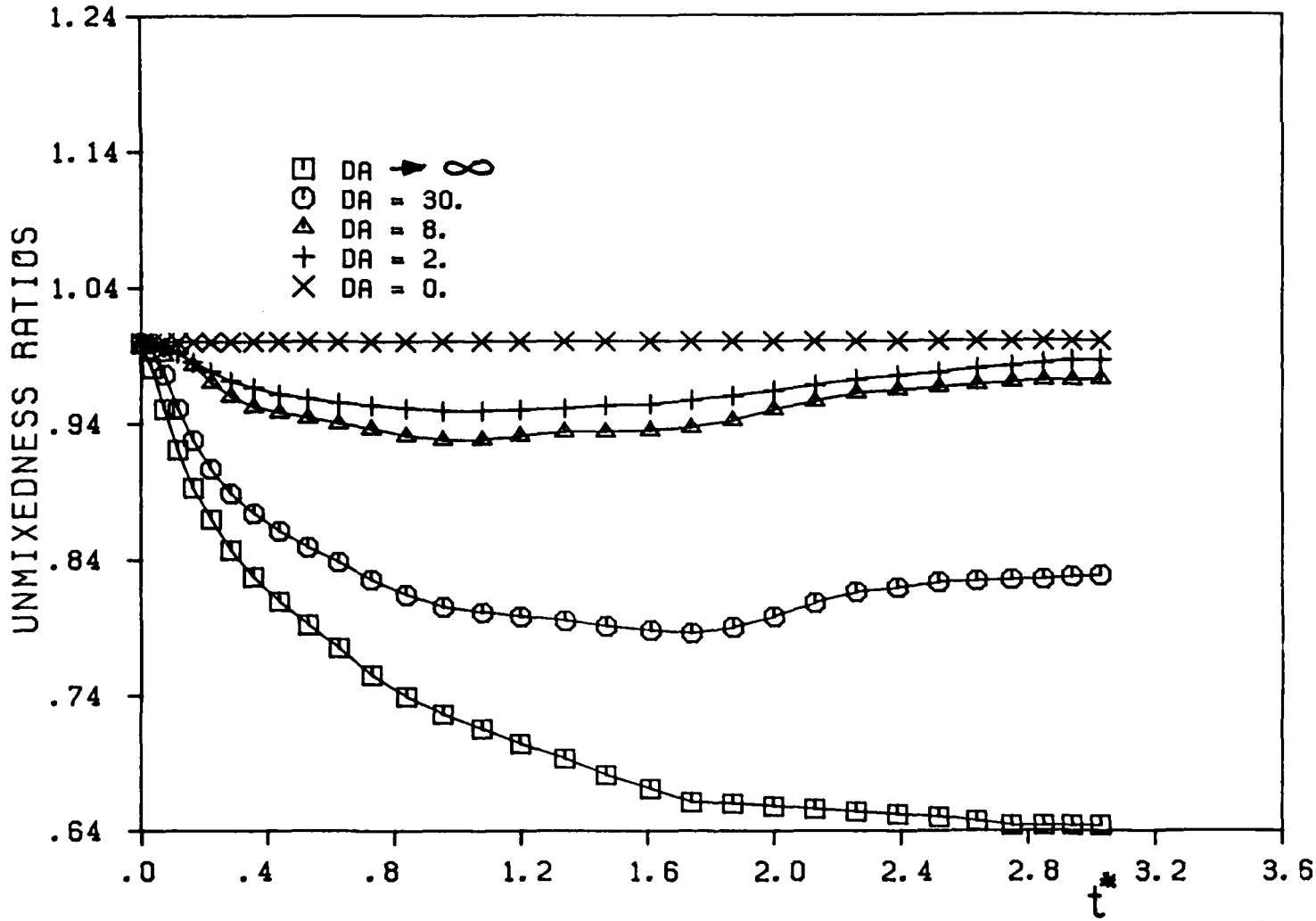
1.24
1.14
1.04
.94
.84
.74
.64
UNMIXEDNESS RATIOS
DA → ∞
DA = 30.
DA = 8.
DA = 2.
DA = 0.
.0
.4
.8
1.2
1.6
2.0
2.4
2.8
3.2
3.6
t*

Figure 9

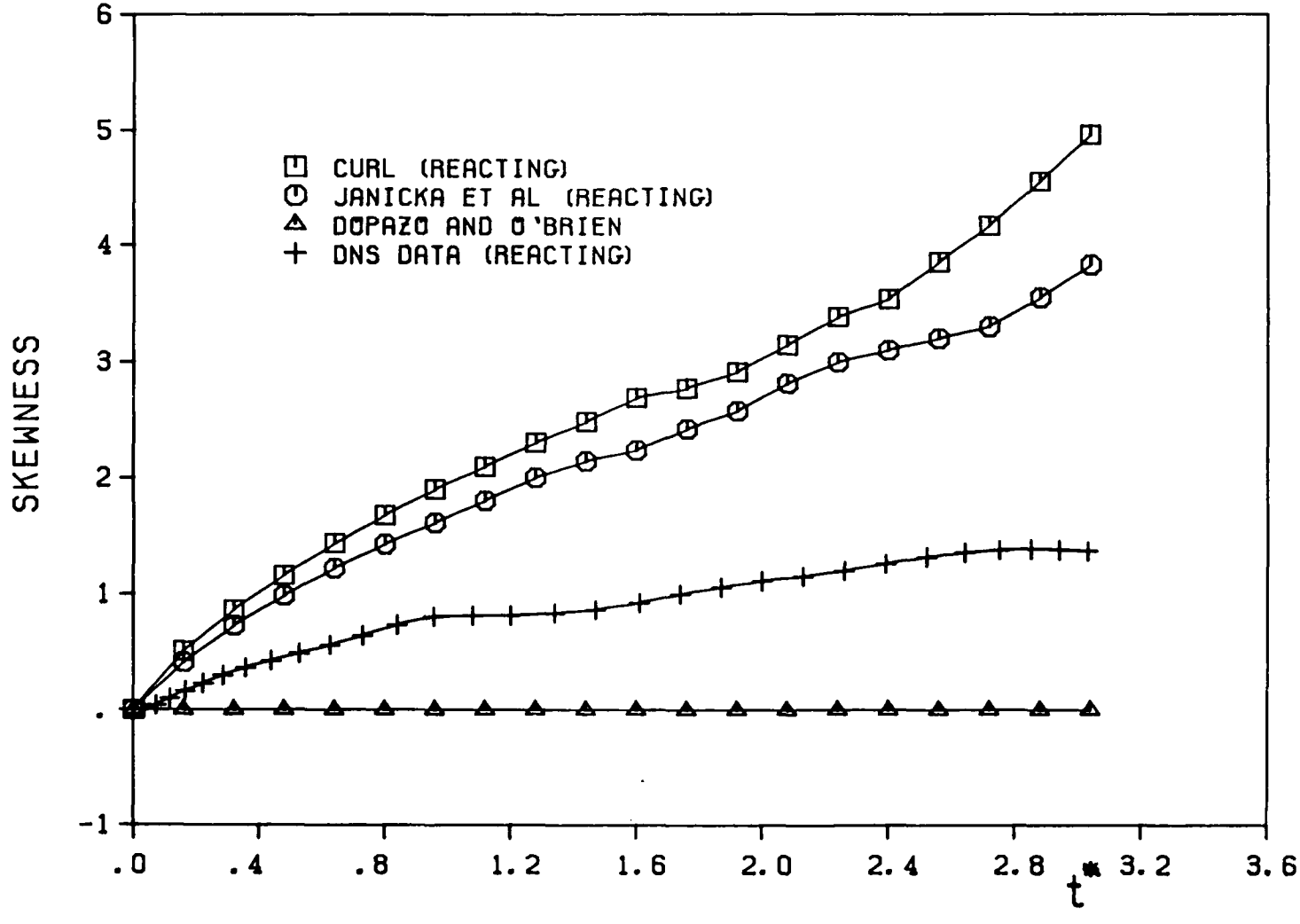
CURL (REACTING)
JANICKA ET AL (REACTING)
DOPAZO AND O'BRIEN
DNS DATA (REACTING)
SKEWNESS
6
5
4
3
2
1
.
-1
.0
.4
.8
1.2
1.6
2.0
2.4
2.8
3.2
3.6
t*

Figure 10

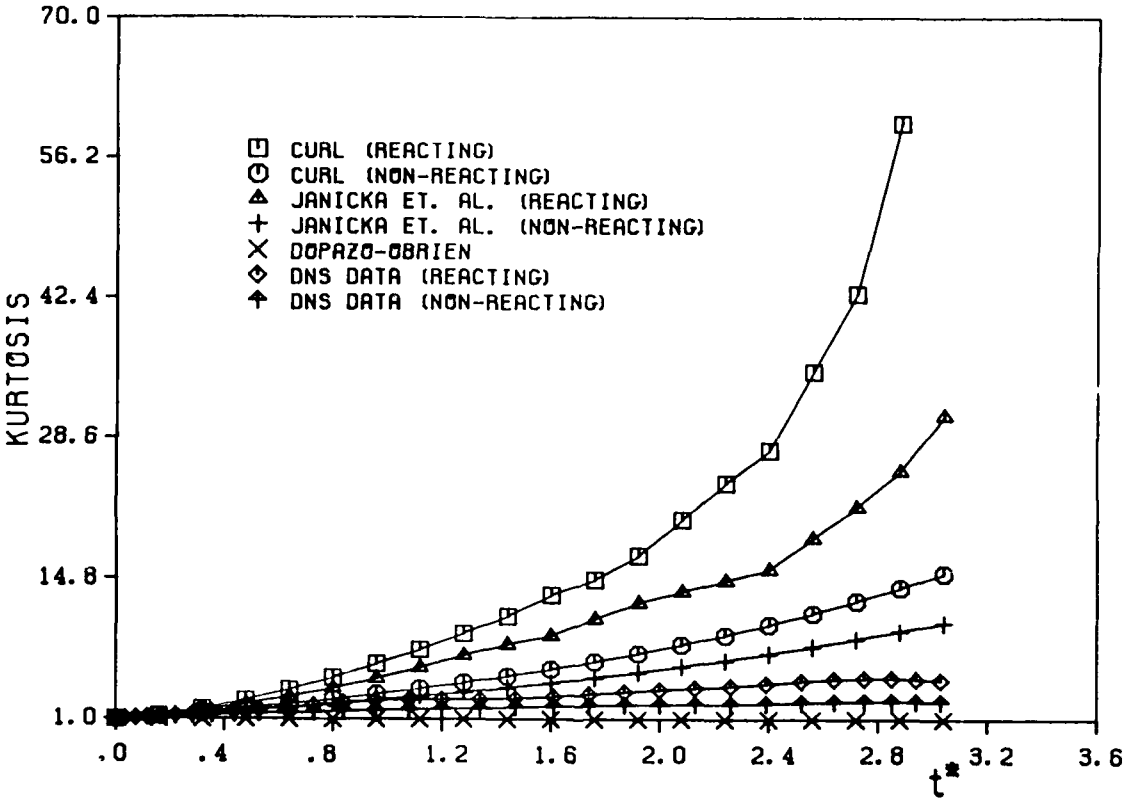
70.0
56.2
42.4
28.6
14.8
1.0
KURTOSIS
CURL (REACTING)
CURL (NON-REACTING)
JANICKA ET. AL. (REACTING)
JANICKA ET. AL. (NON-REACTING)
DOPAZO-OBRIEN
DNS DATA (REACTING)
DNS DATA (NON-REACTING)
.0
.4
.8
1.2
1.6
2.0
2.4
2.8
3.2
3.6
t*

Figure 11